NEW CALIBRATION TECHNIQUES for ONE-PORT MEASUREMENTS using a COMPUTER-CORRECTED NETWORK ANALYSER

by:

E. F. da SILVA, M.Sc., C.Eng., M.I.E.R.E.

A Thesis submitted for the Degree of Doctor of Philosophy

School of Engineering Science
University of Warwick

September, 1978.

CONTENTS

Appendix 12 - Publications

* * * * * * * * * * *

ACKNOWLEDGEMENTS

I wish to express my gratitude to Professor J.A. Shercliffe, Chairman of the Department of Engineering Science, and Professor J. Douce, Head of the Electrical Department of the University of Warwick for the facilities provided for conducting these investigations.

This work was supervised by Dr. M.K. McPhun to whom I am most grateful for his technical and friendly guidance during the past years and for his constructive comments in the preparation of this manuscript. Thanks are also due to Mr R. Anderson of Lanchester Polytechnic for many constructive discussions.

In the Department of Engineering, I am indebted to Dr. H.V. Shurmer and in particular to a former graduate student Dr. N. Hosseini who offered most valuable advice in the writing of the automated programmes. Thanks are also due to Mr A. Hume, Mrs K. Stoneman and Miss L. Harvey of the Departmental Computer Section.

Acknowledgement is also made to the Science Research Council for partial financial support.

Finally, I would like to thank my wife Ann, who endured the many months of "widowhood" whilst this thesis was being finalized.

* * * * * * * * * *

ABSTRACT

The thesis presents three new computer correction methods for measuring immittances and reflection coefficients using an automatic network analyser. The first correction method called the "Three Short Circuit Correction Method" was invented to overcome the difficulty of measuring components embedded in microstrip or in confined environments where sliding matched terminations required by normal correction methods cannot be used. With this new method, error correction is carried out based on calibration measurements produced using three unevenly spaced short circuits. This method was subsequently published in the I.E.E. journal "Electronic Letters" of 22nd March, 1973.

The second correction method using four evenly spaced short circuits was introduced to overcome the difficulty of accurately specifying electrical lengths in microstrip or in a transmission line with non-homogenous medium. The third correction method was evolved to overcome the practical difficulties of constructing good short circuits within microstrip lines. With this method, direct knowledge of the terminations of the calibration standards is unnecessary. Rigorous theoretical derivations for the last two correction methods have been published in the I.E.R.E. journal "Radio and Electronic Engineer" issue of May, 1978. Detailed measurement results and comparisons of the different types of correction measurements have been published in the "Microwave Journal" issue of June, 1978.

The last two correction methods also provide a means of measuring the attenuation and phase changes of transmission lines, and the effective dielectric constant of a non-homogenous line may be calculated if its physical length is known.

Comparative measurements carried out using the new correction systems as opposed to the older established correction systems are included in this thesis. They agree most favourably.

Results obtained using any of the new correction systems have shown that measurement accuracies of $\pm$ 0.5% with a confidence level of 99% are attainable. These results have been confirmed by statistical data obtained from repeated measurements (100 in some cases) of an accurately defined test standard.

* * * * * * * * * * *

DECLARATION

Unless otherwise credited, all the theoretical and practical work described in this thesis is my own.

This work has not been submitted at any other university or institution although some parts of this thesis have been published in technical journals.

* * * * * * * * * * *

PREFACE

Overall Aims

The overall aims of this thesis evolved from necessity. The necessity arose when a team of researchers at the University of Warwick were investigating the application of lumped components, (transistors, resistors, inductors and capacitors) for use at microwave frequencies. As these elements were constructed, it was found that there were no convenient means for accurately characterizing these devices. The author then undertook the task of remedying this deficiency. This work proved to be a far greater task than originally anticipated and the author's original research on inductors had to be cast aside in favour of the measurement problems.

Investigations originally began with the then currently used rapid measurement techniques for evaluating immittances and after this survey (ChapterI), it was decided that the reflectometer would be used. The principles of the reflectometer was subsequently investigated in Chapter II. The peripheral equipment associated with it were investigated in Chapter III.

For measurement accuracy, inherent measurement errors must be recognised and eliminated if possible. Hence, the errors associated with reflectometers had to be investigated. The two main errors, directivity and source match, have been discussed extensively in Chapter IV. A study of these equipment errors revealed that they are extremely difficult to eliminate over large measurement bandwidths. However, these errors can be recognised and cancelled out mathematically by the use of specific calibration procedures. This led to a

hitherto unpublished general mathematical solution for these errors and the invention of the three new correction methods described in Chapter V. These correction methods have now been published. Software correction methods require considerable mathematical manipulation of complex numbers and five manual computer programmes and two automated programmes had to be written. These have been described extensively in Chapter VI.

The calibration procedures required the construction of several calibration pieces such as short-circuits, off-set short circuits etc. These have been shown in considerable detail in Chapter VII.

The determination of the suitability of the equipment for use in computer correction measurements has been established in Chapter VIII.

The results of some measurements carried out with the new correction systems are shown in Chapter IX. A substantial part of this lengthy chapter has been devoted to establishing the accuracy of the corrected measurements. To minimise random errors, many measurements (up to 100 in some cases) have been carried out to determine the accuracy of the measurement procedures.

The final conclusions of the thesis are summarized in Chapter X. Suggestions for further work has also been included in this chapter.

Appendices 11.1 to 11.10 contain details of some fundamental principles used throughout the thesis whilst appendices 12.1 to 12.3 include the published papers that have resulted from this work.

* * * * * * * * * *

CHAPTER I

A BRIEF REVIEW OF SOME REFLECTION COEFFICIENT MEASUREMENT SYSTEMS

1:0 Introduction

The purpose of this thesis is to establish new computer corrected measurement procedures for determining the immittances of lumped components (transistors, resistors, inductors, capacitors etc.,) used at microwave frequencies. The necessity for this thesis arose when a team of researchers at the University of Warwick were engaged in the application of lumped components. As these fundamental devices were constructed, it was found that there was no convenient means for accurately characterizing the devices. The inability to characterize these devices affected the author's work most profoundly as he was then involved in the construction and application of lumped inductors for microwave use. The test jig for measuring these inductors (Figure 1.1) had already been built and specimen components (Figure 1.2) had already been constructed. The same problem was also experienced by fellow researchers D. Michie in his measurement of capacitance and A. Kwesah in his characterization of transistors.

The difficulties shared in common with these fellow researchers were that computer corrected measurements using reflectometers could only take place at a reference plane where calibration standards such as a sliding load could be used. Hence if a device was embedded in a dielectric medium some distance away from this reference plane, then only the transferred immittance i.e., device immittance transferred through a length of transmission line could be measured.

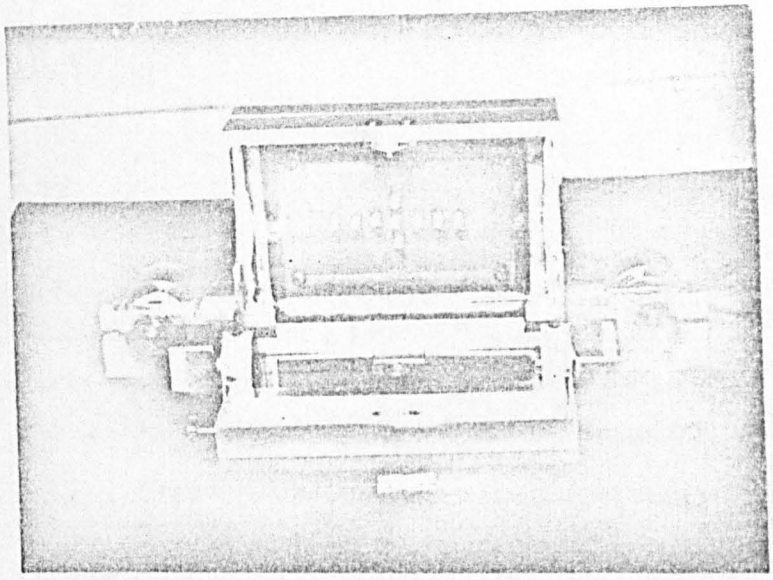

Figure 1.1: Test Jig designed by the author for the measurement of lumped components.

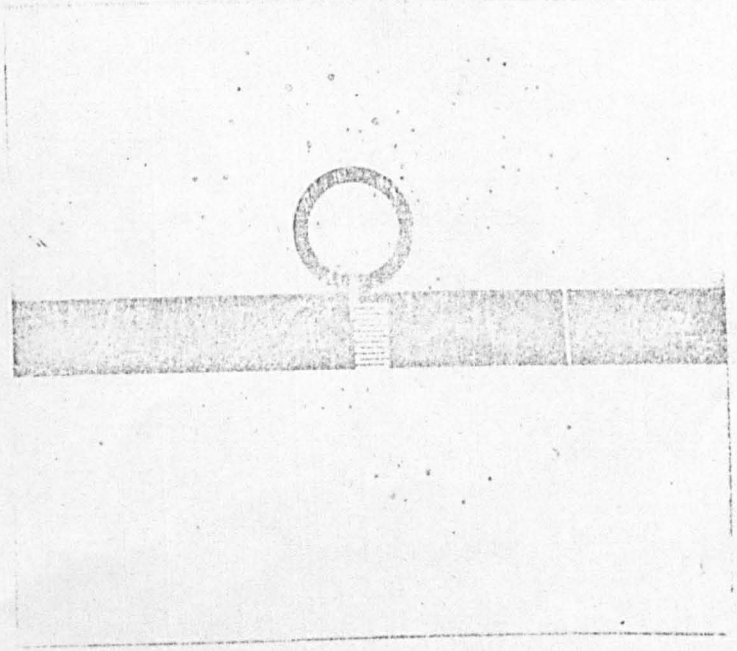

Figure 1.2: A typical lumped tuned circuit constructed by the author on a 10 x 10 mm substrate for the test jig of figure 1.1

This deficiency had to be resolved and the author then abandoned his own work on inductors and undertook the task of providing a solution to the measurement dilemma. However, before this task could be carried out, a survey of the many different methods of measuring immittances had to be investigated.

This chapter presents a brief review of some of the more commonly used systems for measuring immittances using reflection coefficients methods. The measurement systems chosen for discussion are the Rhotector (Section 1:1), the Six Element Reflection Bridge (Section 1:2), Time Domain Reflectometry (Section 1:3) and Swept Slotted Line Frequency Measurements (Section 1:4), Directional Coupler (Section 1:5).

The above methods were selected for investigations chiefly because of the ease of measurement over wide frequency bands. Many other methods of measuring reflection coefficients are also known e.g., Deschamps Method etc., and a comprehensive explanation of these methods may be obtained from the excellent series of books on microwave measurements by Sucher and Fox (Reference 1.1).

1:1 The Rhotector

Figure 1.3

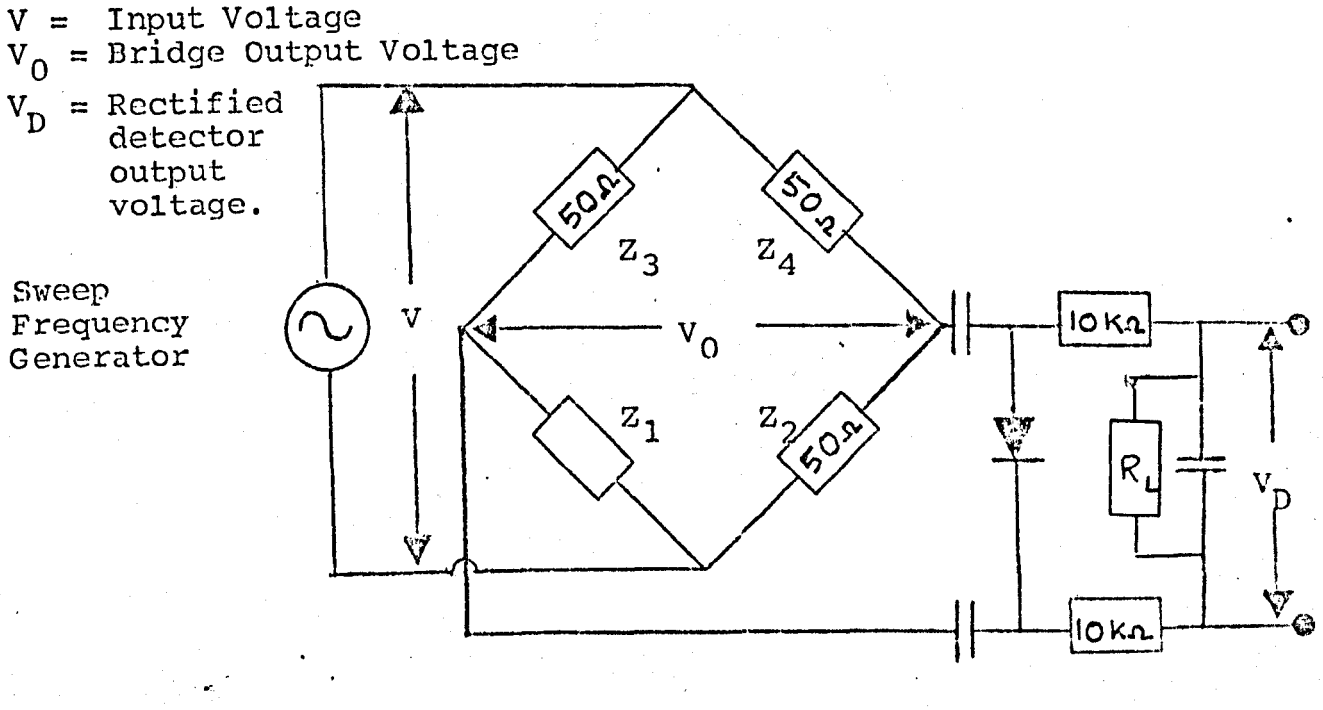

The Rhotector (ref. 1.2) is a reflection coefficient measurement device based on the Wheatstone Bridge principle. Its configuration is shown in figure 1.3 where Z_3 and Z_4 are equal resistances (usually 50 ohms). Z_1 represents the impedance to be measured and Z_2 is the reference impedance.

When the bridge is balanced, the bridge output voltage (V_0) is zero and the detector output voltage (V_D) is also zero. When the bridge is unbalanced, i.e., $Z_1 \neq Z_2$ an output voltage V_0, causes the R.F. diode detector to produce a voltage V_D.

The rhotector is constructed with a 50Ω coaxial measuring port and is supplied with a kit of supplementary coaxial loads having voltage standing wave ratios (VSWR) of 1.0, 1.5, 2.0, and 3.0. For wide band measurements, a sweep signal generator is connected to the input terminals and the detector output signal is normally connected to an oscilloscope whose time base is synchronized to the sweep frequency. Z_2 is externally terminated with a load of VSWR = 1 and values of Z_1 using the calibration standards are used to calibrate the appropriate VSWR's on the display oscilloscope. The device to be measured is then inserted in place of the calibration standards and the VSWR displayed is interpolated.

Referring to figure 1.3 it is seen that provided the diode detector does not load the bridge network, then

$$V_o = V\left[\frac{Z_1}{Z_1+Z_3} - \frac{Z_2}{Z_2+Z_4}\right]$$

and since $Z_3 = Z_4 = Z$ by construction and if Z_2 is chosen to be Z, then

$$\frac{V_o}{V} = \left[\frac{Z_1}{Z_1+Z} - \frac{1}{2}\right]$$

$$\frac{V_o}{V} = \frac{1}{2}\left[\frac{Z_1 - Z}{Z_1 + Z}\right] \quad \ldots\ldots \quad 1.1$$

The above measurements are usually carried out at low signal powers (-10 dBm) in which case the diode detector characteristics may be assumed to be square law i.e., $I_{DIODE} = k\, V^2_{in\ (DIODE)}$ where k = diode constant.

The detector output voltage (V_D)

$$V_D = \left[I_{DIODE} \times R_L\right]$$

where R_L = Diode Load Resistance hence, substituting in equation 1.1

$$V_D = \left|\frac{k R_L V^2}{4}\left[\frac{Z_1 - Z}{Z_1 + Z}\right]^2\right| \quad \ldots\ldots \quad 1.2$$

If $\frac{k R_L}{4}$ is defined as K then equation 1.2 becomes

$$V_D = \left| K V^2 \Gamma^2 \right| \quad \ldots\ldots \quad 1.3$$

It will be shown later (equation 2.19) that $\Gamma = \frac{Z_1 - Z}{Z_1 + Z}$ where Γ is called the reflection coefficient

The voltage standing wave ratio (VSWR) is related to the reflection coefficient (Γ) by the expression

$$\Gamma = \left| \frac{VSWR - 1}{VSWR + 1} \right|$$

and substituting in equation 1.3 yields

$$V_D = KV^2 \left| \frac{VSWR - 1}{VSWR + 1} \right|^2 \quad \ldots\ldots \quad 1.4$$

Figure 1.3(a) is constructed by substituting various values of VSWR in equation 1.4.

Figure 1.3(a)
Relative Output Voltage vs VSWR

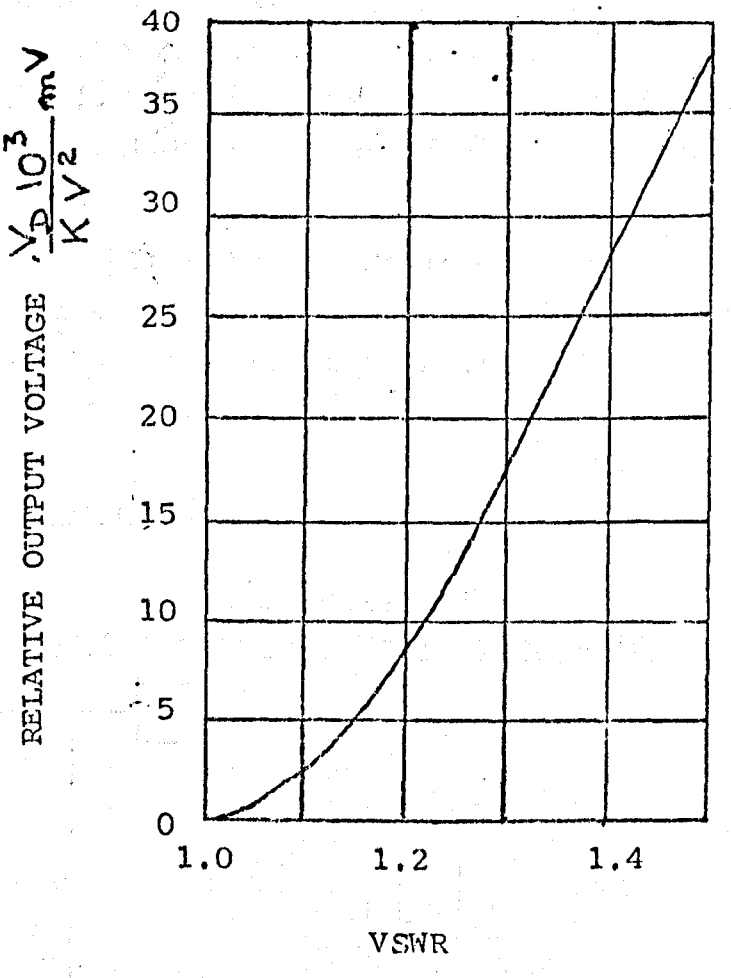

A more detailed analysis of the Rhotector may be found in reference 1.2.

The rhotector is a relatively simple and useful device for measuring reflection coefficients over wide frequency bands and it is an ideal production test instrument as it is relatively robust. It was not selected as the main measurement system because:-

1: Only the modulus of the reflection coefficient is measured. Phasor values cannot be obtained.

2: The reflection coefficient measured is dependent on the accuracy of the main calibration test standards.

3: The reflection coefficient measured is directly proportional to the square of the value of the input voltage (equation 1.2) and over a wide frequency band of measurement the input voltage may vary considerably.

4: The detector output voltage is not linearly related to the reflection coefficient or VSWR (figure 1.2). Furthermore, this output is subject to the temperature vagaries of the diode characteristics.

5: The signal applied to the device under test (Z_1) is always less than the generator applied voltage and could lead to poor signal to noise ratios when low reflection coefficients are measured.

1:2 The Reflection Bridge

Figure 1.4(a)

The Six Element Reflection Bridge

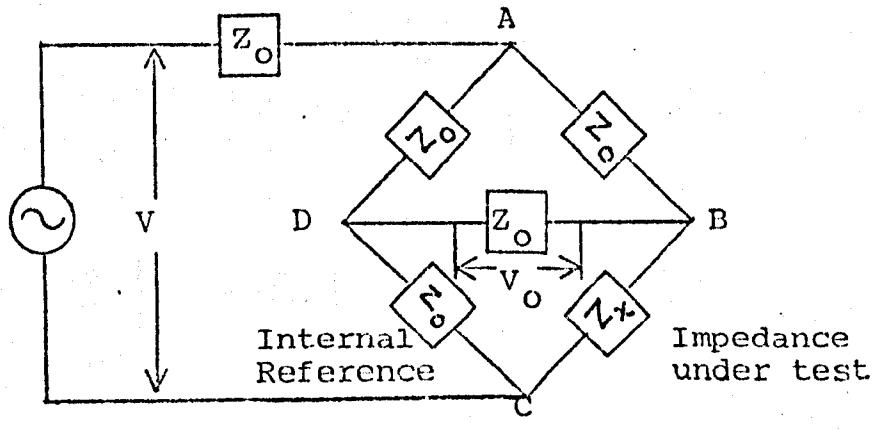

The reflection bridge is a six-element bridge which assumes the configuration shown in figure 1.4(a). This network configuration has the great advantage in that the detector output voltage (V_0) is directly proportional to the reflection coefficient. The network can be analysed by a simple mesh analysis using the notation shown in figure 1.4(b) which is that of figure 1.4(a) re-drawn.

Figure 1.4(b)
The Reflection Bridge of Figure 1.4(a)
Re-drawn for Analysis

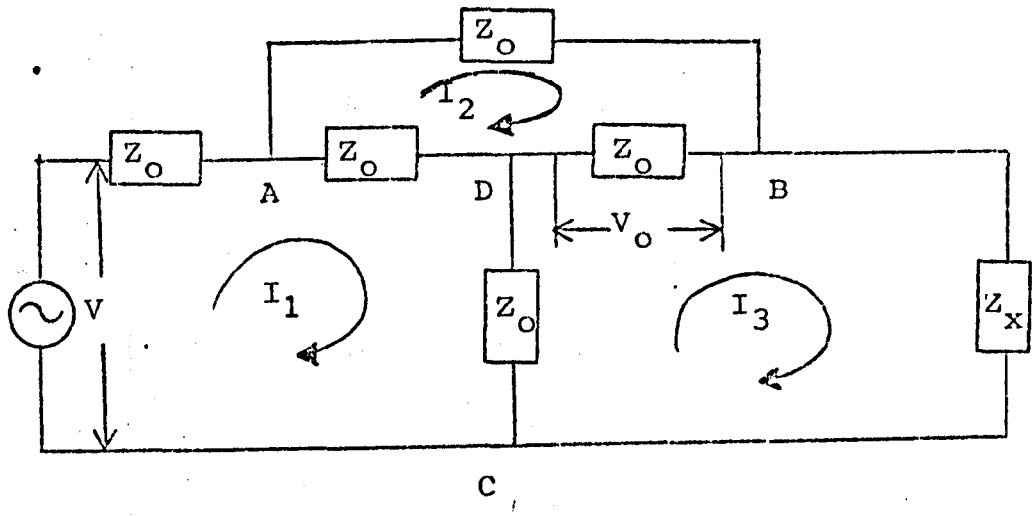

By inspection

$$\begin{bmatrix} V \\ 0 \\ 0 \end{bmatrix} = \begin{bmatrix} 3Z_0 & -Z_0 & -Z_0 \\ -Z_0 & +3Z_0 & -Z_0 \\ -Z_0 & -Z_0 & 2Z_0+Z_x \end{bmatrix} \begin{bmatrix} I_1 \\ I_2 \\ I_3 \end{bmatrix} \quad \ldots\ldots \quad 1.5$$

and defining the determinate (D)

$$D = \begin{vmatrix} 3Z_0 & -Z_0 & -Z_0 \\ -Z_0 & 3Z_0 & -Z_0 \\ -Z_0 & -Z_0 & 2Z_0+Z_x \end{vmatrix}$$

$$D = 8Z_0^2 \left[Z_0 + Z_x \right] \quad \ldots\ldots \quad 1.6$$

The detector output voltage (V_D) is

$$VD = (I_2 - I_3)\ Z_0 \qquad \ldots\ldots \quad 1.7$$

Using Cramer's Rule to solve for I_2 gives

$$I_2 = \begin{bmatrix} 3Z_0 & V & -Z_0 \\ -Z_0 & 0 & -Z_0 \\ -Z_0 & 0 & 2Z_3+Z_2 \end{bmatrix} \Big/ D$$

$$\dot{I}_2 = \left[3VZ_0^{\,2} + VZ_0Z_x \right] / D \qquad \ldots\ldots \quad 1.8$$

and

$$I_3 = \begin{bmatrix} 3Z_0 & -Z_0 & V \\ -Z_0 & 3Z_0 & 0 \\ -Z_0 & -Z_0 & 0 \end{bmatrix} \Big/ D$$

$$\therefore\ I_3 = \left[4\ V\ Z_0^{\,2} \right] / D \qquad \ldots\ldots \quad 1.9$$

Combining equations 1.6, 1.7, 1.8 and 1.9,

$$V_0 = (I_2 - I_3)Z_0 = \frac{\left[3V\ Z_0^{\,2} + V\ Z_0\ Z_x - 4V\ Z_0^{\,2} \right] Z_0}{8\ Z_0^{\,2}\left[Z_0 + Z_x \right]}$$

$$V_0 = \frac{V\left[Z_x - Z_0 \right]}{8\left[Z_x + Z_0 \right]} \qquad \ldots\ldots \quad 1.10$$

$$\text{or} \quad V_0 = \frac{V}{8}\left[\Gamma \right] \qquad \ldots\ldots \quad 1.11$$

where $\Gamma = \dfrac{Z_x - Z_0}{Z_x + Z_0}$ as shown in equation 2.19.

Hence the output voltage V_0 is directly proportional to the reflection coefficient Γ . PROVIDED THAT A LINEAR DETECTOR (REF 1.3) IS USED.

The insertion loss of the bridge is high, the output voltage being one eighth of the open circuit generator voltage or ¼ of the voltage that would be delivered by the generator if it was correctly terminated by an impedance Z_0 in place of the bridge. Thus the insertion loss is 12dB. Practical realisations of the bridge circuit have losses slightly greater than this. This high insertion loss has the advantage that source mismatch error (section 4:3) is reduced but it also causes reduced signal level to the device under test.

The greatest problem with the bridge described is that a balun must be provided for the R.F. Source or the detector. This condition is most difficult to satisfy where microwave frequencies operating over several octave bandwidths are desired. If a crystal detector is placed across the detector load such as in the Wiltron Autotester (reference 1.4) the baluns problem is overcome but then only the magnitude of the reflection coefficient $|\Gamma|$ will be obtained and many of the disadvantages common to the Rhotector (section 1:1) will be evident. A more detailed analysis of this bridge may be found in references 1.3 and 1.4.

This bridge was not favoured for the measurement of complex reflection coefficients for the reasons discussed in sections 1:1 and 1:2. in spite of its higher directivity. The problem of directivity errors will be discussed fully in section 4:2.

1:3 Time Domain Reflectometry Measurements

Time Domain Reflectometry employs a pulse generator which sends a voltage step [incident wave] along a transmission line towards the terminating impedance to be measured (fig. 1.5).

If the terminating impedance is not matched to the line, then reflection occurs. Both the incident and reflected steps are monitored by an oscilloscope at a fixed point.

Figure 1.5
Block Diagram of a Simple Time Domain Reflectometry System

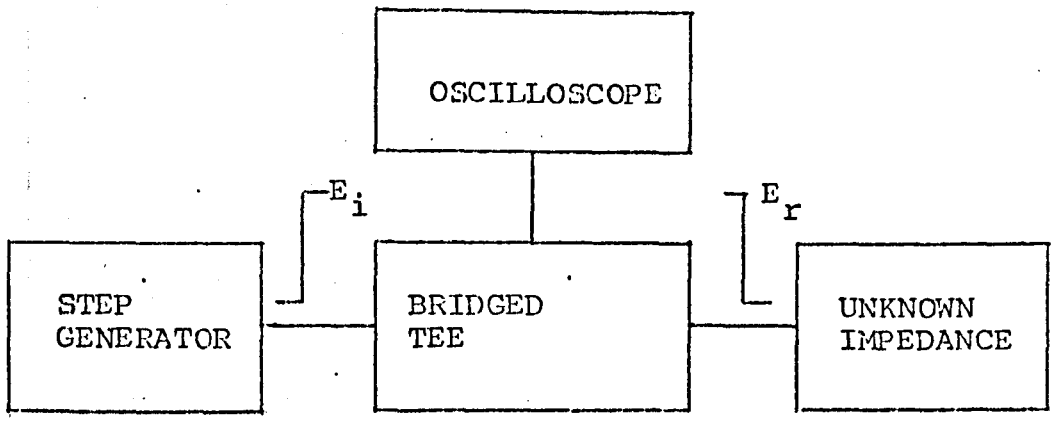

The following can be deduced from an intelligent comparison of the incident and reflected step waveforms.

1: Any discontinuities in the line can be located by virtue of the propagation velocity of the step function and the time (measured on the time base of the oscilloscope) required for the reflected voltage to return. This feature is extremely useful for locating poor connections etc., within a system.

2: The waveform of the reflected wave from any discontinuities or terminations is most valuable for it reveals both the nature and the magnitude of the mismatched termination. Eight ideal oscilloscope displays of this nature are shown in figures 1.6 and 1.7. These diagrams have been taken from reference 1.5. The terminating impedance and/or reflection coefficients may also be calculated using the expressions with figure 1.6 and 1.7.

Figure 1.6

TDR Displays for Typical Loads

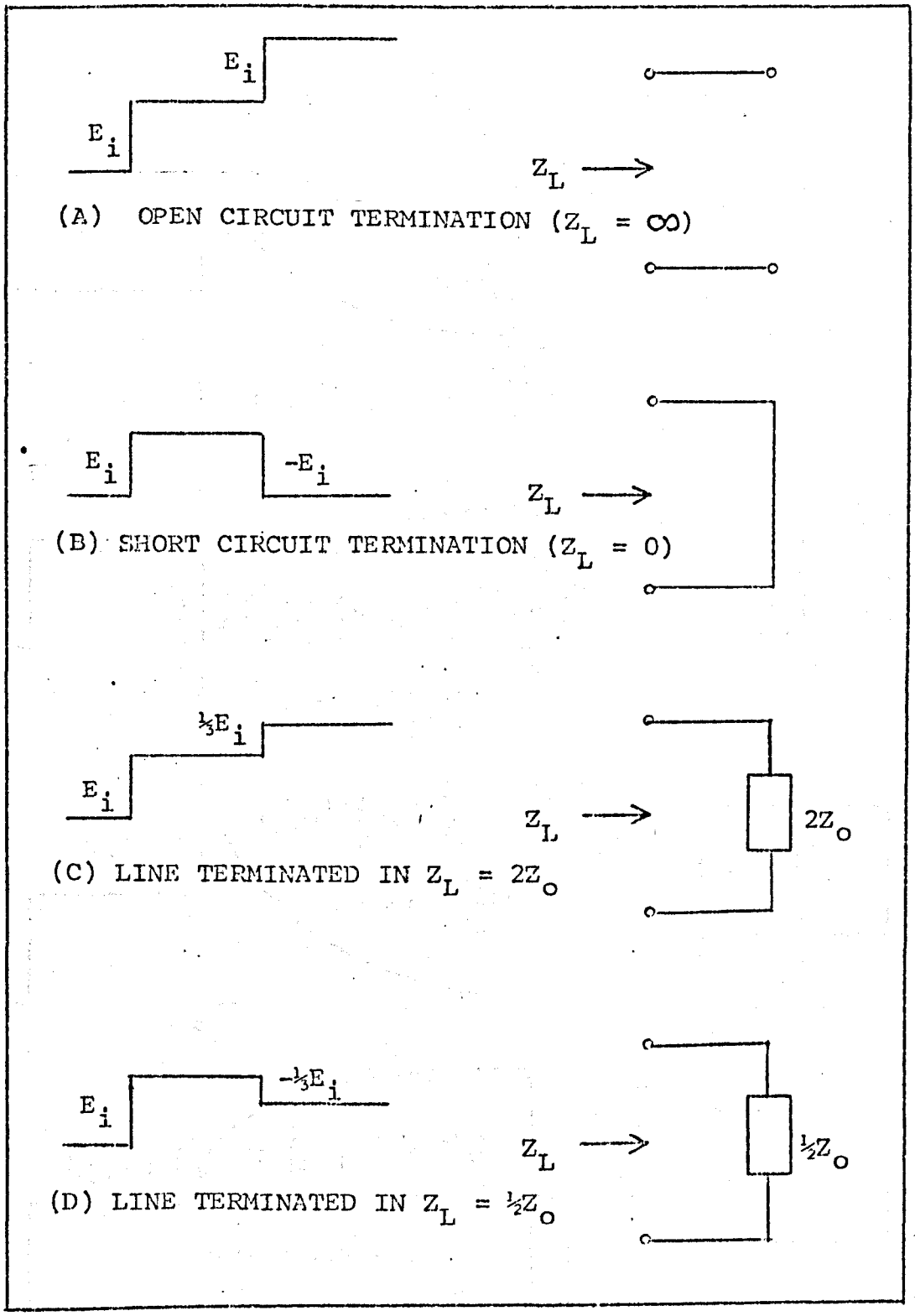

Figure 1.7

Oscilloscope Displays for Complex Load Impedances Z_L

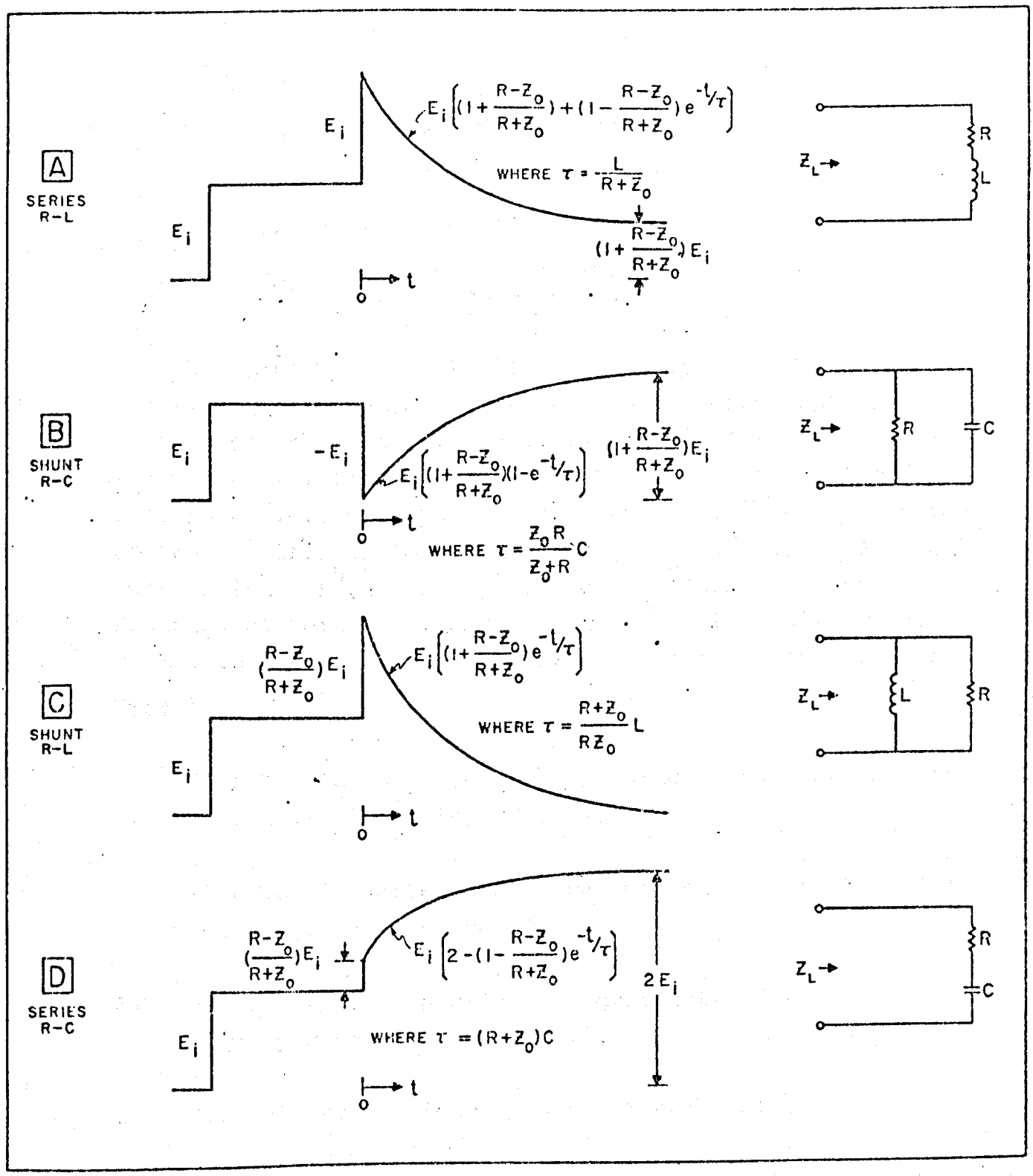

These expressions may be derived by recalling that the reflection coefficient (Γ) is given by:

$$\Gamma = \frac{E_R}{E_i} = \frac{Z_L - Z_0}{Z_L + Z_0}$$

..... (Ref 1.5)

where E_R = Reflected Waveform

E_I = Incident Step Waveform

Z_L = Terminating Impedance

Z_0 = Characteristic Impedance of the Transmission Line.

Assuming Z_0 is real, it become only a matter of simple substitution in the above expression to derive the four expressions shown in figure 1.6. The waveforms for figure 1.7 can be verified by resorting to the use of Laplace Transform i.e., writing the expression for $\Gamma(s)$ in terms of the specific Z_L for each example ($Z_L = R + sL$, $\frac{r}{1+sC}$, etc.) multiplying $\Gamma(s)$ by $\frac{E_i}{s}$, the transform of a step function of height E_i, and then transforming this product back into the time domain to find an exact expression for $E_{R(t)}$.

Time Domain Reflectometry was used in the development of the test jig shown in figure 1.1.

Time Domain Reflectometry was not chosen for the main measurement system because of:

1: Difficulty in measuring the gradients of the display waveforms accurately.

2: Multiple reflections in a practical system.

3: Relatively poor rise time of step generator at that time for high frequency work (6 GH_Z)

4: Difficulty in observing the waveform accurately, resulting in relatively poor accuracy.

1:4 Swept Frequency Slotted Line Measurements

A basic block diagram of how a slotted line may be used in swept frequency measurements is shown in figure 1.8.

Figure 1.8
Block Diagram of VSWR Measurements
Using the Sweep Frequency Slotted Line Method

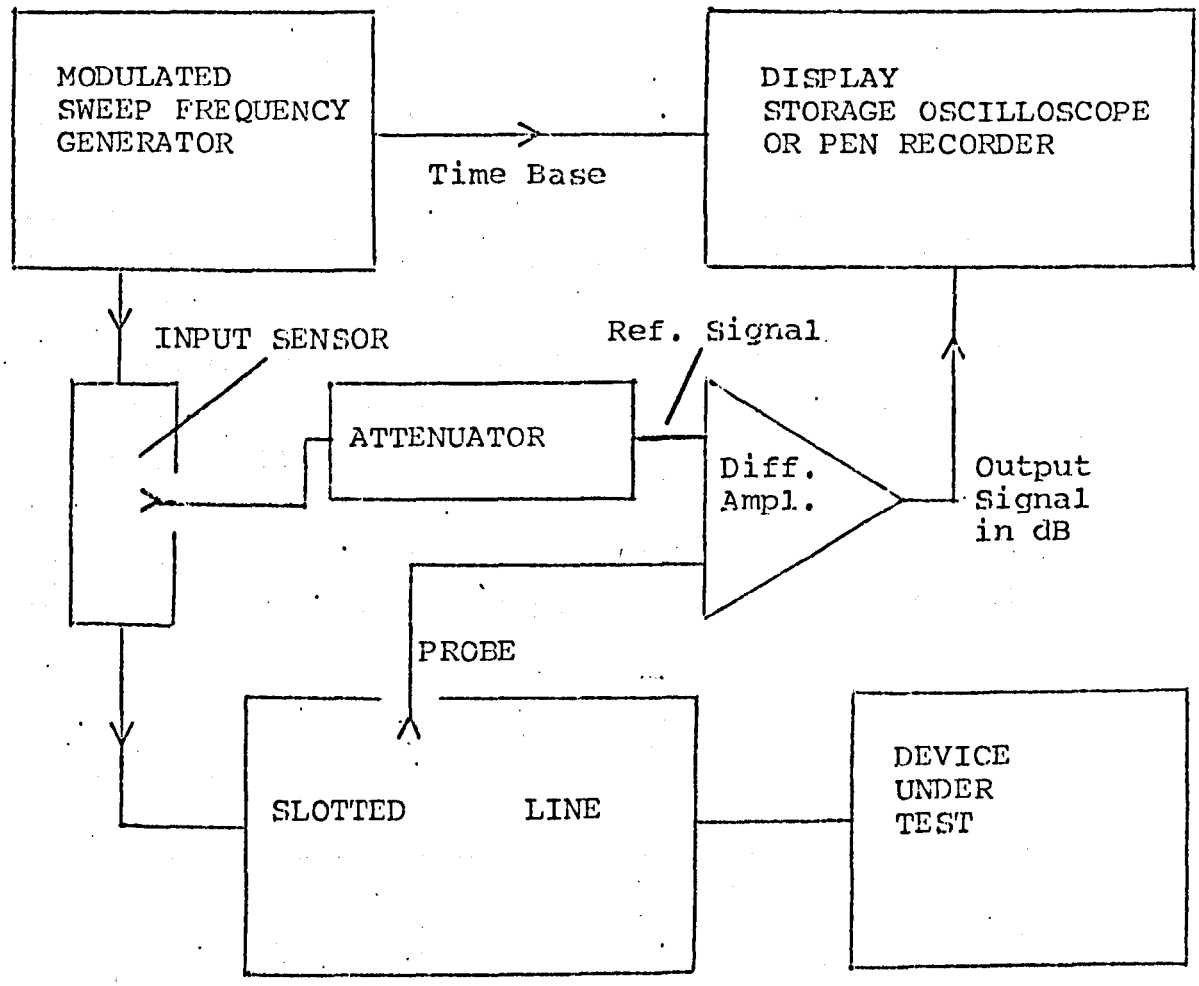

Measurement is relatively easy to carry out. The frequency generator is set to sweep the desired frequency band. The device under test is removed and a power meter is connected to the output port of the slotted line. The generator is adjusted until the desired output power e.g., 0dBm is obtained.

The power meter is removed and replaced by a good termination e.g., a sliding load. One input (carriage input) of the differential amplifier is grounded and the other input (reference input) is adjusted by the attenuator to produce a suitable output e.g.,— 25dBm. The carriage input to the differential amplifier is then re-introduced and the probe penetration adjusted until the two inputs are equal, i.e., no output from the differential amplifier. At this stage, movement of the carriage assembly on the line should theoretically produce no change in output from the differential amplifier. In practice slight changes occur because of an imperfect slotted line and termination. The advantage of using a differential amplifier lies in the fact that small changes in input power do not introduce large errors in VSWR measurements (reference 1.6). The output of the amplifier is then connected to a pen recorder or storage scope whose ordinate axis is initially set at its mid-position in order to allow measurement in either direction. The slotted line termination is then removed and the device under test (DUT) is reconnected. The probe carriage on the slotted line is slid manually to and fro over a distance (d). The distance (d) must exceed half an electrical wavelength of the lowest frequency to be measured. The resultant plot of a typical set of measurements is shown in figure 1.9.

Figure 1.9

Typical VSWR Plot of a Swept Slotted Line Measurement

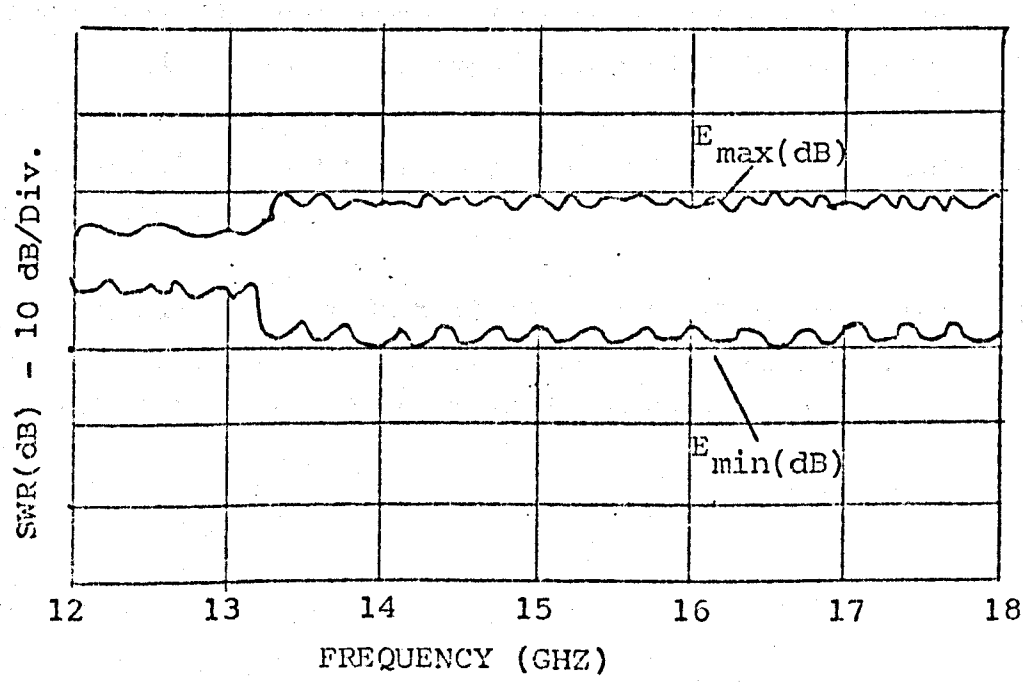

The SWR(dB) at a particular frequency is denoted by the distance between E_{MAX}(dB) and E_{MIN}(dB) (figure 1.9) at that particular frequency. The VSWR ratio and hence the magnitude of the reflection coefficient can be calculated in the usual manner.

A simple explanation of the above procedure can be obtained by first considering operation at one frequency only. E_{MAX} and E_{MIN} of this particular frequency can be obtained by sliding the carriage probe along the slotted line over a distance (d) greater than half a wavelength. This information will enable the VSWR to be calculated. Phase information will only be obtained in the distance through which a fixed reading, e.g., E_{Min} has moved is known when the device under test at the end of the slotted line has been substituted for a reference termination e.g., a short circuit. If the recorder or storage scope is capable of recording E_{MAX} and E_{MIN} in dB then since

$$\text{VSWR(dB)} = 20 \log \left| \frac{E_{MAX}}{E_{MIN}} \right| = 20 \log |E_{MAX}| - 20 \log |E_{MIN}|$$

it follows that the difference between $|E_{MAX}(dB)|$ and $|E_{MIN}(dB)|$ will yield VSWR in dB. If another frequency is chosen, E_{MAX} and E_{MIN} will occur at different points along the slotted line. For a series of different frequencies (swept frequencies), the series of E_{MAX} and E_{MIN} will be located as the carriage probe is moved slowly along the slotted line and their amplitudes will be recorded. Hence the VSWR at any one frequency can be obtained. It should be noted that there is no phase information in this series of measurements.

An alternative but similar method of carrying out swept frequency slotted line measurements has also been described by Hewlett Packard in reference 1.7.

This type of measurement was not selected as the phase information cannot be easily obtained in these swept measurements.

1:5 Directional Couplers

Directional Couplers are devices which sample a wave moving in one direction but not in the other. Such a device can be used to measure the reflected and incident waves in a measurement system and permit the calculation of the reflection coefficient. The construction of a very simple directional coupler is shown in figure 1.10 and a simplified circuit showing the capacitive and mutual inductive coupling and the inner conductor of the coaxial line is shown in figure 1.11.

An extensive analysis of the dual directional coupler is carried out in Chapter II. The analysis carried out in this section is a very approximate solution and is based on that by Carson (reference 1.8) but it does demonstrate the principle of single frequency operation clearly. It also explains why the directional coupler was adopted as the main device for measurement of reflection coefficients and impedances.

Figure 1.10
Basic Construction of One Type of Directional Coupler

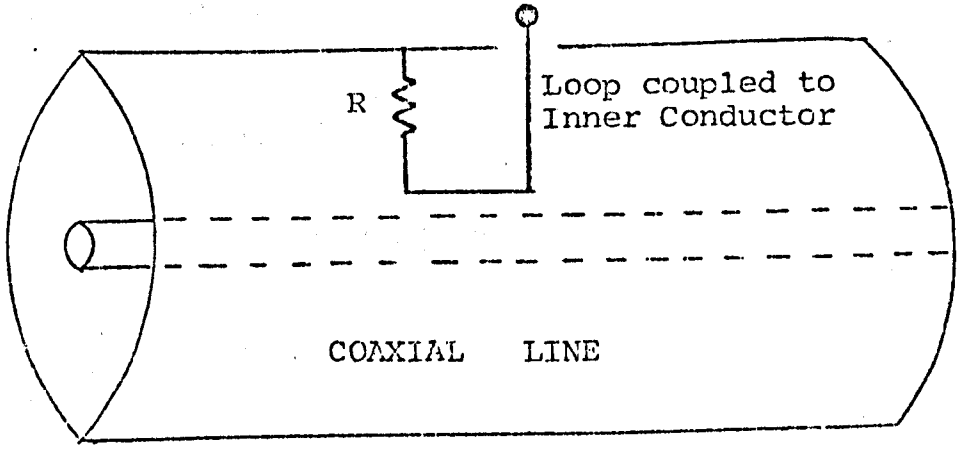

Figure 1.11

Simplified Circuit showing Capacitive and Mutual Inductive Coupling Between the loop and Inner Conductor of a Coaxial Line Coupler.

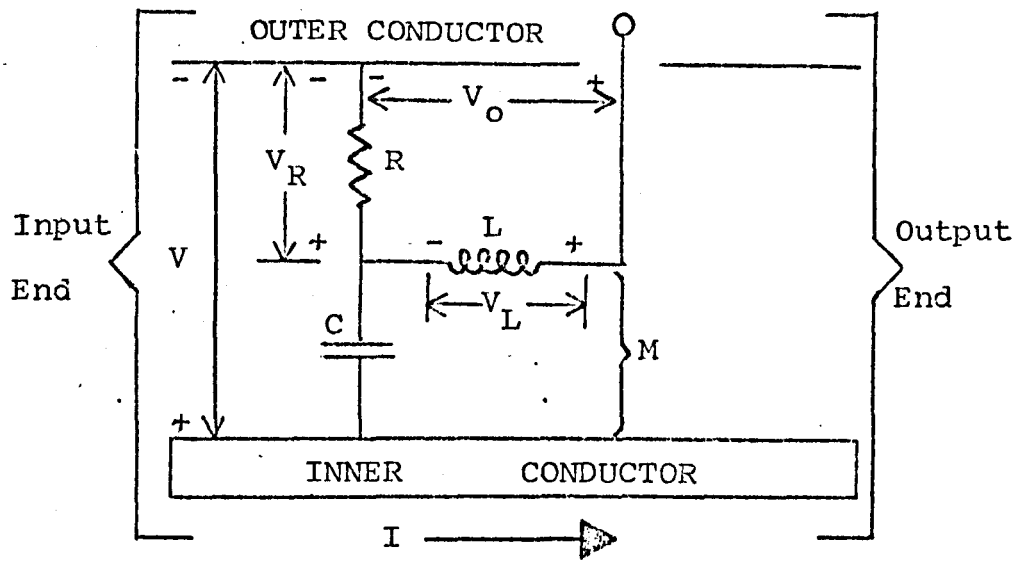

By inspection of figure 1.11, it can be seen that

$$V_R = V \frac{R}{R + \frac{1}{jwc}}$$

If $R \ll \frac{1}{jwc}$ then $V_R \simeq jw\,CRV$ ..... 1..12

Current I in the inner conductor induces V_L in the loop. Thus,

$$V_L \simeq -jw\,MI \qquad \text{.....} \quad 1.13$$

The output voltage is

$$V_O = V_R + V_L = jw\,CRV - jw\,MI \qquad \text{.....} \quad 1.14$$

If the coupler is designed such that

$$CR = \frac{M}{R_O} \qquad \text{.....} \quad 1.15$$

where R_0 = characteristic resistance of the coaxial line, then equation 1.14 becomes

$$V_0 = jw\,M\,(\frac{V}{R_0} - I) \qquad \ldots\ldots \quad 1.16$$

The voltage and current decomposition equations are

$$V = V_i + V_r \qquad \ldots\ldots \quad 1.17$$

and $$I = I_i - I_r = \frac{V_i}{R_0} - \frac{V_r}{R_0} \qquad \ldots\ldots \quad 1.17(a)$$

where the subscripts $_i$ and $_r$ represent the incident and reflected directions. Thus equation 1.16 becomes

$$V_0 = jwM\,(\frac{V_i + V_r}{R_0} - I_i + I_r)$$

$$= jwM\,(I_i + I_r - I_i + I_r)$$

$$V_0 = jw\,M\,2\,I_r \qquad \ldots\ldots \quad 1.18$$

Therefore the output voltage is proportional to the reflected phasor current (or phasor voltage) because the incident components cancel when the coupler is connected as shown in figure 1.11. If the coupler is reversed, its output voltage is proportional to the incident phasor current and the reflected components cancel. In many cases, it is not convenient to keep reversing the coupler, and dual directional couplers, one to measure the incident wave and the other to measure the reflected wave are used. A reflectometer is a dual directional coupler specially manufactured for good amplitude and phase coupling match over a wide frequency band of operation. Reflectometer design is complicated. Harvey (reference 1.10) offers a good bibliography on the subject.

In practice, the directional effect is not perfect and leads to a type of error called "Directivity Error". Directivity Error is investigated extensively in Chapter IV. However in spite of the errors associated with reflectometer measurements, this method was chosen as the most suitable because:

1: The reflectometer method provides a quick and easy method of measuring reflection coefficient and hence impedances if the reference impedance is well defined.

2: Swept frequency measurements are easily carried out.

3: The reflected and incident measurements carried out yield both amplitude and phase information. See equation 1.18 where I_r is a phasor quantity.

4: Error correction systems are relatively easy to incorporate.

5: The signal loss between the sweep frequency signal generator and the device to be measured can be less than 1dB. Thus low-power signal generators can be used or alternatively larger powers can be fed to devices such as transistors if desired.

6: The sampling loss associated with the incident and reflected waves can be easily controlled in the initial design of the reflectometer. A commonly used coupling factor is 20dB nominally.

1:6 Conclusions

The necessity for new rapid and computer correction systems has been established in the early part of this chapter. The latter part of this chapter has presented a brief review of some of the various methods of measuring reflection coefficients rapidly. Each of the methods

investigated has several desirable properties. The Rhotector and the Wiltron Auto tester are ideal production test instruments, robust and simple to use for rapid magnitude measurements of reflection coefficients. Time Domain Reflectometry locates discontinuities rapidly and Loeb (reference 1.9) and his team have used it most successfully in the measurement of lumped components. The Swept Slotted Line Measurements Technique, although relatively accurate does not provide phase information. The Directional Coupler provides both amplitude and phase information rapidly and does not suffer from the baluns and higher loss problems associated with the reflection bridge. Hence, the Directional Coupler was selected as the basis for the measurement system.

The remaining chapters will be devoted to the application and error correction methods published by the author for the measurement of reflection coefficients and immittances using reflectometers.

* * * * * * * * * * *

References

1.1 Sucher, M and Fox, J; "Handbook of Microwave Measurements" 3rd Edition, Volumes I, II, III, John Wiley & Sons Ltd., London.

1.2 Telonic Engineering Co "RHO-Tector VSWR Detector" Application Bulletin 301.

1.3 Oldfield, W.W. "Present-Day Simplicity in Broadband SWR Measurements" Wiltron Technical Review Vol 1, No 1, 930 Meadow Drive Palo Alto, Ca.

1.4 Dunwoodie, D, & Lacy, P "Why Tolerate Unnecessary Measurement Errors?" Wiltron Technical Review No 5 March 1975. 930 Meadow Drive, Palo Alto, Ca.

1.5 Hewlett Packard Application Note 62 "Time Domain Reflectometry" Hewlett Packard Ltd., 1501 Page Mill Road, Palo Alto, Ca.

1.6 Weinschel, B "Measurement of Microwave Parameters by the Ratio Method" Publication by Weinschel Engineering, Gaithersburg, Md, U.S.A.

1.7 Hewlett Packard Application Note 183 "High Frequency Swept Measurements" Hewlett Packard Ltd., 1510 Page Mill Road, Palo Alto, Ca, U.S.A.

1.8 Carson, R.S. "High Frequency Amplifiers" John Wiley & Sons 1975.

1.9 Loeb, H "Private Visit to Cranfield Institute of Technology" Bedfordshire.

1.10 Harvey, A.F. "Microwave Engineering" Academic Press, London 1963.

* * * * * * * * * * *

CHAPTER II

THE THEORY of the MEASURING SYSTEM

2:0 Introduction

The correct choice of a measurement system must ultimately depend on the type of measurement required and on the financial resources available. Various measuring systems were considered for the rapid measurement of reflection coefficients. Among the systems investigated were the Rhotector (Section 1:1), the Reflection Bridge (Section 1:2), Time Domain Reflectometry (Section 1:3) and Swept Slotted Line Measurements (Section 1:4). The advantages and disadvantages of each system has been discussed extensively in Chapter I and only a brief summary is necessary here. Time Domain Reflectometry (TDR) is ideal for physically locating a discontinuity with a system. In fact, it was used extensively for that purpose in the final measurement system. Single frequency or swept frequency slotted line measurements provide accurate results but the measurement method is extremely tedious and time consuming.

The Rhotector, Reflection Bridge and the Dual Directional Coupler (reflectometer) certainly excel as rapid wide band reflection coefficient measurement systems. The first two are variants of the Wheatstone Bridge Principle. With the Rhotector and the Reflection Bridge, the signal level available for test is inherently 12 dB less than the applied level from the signal generator and this could result in poorer signal to noise ratios when large return losses are measured. Dual Directional Couplers (Reflectometers) may be constructed to have low inherent losses, which means that the difference between the signal level available for test purposes and that available from the signal generator could be less that 1 dB.

Commercial wide frequency band coaxial directional couplers have relatively poor directivity characteristics when compared with bridges and waveguide directional couplers. At the commencement of this investigation, wide frequency band, coaxial couplers with a directivity ratio of more than 30 db were not generally available. However, commercial coaxial couplers (Ref 2.1) with greater than 50 db directivity ratios are now common. After much deliberation and discussion, the reflectometer method of measurement using dual directional couplers was finally chosen as the desired measurement system. This chapter will be devoted to the theoretical aspects of such a measurement system.

A brief summary of fundamentals concerning the measurement system is presented in Sections 2:1 and 2:2. A more detailed analysis can be found in any text book (Ref 2.15, 2.16, 2.17). However, the above sections are required to establish the foundations for the analysis of Section 2:3 which has not been presented elsewhere. Section 2:4 analyses the problems associated with the measurement of incident and reflected powers and the errors resulting from it. This is an adaption of an analysis carried out by Warner (Ref 2.8).

2:1 The Theory of Reflectometer Measurement

The use of reflectometers for measuring the incident (a) and reflected wave (b) has been described by many authors, e.g., Hunton and Pappas (Ref 2.4) and Engen and Beatty (Ref 2.5). In this Thesis, the incident wave (a_i) and the reflected wave (b_i) with respect to the "i" th port are defined in the manner described in detail by Warner (Ref 2.8 - Appendix 1).

Figure 2.1

A Simple Reflectometer System

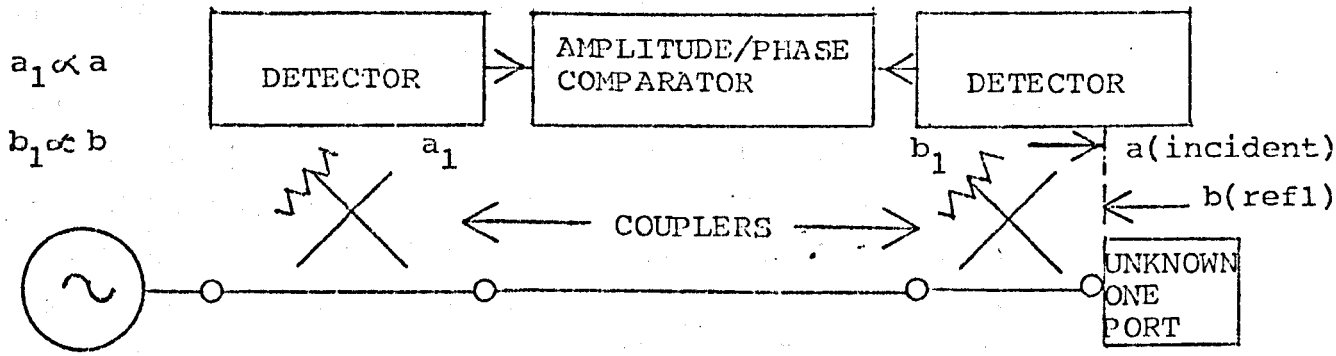

In its simplest form, the reflectometer measures a portion (a_1) of the incident wave (a_i) and a portion (b_1) of the reflected wave (b_i) at a specified plane in a system. For the system to function correctly, it is essential to establish that there is no mutual interaction between the incident and reflected power flow when the wave impedance (Z_w) is real. Hence some fundamental concepts will inevitably have to be reviewed.

Figure 2.2

Propagation of a TE_{10} mode wave in a perfectly conducting, infinitely long wave guide with a homogeneous loss free dielectric.

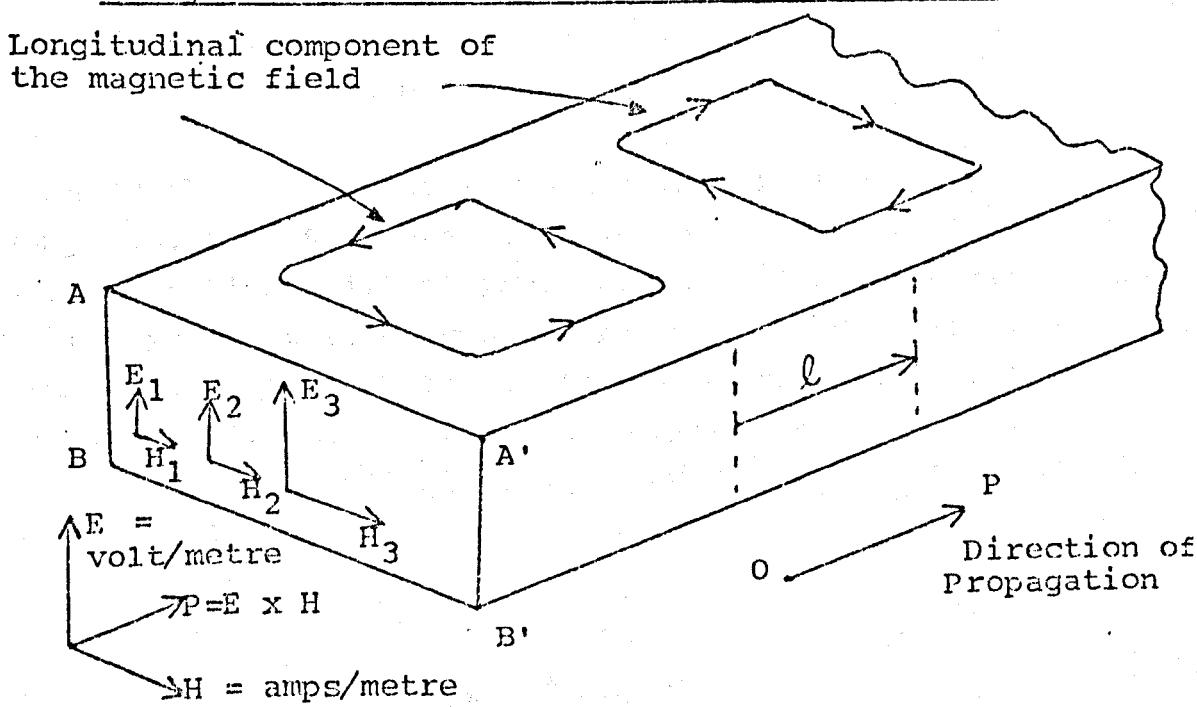

Consider the propagation of electro-magnetic energy (Fig 2.2) in a medium bounded by AA' BB' e.g., an infinitely long wave guide. The modes of wave discussed will be limited to those modes which possess transverse components of both electric and magnetic fields i.e., TEM, TE or TM waves. Since the longitudinal component of the field may always be found if the transverse components are known, there is no need to retain the former explicitly in theory. In fact, for convenience, it will suffice to work entirely in terms of the transverse components of the electric and magnetic field strengths denoted respectively by the symbols E and H. Both these quantities, E and H vary over the cross-section of the transmission system but because the spatial distribution is the same in each case (Fig 2.2), their ratios $\frac{E_3}{H_3} = \frac{E_2}{H_2} = \frac{E_1}{H_1}$ remains unchanged. Schelkunoff (Refs 2.2; 2.3) recognised this important generalization and introduced the concept of wave impedance (Z_w) which is the ratio of these field strengths so that at a given point along the guide, we have in general:

$$Z_w = \frac{E}{H} \qquad \ldots\ldots \qquad 2.1$$

where Z_w = impedance in ohms
E = volts per metre
H = amperes per metre.

When the wave guide is not infinitely long or perfectly terminated, then the total transverse electric field (E) at any point will consist of incident and reflected parts. Each of these parts must, of course, be compounded of the transverse electric field components of all waves travelling in the appropriate direction. The same arguement may be applied to the magnetic field (H) at a given point. Hence the two equations below apply, i.e.,

$$E = E^+ + E^- \qquad \ldots\ldots \qquad 2.2$$

$$H = H^+ + H^- \qquad \ldots\ldots \qquad 2.3$$

where the plus superscript denotes an incident wave (direction OP in Fig 2.2) and the minus superscript denotes a reflected wave (direction PO in Fig 2.2). For this case, the wave impedance (Z_w) is then defined as:

$$Z_w = \frac{E^+}{H^+} \qquad \ldots\ldots \qquad 2.1(a)$$

or

$$Z_w = \frac{-E^-}{H^-} \qquad \ldots\ldots \qquad 2.1(b)$$

Substitution of equations 2.1(a) and 2.1(b) into equation 2.3 will result in:

$$H = \frac{E^+}{Z_w} - \frac{E^-}{Z_w} \qquad \ldots\ldots \qquad 2.4$$

If the symbols $\mathcal{E}$ and $\mathcal{H}$ are used to represent the instantaneous values of the complex quantities E and H for a sinusoidal time variation, then:

$$\mathcal{E} = \mathrm{Re}\, E e^{j\omega t}$$
$$\mathcal{H} = \mathrm{Re}\, H e^{j\omega t}.$$

and writing equations 2.2, 2.3 and 2.4 in instantaneous values will result in:

$$\mathcal{E} = \mathcal{E}^+ + \mathcal{E}^- \qquad \ldots\ldots \qquad 2.2(a)$$

$$\mathcal{H} = \mathcal{H}^+ + \mathcal{H}^- \qquad \ldots\ldots \qquad 2.3(a)$$

$$\mathcal{H} = \frac{\mathcal{E}^+}{Z_w} - \frac{\mathcal{E}^-}{Z_w} \qquad \ldots\ldots \qquad 2.4(a)$$

The instantaneous power flux or Poynting Vector, $\underline{P}$, is given by $\underline{P} = \underline{E} \times \underline{H}$. As we have defined $\mathcal{E}$ and $\mathcal{H}$ as the transverse components, which are at right angles, then $P = \mathcal{E}\mathcal{H}$ where P is in the longintudinal direction so that:

$$P = (\mathcal{E}^+ + \mathcal{E}^-)\ \frac{(\mathcal{E}^+ - \mathcal{E}^-)}{Z_w}$$

$$P = \frac{(\mathcal{E}^+)^2}{Z_w} - \frac{(\mathcal{E}^-)^2}{Z_w}$$

or

$$P = \mathcal{E}^+ H^+ - \mathcal{E}^- H^-$$

$$P = P^+ - P^- \qquad \ldots\ldots \quad 2.5$$

which is the desired result.

2:2 Reflection Coefficient (Γ)

The reflection coefficient (Γ) is defined as the complex ratio of the reflected to incident wave at any specified point along the axis of propagation (Fig 2.1).

On the basis of this definition, it follows that there are two alternative ratios which can be used, because the coefficient may be expressed either in terms of the electric or magnetic field. The former definition yields:

$$\Gamma_E = \frac{E^-}{E^+} \qquad \ldots\ldots \quad 2.6$$

where Γ_E = Electric Reflection Coefficient and as before
E^+ = Incident Electric Field
E^- = Reflected Electric Field.

The latter definition yields:

$$\Gamma_H = \frac{H^-}{H^+} \qquad \ldots\ldots \quad 2.7$$

where Γ_H = Magnetic Reflection Coefficient and as before
H^+ = Incident Magnetic Field
H^- = Reflected Magnetic Field

Either of the definitions of 2.6 or 2.7 may be used. However, as it is more convenient to measure the electric field the definition of 2.6 will be used throughout this Thesis. Henceforth, all reflection coefficients will be

assumed to be with respect to the electric field unless otherwise stated.

At this stage, it would be best to refer to Fig 2.2 once again. If E_o^+ is the incident wave at 0, then at any point P, distant "ℓ" to the right of 0 in the direction of propagation, the electric field E_p^+ is given by:

$$E_p^+ = E_o^+ e^{-p\ell} \quad \ldots\ldots \quad 2.8$$

where the propagation constant $(p) = \alpha + j\beta$ and
α = the attenuation constant (Nepers/Metres) and
β = the phase constant (Radians/Metre).

Similarly if E_o^- is the value of the reflected wave at 0, then E_p^- at the point P is given by:

$$E_p^- = E_o^- e^{+p\ell} \quad \ldots\ldots \quad 2.9$$

The nomenclature "incident" and "reflected" assumes the wave source to be somewhere to the left of "0" and the point of reflection somewhere to the right of P. Equation 2.8 is merely a mathematical statement of the well-known fact that the field at P suffers attenuation by a factor $e^{-\alpha\ell}$ and lags $\beta\ell$ radians on the field at 0 for an incident wave. Equation 2.9 is merely a mathematical statement of the same argument for a reflected wave.

Similarly for the magnetic field, we have:

$$H_p^+ = H_o^+ e^{-p\ell} \quad \ldots\ldots \quad 2.10$$

$$H_p^- = H_o^- e^{+p\ell} \quad \ldots\ldots \quad 2.11$$

Hence the resultant transverse, electric and magnetic fields at any point P may be expressed in terms of the values of their forward and backward travelling components at the

point O, thus:

$$E_p = E_o^+ e^{-pl} + E_o^- e^{+pl} \quad \ldots\ldots \quad 2.12$$

$$H_p = H_o^+ e^{-pl} + H_o^- e^{+pl} \quad \ldots\ldots \quad 2.13$$

Defining $$\Gamma = \frac{E_o^-}{E_o^+} \quad \ldots\ldots \quad 2.14$$

and $$\Gamma_H = \frac{H_o^-}{H_o^+} \quad \ldots\ldots \quad 2.15$$

then from equations 2.1(a) and 2.1(b), $\Gamma = -\Gamma_H$ 2.16

Division of equation 2.12 by 2.13 and using the substitutions of 2.14, 2.15 and 2.16 gives:

$$\frac{E_p}{H_p} = \frac{E_o^+ (1 + \Gamma e^{2pl})}{H_o^+ (1 - \Gamma e^{2pl})} \quad \ldots\ldots \quad 2.17$$

If Schelkunoff's definition in equation 2.1 is substituted:

$$Z_L = Z_w \frac{1 + \Gamma e^{+2pl}}{1 - \Gamma e^{+2pl}} \quad \ldots\ldots \quad 2.18$$

The above statement is general. Z_L signifies the wave impedance at any arbitrary point point P, situated a distance "l" from the reference point O (Fig 2.2) Z_w is the characteristic wave impedance of the line.

If constraints are placed on the line length to make $l = 0$, equation 2.18 reduces to another well-known expression:

$$Z_L = \frac{Z_w(1 + \Gamma)}{(1 - \Gamma)} \quad \ldots\ldots \quad 2.18(a)$$

or

$$\Gamma = \frac{Z_L - Z_W}{Z_L + Z_W} \qquad \ldots\ldots \quad 2.19$$

Equation 2.19 is the very important relationship which forms the basis of these measurements. It follows that if the characteristic impedance Z_W can be accurately defined then measuring the complex quantity Γ, will allow Z_L to be evaluated.

In practice, it is not always possible to measure a reflection coefficient, Γ_o directly at the point O (Fig 2.3) and in most cases, it is customary to place the measuring device at any point O" separated from the measuring plane AB by a distance ℓ' . The relationship between the desired reflection coefficient (Γ_o) at point O and that (Γ) measured at point O" will be derived.

Figure 2.3
Relationships between Reflection Coefficients

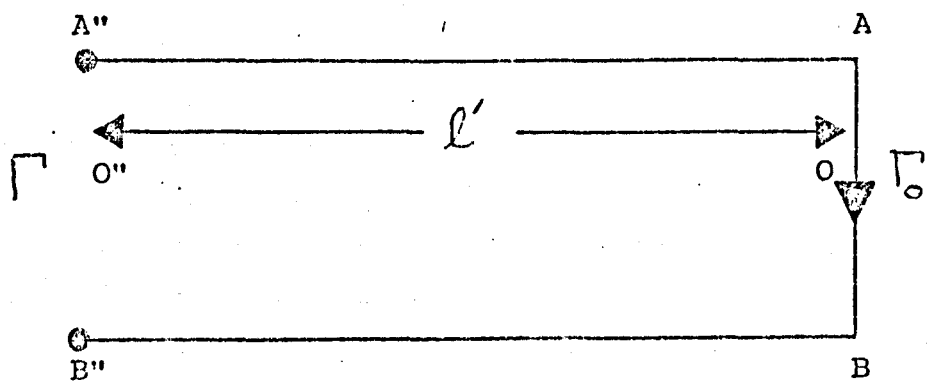

Let E_o^+ and E_o^- represent the incident and reflected waves at AB. Let $E_o^{+''}$ and $E_o^{-''}$ represent the incident and reflected waves respectively on the plane A" B" of Fig 2.3. Using the basic equations of 2.8, 2.9 and 2.14 it follows that:

$$\Gamma_o = \frac{E_o^-}{E_o^+} = \frac{E_o^{-''} e^{p\ell'}}{E_o^{+''} e^{-p\ell'}} = \Gamma e^{2p\ell'} \qquad \ldots\ldots \quad 2.20$$

or

$$\Gamma = \Gamma_o e^{-2p\ell'} \qquad \ldots\ldots \quad 2.21$$

Being complex, the reflection coefficients Γ and Γ_o may be written as $|\Gamma|e^{j\phi}$ and $|\Gamma_o|e^{j\phi_o}$ respectively where ϕ and ϕ_o represent the angle in radians. Substitution in 2.21 results in:

$$|\Gamma|e^{j\phi} = |\Gamma_o|e^{j\phi_o}e^{-2\rho\ell'} = |\Gamma_o|e^{j\phi_o}\, e^{-2\alpha\ell'}\, e^{-j2\beta\ell'}$$

$$|\Gamma|e^{j\phi} = \left[\, |\Gamma_o|e^{-2\alpha\ell'}\right] e^{j(\phi_o - 2\beta\ell')} \qquad \ldots\ldots \qquad 2.22$$

From which it is easily seen that the modulus of the measured reflection coefficient is attenuated by a factor $2\alpha\ell'$ from the true modulus, whilst the angle of the measured reflection coefficient is modified by the difference $2\beta\ell'$ from the true angle.

2.3 Directional Couplers

Many papers (Ref 2.4, 2.5, 2.6, 2.13, 2.14, 2.15) have been published on directional couplers. Harvey (Ref 2.16) gives an extensive list of references. In its basic form (Fig 2.4) a single directional coupler is essentially a 4 port network with one port ideally matched. It has been shown (Ref 2.15 that such a network manifests directional properties. For example, if Port 3' is terminated, then it is theoretically possible to arrange for Port 4 to sample power travelling in the direction from Port 1 to Port 2' but not vice-versa.

Figure 2.4

Single and Dual Directional Couplers

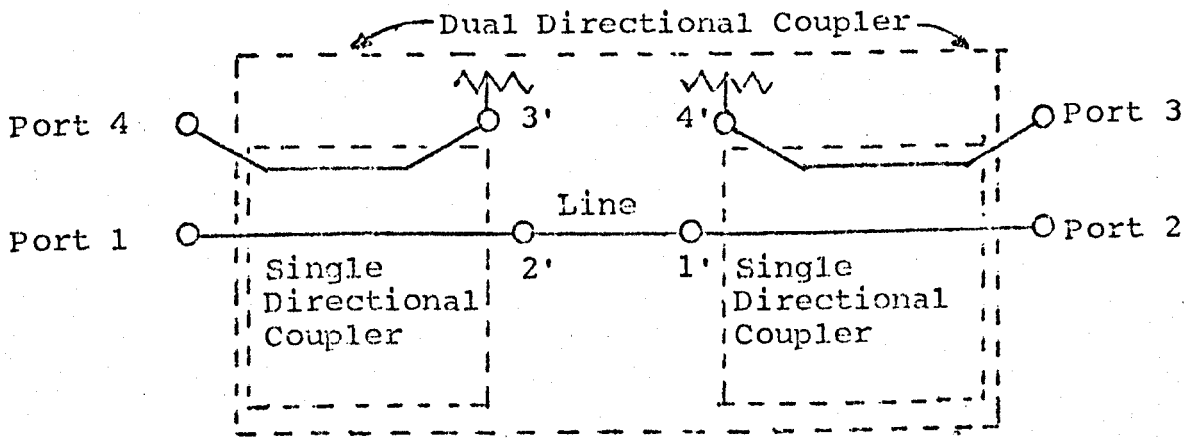

In a practical reflectometer systems, two directional couplers are required, one to sample the incident wave and the other to sample the reflected wave. The use of two separate couplers joined by a connecting line is undesirable because of mis-matches between the units. Difficulty is experienced with attaining amplitude and phase tracking. To alleviate these undesirable effects, manufacturers tend to offer dual directional couplers units for which claims are made that the internal couplers are matched for amplitude and phase.

A dual directional coupler may be analysed as a four port network (Fig 2.4) with the general scattering matrix of equation 2.23.

$$\begin{bmatrix} b_1 \\ b_2 \\ b_3 \\ b_4 \end{bmatrix} = \begin{bmatrix} S_{11} & S_{12} & S_{13} & S_{14} \\ S_{21} & S_{22} & S_{23} & S_{24} \\ S_{31} & S_{32} & S_{33} & S_{34} \\ S41 & S_{24} & S_{43} & S_{44} \end{bmatrix} \begin{bmatrix} a_1 \\ a_2 \\ a_3 \\ a4 \end{bmatrix} \quad \ldots\ldots \quad 2.23$$

All incident waves (a_n) and emergent waves (b_n) are identified by a subscript where "n" denotes the port number. In the diagram of figure 2.4(a), port 1 is the main input port (i.e. connected to the signal source). Port 2 is the main output port. Ports 3 and 4 are intended for sampling the reflected and incident waves respectively. M_3 and M_4 are the indicated sampled reflected and incident powers with the incorporated conversion constants.

Figure 2.4(a)

Signal Flow Graph of a Dual Directional Coupler

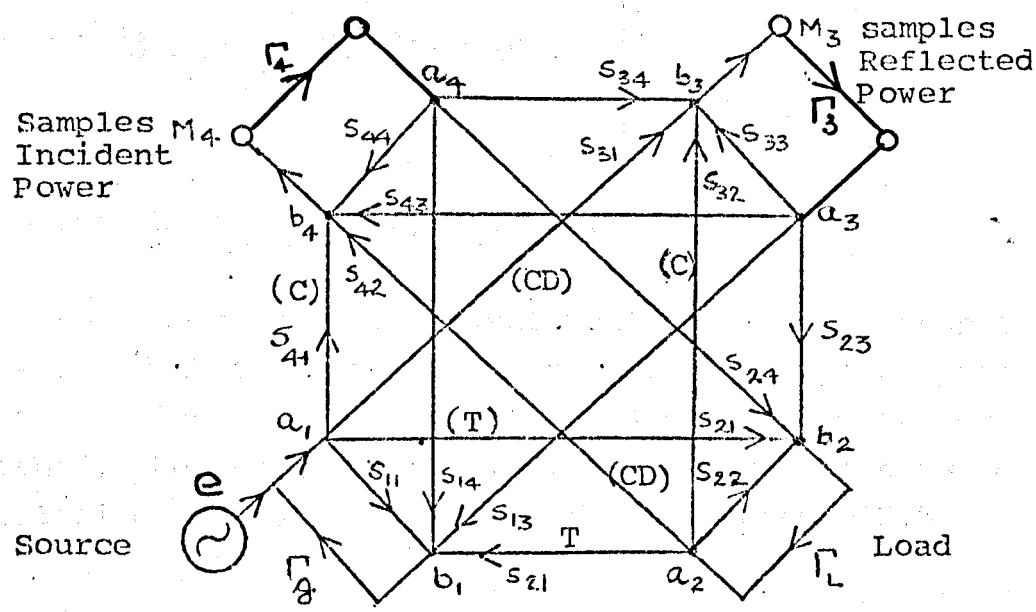

C = Desired coupling paths
CD = Back coupling paths

The Forward Coupling Path (C), is the desired signal path from one port to another. These are S_{41} for port 1 to port 4 and S_{32} for port 2 to 3.

The Back Coupling Paths (CD), are the undesired signal paths to a particular port. The paths are S_{42} for port 4 and S_{31} for port 3.

The Transmission Paths (T), are the main signal propagation paths. These are S_{21} and S_{12} for the main signal paths between ports 1 and 2.

$$\text{Coupling Factor (CF)} = 10 \log_{10} \left| \frac{\text{Incident Power to Port 1}}{\text{Incident Power to Port 4}} \right| \quad \ldots\ldots \quad 2.24$$

$$\text{Directivity Factor (DF)} = 10 \log \left| \frac{\text{Power to Port 4}}{\text{Power to Port 3}} \right| \quad \ldots\ldots \quad 2.25$$

when port 2 is perfectly matched.

For the case of the ideal dual directional coupler, it is assumed that there are no undesirable coupling paths and that the signal source, coupler and detectors are perfectly matched. For such a system, Figure 2.4 may be considerably simplified and reduced to that shown in Figure 2.5 where

$$b_4 = S_{41} a_1; \qquad b_3 = S_{21} S_{32} \Gamma_L a_1$$

and

$$\frac{b_3}{b_4} = \frac{S_{21} S_{32} \Gamma_L}{S_{41}} \quad \ldots\ldots \quad 2.26$$

Note: $\frac{b_3}{b_4}$ is independent of a_1

Figure 2.5

Signal Flow Graph of the Ideal Dual Directional Coupler

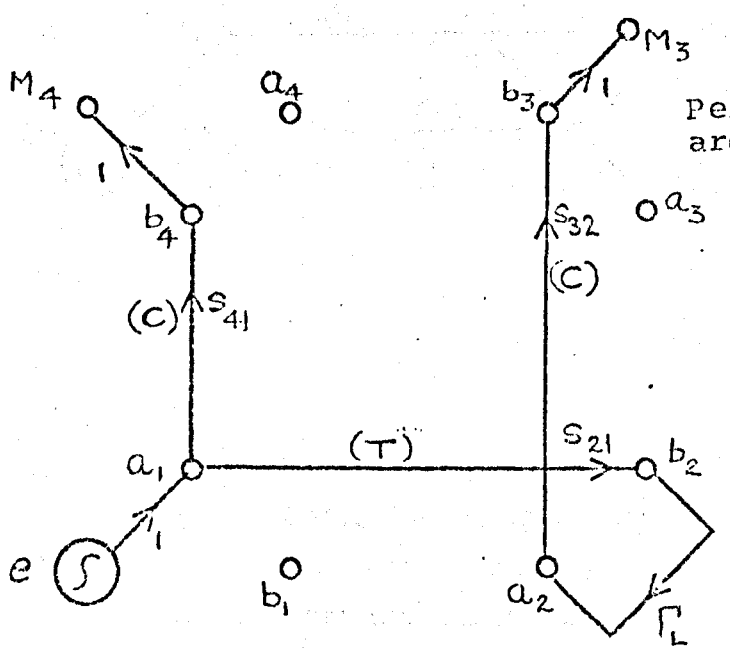

Equation 2.26 states that the ratio of

$$\frac{b_3}{b_4} = \frac{\text{Sampled Reflected Power}}{\text{Sampled Incident Power}}$$ is directly proportional to the unknown reflection coefficient of the load. The constant of proportionality is the factor $\frac{S_{21}\,S_{32}}{S_{41}}$.

For the more practical case of finite coupler directivity and reflection coefficient, let us first assume that the detectors are perfectly matched, i.e., no power is incident on a_3 and a_4 Figure 2.4 may then be reduced to Fig 2.6.

Figure 2.6
The Dual Directional Coupler with Perfectly Matched Detectors

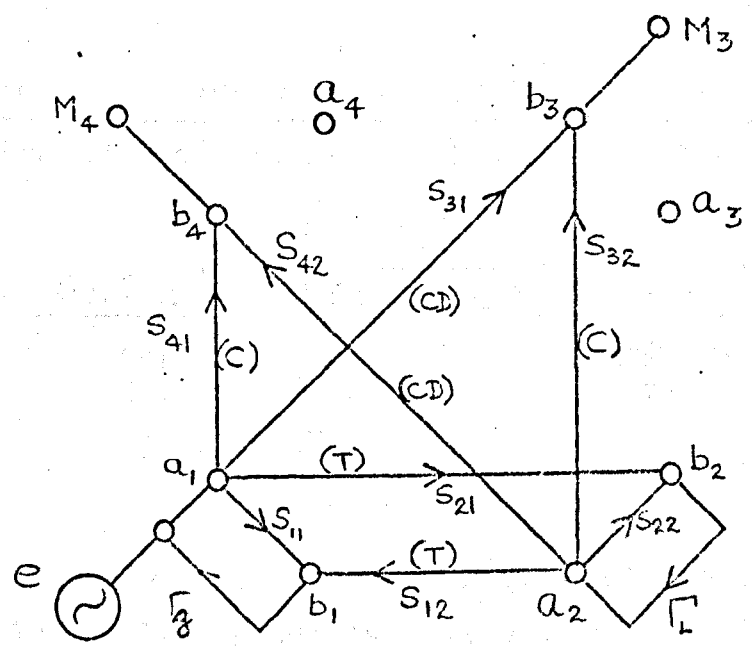

Legend:

Direct Transmission Path (T)
Back Coupling Path (CD)
Coupler VSWR
Forward Coupling Path (C)

By inspection of the signal flow graph, it is seen that

$$a_2 = \Gamma_L (S_{21} a_1 + S_{22} a_2) \text{ or } a_2 = \frac{S_{21}\Gamma_L a_1}{1 - S_{22}\Gamma_L}$$

$$b_3 = S_{31} a_1 + S_{32} a_2$$

$$\therefore \quad b_3 = \left(S_{31} + \frac{S_{21} S_{32} \Gamma_L}{1 - S_{22}\Gamma_L}\right) a_1$$

$$b_4 = S_{41} a_1 + S_{42} a_2$$

$$\therefore b_4 = a_1 \left(S_{41} + \frac{S_{21} S_{42} \Gamma_L}{1 - S_{22}\Gamma_L}\right)$$

Hence,

$$\frac{\text{Indicated Reflected Power (M3)}}{\text{Indicated Incident Power (M4)}} = \frac{b_3}{b_4}$$

$$\frac{b_3}{b_4} = \frac{S_{21} S_{32} \Gamma_L}{S_{41}} \left[\frac{\frac{1}{(1 - S_{22}\Gamma_L)} + \frac{S_{31}}{S_{32}} \times \frac{1}{S_{21}\Gamma_L}}{1 + \frac{S_{42} S_{21}}{S_{41}} \frac{\Gamma_L}{(1 - S_{22}\Gamma_L)}}\right] \quad \ldots\ldots \quad 2.27$$

Comparison of the ideal case (equation 2.26) and the more practical case (equation 2.27) show that the latter differs by the ratio of the error terms within the brackets. This leads to the conclusions that for accurate measurement, S_{22}, S_{31} and S_{42} should be zero. These are partially met by making the main line VSWR (S_{22}) as low as possible and by careful spacing of the two couplers, usually a quarter wavelength apart. This latter condition is not easily met in wide band couplers.

The complexity of the analysis of the dual directional coupler increases for the really practical case where it can no longer be assumed that the detectors are perfectly matched i.e., power is incident on a_3 and a_4 within the system.

Consider again the signal flow graph of figure 2.4; by inspection,

$$\begin{bmatrix} a_1 \\ a_2 \\ a_3 \\ a_4 \end{bmatrix} = \begin{bmatrix} e + \Gamma_g b_1 \\ \Gamma_L b_2 \\ \Gamma_3 b_3 \\ \Gamma_4 b_4 \end{bmatrix} = \begin{bmatrix} e & 0 & 0 & 0 \\ 0 & 0 & 0 & 0 \\ 0 & 0 & 0 & 0 \\ 0 & 0 & 0 & 0 \end{bmatrix} + \begin{bmatrix} \Gamma_g b_1 & 0 & 0 & 0 \\ 0 & \Gamma_L b_2 & 0 & 0 \\ 0 & 0 & \Gamma_3 b_3 & 0 \\ 0 & 0 & 0 & \Gamma_4 b_4 \end{bmatrix}$$

..... 2.28

Substitution of 2.28 into 2.23 gives:

$$\begin{bmatrix} b_1 \\ b_2 \\ b_3 \\ b_4 \end{bmatrix} = \begin{bmatrix} S_{11} & S_{12} & S_{13} & S_{14} \\ S_{21} & S_{22} & S_{23} & S_{24} \\ S_{31} & S_{32} & S_{33} & S_{34} \\ S_{41} & S_{42} & S_{43} & S_{44} \end{bmatrix} \begin{bmatrix} e & 0 & 0 & 0 \\ 0 & 0 & 0 & 0 \\ 0 & 0 & 0 & 0 \\ 0 & 0 & 0 & 0 \end{bmatrix} + \begin{bmatrix} S_{11} & S_{12} & S_{13} & S_{14} \\ S_{21} & S_{22} & S_{23} & S_{24} \\ S_{31} & S_{32} & S_{33} & S_{34} \\ S_{41} & S_{42} & S_{43} & S_{44} \end{bmatrix} \begin{bmatrix} \Gamma_g b_1 & 0 & 0 & 0 \\ 0 & \Gamma_L b_2 & 0 & 0 \\ 0 & 0 & \Gamma_3 b_3 & 0 \\ 0 & 0 & 0 & \Gamma_4 b_4 \end{bmatrix}$$

$$\begin{bmatrix} 1 & 0 & 0 & 0 \\ 0 & 1 & 0 & 0 \\ 0 & 0 & 1 & 0 \\ 0 & 0 & 0 & 1 \end{bmatrix} \begin{bmatrix} b_1 \\ b_2 \\ b_3 \\ b_4 \end{bmatrix} = \begin{bmatrix} S_{11}e \\ S_{21}e \\ S_{31}e \\ S_{41}e \end{bmatrix} + \begin{bmatrix} S_{11}\Gamma_g & S_{12}\Gamma_L & S_{13}\Gamma_3 & S_{14}\Gamma_4 \\ S_{21}\Gamma_g & S_{22}\Gamma_L & S_{23}\Gamma_3 & S_{24}\Gamma_4 \\ S_{31}\Gamma_g & S_{32}\Gamma_L & S_{33}\Gamma_3 & S_{34}\Gamma_4 \\ S_{41}\Gamma_g & S_{42}\Gamma_L & S_{43}\Gamma_3 & S_{44}\Gamma_4 \end{bmatrix} \begin{bmatrix} b_1 \\ b_2 \\ b_3 \\ b_4 \end{bmatrix}$$

$$-\begin{bmatrix} S_{11}e \\ S_{21}e \\ S_{31}e \\ S_{41}e \end{bmatrix} = \begin{bmatrix} (S_{11}\Gamma_g - 1) & S_{12}\Gamma_L & S_{13}\Gamma_3 & S_{14}\Gamma_4 \\ S_{21}\Gamma_g & S_{22}\Gamma_L - 1 & S_{23}\Gamma_3 & S_{24}\Gamma_4 \\ S_{31}\Gamma_g & S_{32}\Gamma_L & S_{33}\Gamma_3 - 1 & S_{34}\Gamma_4 \\ S_{41}\Gamma_g & S_{42}\Gamma_L & S_{43}\Gamma_3 & S_{44}\Gamma_4 - 1 \end{bmatrix} \begin{bmatrix} b_1 \\ b_2 \\ b_3 \\ b_4 \end{bmatrix}$$

..... 2.29

For the ratio b_3/b_4, using Cramers rule:

$$\frac{b_3}{b_4} = \frac{-e\begin{vmatrix} (S_{11}\Gamma_g-1) & S_{12}\Gamma_L & S_{11} & S_{14}\Gamma_4 \\ S_{21}\Gamma_g & (S_{22}\Gamma_L-1) & S_{21} & S_{24}\Gamma_4 \\ S_{31}\Gamma_g & S_{32}\Gamma_L & S_{31} & S_{34}\Gamma_4 \\ S_{41}\Gamma_g & S_{42}\Gamma_L & S_{41} & (S_{44}\Gamma_4-1) \end{vmatrix}}{-e\begin{vmatrix} (S_{11}\Gamma_g-1) & S_{12}\Gamma_L & S_{13}\Gamma_3 & S_{11} \\ S_{21}\Gamma_g & (S_{22}\Gamma_L-1) & S_{23}\Gamma_3 & S_{21} \\ S_{31}\Gamma_g & S_{32}\Gamma_L & (S_{33}\Gamma_3-1) & S_{31} \\ S_{41}\Gamma_g & S_{42}\Gamma_L & S_{43}\Gamma_3 & S_{41} \end{vmatrix}}$$

Simplification may be obtained by multiplying the 3rd and 4th columns respectively in the numerator and denominator by Γ_g and substracting them from their respective column 1 to yield:

$$\frac{b_3}{b_4} = \frac{\begin{vmatrix} (S_{22}\Gamma_L-1) & S_{21} & S_{24}\Gamma_4 \\ S_{32}\Gamma_L & S_{31} & S_{34}\Gamma_4 \\ S_{42}\Gamma_L & S_{41} & (S_{44}\Gamma_4-1) \end{vmatrix}}{\begin{vmatrix} (S_{22}\Gamma_L-1) & S_{23}\Gamma_3 & S_{21} \\ S_{32}\Gamma_L & (S_{33}\Gamma_3-1) & S_{31} \\ S_{42}\Gamma_L & S_{43}\Gamma_3 & S_{41} \end{vmatrix}} \quad \ldots\ldots \quad 2.30$$

which when expanded will result in:

$$\frac{b_3}{b_4} = \frac{(S_{22}\Gamma_L-1)\left[\Gamma_4(S_{31}S_{44}-S_{34}S_{41})-S_{31}\right]+S_{21}\Gamma_L\left[\Gamma_4(S_{34}S_{42}-S_{32}S_{44})+S_{32}\right]+S_{24}\Gamma_4\Gamma_L\left[S_{32}S_{41}-S_{31}S_{42}\right]}{(S_{22}\Gamma_L-1)\left[\Gamma_3(S_{33}S_{41}-S_{31}S_{43})-S_{41}\right]+S_{21}\Gamma_L\left[\Gamma_3(S_{32}S_{43}-S_{33}S_{42})-S_{42}\right]+S_{23}\Gamma_3\Gamma_L\left[S_{31}S_{42}-S_{32}S_{41}\right]}$$

$\ldots\ldots$ 2.31

Equations 2.26 and 2.27 may also be obtained from equation 2.31 by making the previous suppositions. As it stands, the equation does not present a very clear picture of what is happening. However, by expanding the expression and by judicious collection of the terms, some conclusions will be found.

Should be +

$$\frac{b_3}{b_4} = \frac{(S_{22}\Gamma_L - 1)\left[\Gamma_4(S_{31}S_{44} - S_{34}S_{41})\right] - S_{22}S_{31}\Gamma_L + S_{31} + S_{21}S_{32}\Gamma_L\left[\Gamma_4(S_{34}S_{42} - S_{32}S_{44})/S_{32} - 1\right] + S_{24}\Gamma_4\Gamma_L\left[S_{32}S_{41} - S_{31}S_{42}\right]}{S_{22}S_{33}S_{41}\Gamma_3\Gamma_L - S_{33}S_{41}\Gamma_3 - (S_{22}\Gamma_L - 1)S_{31}S_{43}\Gamma_3 - S_{22}S_{41}\Gamma_L + S_{41} + S_{21}\Gamma_L\left[\Gamma_3(S_{32}S_{43} - S_{33}S_{42}) - S_{42}\right] + S_{23}S_{31}S_{42}\Gamma_3\Gamma_L - S_{23}S_{32}S_{41}\Gamma_3\Gamma_L}$$

$$= \frac{S_{21}S_{32}\Gamma_L\left[1 + \frac{S_{31}}{S_{21}S_{32}\Gamma_L} - S_{44}\Gamma_4 + \frac{S_{34}S_{42}\Gamma_4}{S_{32}} - \frac{S_{22}S_{31}}{S_{21}S_{32}} + \frac{S_{22}S_{31}S_{44}\Gamma_4}{S_{21}S_{32}} - \frac{S_{31}S_{44}\Gamma_4}{S_{21}S_{32}\Gamma_L} - \frac{S_{22}S_{34}S_{41}\Gamma_4}{S_{21}S_{32}} + \frac{S_{34}S_{41}\Gamma_4}{S_{21}S_{32}\Gamma_L} + \frac{S_{24}S_{41}\Gamma_4}{S_{21}} - \frac{S_{24}S_{31}S_{42}\Gamma_4}{S_{21}S_{32}}\right]}{S_{41}\left[1 - S_{22}\Gamma_L - S_{33}\Gamma_3 + S_{22}S_{33}\Gamma_3\Gamma_L - S_{23}S_{32}\Gamma_3\Gamma_L + \frac{S_{21}S_{32}S_{43}\Gamma_3\Gamma_L}{S_{41}} - \frac{S_{21}S_{33}S_{42}\Gamma_3\Gamma_L}{S_{41}} - \frac{S_{21}S_{42}\Gamma_L}{S_{41}} + \frac{S_{23}S_{31}S_{42}\Gamma_3\Gamma_L}{S_{41}} - \frac{S_{22}S_{31}S_{43}\Gamma_3\Gamma_L}{S_{41}} + \frac{S_{31}S_{43}\Gamma_3}{S_{41}}\right]}$$

$$\frac{b_3}{b_4} = \frac{S_{21}S_{32}\Gamma_L}{S_{41}} \times \frac{\left[1 + \Gamma_4\left\{\frac{S_{22}S_{31}S_{44}}{S_{21}S_{32}} - \frac{S_{22}S_{34}S_{41}}{S_{21}S_{32}} - \frac{S_{24}S_{31}S_{42}}{S_{21}S_{32}} + \frac{S_{24}S_{41}}{S_{21}} - \frac{S_{31}S_{44}}{S_{21}S_{32}\Gamma_L} + \frac{S_{34}S_{41}}{S_{21}S_{32}\Gamma_L} + \frac{S_{34}S_{42}}{S_{32}} - S_{44}\right\} - \frac{S_{22}S_{31}}{S_{21}S_{32}} + \frac{S_{31}}{S_{21}S_{32}\Gamma_L}\right]}{\left[1 + \Gamma_3\left\{\frac{S_{21}S_{32}S_{43}\Gamma_L}{S_{41}} - \frac{S_{21}S_{33}S_{42}\Gamma_L}{S_{41}} + S_{22}S_{33}\Gamma_L - \frac{S_{22}S_{31}S_{43}\Gamma_L}{S_{41}} + \frac{S_{23}S_{31}S_{42}\Gamma_L}{S_{41}} - S_{23}S_{32}\Gamma_L + \frac{S_{31}S_{43}}{S_{41}} - S_{33}\right\} - S_{22}\Gamma_L - \frac{S_{21}S_{42}\Gamma_L}{S_{41}}\right]}$$

..... 2.32

Note: 2.32 can also be easily resolved to 2.26 and 2.27.

Equation 2.32 may also be written in the form:

$$\frac{b_3}{b_4} = \frac{\{S_{21}S_{32} - S_{21}S_{32}S_{44}\Gamma_4 + S_{21}S_{34}S_{42}\Gamma_4 - S_{22}S_{31} + S_{22}S_{31}S_{44}\Gamma_4 - S_{22}S_{34}S_{41}\Gamma_4 + S_{24}S_{32}S_{41}\Gamma_4 - S_{24}S_{31}S_{42}\Gamma_4\}\Gamma_L + \{S_{31} - S_{31}S_{44}\Gamma_4 + S_{34}S_{41}\Gamma_4\}}{\{-S_{22}S_{41} + S_{22}S_{33}S_{41}\Gamma_3 - S_{23}S_{32}S_{41}\Gamma_3 + S_{21}S_{32}S_{43}\Gamma_3 - S_{21}S_{33}S_{42}\Gamma_3 - S_{21}S_{42} + S_{23}S_{31}S_{42}\Gamma_3 - S_{22}S_{31}S_{43}\Gamma_3\}\Gamma_L + \{S_{41} - S_{33}S_{41}\Gamma_3 + S_{31}S_{43}\Gamma_3\}}$$

Let $\frac{b_3}{b_4} = \rho_m$ i.e. the measured reflection coefficient, then

$$\rho_m = \frac{A\Gamma_L + B}{C\Gamma_L + D} \qquad \ldots\ldots \quad 2.33$$

Where

$$A = \{S_{21}S_{32} - S_{21}S_{32}S_{44}\Gamma_4 + S_{21}S_{24}S_{42}\Gamma_4 - S_{22}S_{31} + S_{22}S_{31}S_{44}\Gamma_4 - S_{22}S_{34}S_{41}\Gamma_4 + S_{24}S_{32}S_{41}\Gamma_4 - S_{24}S_{31}\Gamma_4\} \qquad \ldots\ldots \quad 2.33(a)$$

$$B = \{S_{31} - S_{31}S_{44}\Gamma_4 + S_{34}S_{41}\Gamma_4\} \qquad \ldots\ldots \quad 2.33(b)$$

$$C = \{-S_{22}S_{41} + S_{22}S_{33}S_{41}\Gamma_3 - S_{23}S_{32}S_{41}\Gamma_3 + S_{21}S_{32}S_{43}\Gamma_3 - S_{21}S_{33}S_{42}\Gamma_3 - S_{21}S_{42} + S_{23}S_{31}S_{42}\Gamma_3 - S_{22}S_{31}S_{43}\Gamma_3\} \qquad \ldots\ldots \quad 2.33(c)$$

$$D = \{S_{41} - S_{33}S_{41}\Gamma_3 + S_{31}S_{43}\Gamma_3\} \qquad \ldots\ldots \quad 2.33(d)$$

Equation 2.33 is vitally important because:

(1) It shows that the measured reflection coefficient " ρ_m " is related to the true Γ by a bilinear transformation (Appendix 11.1).

(2) The constants of a passive bilinear transformation, A, B, C, D, may be obtained by three measurements (Ref 2.17). It is unnecessary to know the individual 'S' parameters but the scattering parameters may be calculated by use of Appendix 11.2.

(3) If the constants A, B, C, D of the bilinear transformation are known then Γ may be calculated. (Fig 2.7).

(4) Item 3 is of the utmost importance for it clearly demonstrates that an imperfect dual directional coupler used with un-matched detectors may be used to yield the true measurement of a reflection coefficient if the constants of item 2 are known. This is the basis of Computer Corrected Measurements in One Port Reflection Measurements.

Figure 2.7
Basis of Error Correction

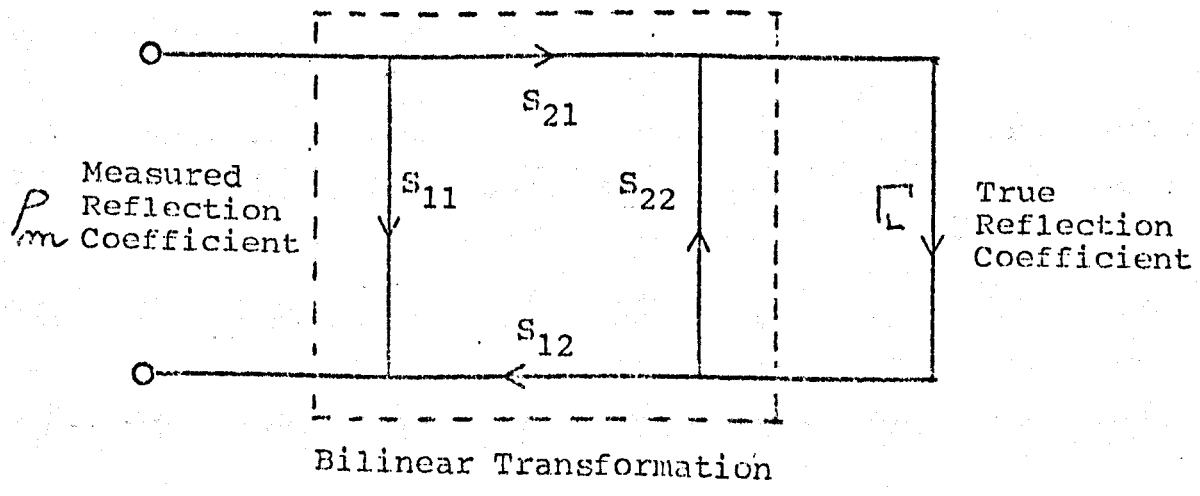

2:4 The Measurement Uncertainty of Incident and Reflected Power

In the foregoing section (2.3) analyses have been made of the process of identifying the incident and the reflected waves. This section expounds the problems associated with the measurement of the incident and reflected waves in coaxial couplers.

For these purposes, the incident (a_i) and the reflected (b_i) complex voltage wave amplitudes are normalized with respect to the real characteristic impedance (Z_o) * in the manner defined by Warner (Ref 2.8).

Hence:

$$\frac{|a_i|^2}{Z_o} = P_i \qquad \ldots\ldots \quad 2.34$$

$$\frac{|b_i|^2}{Z_o} = P_r \qquad \ldots\ldots \quad 2.35$$

where P_i = incident power
and P_r = reflected power

* The effect of conductor resistance on the characteristic impedance is negligible at frequencies above 2 GHz and for practical purposes, the line is assumed to have negligible loss.

Consider for example, the transfer of power from port 1 to port 4 (Figs 2.8 and 2.9) of a directional coupler in which the effects of the other ports are negligible.

Figure 2.8
Power Transfer through a 2 Port Network

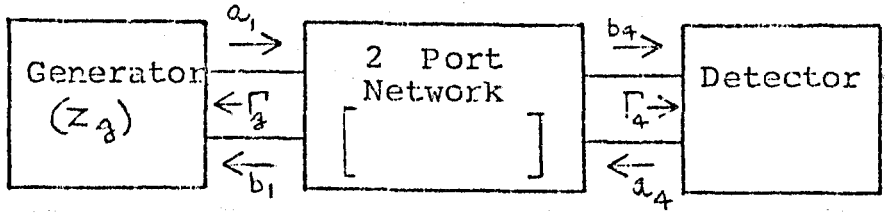

Let Γ_g and Γ_4 be the respective source and load reflection coefficients. Let the power dissipated in the load be denoted by P_1 when the generator and load are connected directly.

Let P_4 be the power dissipated in the load when the two port network shown in Figs 2.8 and 2.9 is connected between the generator and the load.

By definition, the power insertion loss (I.L.) of this 2 port network is given in decibels by:

$$I.L. = 10 \log \frac{P_1}{P_4} \qquad \ldots\ldots \quad 2.43$$

Figure 2.9
Signal Flow Graph for the Configuration shown in Figure 2.8

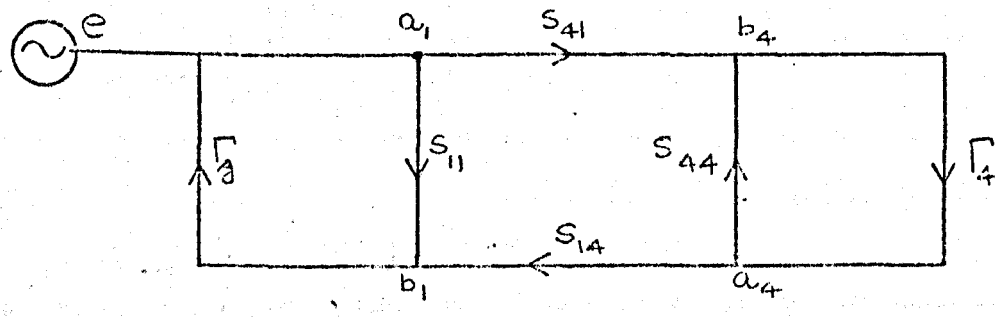

If the scattering coefficients of Figure 2.8 are used to define the two port network, the complex wave amplitudes are related as follows:

$$b_1 = S_{11} a_1 + S_{14} a_4$$

$$b_4 = S_{41} a_1 + S_{44} a_4$$

If Mason's non-touching loop rule (Refs 2.11 and 2.12) is used,

$$\frac{b_4}{e} = \frac{S_{41}}{1-(S_{11}\Gamma_g + S_{44}\Gamma_4 + S_{14}S_{41}\Gamma_g\Gamma_4) + S_{11}S_{44}\Gamma_g\Gamma_4} \quad \ldots\ldots \quad 2.44$$

The power absorbed by the detector (Z_4) is:

$$P_4 = \frac{|b_4|^2}{Z_0} - \frac{|a_4|^2}{Z_0} = \frac{|b_4|^2}{Z_0}\left(1-|\Gamma_4|^2\right) \quad \ldots\ldots \quad 2.45$$

If equation 2.44 is inserted into 2.45 and the denominator is re-arranged:

$$P_4 = \frac{|e|^2|S_{41}|^2(1-|\Gamma_4|^2)}{Z_0\left|(1-S_{11}\Gamma_g)(1-S_{44}\Gamma_4) - S_{14}S_{41}\Gamma_g\Gamma_4\right|^2} \quad \ldots\ldots \quad 2.46$$

The power P_1 , dissipated in Z_4 when the generator is connected directly to it can be found from 2.46 by letting $S_{11} = S_{44} = 0$ and $S_{14} = S_{41} = 1$.

Thus:

$$P_1 = \frac{|e|^2(1-|\Gamma_4|^2)}{Z_0|1-\Gamma_g\Gamma_4|^2} \quad \ldots\ldots \quad 2.47$$

Substitution of 2.46 and 2.47 in 2.43 would result in:

$$\text{I.L.} = 10\log_{10}\frac{\left|(1 - S_{11}\Gamma_g)(1 - S_{44}\Gamma_4) - S_{14}S_{41}\Gamma_g\Gamma_4\right|^2}{\left|S_{41}\right|^2\left|1 - \Gamma_g\Gamma_4\right|^2} \quad \ldots\ldots \quad 2.48$$

which can be simplified further to

$$\text{I.L.} = 20\log_{10}\frac{\left|(1 - S_{11}\Gamma_g)(1 - S_{44}\Gamma_4) - S_{14}S_{41}\Gamma_g\Gamma_4\right|}{\left|S_{41}\right|\left|1 - \Gamma_g\Gamma_4\right|} \quad \ldots\ldots \quad 2.49$$

In an ideal coupler, the insertion loss between port 1 and port 4 is really the coupling loss (CL) when the source Γ_g and detector Z_4 are matched. In such a case, equation 2.49 reduces to:

$$\text{CL} = 20\log_{10}\frac{1}{\left|S_{41}\right|} \quad \ldots\ldots \quad 2.50$$

which is the usual definition for coupling factor (Section 2:3)

Note also that in such a case, the insertion loss (I.L.) becomes equal to the attenuation (A) of the network.

Returning to equation 2.46, the measured power P_4 is dependent on many factors, most of which are controlled in the design of the coupler. However Γ_g is definitely not a feature of the coupler and its magnitude and phase will undoubtedly affect P_4 . Hence it becomes necessary to investigate the mis-match errors and power uncertainity which will arise.

To begin with, insertion loss (I.L.) is merely the sum of the coupling loss (CL) and the mis-match loss (M.L.) Using equations 2.49 and 2.50 results in:

$$M.L. = I.L. - CL$$

$$M.L. = 20 \log_{10} \frac{\left|(1 - S_{11}\Gamma_g)\ (1 - S_{44}\Gamma_4) - S_{14}S_{41}\Gamma_g\Gamma_4\right|}{\left|1 - \Gamma_g\Gamma_4\right|} \quad \ldots\ldots \quad 2.51$$

All of the independent variables in equation 2.51 are complex quantities and all phase relationships are possible. If both the magnitude and phase of all of these quantities are known, M.L. can be calculated precisely. However, if only their magnitudes are known, as is often the case, then the mis-match uncertainty is given by

$$M.L._{(LIMIT)} = 20 \log_{10} \left[\frac{1 \pm \left\{|S_{11}\Gamma_g| + |S_{44}\Gamma_4| + |S_{11}S_{44}\Gamma_g\Gamma_4| + |S_{14}S_{41}\Gamma_g\Gamma_4|\right.}{1 \mp |\Gamma_g\Gamma_4|}\right] \quad \ldots\ldots \quad 2.52$$

Since $P_4 = \frac{P_1}{\text{Insertion loss Ratio}}$ it follows that the absolute power measured by P_4 will be subject to a power uncertainty equal to the reciprocal of equation 2.52.

Hence, it can be concluded that although the source impedance does not affect the incident and reflected wave ratio (equation 2.32), it does affect the absolute value of power in the detectors and will introduce errors in the powers measured by the detectors, if their efficiencies are sensitive to varying power levels. If this error is to be minimised then Γ_g and Γ_4 should be made to approach the ideal case of zero.

A similar treatment may also be used for the power transfer from port 2 to port 3.

2:5 Conclusions

The principle of how an impedance or admittance may be measured using incident and reflected waves has been established in Sections 2:1 and 2:2. A thorough analysis of the dual directional coupler has been made to demonstrate how it measures the incident and reflected waves. The errors associated with the coupler have been derived and the basis for computer corrected systems have been shown in Section 2:3. The equations relating the uncertainty in the measurement of power in the measuring ports with respect to the source match has also been derived.

* * * * * * * * * *

2:6 References

2.1 Stager C, and Kartaschoff P, "Measurement Accuracy Hinges on Coupler Design" Microwave Journal, April 1977.

2.2 Schelkunoff S.A., "The Impedance Concept" B.S.T.J., 1938 17,7.

2.3 Schelkunoff S.A., "Impedance Concept in Waveguides" Quarterly Applied Mathematic, 1944. 2 ppl.

2.4 Hunton, J.K. and Pappas N.L. "The hp Microwave Reflectometers" Hewlett Packard J. Vol 6 pp 1-7 Sept-Oct 1954.

2.5 Engen G.F. and Beatty R.W., "Microwave Reflectometer Techniques" I.R.E. Trans on Microwave Theory and Techniques Vol MTT - 7 pp 351-355 July 1959.

2.6 Kuhn N, "Simplified Signal Flow Graph Analysis" Microwave Journal Nov 1963 pp 59-66.

2.7 Hewlett Packard Catalogue 1973 - pg 336. Directional Couplers 8690B Series.

2.8 Warner F, "Microwave Attenuation Measurement" I.E.E. Monograph Series 19 - Appendix 1 pp 270-272

2.9 Woods D, "Concepts of Voltage Waves, Current Waves and Power Waves in S Parameter Definitions and Measurements" Manuscript M32 (1st May 1972) which is deposited in the I.E.E. library, Savoy Place, London.

2.10 Woods D. "Concepts of Voltage Waves, Current Waves and Power Waves in S Parameter Definitions and Measurements". Proc I.E.E. Vol 119 No 12 Dec 1972.

2.11 Mason S.J., "Feedback Theory - Some Properties of Signal Flow Graphs" Proc I.R.E. Vol 41 pp 1144-1156 Sept 1953; also Mason S.J. "Feedback Theory - Further Properties of Signal Flow Graphs" Proc I.R.E. Vol 44 pp 920-926 July 1956.

2.12 Hunton J.K., "Analysis of Microwave Measurement Techniques by Means of Signal Flow Graphs" Trans I.R.E. Vol MTT-8 pp 206-212, March 1960.

2.13 Carson R, "High Frequency Amplifiers" John Wiley and Sons 1975 pp 165-167

2.14 Sucher M, and Fox, J. Handbook of Microwave Measurements. Volume II, John Wiles and Sons, London 1963.

2.15 Montgomery C.G., Dicke R.H. and Purcell E.M. "Principles of Microwave Circuits . McGraw Hill, New York 1948).

2.16 Harvey A.F., "Microwave Engineering" Academic Press, New York 1963.

2.17 Barlow H.M. and Cullen A.L., Microwave Measurements, Constable & Co., London 1950.

* * * * * * * * * * *

CHAPTER III

THE MEASURING SYSTEM (Hardware)

3:0 Introduction

The theory and associated theoretical problems relating to reflectometer measurement of immittances has been derived in Chapter II. This chapter will explain and justify the choice of equipment used in the measuring system.

The system described is the manual system originally used to verify the theoretical expressions. A later chapter will show how this system was modified to produce a fully automated computer corrected system.

3:1 Description of the Measuring System

A block diagram of the manual operating system is shown in Figure 3.1. A photograph of the equipment used is shown in Figure 3.2.

Figure 3.1

Block Diagram of Measuring System

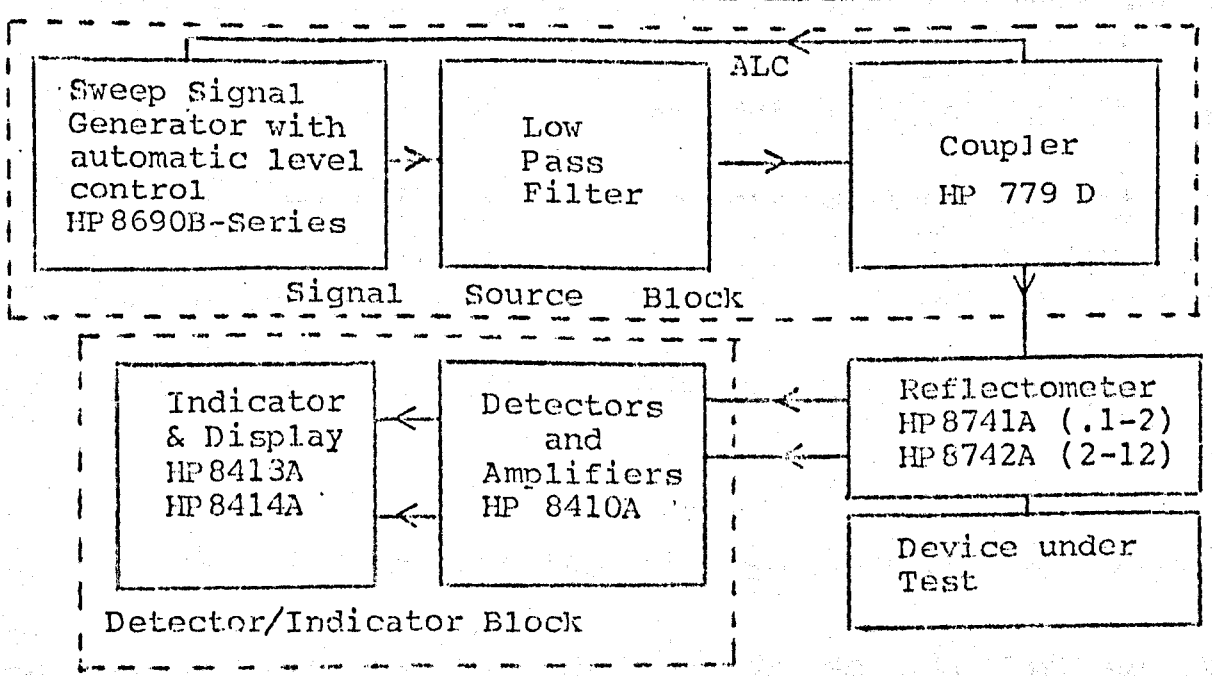

Figure 3.2

Photograph of Equipment Used

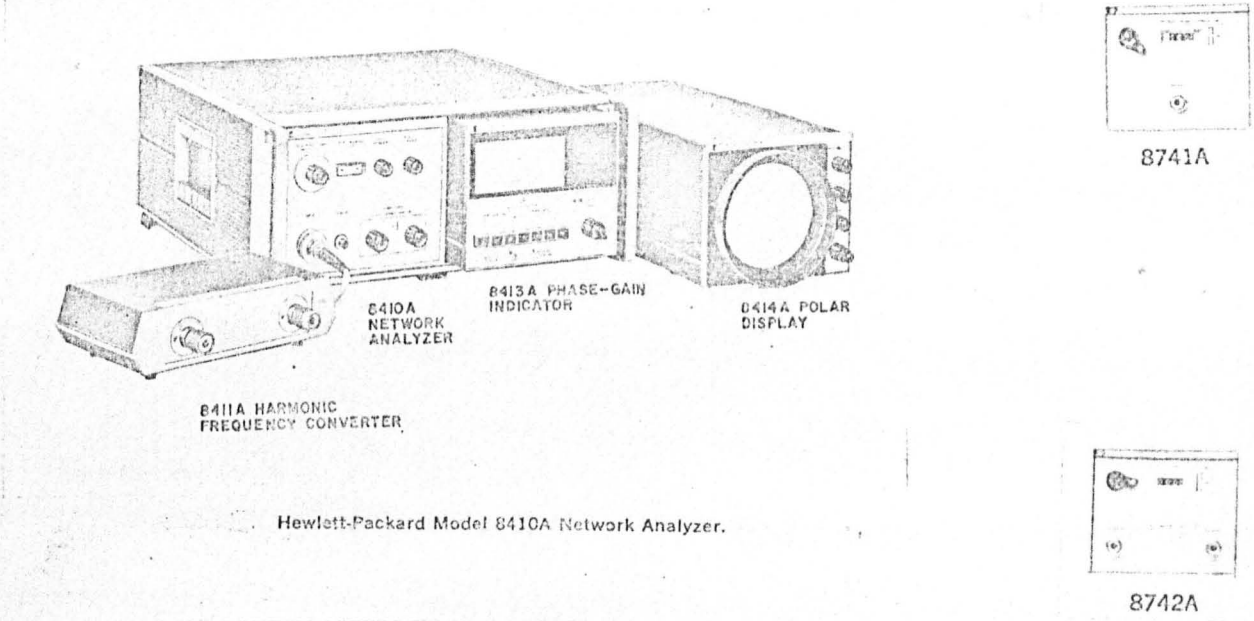

Hewlett-Packard Model 8410A Network Analyzer.

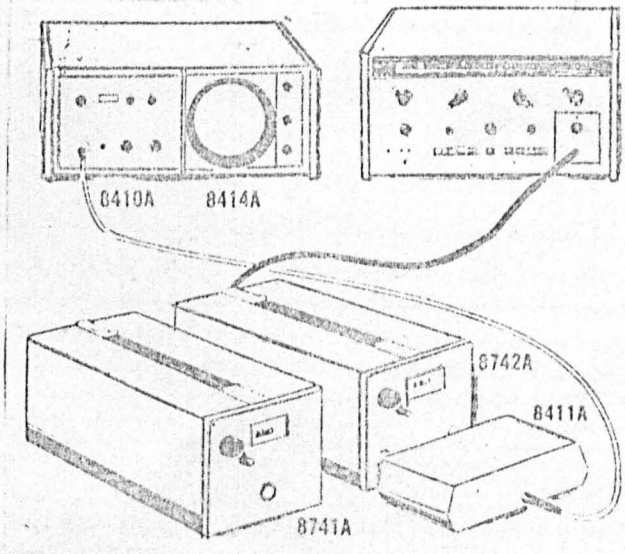

8414A Polar Display Plug-in module for 8410A mainframe. CRT polar display for direct readout of reflection coefficient and angle. Smith Chart overlays included for direct impedance or admittance readout.

8413A Phase-Gain Indicator (Optional) Alternate plug-in module for 8410A mainframe provides meter display of dB return loss and reflection coefficient angle.

8741A Reflection Test Unit 0.11 to 2.0 GHz Wideband reflectometer phase balanced for swept or spot frequency impedance tests below 2.0 GHz. Accepts RF input and provides connections for unknown test device and 8411A. Calibrated variable reference plane.

8742A Reflection Test Unit 2.0 to 12.4 GHz Wideband reflectometer phase balanced for impedance tests above 2.0 GHz. Calibrated variable reference plane.

The system may be divided into three basic blocks. A signal source block which generates the signal, a reflectometer block which recognises the incident and reflected waves from the device under test(DUT) and a Detector-Indicator system block which interprets the reflectometer outputs. Details of the three basic blocks will be discussed in Sections 3:2, 3:3 and 3:4 respectively.

In using the equipment the desired frequency is selected, and two calibration pieces, a sliding load ($|\Gamma| = 0$) and a short ($\Gamma = 1/180°$) are used to establish the limits of Γ_L in the measuring system. The device under test (DUT) or test piece (Z_L) is then measured to yield Γ_L .

The test piece impedance (Z_L) is then calculated by means of Equation 2.18, hence;

$$Z_L = \frac{Z_0(1+\Gamma_L)}{(1-\Gamma_L)}$$

or

$$Y_L = \frac{Y_0(1-\Gamma_L)}{(1+\Gamma_L)} \qquad \ldots\ldots \qquad 3.0$$

3:2 The Signal Source Block

The signal source block comprises a signal generator, a low pass filter and a directional coupler-detector system for automatic level control.

The basic requirements of the signal generator may be summed up as

(a) Good frequency stability.
(b) A good source match, i.e. low SWR.
(c) Sufficient output level (-20 dBm to +10 dBm)
(d) Low distortion, i.e., low harmonic content.
(e) An electronic means of keeping the signal output constant.

3:2.1 Frequency Stability

The signal source should be ideally a phase locked source with a spectral purity of such order that all harmonics are unmeasurable. In addition, there must be complete reliability and repeatibility in frequency selection. Microwave Synthesized Signal Generators (Ref. 3.1) approaching the idealized case are now available. However, these generators were not available and one had to manually phase lock the signal generator to a comb generator (Ref 3.2). This unit incorporates ten pre-selected crystals to stabilize an oscillator operating in the region of 15 MHz. This stable low frequency signal is used to drive a harmonic generator. By suitable choice of crystal switching, it would be possible to derive a harmonic to mix with the main R.F. signal to provide a D.C. control voltage to the signal generator to maintain the desired radio frequency constant.

In practice, it was found that phase lock could only be maintained for about 20 minutes because the drift in the R.F generator would be such that it would drift outside the "lock range" of the system. A slightly longer period of "phase lock" could be maintained if the R.F. generator was switched on for approximately two hours before measurement.

The main R.F. signal source used in all the measurements is the Hewlett Packard 8690B Series of Generators (Ref 3.4). These consist of a main control unit 8706A, a signal multiplexer 8705A, and a R.F. Unit Holder 8707A with three Grid or PIN levelled BWO R.F. Plug-ins. The plug-ins are 8699B (0.1-2GHz and 2-4GHz) 8693A (4-8GHz) and 8694A (8-12.4GHz).

Full details of the equipment is of course available in the respective handbooks but it can generally be said that these generators are capable of fixed or sweep frequency operation, using either manual or electronic controls. When levelled, the power output is greater than 25 mW ($\simeq$ 14 dBm). The spurious signals, i.e., harmonic and non harmonic signals for all the 3 plug-in units are 20 and 40 dB down on the desired signal respectively. The output port reflection coefficient is quoted as ≤ 0.25 (VSWR ≤ 1.67). Such a poor source match is definitely disadvantageous and is explained in Section 3:2.2.

3:2.2 The Importance of Source Match

The importance of source match can be easily visualized by a study of the incident, reflected and re-reflected waves in a typical measurement enviroment. Such a situation is depicted in Figure 3.3 where a dual directional coupler undergoing multiple reflections is used to measure a reflection coefficient. The dual directional coupler is driven from a generator with a reflection coefficient Γ_g which produces a wave (e) incident at a_1 and emergent at b_1 and it is used to measure the reflection coefficient Γ_L of an unknown device. To simplify matters in Figure 3.3 the effects of S_{11} and S_{22} of the coupler have been temporarily ignored.

Figure 3.3
Multiple Reflections in a Reflectometer System

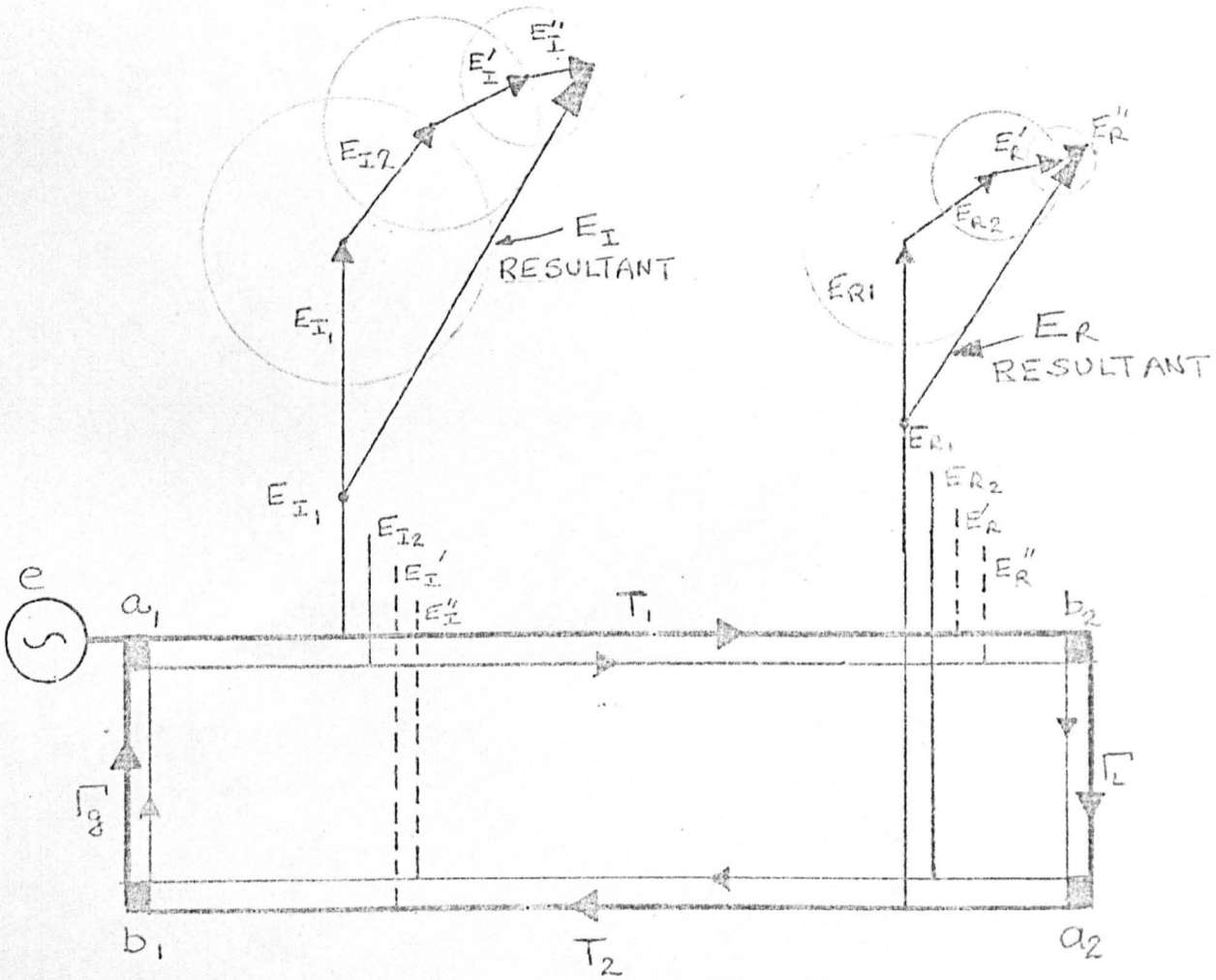

In Figure 3.3, the first incident and reflected paths are denoted by the bold lines and larger arrows, whilst the second incident and reflected paths are denoted by the bold lines and smaller arrows.

The dotted lines represent the unwanted coupling to the individual couplers. E'_I and E''_I represent the undesired waves to the first coupler and E'_R and E''_R represent the undesired waves to the second coupler. The superscripts, $'$ and $''$ denote that the components are due to the first and second incident and reflected waves respectively.

Let the desired and undesired coupling for the first coupler be C_1 and CD_1 respectively. Let C_2 and CD_2 be the desired and undesired coupling for the second coupler.

The first incident and reflected waves are denoted by a_1 and b_1 respectively.. The second incident and reflected waves by a'_1 and b'_1 respectively and so on. T_1 and T_2 represent the main transmission paths.

By inspection from figure 3.3;

$$E_{I_1} = C_1 a_1 \quad \ldots\ldots \quad 3.1$$

$$E_{I_2} = C_1 \Gamma_g \Gamma_L T_1 T_2 a_1 \quad \ldots\ldots \quad 3.2$$

$$E_{R_1} = C_2 a'_2 = C_2 \Gamma_L T_1 a_1 \quad \ldots\ldots \quad 3.3$$

$$E_{R_2} = C_2 a'_2 = C_2 \Gamma_g \Gamma_L T_1^2 T_2 a_1 \quad \ldots\ldots \quad 3.4$$

Comparison of the above terms gives:

$$\frac{E_{I_2}}{E_{I_1}} = \frac{C_1 \Gamma_g \Gamma_L T_1 T_2 a_1}{C_1 a_1} = \Gamma_g \Gamma_L T_1 T_2 \quad \ldots\ldots \quad 3.5$$

$$\frac{E_{R_2}}{E_{R_1}} = \frac{C_2 \Gamma_g \Gamma_L^2 T_1^2 T_2 a_1}{C_2 \Gamma_L T_1 a_1} = \Gamma_g \Gamma_L T_1 T_2 \quad \ldots\ldots \quad 3.6$$

Hence for each complete wave journey around the loop both E_{I_m} and E_{R_m} are altered by the same quantity, i.e., $\Gamma_g \Gamma_L T_1 T_2$. The resultant reflected versus incident ratio $\frac{E_{R(TOTAL)}}{E_{I(TOTAL)}}$ remains unaltered. (Figure 3.3). Note particularly that the above is true regardless of the directivity of the individual couplers.

The above result is not surprising as it has already been proven indirectly in Section 2:3. However, in theory, the loop product ($\Gamma_g \Gamma_L T_1 T_2$) could be $1 \angle 180°$ in which case the incident and reflected signals would cancel each other rendering the coupler useless on these occasions. In practice, $(\Gamma_g \Gamma_L T_1 T_2)$ is seldom $1 \angle 180°$ and this does not occur.

If the product $(\Gamma_g \Gamma_L T_1 T_2)$ is examined, it is evident that T_1 and T_2 are determined by the coupling, attenuation, source and load match. For example, a 20 dB coupler with no line losses would result in $T_1 \simeq 0.995$ (Ref. 3.3). The reflection coefficient, Γ_L, of the test device may range from a perfect match $|0|$ to a perfect open or short circuit $|1|$. Hence, if $(\Gamma_g \Gamma_L T_1 T_2)$ is to approach 0 then Γ_g must be controlled and should ideally be zero.

It was mentioned earlier that the sweep generator system used (Ref 3.4) has an output VSWR $\leq$ 1.67 (Γ_g = 0.25). A trivial calculation for the case of a 20 dB coupler and a load reflection coefficient $|1|$ will show that it is possible for the signal to be reflected thrice before it is reduced to less that 1% of its original value.

These reflections cause a poor passband response in a measuring system, particularly if swept frequency measurements are being taken. If wide band attenuators are used to improve the passband characteristics, then for the same oscillator power, the incident wave is reduced, and for the same reflection coefficient, the magnitude of the reflected waves will also be reduced and in the limit, it will be comparable to the inherent noise power within the detecting system. This results in further unecessary errors in the measurement. Poor passband response also introduces errors in the measurement of power sensitive devices e.g., transistors, varactor diodes etc.

Source match may be improved by the use of isolators/ circulators and even attenuation - matching networks. The former are more efficient but usually lack the multi-octave bandwidths required and as mentioned above, the attenuators introduce unnecessary loss. In either case, both methods do not inhibit the output variations within thesweep generator.

The well established methods to minimise signal output variations and also to present a good source match is the system presented in Figure 3.1. This system is similar to that described by Engen (Ref. 3.5). The sweep signal generators used incorporate voltage variable attenuators. The output signal (forward wave) is detected by the directional coupler just prior to entry into the reflectometer. The entire signal source block of Fig 3.1 will now be shown to be equivalent to a constant levelled source with an output match approaching that of the directional coupler, which is considerably better than that of the sweep generator itself.

Figure 3.4
Effective Source System

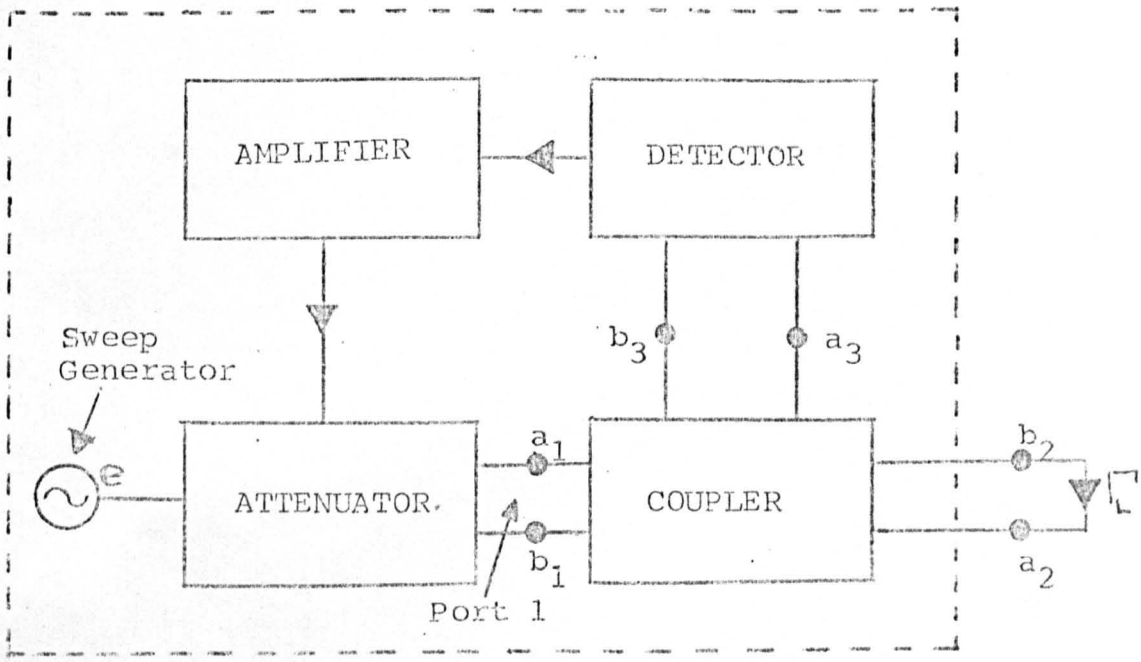

In Figure 3.4, let a_1 represent the incident wave which the generator presents to the coupler. By reference to the signal flow graph of Figure 3.5, it is seen that:

$$a_1 = e + \Gamma_g b_1 \qquad \ldots\ldots \qquad 3.7$$

Figure 3.5

Signal Flow Graph for Effective Signal Source of Figure 3.4

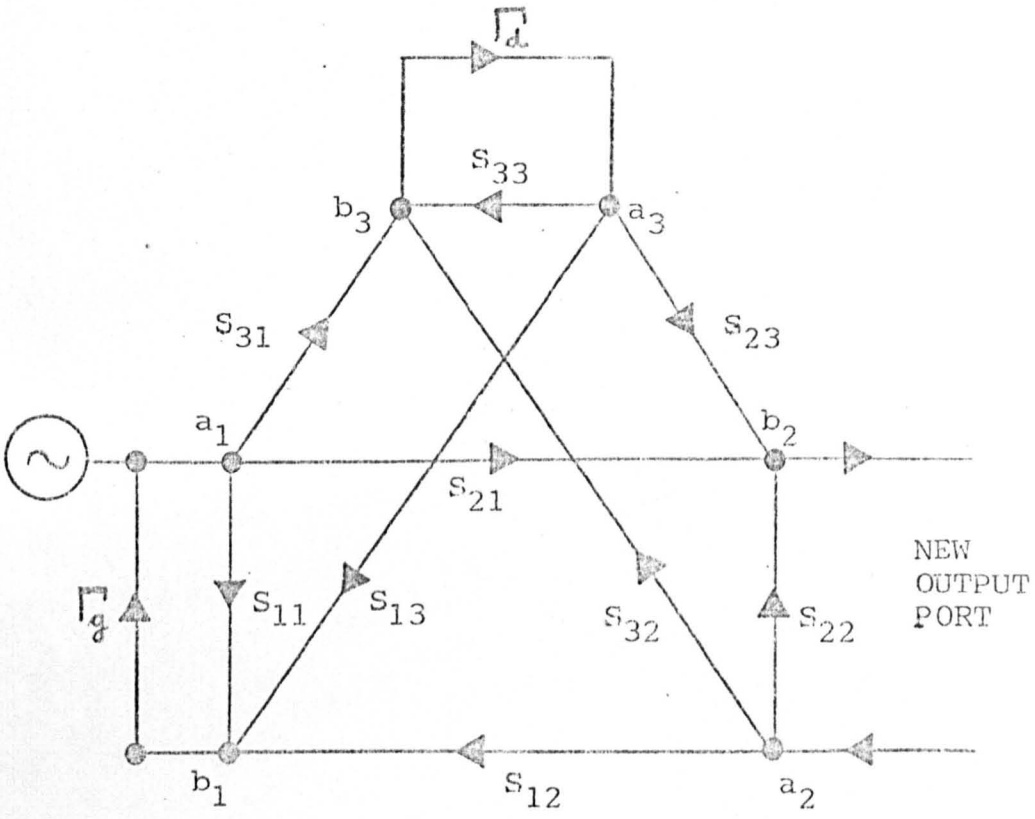

With the coupler network of Figure 3.5 connected, Port 2 is the main signal output port with the wave being emergent at b_2, and a_2 is where the reflected wave re-enters the system. Hence,

$$b_2 = S_{21}a_1 + S_{22}a_2 + S_{23}a_3$$
$$= S_{21}a_1 + S_{22}a_2 + S_{23}\Gamma_d b_3 \quad \ldots\ldots \quad 3.8$$

$$b_3 = S_{31}a_1 + S_{32}a_2 + S_{33}a_3$$
$$= S_{31}a_1 + S_{32}a_2 + S_{33}\Gamma_d b_3 \quad \ldots\ldots \quad 3.8a$$

From 3.8 $$a_1 = \frac{b_2 - S_{22}a_2 - S_{23}\Gamma_d b_3}{S_{21}}$$

and substituting in 3.8a

$$b_3 = \frac{S_{31}b_2}{S_{21}} - \frac{S_{22}S_{31}a_2}{S_{21}} - \frac{S_{23}S_{31}\Gamma_d b_3}{S_{21}} + S_{32}a_2 + S_{33}\Gamma_d b_3$$

$$b_3\left[1 + \Gamma_d\left(\frac{S_{23}S_{31}}{S_{21}} - S_{33}\right)\right] = \frac{S_{31}}{S_{21}}b_2 - a_2\left[\frac{S_{22}S_{31}}{S_{21}} - S_{32}\right]$$

and $$b_2 = b_3\left[\frac{S_{21}}{S_{32}} + \Gamma_d\left(S_{23} - \frac{S_{21}S_{33}}{S_{31}}\right)\right] + a_2\left[S_{22} - \frac{S_{21}S_{32}}{S_{31}}\right] \quad \ldots\ldots \quad 3.9$$

or $$b_2 = e' + \Gamma_g' a_2 \quad \ldots\ldots \quad 3.10$$

where $$e' = b_3\left[\frac{S_{21}}{S_{32}} + \Gamma_d\left(S_{23} - \frac{S_{21}S_{33}}{S_{31}}\right)\right] \quad \ldots\ldots \quad 3.10A$$

$$\Gamma_g' = \left[S_{22} - S_{21}\frac{S_{32}}{S_{31}}\right] \quad \ldots\ldots \quad 3.10B$$

Note the first term of 3.9 represents the ALC generator output whilst the second term is the effective generator reflection coefficient.

The directivity of the coupler has already been defined as:

$$D = 20\log_{10}\left|\frac{S_{31}}{S_{32}}\right| \text{ and since}$$

S_{21} is close to unity ($\simeq$0.95 & 0.995 for a 10 dB and a 20 dB coupler resp - Ref 3.3) it can be written:

$$\frac{S_{32}}{S_{31}} = 10^{-(D/20)} \quad \ldots\ldots \quad 3.11$$

If 3.11 is substituted in 3.10B for the worst case source match

$$\left|\Gamma_g'\right| = \left|S_{22}\right| + \left|10^{-(D/20)}\right| \qquad \ldots\ldots \quad 3.12$$

Figure 3.6
Maximum VSWR of the Effective Source when used in a closed Loop Control Circuit.

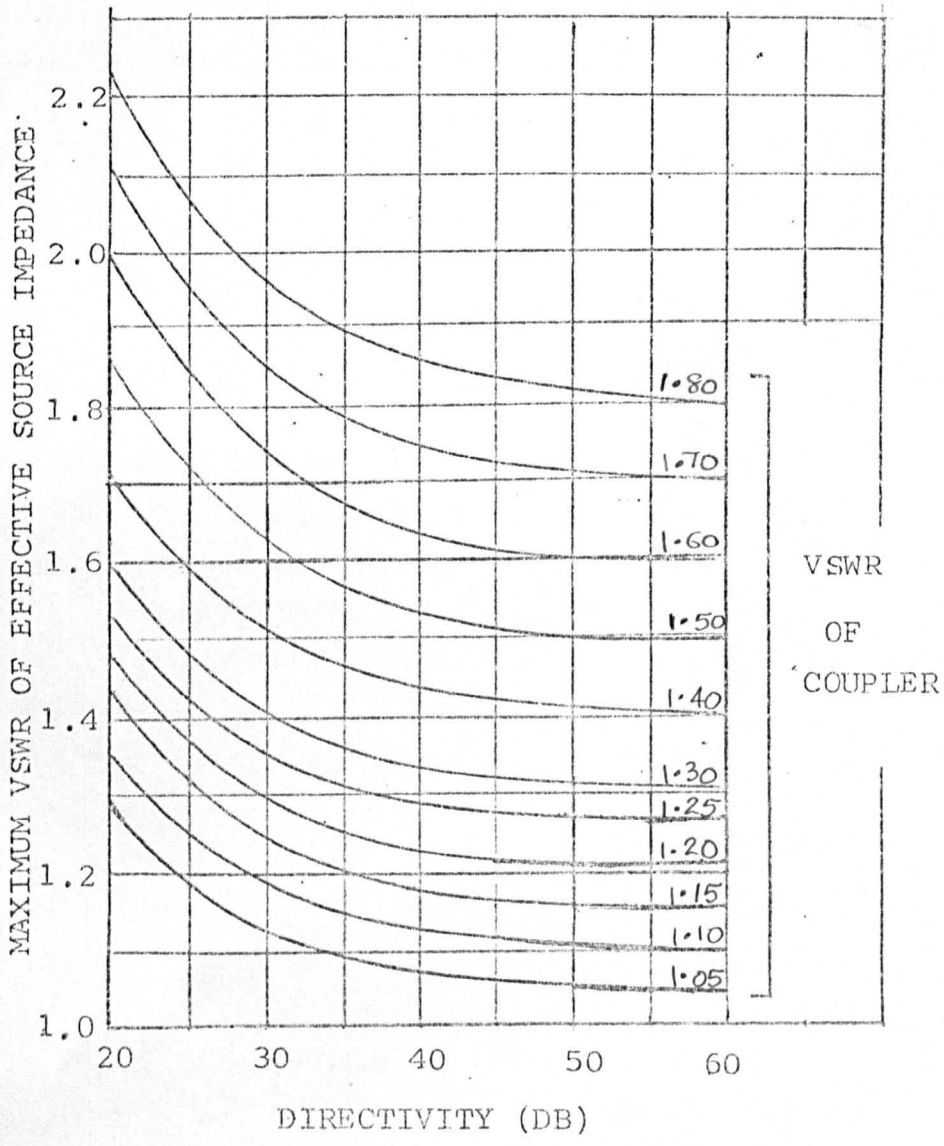

In the actual test set used, the directional coupler used was the Hewlett Packard Type 779D (Ref. 3.1) This has a mean coupling of 20 $\pm$ 0.5 dB and a main and auxiliary line SWR of 1.2 maximum. The minimum directivity for this coupler is 30 dB (1.7 - 4 GHz) and 26 dB (4 - 12.4 GHz). When this coupler is used in a good closed loop automatic level control system, the worst case source match, calculated from equation 3.10B is summarized as follows:

Worst Source Match using HP779D Coupler *

HP 779D			Worst Source Match
Frequency GHz	Directivity dB	Mainline and Auxiliary Line VSWR	VSWR
1.7 - 4.0	30	1.2	1.279
4 - 12.4	26	1.2	1.328

* Assuming sufficient loop gain.

Note: Hewlett Packard quotes an effective source of 1.2 SWR (Ref 3.1) but does not state the frequency. However, the figures calculated are considerably better than the 1.67 SWR quoted for the generator alone.

The Low Pass Harmonic Filter

This should be used whenever possible and should be placed before the levelling coupler, as the coupler detector is frequency insensitive and might be affected by the spurious signals. The spurious signals do not effect the measured results in the same manner because the signals are detected through tuned amplifiers.

3:3.0 Choice of the Reflectometer

Two reflectometers were used. These are the HP 8741A for 0.11 to 2.0 GHz and HP 8742A for 2.0 to 12.4GHz. A block diagram of these systems is shown in Figure 3.7. The signal is fed to the device under test via a dual directional coupler. The incident and reflected signals are fed into a dual channel receiver for processing.

Figure 3.7
Basic Diagram of the HP 8741A and HP 8742A Reflectometers

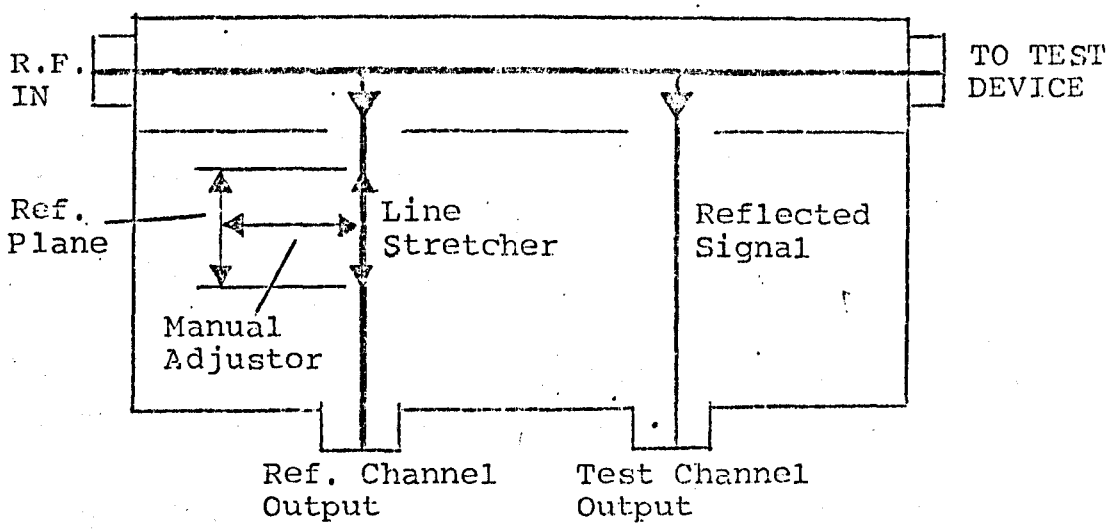

Both reflectometers employ a calibrated line stretcher to enable the electrical path lengths to the receiver to be identical. This is of considerable advantage as it allows direct readings of the display systems for phase changes. The coupling factors for all the reflectometers are a nominal 20 dB and the insertion loss is less than 1 dB.

Two sets of Directivity Figures are claimed by the manufacturers (Ref 3.6 and 3.9), these are tabulated below:

Type	Frequency (GHz)	Directivity	
		Before 1970	After 1970
8741A	0.11 to 1.0	$\geq$ 40 dB	$\geq$ 36 dB
	1.0 to 2.0	$\geq$ 34 dB	$\geq$ 32 dB
8742A	2.0 to 12.4	$\geq$ 30 dB	$\geq$ 30 dB

As the reflectometer forms the "heart" of the measuring system, its choice is of considerable importance. The mathematical analysis of Section (2.3) has shown what is desired. The important characteristics may be classified into five important properties, namely;

1: Directivity.
2: SWR
3: Frequency Range.
4: Coupling Coefficient.
5: Transmission Loss.

The following sub-sections are an intuitive discussion of the mathematical analysis carried out in Chapter 2.

3:3.1 Directivity

Directivity is a measure of the ability of a coupler to isolate two signals, for example, the incident and reflected wave. It therefore sets the limits on how accurately a coupler can perform a specific measurement. As an example when making reflection measurements a dual directional coupler is required and the directivity of the test port is the most important parameter. Subsequent mathematical treatment will confirm this. Ideally, it would be desirable to measure the reflected signal alone. However, because of directivity, the reflected signal is combined with a small portion of the incident wave. This can be easily explained by reference to the phasor diagram of Figure 3.8.

Figure 3.8 EFFECT OF DIRECTIVITY ON REFLECTION COEFFICIENT MEASUREMENT.

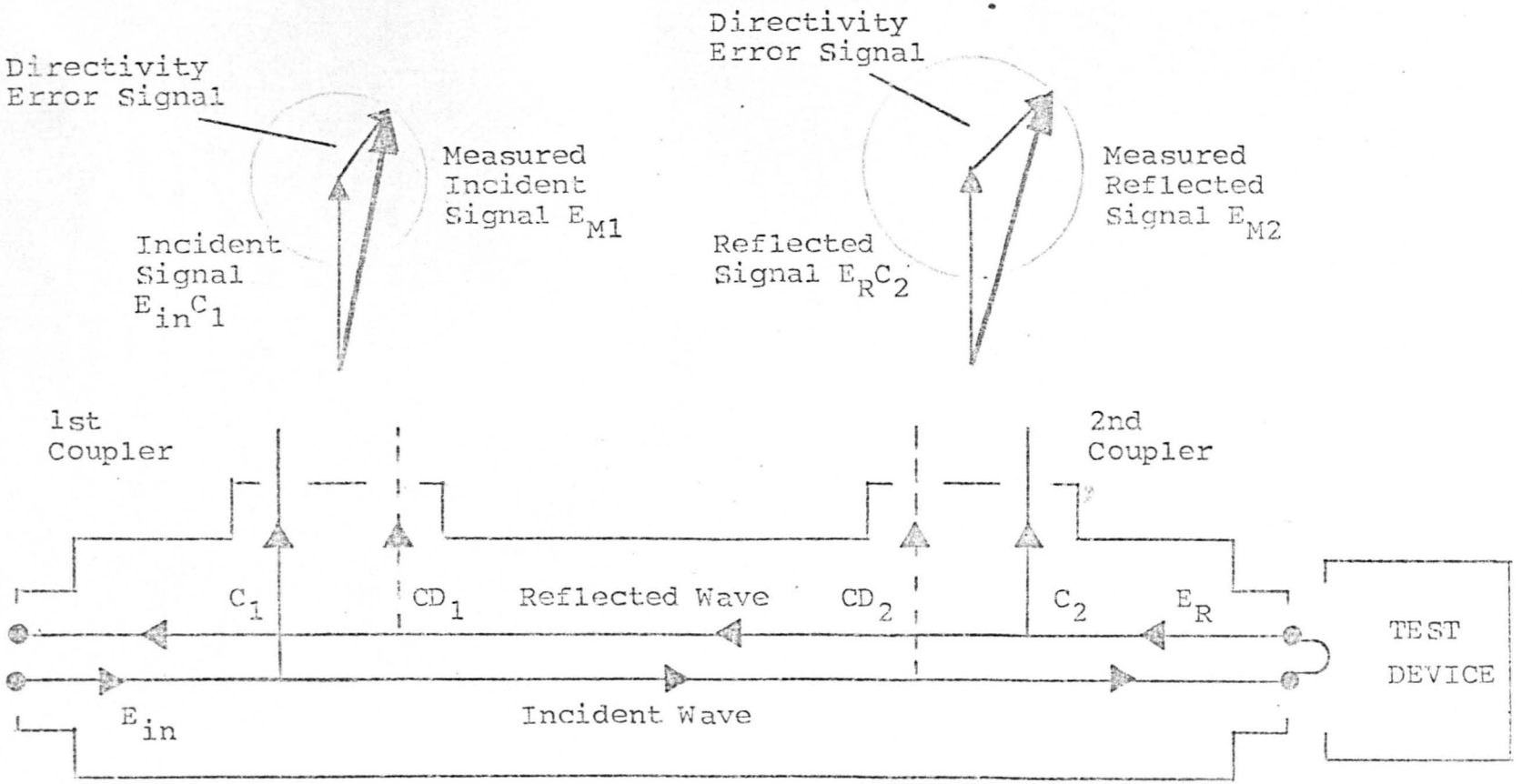

C_1 and C_2 = desired coupling factors; CD_1 and CD_2 = undesired coupling factors;
E_{M1} & E_{M2} = measured signals; E_{in} = input signal; E_R = reflected signal

In the 1st coupler, the small portion of the reflected wave which combines with the incident signal leads to an error in the measured incident signal. However as the incident signal is much larger than the directivity error signal, the magnitude of the measured incident signal is approximately unaltered.

In the 2nd coupler, the small portion of the incident signal which combines with the reflected signal results in a phase which is directly additive to the measurement uncertainty. Thus the higher the directivity (i.e., a smaller directivity error signal) the higher will be the measurement accuracy.

When measuring large reflections, the small portion of the incident signal that mixes with the reflected signal is very small, and it adds a negligible amount of uncertainty as in the first coupler. As the reflected signal becomes smaller, the small portion of the incident signal becomes more significant. When the reflected signal in dB (return loss) equals the directivity of the coupler, the measurement can result in a -6dB to $+\infty$ dB error. The importance of this cannot be overlooked and a mathematical analysis showing the practical limits of measurement will be given in Chapter IV.

3:3.2 Voltage Standing Wave Ratio (VSWR)

The VSWR of the coupler is important since it minimises the simple and multiple mis-match errors thus improving the accuracy of the measurement. For example, when making swept reflection measurements, it is customary to set a full reflection (0dB return loss) reference by connecting a short circuit at the output of the coupler. Some of the reflected signal will be re-reflected due to the output port (test port) of the coupler. This re-reflected signal will go through a wide phase variation due to the width of the frequency sweep, adding and subtracting from the reflection signal, thus creating a ripple in the full reflection (0dB return loss). The above effects can also be caused by detector mis-matches.

The magnitude of the re-reflected signal and thus the measurement uncertainty can be minimised by selecting couplers with as low a SWR as possible, and by the use of detectors with low SWR's.

3:3.3 Frequency Range

Broadband operation is important because it eliminates the necessity for several octave band couplers to cover a wide frequency range. For example, with broadband sources capable of up to four octave band sweeps, it is a real convenience to be able to have a wideband coupler to obviate the need for time consuming costly calibration techniques.

3:3.4 Coupling Coefficient

The choice of coupling coefficient is important because it determines the level of signal with which the detection circuits will have to operate. Most sweep generators have limited outputs (usually +5 to + 10 dBm at 12 GHz) and a convenient coupling coefficient is 20dB down on the main signal. Such a coupler would extract 1% of the main signal. On the other hand, a 10dB coupler would extract a full 10% of the main signal. Furthermore, in power sensitive measurements, e.g., transistors, it is important that the coupling coefficient remains constant over the frequency range of measurement. Hewlett Packard claims that this feature is enhanced in their couplers by the use of exponential coupling designs and lower coupling coefficients which introduce less perturbations into the main signal line, thus favouring lower SWR's and better directivity.

3:3.5 Transmission Loss

Transmission loss is the total loss in the mainline of a directional device and includes insertion loss and coupling loss. It assumes importance at the higher frequencies where sweep generators have a limited output often less than + 10dBm.

In general, broadband coaxial couplers have transmission losses of the order of 1 dB. This loss should be as constant with frequency as possible.

3:4 The Detection and Indication Block

The detection system used is the Hewlett Packard Network Analyser 8410A operating with its auxiliaries HP 8411A and HP 8413A or HP 8414A. Detailed descriptions of all these can be found in their respective hand-books. The information given here is only for the understanding of the measuring system used.

Figure 3.9

Basic System used in the Network Analyser to achieve Frequency Translation by a Sampling Technique

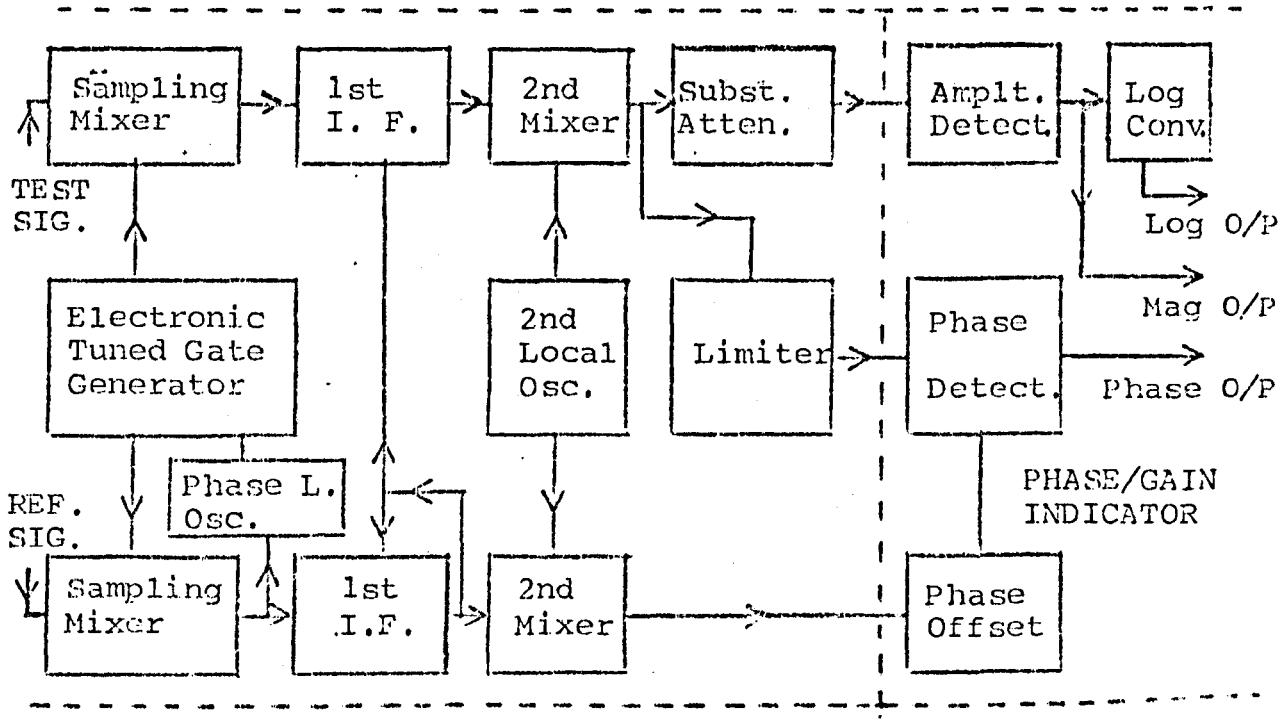

The basic system consists of three units, a harmonic frequency converter (HP 8411A), a main frame unit (HP 8410A) and a plug-in display unit, either a phase-gain indicator (HP 8413A) or a polar display unit (HP 8414A) (Fig. 3.1). In its broadest sense, the system is a dual channel self tuning double super-heterodyne receiver which operates between 110 MHz and 12.4 GHz. A block diagram is shown in figure 3.9.

The key technique that allows the analyser to measure complex ratios is the technique of frequency translation by sampling. Sampling as used in this system is a special case of heterodyning which translates the input R.F. frequencies to a lower I.F. frequency where normal circuitry is used to measure amplitude and phase relationships. The principle is to exchange the local oscillator of a conventional heterodyne system with a pulse generator which generates a train of very narrow pulses. If each pulse within the train is narrow compared to a period of applied R.F. signals, the sampler becomes a harmonic mixer with equal efficiency for each harmonic. This sampling-type mixing has the advantage that a single system can operate over an extremely wide input frequency range.

In order to make the system capable of swept frequency operation, an internal phase-lock loop keeps one channel of the two channel network analyser tuned to the incoming signal. Tuning of the phase-lock loop is entirely automatic. When the loop is unlocked, it automatically tunes back and forth across a portion of whatever octave-wide frequency band has been selected by the user. When any harmonic of the tracking oscillator frequency is 20.278 Mhz below the input frequency the loop stops searching and locks. Search and lock-on are normally completed in about 20 μS . The loop will remain locked for sweep rates as high as 220 GHz/sec (a rate corresponding to about 30 sweeps per second over the highest frequency band 8 to 12.4GHz). Initially this fact was not observed in the computerized systems (described later)

and considerable measurement error was experienced. Ryttling and Sanders (Ref 3.11) provides further details of this sampling, search and phase-locking design.

The I.F. signals reconstructed from the sampler outputs have the same relative amplitudes and phases as the microwave reference and test signals, because the frequency conversion is a linear process Referring again to Figure 3.9, the I.F. signals are first applied to a pair of matched AGC (automatic gain control) amplifiers. These AGC amplifiers perform two functions; they keep the signal level in the reference channel constant and they vary the gain in the test channel so that the test signal level does not change when variations common to both channels occur. This action is equivalent to taking a ratio. It removes the effects of power variations in the signal source, frequency response characteristics common to both channels and other similar common-mode variations.

The two signals (reference and test) are then down-converted once more to 278 kHz (2nd. I.F.) to enable good amplitude and phase detection. This intermediate frequency of 278 kHz has proved useful in checking the phase accuracy of the receiver. This is because the period (T)

$T = \frac{1}{278\ \text{kHz}}$, i.e 3.6 μs corresponds to 360° of phase or

10 picoseconds = 1°

To obtain the desired magnitude (dB) and phase comparisons (degrees) the phase-gain indicator plug-in display unit (HP 8413A) contains a linear phase detector and an analogue to logarithmic converter which is claimed to be accurate to within ± .2 dB over a 60 dB overall range of test signal amplitudes. Voltage Ratios (dB) and relative phase (degrees) can be read on the meter of the display unit (used for manual readings) but the plug-in also provides calibrated d.c. coupled voltages proportional to gain (as a linear ratio or in dB) and phase for graphical or electronic displays.

An alternative display used was the Polar Display Unit (HP 8414A). A block diagram of this is shown in Figure 3.10.

Figure 3.10

Block Diagram of Polar Display Unit

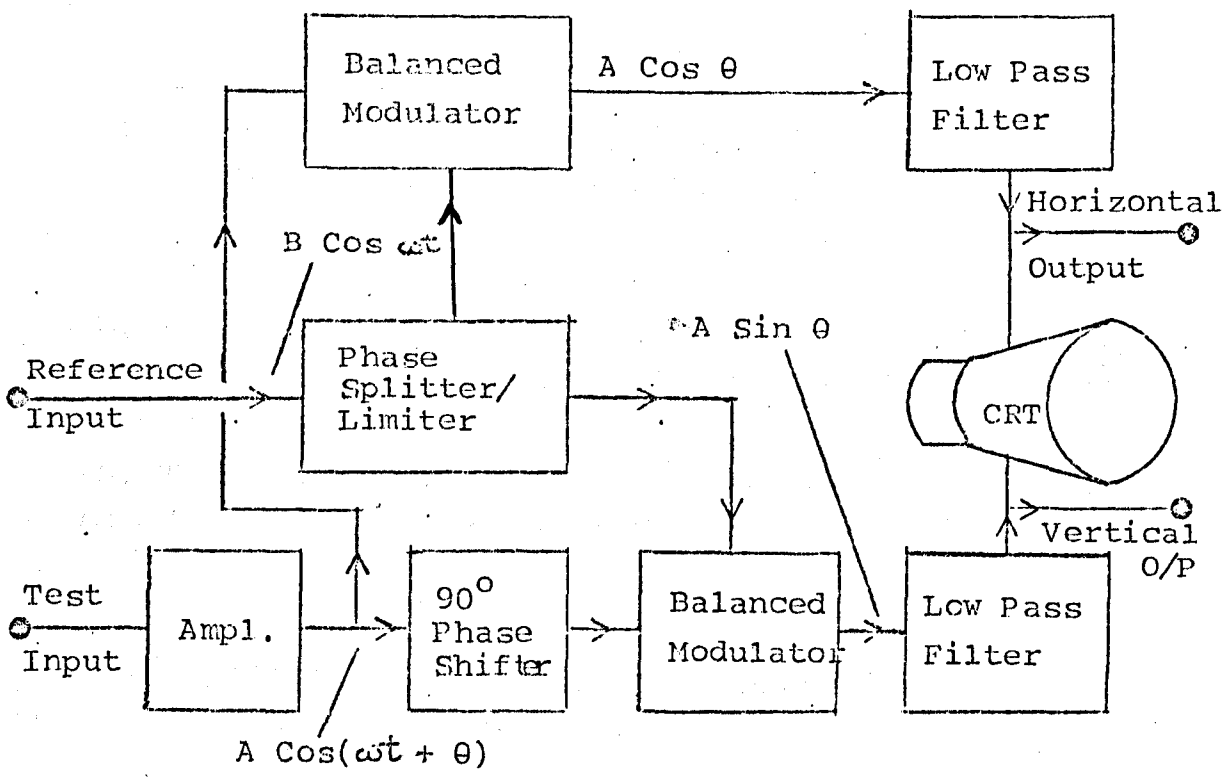

The unit converts polar quantities into a form suitable for display on the cathode ray tube (CRT). This is accomplished by using two balanced modulator phase detectors. The phase of the test channel is shifted 90^{o} with respect to the reference channel before being applied to the balanced modulators. The output of one modulator is proportional to A Sin θ. This signal is amplified and fed to the vertical deflection plates of the CRT. The output of the other modulator is proportional to A Cos θ and this signal is applied to the horizontal deflection plates of the CRT. Thus the polar phasor can be displayed in the rectangular coordinates of an oscilloscope or an X-Y recorder.

The polar display was the unit most frequently used (especially in computer controlled measurements) as it would instantly demonstrate any mal-function in the equipment, e.g., loss of phase lock, improper calibration of standards etc.

3:5 System Accuracy

Hewlett Packard (Ref 3.9) claim the following when the system is used without computer correction:

Overall Uncertainty* Reflection coefficient magnitude of unknown (Γ_L) is measured to within Γ_u =

$\pm$ (0.01 + 0.02 $|\Gamma_L|$ + 0.05 $|\Gamma_L|^2$), 0.11 to 1.0 GHz)
$\pm$ (0.02 + 0.02 $|\Gamma_L|$ + 0.05 $|\Gamma_L|^2$), 1.0 to 2.0 GHz) HP 8742A

$\pm$ (0.032 + .052 $|\Gamma_L|$ + 0.036 $|\Gamma_L|^2$), 2.0 to 8.0 GHz)
$\pm$ (0.032 + 0.04 $|\Gamma_L|$ + 0.07 $|\Gamma_L|^2$), 8.0 to 12.4 GHz) HP 8742A

Reflection coefficient angle uncertainty:

$\pm$ Arc Sin $\frac{\Gamma_u}{\Gamma_L}$, for $\phi \leq 90^\circ$

*Note:

Overall uncertainty includes the effects of coupler directivity, source match, and system tracking with frequency.

The following information on the system is taken from the Hewlett Packard Catalogue Sheet (Ref. 3.9).

8410A NETWORK ANALYZER

(Operating with 8411A)

Instrument Type: Measures relative amplitude and phase of two RF input signals; choice of two plug-in display modules for meter readout (8413A), or CRT polar display (8414A).

Frequency Range: 0.11 to 12.4 GHz.

Tuning: Automatic over octave band selected by front panel switch.

Swept Operation: Sweeps in octave bands; apply sweep reference voltage for fast sweep operation (compatible with sweep reference out of Model 8690A Sweep Oscillators*).

Input Impedance: 50Ω, SWR < 1.4 to 8 GHz, < 2.0 to 12.4 GHz, connectors precision 7 mm coax (APC-7).

Channel Isolation: > 70 dB, 0.11 to 6.0 GHz; > 60 dB, to 12.4 GHz.

Amplitude

Input Power Range

Reference Channel: 20 dB variation causes less than ± 0.75 dB and ± 2° change in amplitude and phase readings. 20 dB range will be within — 16 to — 44 dBm.

Test Channel: — 10 (± 2) dBm maximum. Not to exceed reference channel power by more than 20 dB.

Dynamic Range

Reference Channel: 20 dB or more.

Test Channel: 60 dB or more.

Test Channel Noise: Less than — 78 dBm equivalent input noise (measured on 8413A Meter).

Maximum RF Input to Either Channel: 50 mW (damage level).

Maximum DC on RF Line: ± 3 V (damage level).

Amplitude Control: Adjusts gain of test channel relative to reference channel.

Range: 69 dB total in 10 and 1 dB steps; vernier provides continuous adjustment over at least 2 dB.

Accuracy: ± 0.1 dB per 10 dB step, not to exceed ± 0.2 dB cumulative. ± 0.05 dB per 1 dB step, not to exceed ± 0.1 dB cumulative.

General

Phase Control: Vernier provides continuous phase reference adjustment over at least 90°.

Outputs: Two rear panel auxiliary outputs provide 278 kHz IF signals; outputs may be used for signal analysis, special applications, and convenient test points; modulation bandwidth nominally 10 kHz.

Reference Channel IF: 2 volts peak-to-peak nominal.

Test Channel IF: 10 volts peak-to-peak or less, depending on signal level and test channel gain setting.

Sweep Reference Input. Accepts DC voltage proportional to frequency for optimum swept-frequency operation; compatible with 0 to 40 volt per octave (nominal) sweep reference output of 8690-series Sweep Oscillators.

Power: 115 or 230 volts ± 10%, 50 to 400 Hz, 70 watts (includes 8411A).

Weight: 8410A, 32 lbs.; 8411A, 6½ lbs.

Dimensions: 8410A, 7½ in. high, 18⅛ in. deep, 16¾ in. wide. 8411A, 2⅝ in. high, 5⅝ in. deep, 9 in. wide exclusive of connectors; 5 ft. cable permanently attached for connection to 8410A.

Price: 8410A, $1,700; 8411A, $2,200.

* Simple resistive network required for 8690-series Sweep Oscillators.

8413A PHASE-GAIN INDICATOR

(Installed in 8410A)

Instrument Type: Plug-in meter display unit for 8410A. Displays relative amplitude in dB between reference and test channel inputs or relative phase in degrees. Push-button selection of meter function and range.

Amplitude

Range: ± 30, 10 and 3 dB full scale.

Accuracy: ± 3% of end scale.

Amplitude Output: 50 millivolts per dB up to ± 30 dB total; bandwidth 10 kHz nominal depending on signal level; source impedance 1 kΩ; accuracy, ± 3%.

Linear Output (rear panel): 0 to 1 V maximum; 10 kHz bandwidth; source impedance approx. 250Ω.

Maximum Drift

Log: < ± 0.1 dB per degree C.
Linear: < ± 5 mV per degree C.

Phase

Range: ± 180, 60, 18, 6 degrees full scale.

Accuracy: ± 2% of end scale.

Phase Output: 10 millivolts per degree; 10 kHz bandwidth; 1 kΩ source impedance. Accuracy ± 2% of reading on auxiliary display.

Maximum Drift: < ± 0.2 degree per degree C.

Phase Offset: ± 180 degrees in 10 degree steps.

Accuracy: ± 0.2° ± 0.3°/10° step, not to exceed ± 1.5 degrees cumulative.

Phase Response Versus Signal Amplitude: 4 degrees maximum phase change for 60 dB amplitude change in test channel.

General

Power: Additional 15 watts supplied by 8410A.

Weight: 11 lbs.

Dimensions: 6 in. high, 15⁹⁄₁₆ in. deep, 7³⁄₃₂ in. wide (excludes front panel knobs).

Price: $825.

8414A POLAR DISPLAY

(Installed in 8410A)

Instrument Type: Plug-in CRT display unit for 8410A. Displays amplitude and phase data in polar coordinates on 5-in. cathode ray tube.

Range: Normalized polar coordinate display; magnitude calibration 20% of full scale per division. Scale factor is a function of GAIN setting on 8410A. Maximum scale factor 10. (for 0 dB setting) decreasing to at least 0.0316 (for 50 dB setting); phase calibrated in 10 degree increments over 360 degree range.

Accuracy: Error circle on CRT ± 3 mm radius.

Outputs: Two DC outputs provide horizontal and vertical components of polar quantity. Maximum output ± 10 volts, < 100Ω source impedance, bandwidth (3 dB) 10 kHz.

Drift:

Beam center drift: CRT, ± 0.2 mm/° C; auxiliary outputs, < ± 5 mV/° C.

Measurement drift: amplitude, less than 2% of reading/° C; phase, less than 0.2° C (not including beam center drift).

Beam Center: Pressing BEAM CENTER simulates zero-signal input to test channel. Allows convenient beam position adjustment for reference.

SPECIFICATIONS

General

CRT: 5-inch, 5 kV post accelerator tube with P-2 phosphor; internal polar graticule.

Marker Input (rear panel): Accepts frequency marker output pulse from HP 8690-series and 690-series Sweep Oscillators, — 5 volts peak. Markers displayed as intensified dot on CRT display.

Blanking Input (rear panel): Accepts — 5 volt blanking pulse from HP 8690-series and 690-series Sweep Oscillators to blank retrace during swept operation.

Background Illumination: Controls intensity of CRT background illumination for photography. Eliminates need for ultraviolet light source in oscilloscope camera when photographing internal graticule.

Accessories Furnished: Three Smith Chart overlays for CRT.

Power: Additional 35 watts supplied by 8410A.

Weight: 13 lbs.

Dimensions: 6 in. high, 15⅝ in. deep, 7⅜₂ in. wide (excludes front panel knobs).

Price: $825.

8740A TRANSMISSION TEST UNIT

Instrument Type: RF power splitter and calibrated line stretcher for convenient transmission tests with 8410A. Provides reference and test channel RF outputs for connection to unknown device and the 8411A Converter.

Frequency Range: DC to 12.4 GHz.

Frequency Response: Measurement errors from frequency response variations between reference and test channels $< \pm 0.5$ dB amplitude and ± 3 degrees phase to 8.0 GHz; ± 0.75 dB and ± 5 degrees to 12.4 GHz (includes frequency response of 8411A Converter).

Output Impedance: 50 ohms, reflection coefficient 0.07 (1.15 SWR, 23 dB return loss) DC to 8 GHz; 0.11 (1.25 SWR, 19 dB return loss) 8.0 to 12.4 GHz.

Maximum RF Input Power: 1 watt. 0.5 milliwatt when connected directly to 8411A Converter.

Insertion Loss: 17 dB nominal.

Connectors: Input, compatible Type N female stainless steel; output, APC-7.

Reference Plane Extension:

Electrical; 0 to 30 centimeters.
Mechanical; 0 to 10 centimeters.
Both extensions calibrated by digital indicators.
Electrical extension indicator adjustable for initial calibration.

Power: Passive, no primary power required.

Weight: 17½ lbs.

Dimensions: 6 in. high, 16⅜₆ in. deep, 7⅜₂ in. wide (excluding knobs and connectors).

Price: $1,100.

8741A AND 8742A REFLECTION TEST UNITS

Instrument Type: Wideband reflectometer, phase-balanced for swept or spot frequency impedance tests with 8410A. Calibrated variable reference plane.

Frequency Range: 0.11 to 2.0 GHz (8741A); 2.0 to 12.4 GHz (8742A).

Impedance: 50 ohms.

Overall Uncertainty: Reflection coefficient magnitude of unknown (Γ_L) is measured to within $\Gamma_u =$

$\pm (0.01 + 0.02 |\Gamma_L| + 0.05 |\Gamma_L|^2)$, 0.11 to 1.0 GHz.
$\pm (0.02 + 0.02 |\Gamma_L| + 0.05 |\Gamma_L|^2)$, 1.0 to 2.0 GHz.
$\pm (0.032 + 0.052 |\Gamma_L| + 0.036 |\Gamma_L|^2)$, 2.0 to 8.0 GHz.
$\pm (0.032 + 0.04 |\Gamma_L| + 0.07 |\Gamma_L|^2)$, 8.0 to 12.4 GHz.

Reflection Coefficient Angle Uncertainty: $\pm$ arc sin $\frac{\Gamma_u}{\Gamma_L}$, for $\phi \leq 90°$.

Note: Overall Uncertainty includes the effects of coupler directivity, source match, and system tracking with frequency.

Directivity: $\geq$ 40 dB, 0.11 to 1.0 GHz; $\geq$ 34 dB, 1.0 to 2.0 GHz (8741A*); $\geq$ 30 dB, 2.0 to 12.4 GHz (8742A).

Maximum RF Input: 30 watts. 1 milliwatt when connected to 8411A Converter.

Insertion Loss to Test Device: 1 dB nominal.

Reflectometer Coupling Coefficient: 20 dB nominal.

Reference Plane Extension: 0 to 15 cm (8741A); 0 to 17 cm (8742A); calibrated by digital dial indicator. Indicator is adjustable for initial calibration.

Connectors: Input, Type N female, stainless steel; incident, reflected, and unknown reflectometer ports APC-7.

Accessory Furnished: 11565A APC-7 short for Reflectometer Calibration.

Power: Passive, no primary power required.

Weight: 16½ lbs. (8741A); 15½ lbs. (8742A).

Dimensions: 6 in. high, 16⅜₆ in. deep, 7⅜₂ in. wide (not including connectors and knobs).

Prices: Model 8741A: $1,500.00.
Model 8742A: $1,500.00.

* 8741A directivity typically > 30 dB, 2.0 to 2.4 GHz.

IMPEDANCE OVERLAYS FURNISHED WITH 8414A POLAR DISPLAY

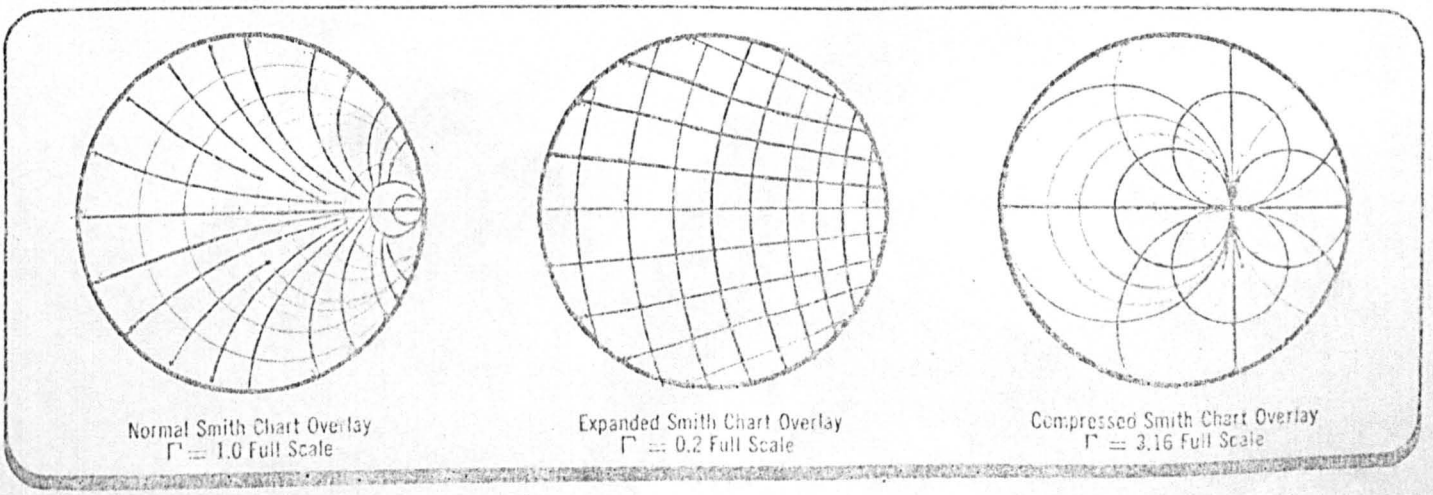

Normal Smith Chart Overlay
$\Gamma = 1.0$ Full Scale

Expanded Smith Chart Overlay
$\Gamma = 0.2$ Full Scale

Compressed Smith Chart Overlay
$\Gamma = 3.16$ Full Scale

3.6 Conclusions.

A brief description of the equipment used in this thesis for the measurement of reflection coefficients has been presented in Chapter III. Detailed descriptions of the individual circuits have not been given as these can be easily obtained from the individual handbooks.

The two main errors associated with the equipment have been introduced. The first error, poor source match, can be alleviated by the use of a suitable automatic gain control system. This has been discussed in Section 3.2.2. An introduction into the errors caused by poor directivity has been carried out in section 3.3.1. Both these errors and the manner in which they limit the measurement accuracy will be extensively discussed in Chapter IV.

3:7 References

3.1 Hewlett Packard "Co-axial and Waveguide Catalogue 1977-1978.

3.2 Phase Lock Source in Department.

3.3 Hewlett Packard "High Frequency Swept Measurements" Application Report 183.

3.4 Hewlett Packard "Electronic Instruments and Systems for Measurement/Analysis/Computation 1973 Catalogue.

3.5 Engen, Glen. F. "Amplitude Stabilization of a Microwave Signal Source" I.R.E. M.T.T. April 1958 pp 202-206.

3.6 Hewlett Packard - Network Analysor Data Catalogue Sheet - 1st March 1970.

3.7 Dunwoodie,D. and Lacy, P. "Why Tolerate Unnecessary Measurement Errors" Wiltron Technical Review Number 5 - March 1975.

3.8 Lacy, P. and Oldfield, W. "A Precision Swept Reflectometer" Microwave Journal April 1973 pp 31 to 34 & 50.

3.9 Hewlett Packard - Network Analyser Data Catalogue Publication 1st June 1967.

3.10 Anderson, R.W. & Dennison, O.T. "An Advanced New Network Analyser for Sweep-Measuring Amplitude and Phase from 0.1 to 12.4 GHz". Hewlett Packard Journal, February 1967 pp 2-10.

3.11 Rytting,D.K. and Sanders,S.N. "A System for Automatic Network Analysis" Hewlett Packard Hewlett Packard Journal February 1970 pp 2-10.

* * * * * * * * * *

CHAPTER IV

UNCORRECTED REFLECTOMETER MEASUREMENT

4:0 Introduction

The overall aims of this chapter are to discuss the errors and to establish the accuracy limits to which a reflectometer may be used.

Section 4:1 establishes the directivity and mis-match error. The former is analysed in section 4:2, whilst the latter is examined in section 4:3. The effect of the errors in measurement vary with the device being measured. For example, the directivity error becomes increasingly large as smaller reflection coefficients are measured. Graphs are therefore provided to establish quickly the accuracy limits to which measurements may be made for a given system. These are given in Section 4:4. The effects of inter-series connectors and adapters are examined in section 4:5.

An alternative method of deriving accuracy specificatins is given in section 4:6. This method is important because the instruments used for the measurements of this thesis are specified by the manufacturer in this manner. Finally comparisons are made between the various methods to determine the accuracy limits for the uncorrected measurement system.

4:1 The Limits of Reflectometer Accuracy

The theory of the reflectometer (dual directional coupler) has already been derived in section 2:3. Equation 2.33 has established that the measured reflection coefficient (ρ_m) is related to the reflection coefficient (Γ_L) of the device under test (DUT) by a bilinear transformation of the form:

$$\rho_m = \frac{A\,\Gamma_L + B}{C\,\Gamma_L + D} \qquad \ldots\ldots \quad 4.1$$

where A, B, C and D are the complex constants defined by equations 2.33(a) to 2.33(d) respectively.

In appendix 11:2, it has been shown that a bilinear transformation of equation 4.1 can also be expressed by a general set of scattering parameters of the form shown in figure 4.1, where:

$$A = -(S_{11}\,S_{22} - S_{12}\,S_{21}); \qquad B = S_{11}$$

$$C = -S_{22}; \qquad D = 1$$

as defined by equations 11.2.7(a) to 11.2.7(d) respectively.

Figure 4.1

General Scattering Parameter
Representation of a Bilinear Transformation

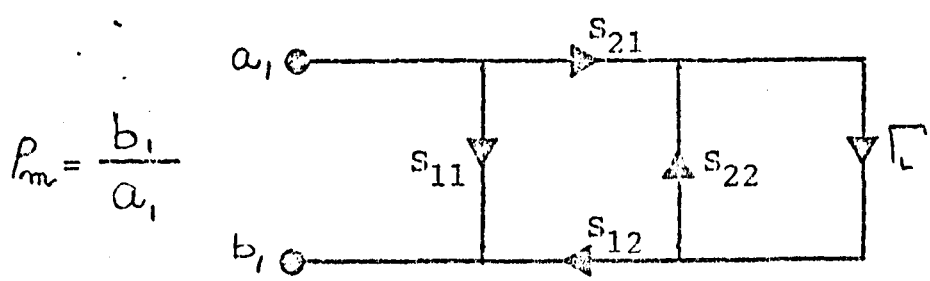

The general set of scattering parameters (Fig 4.1) used here should not be confused with the set used in Chapter II for the derivation of the bilinear relationship in the reflectometer.

In future, unless specifically stated, the general form of the scattering parameters will be used throughout this thesis.

In figure 4.1, b_1 represents the reflected wave sampled by the reflectometer, and a_1 represents the incident wave sampled by the reflectometer. S_{11} is the path of

the signal leaked directly from the incident wave to the reflected wave detector of the reflectometer independent of the device under test. Directivity is the major contributor in the practical case.

S_{21} represents the forward incident signal path to the device under test and S_{12} represents its return path to the detector. S_{22} is the effective reflection coefficient at the output port.

The following are defined:

1: $\rho_m = \frac{b_1}{a_1}$ = indicated measured reflection coefficient.

2: $\rho_t = \frac{b'_1}{a'_1}$ = Indicated true reflection coefficient and is that measured when the directivity is infinite and a perfect output port match exists.

Hence, using Mason's non-touching rule:

$$\frac{b_1}{a_1} = \rho_m = S_{11} + \frac{S_{12}\, S_{21}\, \Gamma_L}{1 - S_{22}\, \Gamma_L} \quad \ldots\ldots \quad 4.2$$

and for the perfect case:

$$\frac{b'_1}{a_1} = \rho_t = S_{12}\, S_{21}\, \Gamma_L \quad \ldots\ldots \quad 4.3$$

The relative measurement uncertainty is defined as

$$\pm \frac{\text{True Indicated Reading - Measured Indicated Reading}}{\text{True Indicated Reading}}$$

$$\rho_t - \rho_m = S_{12}\, S_{21}\, \Gamma_L - S_{11} - \frac{S_{12}\, S_{21}\, \Gamma_L}{1 - S_{22}\, \Gamma}$$

$$\rho_t - \rho_m = -\left[S_{11} + \frac{S_{12}\, S_{21}\, S_{22}\, \Gamma_L^2}{1 - S_{22}\, \Gamma_L} \right]$$

By defining $P_t - P_m = \Delta P$ and substituting equation 4.3,

$$\frac{P_t - P_m}{P_t} = \frac{\Delta P}{P_t} = -\left[\frac{S_{11}}{S_{12}\,S_{21}\,\Gamma_L} + \frac{S_{22}\,\Gamma_L}{1 - S_{22}\Gamma_L}\right] \quad \ldots\ldots \quad 4.4$$

from which both magnitude and phase uncertainty may be calculated. The phase angle can be ascertained by an inverse tangent series (Ref 4.1) of the form:

$$\text{Tan}^{-1}\left(\frac{\Delta P}{P_t}\right) = \left(\frac{\Delta P}{P_t}\right) - \left(\frac{\Delta P}{P_t}\right)^3 + \left(\frac{\Delta P}{P_t}\right)^5 \quad \left(\frac{\Delta P}{P_t}\right)^7 \quad \ldots\ldots \quad 4.5$$

where $\left(\frac{\Delta P}{P_t}\right)^2 < 1$

Equation 4.4 may also be written in modulus form, hence:

$$\left|\frac{P_t - P_m}{P_t}\right| = \left|\mathcal{E}_d\right| + \left|\mathcal{E}_m\right| \quad \ldots\ldots \quad 4.6$$

where $\mathcal{E}_d = \frac{S_{11}}{S_{12}\,S_{21}\,\Gamma_L}$ or if effective directivity (D) is defined as $S_{11}/(S_{12}\,S_{21})$, then

$$\mathcal{E}_d = \frac{D}{\Gamma_L} \quad \ldots\ldots \quad 4.6(a)$$

and

$$\mathcal{E}_m = \frac{S_{22}\,\Gamma_L}{1 - S_{22}\Gamma_L} \quad \ldots\ldots \quad 4.6(b)$$

Both $\mathcal{E}_d$ (Directivity Error) and $\mathcal{E}_m$ (Mis-match Error) are phasors and because of their great importance, a detailed examination of each is essential.

4:2 Directivity Error (ε_d)

The directivity error arises from physical deviations from the ideal within the directional devices and can come from many sources, such as deviations from the prescribed geometry, connector mis-matches or imperfect internal terminations. The manner in which directivity influences an actual measurement is shown in figure 4.2 where the amplitude of the sampled incident wave (a_1) is considered to be unity. The resultant waves at b_1 is the phasor sum of the directivity error wave (ε_d) and the reflected wave (ε_L) from the device under test. The measured reflection coefficient (ρ_m) is the phasor sum (b_1) referenced to (a_1) unity.

Figure 4.2

Possible Error Caused by Directivity

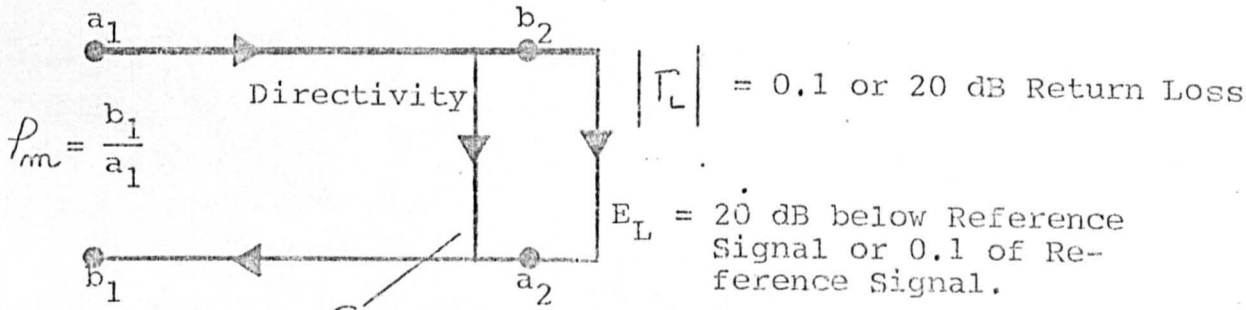

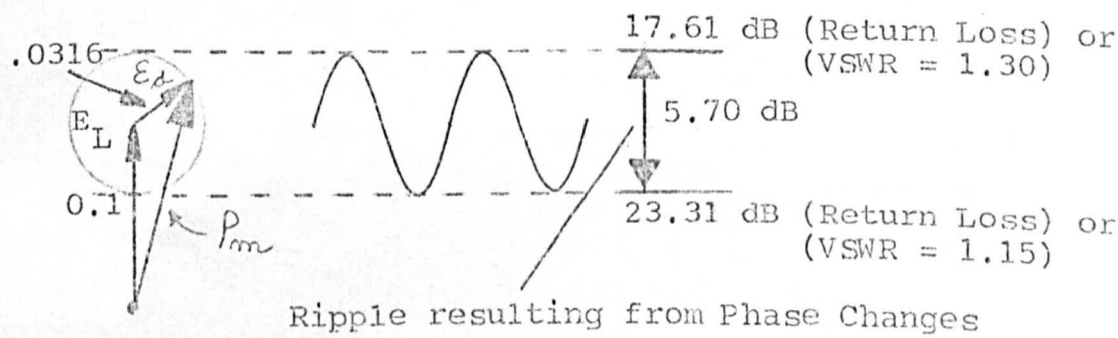

The reflectometers used in the measurements are Hewlett Packard Models 8741A (o.11 to 2.0 GHz) and 8742A (2.0 to 12.4 GHz). The directivities quoted (Ref 4.2) are $\geq$ 36 dB (0.11 - 1 GHz) $\geq$ 32 dB (1 - 2 GHz) and $\geq$ 30 dB (2 - 12.4 GHz). The case presented in figure 4.2 is the case where a coupler with an effective directivity of 30 dB is used to measure a device having a reflection coefficient of 0.11 (SWR = 1.22 or 20 dB return loss).

If the directivity error is in phase with E_L, the resultant is 0.1 + 0.0316 = 0.1316 or 17.61 dB down on the incident wave. If the directivity error (ε_d) opposes the reflected wave, the resultant is 0.1 - 0.0316 = 0.0684 or 23.30 dB down on the incident wave.

Summing up, it is seen that if a 30 dB coupler is used to measure a 20 dB return loss, the result would be a return loss of $20.0 \begin{smallmatrix} + 2.39 \\ - 3.30 \end{smallmatrix}$ dB, i.e there is an uncertainty region of 5.7 dB because of the poor coupler directivity. This error will increase with smaller measured reflection coefficients and will decrease when larger reflection coefficients are measured. A curve (Ref 4.3) showing the possible return loss error for a 35 dB coupler is shown in figure 4.4. Similar curves to Figure 4.3 are also given by Lacy and Oldfield (Ref. 4.4)

Figure 4.3

Possible Return Loss Error Caused by a Directivity of 35dB as a Function of Return Loss Measurement.

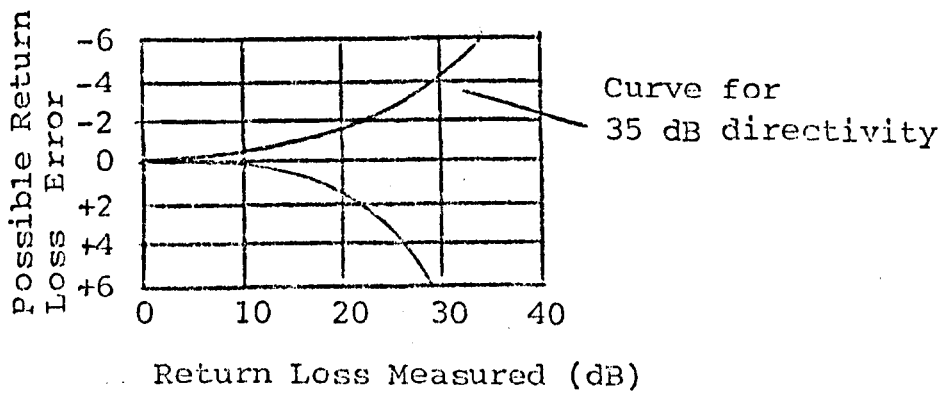

4:3 Source Mis-Match Error (ε_m)

Source mis-match error (ε_m) occurs when a reflectometer is incapable of completely absorbing the reflected wave from a device under test. This error arises because the VSWR of the output port of the reflectometer which is also the source port for the device under test is not unity.

The error consequence of test port mis-match is demonstrated in figure 4.4 where the main reflected signal (solid lines) undergoes multiple reflections at a_2 (dashed lines) and emerges as

Figure 4.4

Possible Errors Due to Output Port Mis-match

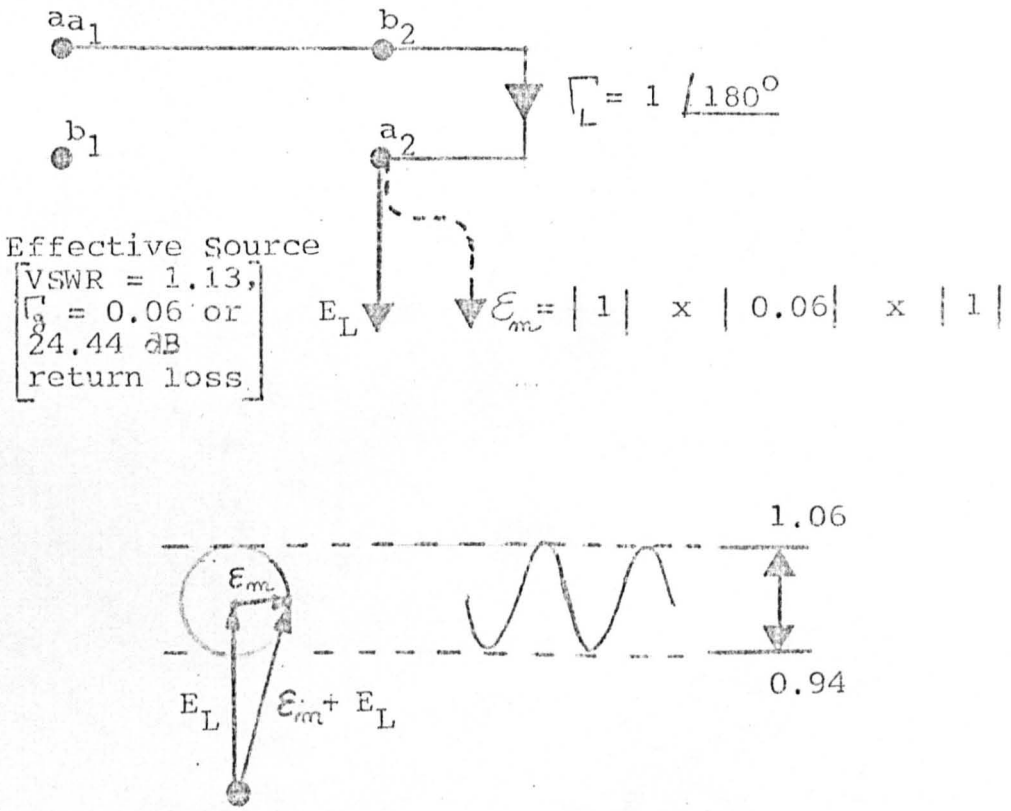

In figure 4.4, the graphical display is shown for the case of a reflectometer (VSWR 1.13) terminated by a short circuit. The resultant phasor ($\varepsilon_m + \varepsilon_L$) varies between 0.94 and 1.06.

This may seem somewhat contradictory to transmission line theory where for the case of real normalization and positive real loads the reflection coefficient $\leq |1|$. However, this resultant is really the result of multiple reflections and should not be confused with a single reflected wave. Note this error is at its worst when the device under test (DUT) has a reflection coefficient of unity. In cases where it has been necessary to establish a reference coefficient of unity, the open/short reference method (Ref 4.3) has been used. (Fig 4.5). This method is not exact and provides a marginally better reference.

Figure 4.5

Preferred Reflection Calibration with Open/Short Reference

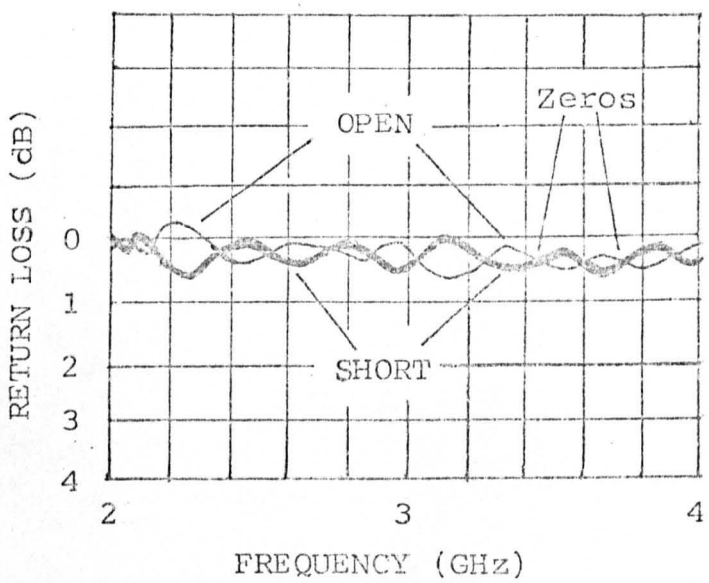

The figure is largely self-explanatory and shows how the average reference may be established by taking the mean between a reference short circuit and a reference open circuit. Sometimes difficulties have been encountered in locating the zeroes to the presence of harmonics in the signal. In such a case, a low pass filter has helped considerably.

4:4 The Combined Measurement Errors

The two errors, directivity ($\mathcal{E}_d$) and mis-match ($\mathcal{E}_m$) discussed previously have been combined by Dunwoodie (Ref 4.10) into a very convenient graph to establish the accuracy limits of a reflectometer. This is shown in figure 4.6

Figure 4.6
General Error Limit Curves
for a Directional Device

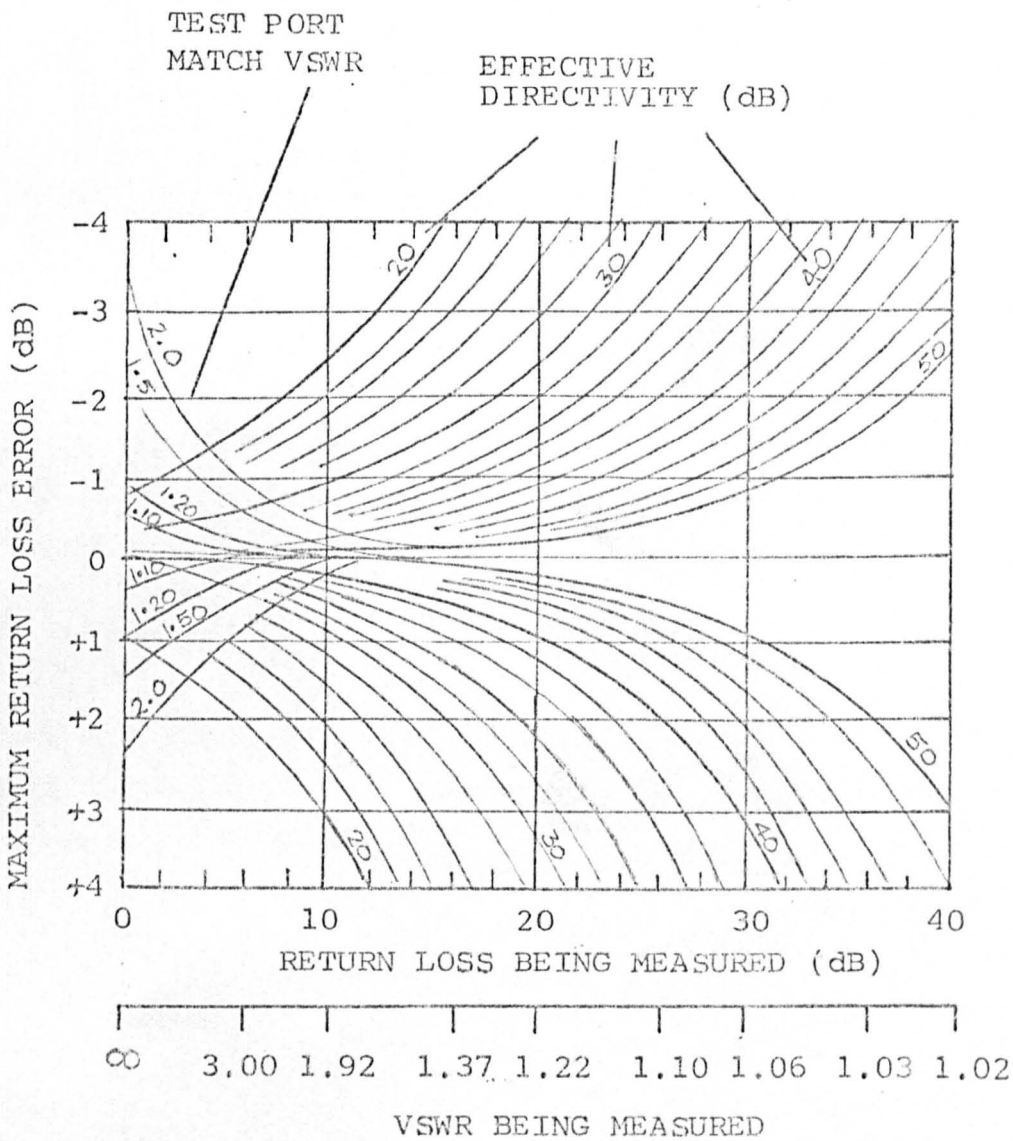

For the case of the reflectometer used, (HP8742A) with a directivity of 30 dB and an effective source match of 1.13, the following can be established.

Table 4.1

Return Loss Measured (dB)	Maximum Return Loss Error (dB)		Total Return Loss Error (dB)
	+	-	
0	0.2	0.6	0.8
10	0.9	0.8	1.7
20	3.3	2.39	5.67
30	∞	6.0	∞

4:5 The Effects of Adapter/Connector Errors

Refelectometer measurements frequently have to be made on devices which are fitted with a different connector to that of the reflectometer measurement port. When this occurs, an inter-series adapter/connector is used and the measurement accuracy is degraded. The effective directivity (magnitude and phase) of the reflectometer is reduced and the test port (source) match is degraded because of the additional wave reflections from the adapter.

An analysis of adapter degradation may be carried out by reference to the signal flow graphs of figure 4.7(a) and its topological equivalent in figure 4.7(b).

Figure 4.7(a)

Signal Flow Graph of Reflectometer and Adapter

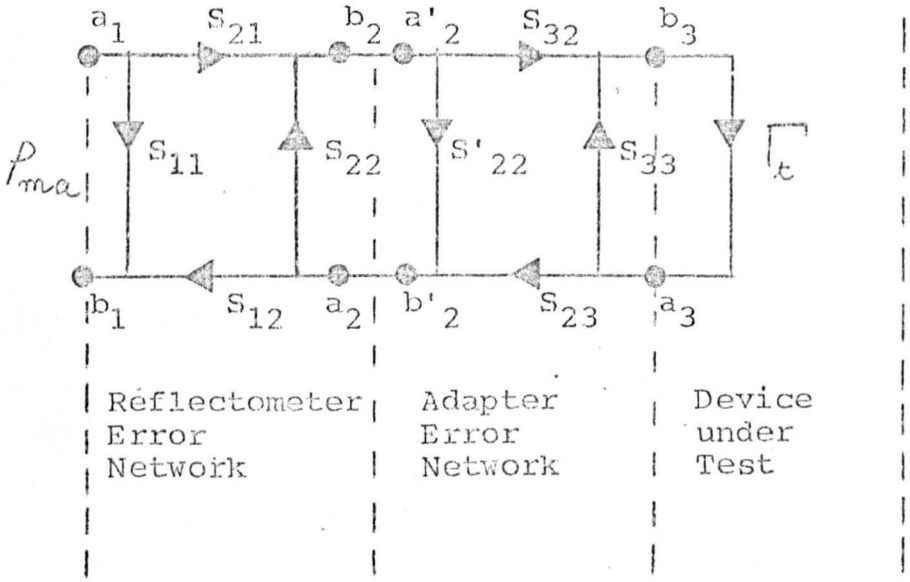

Figure 4.7(b)

Topological Equivalent of Figure 4.7(a)

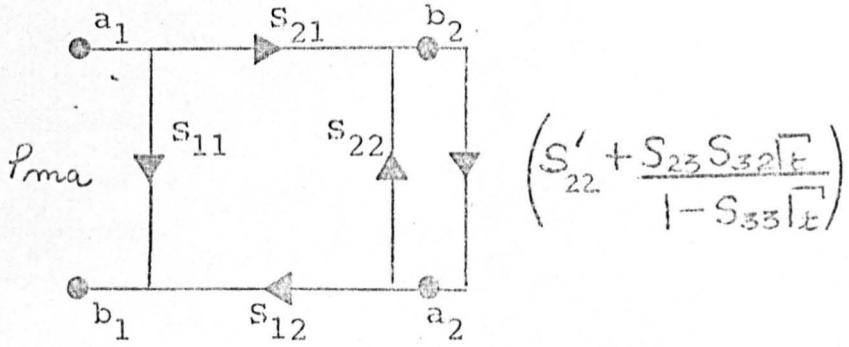

Let Γ_t = reflection coefficient of device to be measured.

Let $\rho_{ma} = b_1/a_1$ = the measured reflection coefficient when an adapter is used.

and $\rho_{wa} = b_1/a_1 = S_{11} + \frac{S_{12}S_{21}\Gamma_t}{1-S_{22}\Gamma_t}$ when no adapter is used.

The additional reflection coefficient measurement uncertainty (ρ_a) is defined as the difference between ρ_{ma} and ρ_{wa}. Hence:

$$\rho_a = \rho_{wa} - \rho_{ma} = S_{11} + \frac{S_{12}S_{21}\Gamma_t}{1 - S_{22}\Gamma_t} - S_{11} - \frac{S_{12}S_{21}\left[S'_{22} + \frac{S_{23}S_{32}\Gamma_t}{1 - S_{33}\Gamma_t}\right]}{1 - S_{22}\left[S'_{22} + \frac{S_{23}S_{32}\Gamma_t}{1 - S_{33}\Gamma_t}\right]}$$

$$\rho_a = \frac{S_{12}S_{21}\Gamma_t}{1 - S_{22}\Gamma_t} - S_{12}S_{21}\left[\frac{S_{22}'(1 - S_{33}\Gamma_t) + S_{23}S_{32}\Gamma_t}{(1 - S_{33}\Gamma_t) - S_{22}S'_{22}(1 - S_{33}\Gamma_t) + S_{23}S_{32}\Gamma_t}\right]$$

..... 4.7

Although mathematically useful, equation 4.7 does not present a very lucid picture of the adapter's effects because the parameters involved are seldom known. Most manufacturers prefer to issue their adapter specifications in terms of VSWR. However useful information may be obtained by consideration of the vectorial properties. In figure 4.8(a), 4.8(b) and 4.8(c) let

Γ_t = the true reflection coefficient.

ρ_u = the error vector due to the imperfect reflectometer.

ρ'_m = the measured reflection coefficient without adapter.

ρ_m = the measured reflection coefficient with adapter.

ρ_a = the additional error due to the adapter.

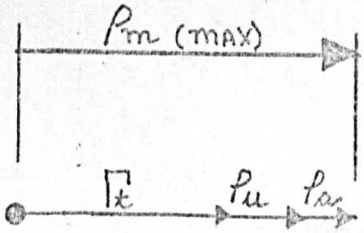

Fig. 4.8a
Lowest Return Loss

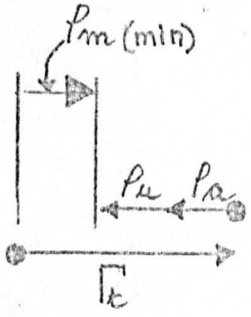

Fig. 4.8b
Highest Return Loss

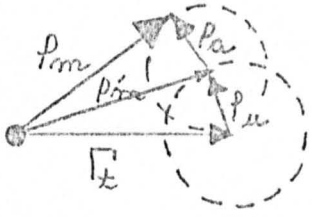

Fig. 4.8c
Largest Phase Error

From figures 4.8(a) 4.8(b), it can be seen that for the worst case errors, the magnitude error simply adds or subtracts from the true reflection coefficient. From figure 4.8(c) the maximum phase error occurs when ρ_m is tangential to the circle described by ρ_a and when ρ'_m is tangential to the circle described by ρ_a . The additional phase error

$$\psi = \tan^{-1} (\rho_a / \rho_m) \quad \ldots\ldots \quad 4.8$$

or $$\psi = \sin^{-1} (\rho_a / \rho'_m) \quad \ldots\ldots \quad 4.8(a)$$

Consider the case for the Hewlett Packard 8742A reflectometer used when it has an effective source reflection coefficient of $|0.06|$, (VSWR = 1.3) and a directivity of 30dB i.e. ($|E \text{ ref}| / |E \text{ inc}| = |0.0316|$).

Let an adapter with a VSWR of 1.05 (32dB return loss or reflection coefficient of 0.025) be used with the coupler (Fig. 4.9).

The two reflections when in phase can add up to (0.0316 + 0.025) i.e., 0.0566 of the incident wave which makes the new effective directivity approximately 25dB.

The test port match of SWR 1.13 ($\Gamma_g' = 0.06$) can become 0.06 + 0.025 = 0.085 when the adapter reflection adds in phase. The new effective test port source match is VSWR = 1.18 or a return loss of 21.4dB. Hence it can be concluded that there is a considerable degradation of the measurement system.

Figure 4.9

Adapter Error Effects on Reflectometer

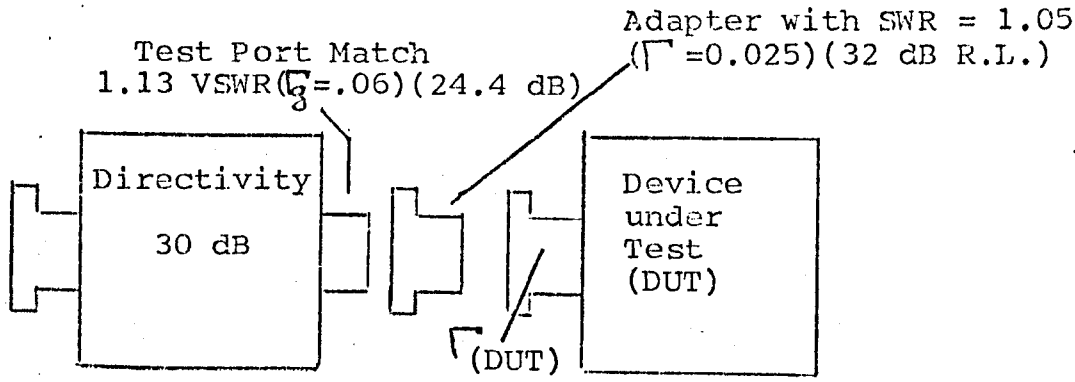

Effective Directivity.	Effective Test Port Match
Directional Coupler = 0.0316 Adapter = 0.025 0.0566 New Directivity is 20 log(1/.0566) = 25 dB	Coupler SWR 1.13 = 0.06 Adapter SWR 1.05 = 0.025 New Match Γ = 0.085 or VSWR = 1.18

It is important to examine the measurement limits for a 20 dB return loss when the reflectometer (HP 8742A) is used with and without an adapter (VSWR 1.05). Using the figures above and going through the calculations of this section, it can be written:

Return Loss of Device (dB)	Measurement Uncertainty	
	Coupler only (dB)	Coupler & Adapter(dB)
20	+2.39 to -3.30 = 5.7 dB (total)	+3.87 to -7.18 = 10.0 dB (total)

Note that a 5.7 dB return loss uncertainty has been increased to a 10 dB uncertainity simply as a result of adding an adapter with a VSWR of 1.05!

To avoid having to calculate the above results, Dunwoodie and Lacy (Ref. 4.3) have presented another graph (Fig 4.10).

Figure 4.10
Uncertainty due to Adapter Error

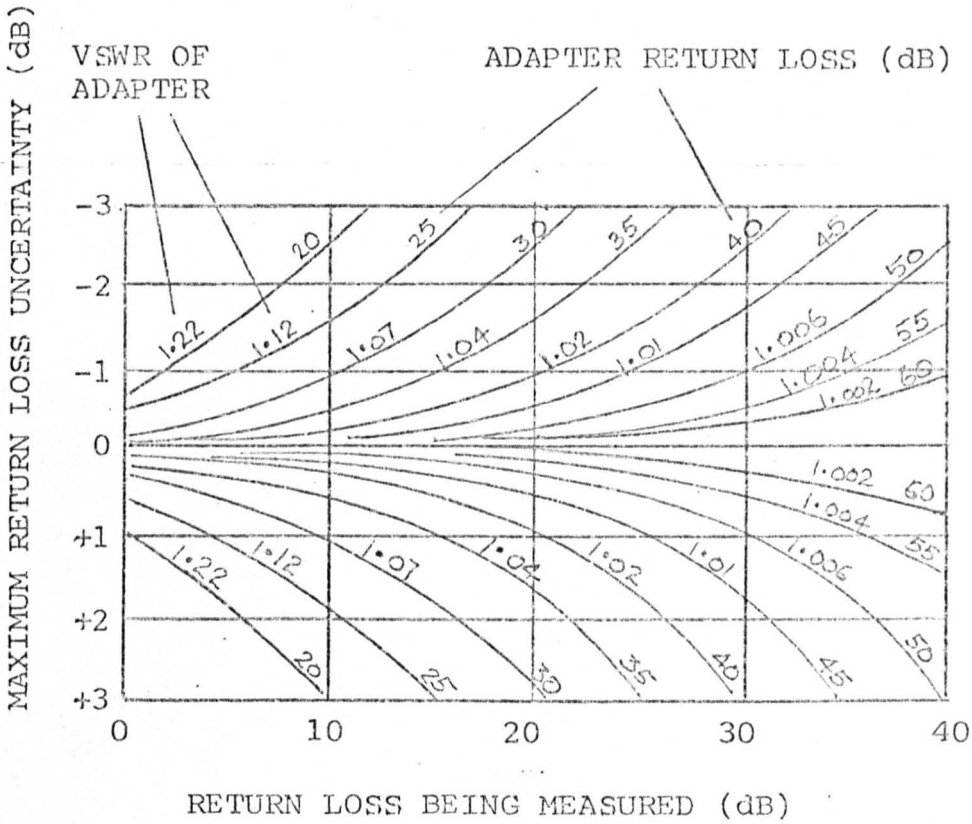

This graph may be used in two ways, (a) to evaluate the effects of the adapter alone or (b) in conjunction with Figure 4.6 when used in the latter manner, the maximum return loss uncertainty (dB) of both graphs are added together to yield the total return loss measurement uncertainty.

4:6 An Alternative Method of Specifying Reflectometer Accuracy

Another form frequently used to quantify reflection coefficient measurement uncertainty is that given by a power series equation where

$$\Gamma_\mu = A + B\Gamma_L + C\Gamma_L^2$$

Γ_μ = Measured Reflection Coefficient Uncertainty

Γ_L = Actual Reflection Coefficient of the Device Under Test and A, B & C are Phasor Constants.

These constants A, B & C can be readily derived by reference to the signal flow graph of figure 4.11, where the justification for using a bilinear transformation has already been shown in section 2:3.

Figure 4.11

Signal Flow Graph of a Reflection Measuring System

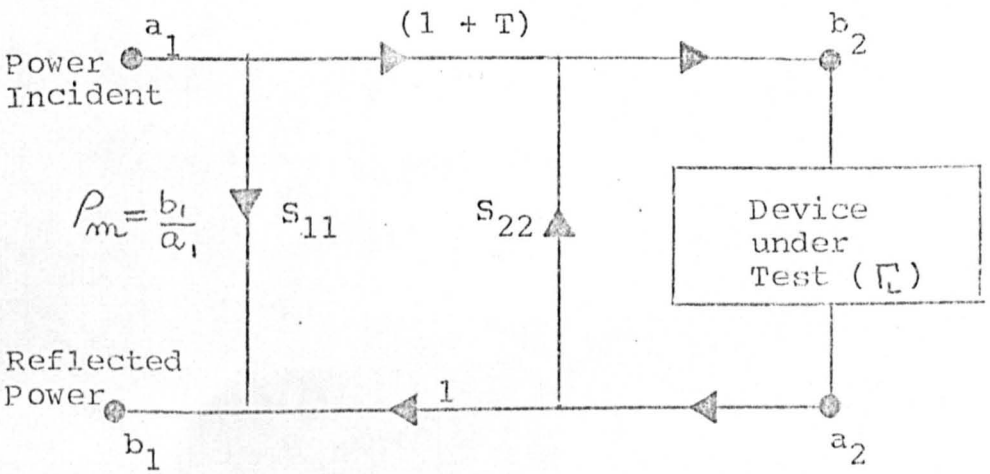

In this diagram, S_{11} represents the power transferred directly from the input terminal (a_1) of the reflectometer to its output (b_1) independent of the device under test. Directivity in the coupler is the major contributor but this also includes leakage between the various connectors and the detection systems.

T represents the system scaling factor. The coupling of the test set and the detector and display sensitivities are the major contributors to the scaling factor.

S_{22} represents the effective source match to the device under test, i.e. the effective reflection coefficient "looking back" into the test coupler from the device under test.

ρ_m is the measured reflection coefficient.
Γ_L is the true reflection coefficient.

From figure 4.11 and the application of Mason's Non-Touching Loop Law (Refs 4.11 and 4.12) it can be written:

$$\rho_m = S_{11} + \frac{1(1+T)\Gamma_L}{1 - S_{22}\Gamma_L} \qquad \ldots\ldots \quad 4.9$$

and since $S_{22}\Gamma_L \ll 1$, the binomial expansion is applicable,

$$\rho_m = S_{11} + (1+T)\Gamma_L \left[1 + (S_{22}\Gamma_L) + (S_{22}\Gamma_L)^2 + (S_{22}\Gamma_L)^3 \ldots\right]$$

The higher order terms are sufficiently small to be neglected, hence

$$\rho_m \simeq S_{11} + \Gamma_L(1+T)\left[1 + S_{22}\Gamma_L\right]$$

$$= S_{11} + \Gamma_L + T\Gamma_L + S_{22}\Gamma_L^2 + T S_{22}\Gamma_L^2$$

Since $T\,S_{22}\Gamma_L^2$ is comparatively small

$$\rho_m \simeq \left[S_{11} + T\Gamma_L + S_{22}\Gamma_L^2\right] + \Gamma_L \qquad \ldots\ldots \quad 4.10$$

The difficulty with equation 4.10 is that "T" is unknown as yet but it can be found by the use of a calibrating short-circuit provided the bilinear transformation constants remain invariant. Hence, if $\Gamma_L = 1\angle 180^o$ and the measured short-circuit coefficient is $\rho_m(\text{short})$, equation 4.10 becomes:

$$\rho_{m(\text{short})} = \left[S_{11} - T + S_{22} - 1\right].$$

and by setting $\rho_{m(\text{short})}$ on the instrument output to be the reference $= 1\angle 180^o$, the above equation reduces to

$$T = (S_{11} + S_{22}) \qquad \ldots\ldots \quad 4.11$$

and substituting equation 4.11 into 4.10 results in

$$\rho_m = S_{11} + (S_{11} + S_{22})\Gamma_L + S_{22}\Gamma_L^2 + \Gamma_L \qquad \ldots\ldots \quad 4.12$$

If the <u>reflection coefficient uncertainty (ρ_u)</u> is defined as $\rho_m - \Gamma_L$, then from equation 4.12

$$\rho_u = S_{11} + (S_{11} + S_{22})\Gamma_L + S_{22}\Gamma_L^2 \qquad \ldots\ldots \quad 4.13$$

or in modulus form for maximum magnitude error

$$\rho_u = \pm\left[|S_{11}| + |(S_{11}+S_{22})||\Gamma_L| + |S_{22}||\Gamma_L|^2\right] \qquad \ldots\ldots \quad 4.14$$

or $\rho_u = A + B\Gamma + C\Gamma^2$ $\qquad \ldots\ldots \quad 4.14(a)$

where Γ = Scalar equivalent of Γ_L; $A = S_{11}$ = Effective Directivity. $B = (S_{11}+S_{22})$ = Calibration Error; C = Effective Source Match.

The reflection coefficient angle uncertainty (ϕ) can be derived directly by a trigonometrical derivation similar to that of equation 4.5 or by reference to the phasor diagram of figure 4.12. The measured reflection coefficient ρ_m is at all times the phasor sum of the true reflection coefficient (ρ_t) and the reflection coefficient uncertainty (ρ_u). The angle ϕ represents the error angle between the true reflection coefficient (ρ_t) and the measured reflection coefficient (ρ_m) and it will be at its maximum when ρ_m is tangential to the circle of movement of ρ_u .

Figure 4.12

Phasor Diagram the Reflection Coefficient Angle Uncertainty

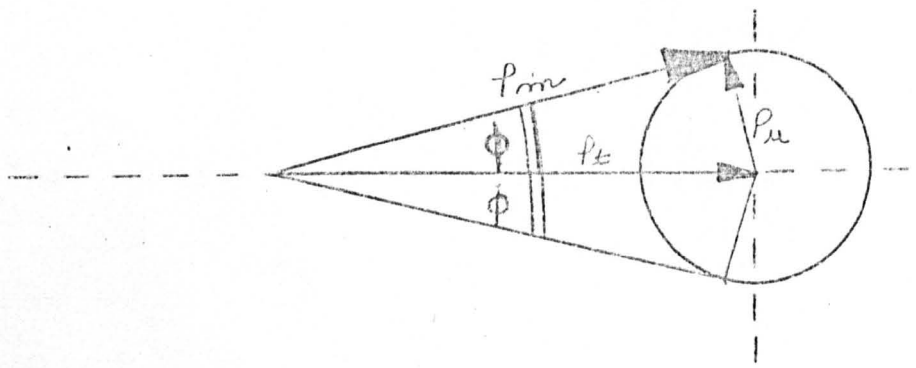

Hence:

$$\text{SIN } \phi_{MAX} = \frac{\rho_u}{\rho_t} \quad \text{or}$$

$$\phi_{MAX} = \pm \text{ Arc Sin } \frac{\rho_u}{\rho_t} \quad \ldots\ldots \quad 4.15$$

For small angles, $\rho_t \simeq \rho_m$ and equation 4.15 may be written as:

$$\phi_{MAX} = \pm \text{ Arc Sin } \frac{\rho_u}{\rho_m} \quad \ldots\ldots \quad 4.16$$

4:6.1 Application of Error Equations

The equations 4.13, 4.14, 4.15 and 4.16 are reasonably good approximations. Take for example the Hewlett Packard reflectometer type 8742A which is used in themeasurement system. The manufacturer's data (Refs 4.2 and 4.7) quote the following for 8-12 GHz operation:-

Directivity $\geq$ 30 dB, Residual Reflection Coefficient = 0.03 and coupling factor = 20 dB.

Hence, taking the transmission factor as 0,995 applying equation 4.14(a) and 3.10(b),

$A = S_{11} = 0.03162;$

C = Effective Source Match (see equation 3.10(b))
$= 0.03 + .995 \times .03162 = 0.06142$

$B = A + C = .09308$

$$\therefore \quad \rho_u = \pm \left[0.0316 + 0937 \left|\Gamma_L\right| + .061 \left|\Gamma_L\right|^2\right] \quad \ldots\ldots \quad 4.17$$

When it was desired to corroborate these figures with the Hewlett Packard figures, great difficulty was experienced because the manufacturer does not publish figures for the reflectometer on its own. However, values can be inserted into equation 4.17 and the results compared with the graph of figure 4.6. For example if $\Gamma_L = 0.1$ i.e., a return loss of 20 dB,

$$\rho_u = \pm \ 0.04172$$

giving a measured ρ_m of 0.1 ± 0.04172

$= 0.14172$ or 0.05828

i.e., a return loss of 16.64 dB or 24.69 dB. When this was compared with the maximum return loss given by figure 4.6, it was found to be within 1 dB of the calculated values.

4:7 System Accuracy

The reflectometer system used for uncorrected measurements is the Hewlett Packard HP8410A. (Ref 4.2). For the overall uncertainty of the complete system i.e., including the effects of coupler directivity, source match and system tracking with frequency, the manufacturer's claim that the reflection coefficient magnitude of the unknown (ρ_m) is measured to within (ρ_u) where

$$\rho_u = \pm (0.01 + 0.02 |\rho_m| + 0.05 |\rho_m|^2 \text{ for } 0.11 \text{ to } 1.0 \text{ Ghz} \quad \ldots 4.18$$

$$\rho_u = \pm (0.02 + 0.02 |\rho_m| + 0.05 |\rho_m|^2 \text{ for } 1.0 \text{ to } 2.0 \text{ Ghz} \quad \ldots 4.19$$

$$\rho_u = \pm (0.032 + 0.052 |\rho_m| + 0.036 |\rho_m|^2 \text{ for } 2 \text{ to } 8 \text{ Ghz} \quad \ldots 4.20$$

$$= \pm (0.032 + 0.04 |\rho_m| + 0.07 |\rho_m|^2 \text{ for } 8.0 \text{ to } 12.4 \text{ Ghz} \quad \ldots 4.21$$

and the reflection coefficient angle uncertainty is givenby $\pm$ Arc Sin $\frac{\rho_u}{\rho_m}$ for $\phi \leq 90^\circ$.

The results of equation 4.18 to 4.21 for the magnitude and phase angle system uncertainty are shown in figures 4.13 and 4.14. The case for the same equations when the directivity error is cancelled are shown in figures 4.15 and 4.16.

Hewlett Packard arrive at the figures by using a single combined bilinear transformation to represent all the errors in the system. The justification and the conditions by which such an assumption may be made are discussed in detail in Chapter 5. They then follow a derivation similar to that of Section 4.6. Their method for the determination of the magnitude error can be found in Appendix B of Reference 4.9. The phase error is not derived but it is almost certainly derived in the manner of section 4.6.

TYPICAL SYSTEM UNCERTAINTY vs. REFLECTION COEFFICIENT MEASURED

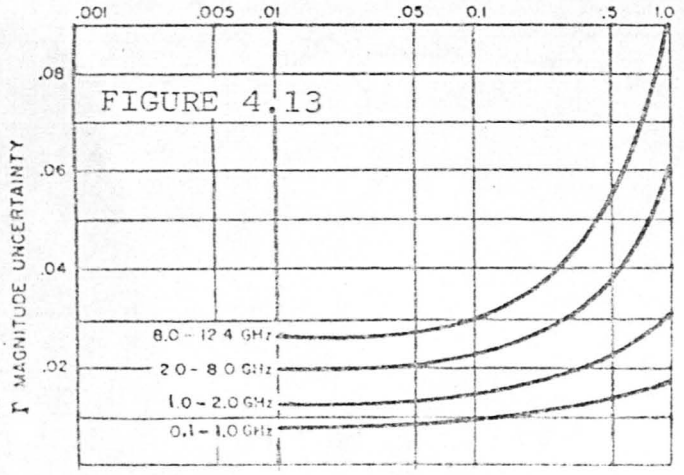

A

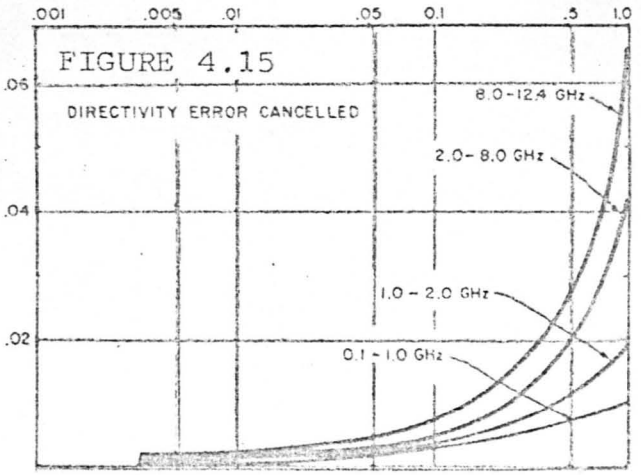

B

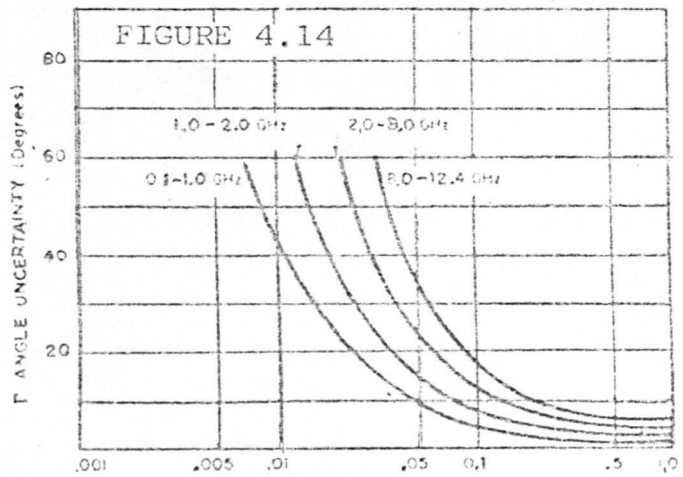

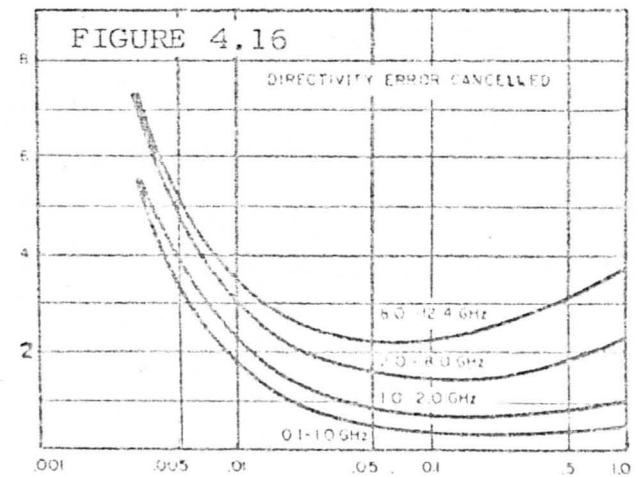

REFLECTION COEFFICIENT MEASURED

One interesting item that has emerged from Appendix A of Reference 4.9 is that Hewlett Packard do not always calculate the full effect of the effective source match in their reflectometer. The following paragraph is taken from Appendix 'A' of reference 4.9:

> "The above solutions do represent absolute worst cases but are usually modified somewhat. The through-line mis-match of a coaxial coupler is largely due to the effects of both input and output connectors. Since the input connector is within the loop and its effect thus removed, some recommend including only 50 to 70% of the specified through-line match."

Hewlett Packard also quote their accuracy specifications with the directivity error cancelled. Such curves are shown in fig. 4.15 and 4.16. Cancellation of directivity errors within a small frequency band is practical. For example in some microstrip reflectometers (Ref. 4.13) the secondary line load is adjusted for magnitude and phase so that equal but opposite signals cancel the directivity error signals at the detector. An alternative method is described in Ref. 4.14

In wide band frequency measurements, this cancellation is not really practical as both the magnitude and phase required for cancellation at each frequency should be known.

4:8 Conclusions

The two main errors of reflectometer measurements, directivity and source match have been discussed extensively in this chapter. Dunwoodie's chart of figure 4.6 is extremely useful for it determines the maximum return loss error for various directivites and source match. The limits of measurement accuracy of the equipment used in this thesis has been summarized in Table 4.1 but it may also be calculated using the alternative methods derived in Section 4:6 and 4:7.

Additional errors due to connector/adapter transistions can deteriorate disastrously a measurement system. Both a mathematical treatment and a resultant chart for this error has been included in Section 4:5.

For this chapter, an extensive search had to be made of the literature because many of the instrument specifications had been changed by the manufacturers as production problems were encountered. Careful cross-checks had to be made to ensure that the data obtained were pertinent to the equipment used.

* * * * * * * * * * *

4:9 References

4.1 Dwight, H.B. "Tables of Integrals and other Mathematical Data. MacMillan & Co. , New York, 4th Edition, 1972 pp 118.

4.2 Hewlett Packard Technical Data Sheets "Network Analyser Model 8410A" dated 1st July 1967 8 pages.

4.3 Dunwoodie, D and Lacy P, "Why Tolerate Unnecessary Measurement Error?" Siltron Technical Review Vol 3 No 1, 1975.

4.4 Lacy, P and Oldfield, W "A Precision Swept Reflectometer" Microwave Journal, April 1973, pp 31-34 & 50.

4.5 Hewlett Packard Catalogue "Electronic Instruments and Systmes for Measurement/Analysis/Computation 1973.

4.6 Hewlett Packard "Coaxial & Waveguide Catalogue and Microwave Measurement Handbook" 1977-78.

4.7 Anderson, R.W. & Dennison, O.T. "An Advanced New Network Analyser for Sweep-Measuring Amplitude and Phase from 0.4 to 12.4 Ghz" Hewlett Packard Journal, Feb. 1967, pp 2-10.

4.8 Hewlett Packard Technical Data Sheet "Network Analyser 8410S (options)" dated 1st March 1970.

4.9 Hewlett Packard "High Frequency Swept Measurements" Application Report 183, Nov 1975.

4.10 Dunwoodie, D.E., "Pin-point Errors in Mismatch Measurements", Microwaves, March 1975. pp 50-60.

4.11 Mason, S.J. "Feedback Theory; Some Properties of Signal Flow Graphs" Proc. I.R.E. Vol 41, No9 pp1144-56, Sept 1953.

4.12 Mason, S.J. "Feedback Theory - Further Properties of Signal Flow Graphs" Proc I.R.E. Vol 44, No 7 pp 920-926. July 1955.

4.13 Foster, K "Private Communication with K Foster of Lanchester Polytechnic, Coventry. 1978.

4.14 Hewlett Packard Application Note 117-1 "Microwave Network Analyser Applications." June 1970

* * * * * * * * * *

CHAPTER V

REFLECTOMETER CORRECTION METHODS

5.0 Introduction

The purpose of this chapter is to establish a general error correction bilinear trransformation model that will enable the true reflection coeffcient of a device under test to be determined even when measurement is carried out with imperfect instruments. At the commencement of this research in 1972, there were two preferred methods of one port measurement correction. One method was that suggested by Barlow and Cullen (Ref. 5.1) in 1950 for determing the constants of the bilinear transformation and the other was that due to Hackborn (Ref. 5.9). Barlow and Cullen suggested using a short circuit, an open circuit made by using a short-circuit a quarter of a wavelength away, and a matched load. With the event of broadband measurements, this method lost favour because the open circuit became virtually indefinable; a fixed length of quarter wavelength can vary by as much as 100% for octave band measurements.

The other method which Hackborn described was that using a short circuit, an off-set short, and a sliding load for calibration measurements. The purpose for using the sliding load at three settings was to describe the locus of a circle whose theoretical centre could be calculated to resemble a perfectly matched termination. This method was applied by Adams (Ref. 5.8) in phase-lock correction systems, by Shurmer (Ref. 5.11) in computer controlled measurements and by Reich (Ref. 5.10) in microstrip measurements. Reich used a sliding microstrip load with a length of 100 mm. Twistleton (Ref. 5.12) has also made some sliding microstrip matched loads with VSWR's of 1.03 to 1.05 for the 8-12 GHz frequency band but these loads were large - approximately 500 mm long.

Although these correction systems performed satisfactorily, two main problems remained. Due to dispersion, it is difficult to accurately define an offset electrical length in microstrip and the use of a sliding load particularly on microstrip imposes severe restrictions.

For example two of the requirements at that time were to measure lumped components for use at microwave frequencies and to measure the input and output admittances of transistors. It was clear that the physical size of the components in situ would not permit the use of a sliding load. Hence new correction methods had to be investigated.

In this chapter, various methods of correction including the three methods invented by the author during this research will be presented. The first correction method (The Three Short Circuits) was published in March 1973 (Ref 5.13) The two other correction methods (the "Four Short Circuit Correction Method" and the "Four Unknown Terminations and a Reference Short Method") were submitted for publication to "Electronic Letters" in February 1976. This was rejected by the I.E.E. as being too lengthy to print in the above publication. Consequently two full papers were prepared for publication. One was published in the "Radio and Electronic Engineer" (Ref 5.23) and the other was published in the "Microwave Journal (Ref 5.24).

5:1 The Elements of the Error Correction Model

For the sake of clarity, some reiteration of the points discussed previously is necessary. The system described throughout and represented in Fig 5.1 is the Hewlett Packard Network Analyser 8410A which comprises a dual channel receiver (Type 8411A & 8410A) and a polar display unit (type 8414A). The reflectometers used can be either the Hewlett Packard Type 87410A or 8742A. The connector error network represents any connector or between-series adaptor (e.g., Microstrip to APC7) that connects the device under test to the reflectometer. The signal source used was one of the Hewlett Packard 8690A series oscillators.

Figure 5.1
Block Diagram of Error Networks

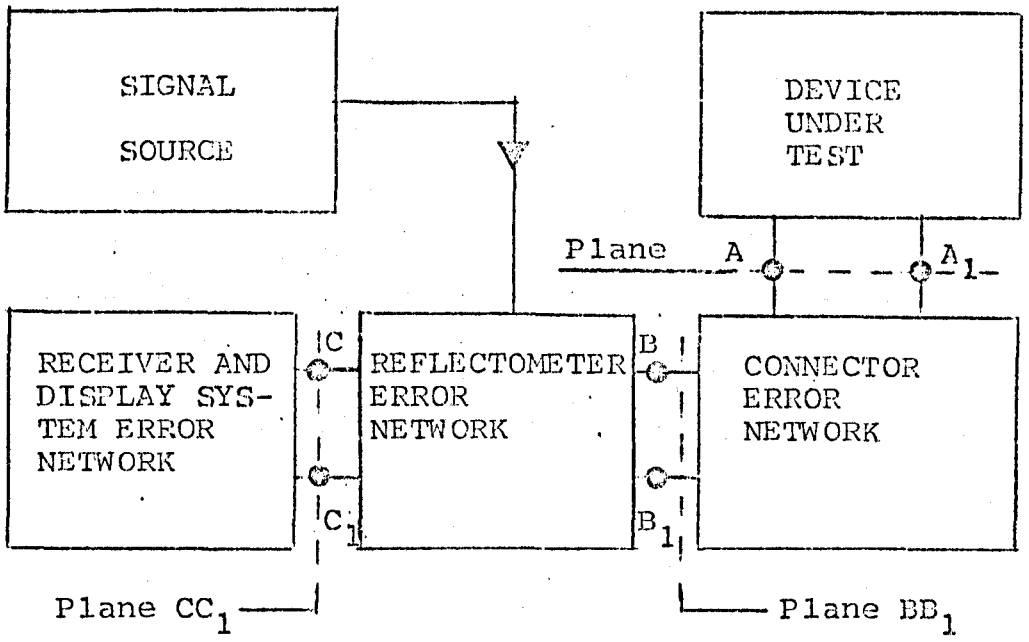

Briefly, the incident wave at B goes through the connector and enters the device under test at A. The reflected signal from the test device is returned through the connector, through the reflectometer and then enters one channel of the dual channel receiver. This signal is then compared with a sample of the incident wave which was fed to the other channel by the reflectometer. The two signals are then displayed on the Polar Display.

To establish an error correction network for the system, it will be shown that the planes AA_1, BB_1, and CC_1 are related by the transformations shown in figure 5.2. And finally, a system bilinear transformation will be derived to replace the three transformations of figure 5.2.

Figure 5.2

Signal Flow Graph Error Networks

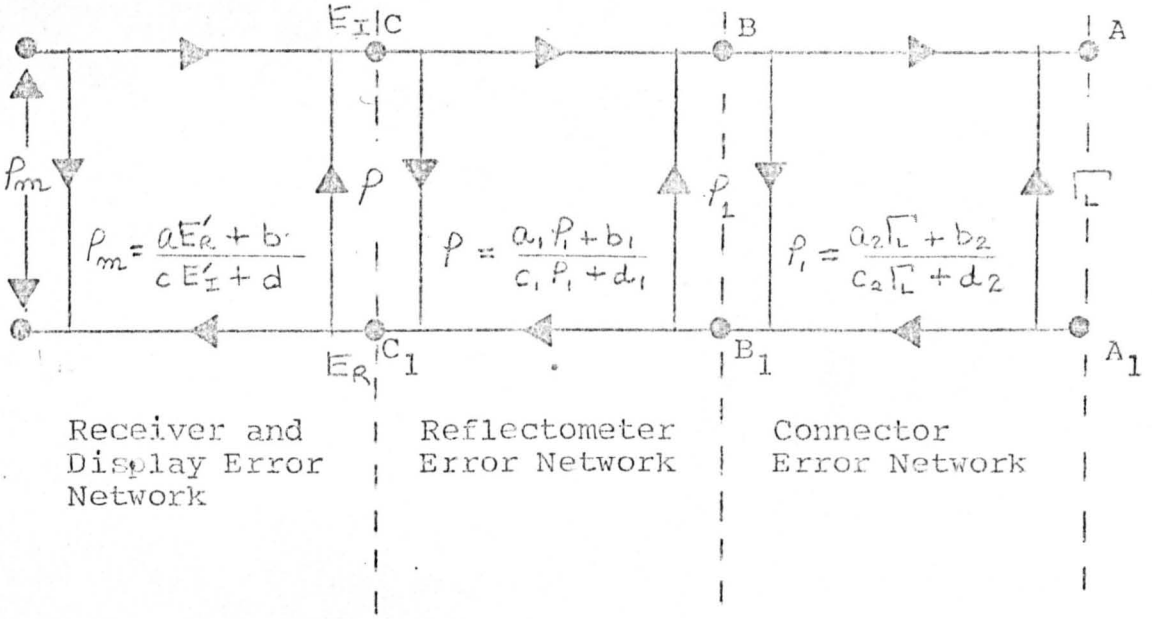

Let Γ_L represent the reflected to incident wave ratio at plane AA_1

ρ_1 represent the reflected to incident wave ratio at plane BB_1

ρ represent the reflected to incident wave ratio at plane CC_1

and ρ_m represent the reflected to incident wave ratio in the display plane.

It has been shown in appendix 11.1 that:

$$\rho_1 = \frac{a_2 \Gamma_L + b_2}{c_2 \Gamma_L + d_2} \qquad \ldots\ldots \quad 5.1$$

where a_2, b_2, c_2 and d_2 are the complex constants of the bilinear transformation between plane AA_1 and plane BB_1.

In equation 2.33 it has been shown that ρ_1 is also related to ρ by a bilinear transformation of the form

$$\rho = \frac{E_R}{E_I} = \frac{a_1 \rho_1 + b_1}{c_1 \rho_1 + d_1} \quad \ldots\ldots \quad 5.2$$

where a_1, b_1, c_1 and d_1 are the complex constants of the reflectometer.

However, ρ is the complex ratio of the reflected wave E_R to the incident wave E_I. The reflected wave E_R is subjected to frequency translation and amplification in one channel of the receiver. Let this effect be denoted by a complex constant "a". The same reflected wave, E_R is also subjected to detector and amplifier offset voltages etc. Let this effect be denoted by another complex constant "b". Hence, the combined effects on the reflected signal results in " $a E_R + b$ ".

Similar conditions are also experienced by the incident signal E'_I, and its final output may also be described by " $c E'_I + d$ " where "c" is the complex amplification factor of the incident receiver channel and "d" represents the complex setector and amplifier offset voltages etc.

The detection and display circuits take the ratio of the reflected signal ($a E'_R + b$) to the incident signal ($c E'_I + d$) to produce a reflection coefficient, ρ_m hence,

$$\rho_m = \frac{a E_R + b}{c E_I + d} \quad \ldots\ldots \quad 5.3$$

This is another bilinear transformation.

The results of appendix 11.2 can be utilized to show that equations 5.2 and 5.3 may be combined to produce

$$\rho_m = \frac{a a_1 \rho_1 + a b_1 + b}{c c_1 \rho_1 + c d_1 + d} \quad \ldots\ldots \quad 5.4$$

Equations 5.1 and 5.4 may also be combined in a similar manner to produce

$$\therefore \rho_m = \frac{[aa_1a_2 + ab_1c_2 + bc_2]\Gamma_L + [aa_1b_2 + ab_1d_2 + bd_2]}{[a_2cc_1 + cc_2d_1 + c_2d]\Gamma_L + [b_2cc_1 + cd_1d_2 + dd_2]} \quad \ldots\ldots \quad 5.5$$

Equation 5.5 is a bilinear transformation and may be written in the general form:

$$\rho_m = \frac{A\Gamma_L + B}{C\Gamma_L + D} \quad \ldots\ldots \quad 5.6$$

where $A = aa_1a_2 + ab_1c_2 + bc_2$ ..... 5.6(a)

$B = aa_1b_2 + ab_1d_2 + bd_2$ ..... 5.6(b)

$C = a_2cc_1 + cc_2d_1 + c_2d$ ..... 5.6(c)

$D = b_2cc_1 + cd_1d_2 + dd_2$ ..... 5.6(d)

Equation 5.6 is of vital importance for this equation is the basis of all single port reflectometer corrected measurements. However, it must be emphasized that for corrected measurements, it is of the utmost importance that the complex constants A, B, C and D remain constant throughout all the measurements. Checks and counter-checks must be made to ascertain that this is the case if accurate measurements are to be obtained.

Theoretical derivation of the bilinear constants of equation 5.6 is simply not practical because the constants themselves are the results of many more unknown constants derived in equations 5.1, 5.2 and 5.3. This can be clearly demonstrated by reference to equation 2.33 which is the basic derivation of equation 5.2.

Therefore the practical approach would be to determine the bilinear constants by measurement. To begin with any one of the four constants may be divided by itself to produce unity provided that the remaining three constants are also divided by the same constant. It follows that if three

calibration measurements, ρ_1 , ρ_2 , ρ_3 are made using three accurately defined calibration pieces, Γ_1 , Γ_2 , Γ_3 then the complex constants of equation 5.6 may be calculated. If a fourth measurement, ρ_m , is then made of a device with an unknown reflection coefficient Γ_x , use of equation 5.6 will permit the accurate calculation of Γ_x .

Many authors (Ref 5.1, 5.2, 5.3,) have suggested means of determining the constants of equation 5.6. One method suggested by Barlow and Cullen (Ref 5.1) is to use a short circuit, an open circuit and a matched load. Other methods involve the use of a short, an off-set short and a sliding load. In theory, there are numerous possibilities that may be used. However, due to practical difficulties; for example, the characterization of an open circuit or a practical matched load, the choice becomes limited. Further details concerning the methods invented by the author will be given in section 5.3.

5:2 Correction Methods Using the Invariance of the Bilinear Transformation Cross-Ratios

In correction systems involving bilinear transformations, the calculation of the corrected result is often tedious and especially time consuming if the complex constants of the bilinear transformations are to be derived. Beatty (ref 5.4) has proposed a simpler mathematical approach by utilising the invariance properties of the cross-ratios of bilinear transformations. It has been shown in appendix 11.4 that any four reflection coefficients Γ_1, Γ_2 , Γ_3 , Γ_4 at a measurement plane, W , can be bilinearly transformed to another measurement plane, Z , to produce reflection coefficients ρ_1 , ρ_2 , ρ_3 , ρ_4 . See figure 5.3. Furthermore, it has also been shown (appendix 11.4) that their resulting cross ratios i.e., $(\Gamma_1 - \Gamma_2)$, $(\rho_1 - \rho_2)$ etc are invariant and are related by:

$$\frac{(\rho_1 - \rho_2)\ (\rho_3 - \rho_4)}{(\rho_2 - \rho_3)\ (\rho_4 - \rho_1)} = \frac{(\Gamma_1 - \Gamma_2)\ (\Gamma_3 - \Gamma_4)}{(\Gamma_2 - \Gamma_3)\ (\Gamma_4 - \Gamma_1)} \quad \ldots\ldots \quad 5.7$$

Figure 5.3
The Invariance of the Bilinear
Transformation Cross-ratios

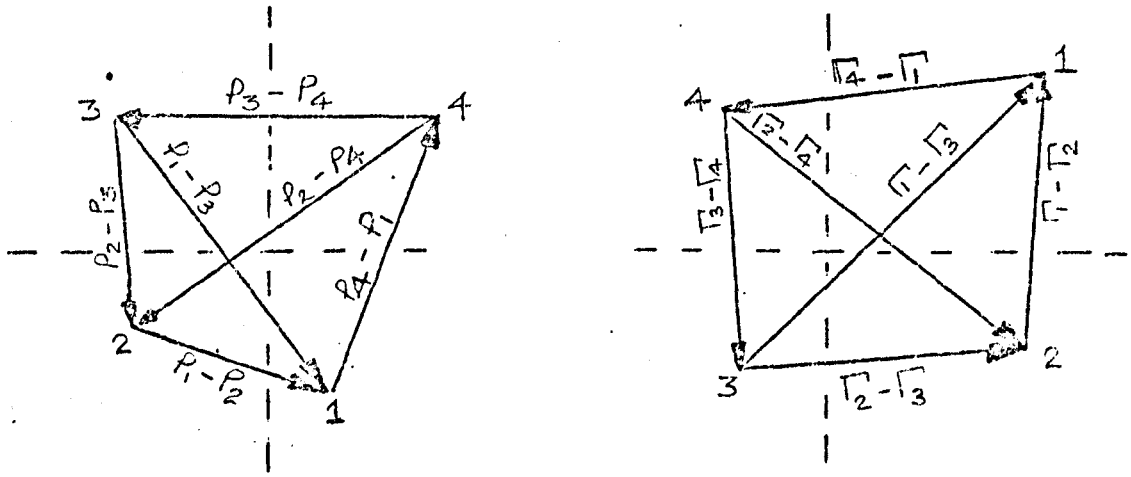

Measurement at "Z" plane

Measurement at "W" plane

Equation 5.7 is extremely useful for it bypasses the need to know the complex constants of equation 5.6 directly. However, it still requires the same three calibration measurements. For example in equation 5.7, let Γ_1, Γ_2, Γ_3 represent three known reflection coefficients (calibration pieces) and let ρ_1, ρ_2, ρ_3 represent their respective measurement values. Let a fourth measurement, ρ_4, be made of an unknown reflection coefficient Γ_4. It follows that a trivial manipulation of equation 5.7 will permit the calculation of Γ_4. Hence, in practical applications, equation 5.7 is invaluable as it permits easy calculation of the corrected

measurements. However, in the analysis of corrected measurement systems, this equation is not as useful for its mathematical simplification has inevitably disguised many practical measuring problems. For example, direct knowledge of the complex constant "B" in equation 5.6 helps to ascertain the effective directivity of the measurement system (see equation 11.2.7(b) and section 5.3). Directivity should be relatively constant at a given frequency in a measurement system. If this differs radically in another set of measurements then equipment malfunction can be easily traced. This problem will not be so easily identified if equation 5.7 was used. Hence the three measurement correction systems presented by the author will be based on the general correction expression of equation 5.6.

5:3 A General Review of One Port Reflectometer Error Correction

5:3.1 Theoretical Error Model

Figure 5.4

Scattering Parameters of the Complete Measuring System

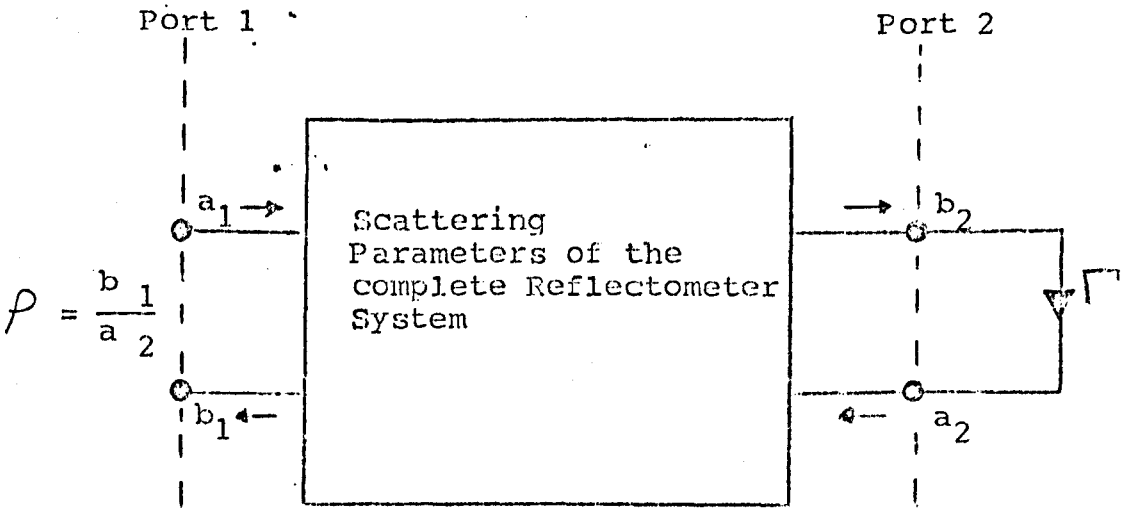

The complete measurement system including reflectometer, receiver, display, connectors etc., is considered as a two port network in figure 5.4. The device to be measured having a true reflection coefficient Γ is connected to port 2. The measured reflection coefficient ρ is that seen at port 1.

The mathematical details of the analysis which follows have been derived in appendix 11.2. To avoid repetition, only the results will be quoted here.

The scattering parameters of the two port network are described by:

$$b_1 = S_{11}a_1 + S_{12}a_2 \quad \ldots\ldots \quad 5.8$$

$$b_2 = S_{21}a_1 + S_{22}a_2 \quad \ldots\ldots \quad 5.9$$

By means of equation 11.2.5,

$$\frac{a_2}{a_1} = \frac{S_{21}\Gamma}{1 - S_{22}\Gamma} \quad \ldots\ldots \quad 5.10$$

By means of equation 11.2.6,

$$\rho = S_{11} + \frac{S_{12}S_{21}\Gamma}{1 - S_{22}\Gamma} \quad \ldots\ldots \quad 5.11$$

The signal flow diagram for equation 5.11 is shown in figure 5.4.

Figure 5.5
Signal Flow Diagram for
Equations 5.6, 5.11 and 5.12

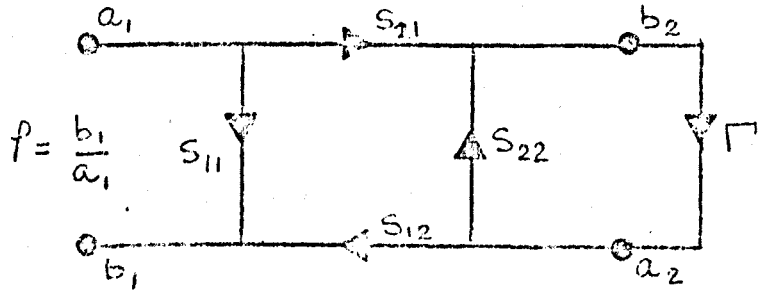

Equation 5.11 may also be modified to the form:

$$\rho = \frac{S_{11} - S_{11} S_{22}\Gamma + S_{12} S_{21}\Gamma}{1 - S_{22}\Gamma}$$

$$\rho = \frac{-(S_{11} S_{22} - S_{12} S_{21})\Gamma + S_{11}}{(-S_{22})\Gamma + 1} \quad \ldots\ldots \quad 5.12$$

Equations 5.6 and 5.12 are of the same form, and for equivalence, then we must have

$$A = (-\Delta^S) = -S_{11} S_{22} + S_{12} S_{21} \quad \ldots\ldots \quad 5.12(a)$$

$$B = S_{11} \quad \ldots\ldots \quad 5.12(b)$$

$$C = (-S_{22}) \quad \ldots\ldots \quad 5.12(c)$$

$$D = 1 \quad \ldots\ldots \quad 5.12(d)$$

Hence it may be concluded that the signal flow graph of figure 5.5 is applicable for reflectometer error correction.

The physical meaning of the scattering parameters when applied in this context, may be likened to the following properties where:

S_{11} represents the effective directivity errors which in addition to the directivity of the measuring coupler also include residual reflection effects of test cables, adapters and leakage signals between the incident (reference) and reflected (test) channels of the receiver etc.

The justification for this representation can be clearly demonstrated in equation 5.12 for the case of a perfectly matched load ($\Gamma = 0$). In this case, the only signal detected will be that due to S_{11} i.e., the effective directivity.

S_{22} may be seen to be the result of an imperfect source match whereby the wave reflected by the device being measured is not completely absorbed and part of this reflected wave is re-reflected to appear as an increment to the main incident

wave. (Note: This source match should not be confused with that of the generator source match mentioned in section 2: 4).

S_{12} S_{21} are referred to as the frequency tracking errors of the system. These are caused by small deviations in gain, phase and frequency response. The errors are caused by differences in the test and reference channel signals due to imperfectly matched cables, differences between the incident and reflected test couplers, difference in receiver channel gain etc.

5:3.2 Practical Error Model

In the practical measurement case, it is not always possible to connect the devices to be measured directly to the reflectometer system and the signal flow graph of figure 5.5 must be modified to include the effects of transformations due to waveguide/cable/connector lengths etc. Furthermore, measurements are frequently required on devices with the same reflection coefficient separated by different electrical lengths of uniform transmission line e.g., a short circuit, an offset short circuit etc.

Figure 5.6

Practical Signal Flow Graph of the Reflectometer Measuring System

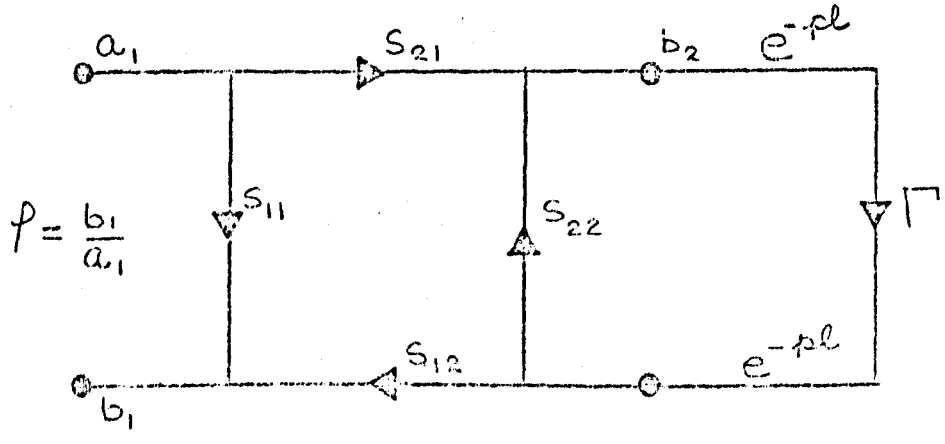

The resulting modified signal flow graph is shown in figure 5.6. For ease in deriving the equations, the following are defined:-

$$\rho' = (\alpha + j\beta)\ell$$

where ρ' represents the total propagation effects for a given uniform transmission line of length "ℓ",

α is the attenuation constant per unit length
β is the phase constant per unit length
ℓ is any fixed length
Γ is the reflection coefficient of a termination.

The suffices, 1 to 4 indicate the ordered set of measurements. For example $\rho'_1 = (\alpha + j\beta)\ell_1$ would refer to the total propagation effects due to a line of length "ℓ_1" with an attenuation and phase constants of α and β respectively.

Hence the general equation of 5.11 adopts the forms shown below:-

For the case $\ell = \ell_1 = 0$,

$$\rho_1 = S_{11} + \frac{S_{12}\, S_{21}\, \Gamma_1}{1 - S_{22}\, \Gamma_1} \qquad \ldots\ldots \qquad 5.13$$

For the case $\ell = \ell_2$,

$$\rho_2 = S_{11} + \frac{S_{12}\, S_{21} \Gamma_2 e^{-2\rho'_2}}{1 - S_{22}\, \Gamma_2 e^{-2\rho'_2}} \qquad \ldots\ldots \qquad 5.14$$

For the case $\ell = \ell_3$,

$$\rho_3 = S_{11} + \frac{S_{12}\, S_{21} \Gamma_3 e^{-2\rho'_3}}{1 - S_{22}\, \Gamma_3 e^{-2\rho'_3}} \qquad \ldots\ldots \qquad 5.16$$

From equations 5.13, 5.14 and 5.16 it is possible to derive the general expressions for the scattering parameters. Detailed derivations have already been published (reference 5.23) by the author. A copy of the paper is included in Appendix 12.2 and only the pertinent results will be quoted. Equations 5.17, 5.18, 5.19, 5.20, 5.22 and 5.23 are extracted from equations, (8), (9), (1), (2), (3), (4), (4a) respectively from Appendix 1 of reference 5.23. For ease of discussion, they are:-

$$S_{22}\Gamma_2 e^{-2\rho_2} = \frac{S_{11}(\Gamma_2 e^{-2\rho_2} - \Gamma_3 e^{-2\rho_3}) + \rho_2\Gamma_3 e^{-2\rho_3} - \rho_3\Gamma_2 e^{-2\rho_2}}{(\rho_2\Gamma_3 e^{-2\rho_3} - \rho_3\Gamma_3 e^{-2\rho_3})} \quad \ldots\ldots \quad 5.17$$

$$S_{22}\Gamma_2 e^{-2\rho_2} = \frac{S_{11}(\Gamma_2 e^{-2\rho_2} - \Gamma_1) + \rho_2\Gamma_1 - \rho_1\Gamma_2 e^{-2\rho_2}}{(\rho_2\Gamma_1 - \rho_1\Gamma_1)} \quad \ldots\ldots \quad 5.18$$

$$S_{11} = \frac{\rho_1\rho_2(\Gamma_2\Gamma_3 e^{-2\rho_2} - \Gamma_1\Gamma_3) - \rho_2\rho_3(\Gamma_1\Gamma_2 e^{2(\rho_3-\rho_2)} - \Gamma_1\Gamma_3) - \rho_3\rho_1(\Gamma_2\Gamma_3 e^{-2\rho_2} - \Gamma_1\Gamma_2 e^{2(\rho_3-\rho_2)})}{\rho_1(\Gamma_1\Gamma_2 e^{2(\rho_3-\rho_2)} - \Gamma_1\Gamma_3) + \rho_2(\Gamma_2\Gamma_3 e^{-2\rho_2} - \Gamma_1\Gamma_2 e^{2(\rho_3-\rho_2)}) + \rho_3(\Gamma_1\Gamma_3 - \Gamma_2\Gamma_3 e^{-2\rho_2})} \quad 5.19$$

$$S_{22} = \frac{\Gamma_1 e^{2\rho_2}(\rho_2 - S_{11}) + \Gamma_2(S_{11} - \rho_1)}{\Gamma_1\Gamma_2(\rho_2 - \rho_1)} \quad \ldots\ldots \quad 5.20$$

$$S_{12}S_{21} = \frac{(\rho_1 - S_{11})(1 - S_{22}\Gamma_1)}{\Gamma_1} \quad \ldots\ldots \quad 5.21$$

$$\Gamma = \frac{\rho_m - S_{11}}{S_{22}\rho_m + S_{12}S_{21} - S_{11}S_{22}} \quad \ldots\ldots \quad 5.22$$

If the device to be measured is connected across a plane situated a distance " ℓ " from the reference plane

$$\Gamma' = \frac{\rho_m - S_{11}}{e^{-2\rho}(S_{22}\rho_m + S_{12}S_{21} - S_{11}S_{22})} \quad \ldots\ldots \quad 5.23$$

where $\rho = (\alpha + j\beta)\ell$ as before.

Several authors (references 5.8, 5.9) have solved specific cases but a general solution for both lossless and loss-free calibration standards have not been available before.

5:4 Specific Calibration Procedures

5:4.1 A considerable amount of work was expended investigating the many methods of measurement correction. The idea of using other than short circuits, open circuits and matched loads as calibration terminations was disliked because of the uncertainty of the characterization of the terminations. Many alternative methods were tried but three methods predominated and these were finally chosen for further work. The three methods are (a) The Three Short Circuit Method (b) The Four Short Circuit Method and (c) The Four Termination and a Reference Short Circuit Method.

5:4.2 The Three Short Circuits Correction Method

In this case, the three terminations used are $\Gamma_1 = \Gamma_2 = \Gamma_3 = 1 \angle 180°$. The electrical length between Γ_2 and Γ_1 is ℓ_2 and the electrical length between Γ_3 and Γ_2 is $(\ell_3 - \ell_2)$. These are shown in figure 5.7.

Figure 5.7

Three Short Circuit Calibration Procedure

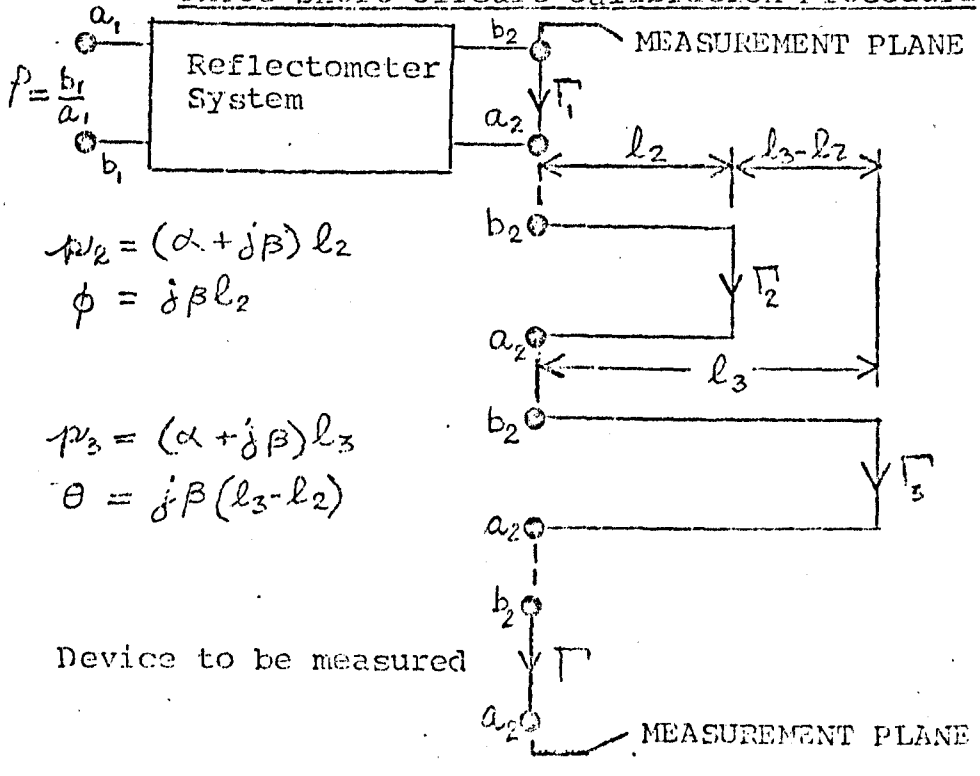

If the above are substituted in the general equations of 5.19 to 5.22, the following results

$$S_{11} = \frac{\rho_1\rho_2(e^{-2\rho_2} - 1) - \rho_2\rho_3(e^{2(\rho_3-\rho_2)} - 1) - \rho_3\rho_1(e^{-2\rho_2} - e^{2(\rho_3-\rho_2)})}{\rho_1(e^{2(\rho_3-\rho_2)} - 1) + \rho_2(e^{-2\rho_2} - e^{2(\rho_3-\rho_2)}) + \rho_3(1 - e^{-2\rho_2})} \quad \ldots\ldots \quad 5.19(a)$$

$$S_{22} = \frac{-e^{2\rho_2}(\rho_2 - S_{11}) - (S_{11} - \rho_1)}{(\rho_2 - \rho_1)} \quad \ldots\ldots \quad 5.20(a)$$

$$S_{12}S_{21} = -(\rho_1 - S_{11})(1 + S_{22}) \quad \ldots\ldots \quad 5.21(a)$$

$$\Gamma = \frac{\rho_m - S_{11}}{S_{22}\rho_m + S_{12}S_{21} - S_{11}S_{22}} \quad \ldots\ldots \quad 5.22(a)$$

If the connecting electrical lines are considered to be lossless, the above equations become:

$$S_{11} = \frac{\rho_1\rho_2(e^{-j2\phi} - 1) - \rho_2\rho_3(e^{+j2\theta} - 1) - \rho_1\rho_3(e^{-j2\phi} - e^{+j2\theta})}{(e^{-j2\phi} - 1)(\rho_2 - \rho_3) - (e^{+j2\theta} - 1)(\rho_2 - \rho_1)} \quad \ldots\ldots \quad 5.19(b)$$

$$S_{22} = \frac{e^{+j2\phi}(\rho_2 - S_{11}) + S_{11} - \rho_1}{(\rho_1 - \rho_2)} \quad \ldots\ldots \quad 5.20(b)$$

$$S_{12}S_{21} = (S_{11} - \rho_1)(1 + S_{22}) \quad \ldots\ldots \quad 5.21(b)$$

$$\Gamma = \frac{\rho_m - S_{11}}{S_{22}\rho_m + S_{12}S_{21} - S_{11}S_{22}} \quad \ldots\ldots \quad 5.22(b)$$

Considerable work was carried out verifying the results of equations 5.19(b) to 5.22(b) experimentally. Very good results were obtained. These results were published in Electronic Letters (Ref 5.13) in March 1973. Since then, this method of measurement has been verified by Gould and Rhodes (Ref 5.14) and Kwesah (Ref 5.15). Warner (Ref 5.16) and Woods (Ref 5.17) have recognised the method as acceptable in their rigorous analysis of reflectometer errors.

5:4.3 The Short/Offset Short/Matched Termination Correction Method

This is the case described by Hackborn (Ref 5.9). For this,

$\Gamma_1 = 1\angle 180^\circ$; $\Gamma_2 = 1\angle 180^\circ$; $\Gamma_3 = 0$

From equation 5.19 to 5.22

$$S_{11} = \rho_3 \qquad \ldots\ldots \qquad 5.19(c)$$

Equation 5.19(c) is only true for a matched termination.

From equation 5.20

$$S_{22} = \frac{S_{11} - \rho_1 + e^{2\gamma_2}(\rho_2 - S_{11})}{\rho_1 - \rho_2}$$

If the transmission line is lossless i.e.

$$S_{22} = \frac{S_{11} - \rho_1 + e^{j2\beta l_2}(\rho_2 - S_{11})}{\rho_1 - \rho_2} \qquad \ldots\ldots \qquad 5.20(c)$$

From equation 5.21

$$S_{12}S_{21} = (S_{11} - \rho_1)(1 + S_{22}) \qquad \ldots\ldots \qquad 5.21(c)$$

From equation 5.22

$$\Gamma = \frac{\rho_m - S_{11}}{S_{22}\rho_m + S_{12}S_{21} - S_{11}S_{22}} \qquad \ldots\ldots \qquad 5.22(c)$$

This method has been compared by the author (Ref 5.23) against other methods and has been found to be that least sensitive to length errors in the offset short.

5:4.4 The Three Open Circuit Correction Method

In this method,

$\Gamma_1 = 1\angle 0°$; $\Gamma_2 = 1\angle 0°$; $\Gamma_3 = 1\angle 0°$

From equation 5.19

$$S_{11} = \frac{\rho_1\rho_2(e^{-2\rho_2}-1) - \rho_2\rho_3(e^{2(\rho_3-\rho_2)}-1) - \rho_3\rho_1(e^{-2\rho_2} - e^{2(\rho_3-\rho_2)})}{\rho_1(e^{2(\rho_3-\rho_2)}-1) + \rho_2(e^{-2\rho_2} - e^{2(\rho_3-\rho_2)}) + \rho_3(1-e^{-2\rho_2})} \quad \ldots\ldots \quad 5.19(d)$$

From equation 5.20

$$S_{22} = \frac{e^{2\rho_2}(\rho_2 - S_{11}) + S_{11} - \rho_1}{\rho_2 - \rho_1} \quad \ldots\ldots \quad 5.20(d)$$

From equation 5.21

$$S_{12}S_{21} = (\rho_1 - S_{11})(1 - S_{22}) \quad \ldots\ldots \quad 5.21(d)$$

From equation 5.22

$$\Gamma = \frac{\rho_m - S_{11}}{S_{22}\rho_m + S_{12}S_{21} - S_{11}S_{22}} \quad \ldots\ldots \quad 5.22(d)$$

This method can be used provided one can really define an open circuit termination. Tests with this method (Ref. 5.7) have shown that the corrected results are susceptible to errors in defining the open circuit terminations.

For co-axial cables, Hewlett Packard (Ref 5.7) and Woods (Ref 5.18) have given figures for various standard connectors. They are tabled below

Connector Type 50 ohm Lines	Open Circuit Capacitance pF	
	Hewlett Packard	Woods, D.
APC7	0.081	0.0807
N - MALE	0.032	
N - FEMALE	- 0.180	
SMA - MALE	- 0.064	
SMA - FEMALE	0.032	
14.2825 mm (Int. Diam)		0.1649
19.05 mm (Int. Diam)		0.2202

However, when microstrip is measured the open circuit capacitance is ill-defined. James and Tse (Ref.5.19) have given some information on calculating microstrip end effects. The author has invented a method whereby the termination immittance can be calculated directly from the calibration measurements. This is explained fully in Section5:5.

5.4.5 The Three Identical Non-Matched Termination Correction Method. This is the case when $\Gamma_1 = \Gamma_2 = \Gamma_3 = \Gamma_x$, where Γ_x is initially unknown. Its use will be shown in Section 5.5

From equation 5.19

$$S_{11} = \frac{\rho_1\rho_2(e^{-2\rho_2}-1) - \rho_2\rho_3(e^{2(\rho_3-\rho_2)}-1) - \rho_3\rho_1(e^{2\rho_2} - e^{2(\rho_3-\rho_2)})}{\rho_1(e^{2(\rho_3-\rho_2)}-1) + \rho_2(e^{2\rho_2}-e^{2(\rho_3-\rho_2)}) + \rho_3(1-e^{-2\rho_2})} \quad \ldots\ldots \quad 5.19(e)$$

From equation 5.20

$$S_{22} = \frac{1}{\Gamma_x}\left\{\frac{e^{2\rho_2}(\rho_2 - S_{11}) + (S_{11}-\rho_1)}{(\rho_2-\rho_1)}\right\} \quad \ldots\ldots \quad 5.20(e)$$

From equation 5.21

$$S_{12}S_{21} = \frac{1}{\Gamma_x}\left\{(\rho_1 - S_{11})(1 - S_{22}\Gamma_x)\right\} \quad \ldots\ldots \quad 5.21(e)$$

From equation 5.22

$$\Gamma = \frac{\rho_m - S_{11}}{S_{22}\rho_m + S_{12}S_{21} - S_{11}S_{22}} \quad \ldots\ldots \quad 5.22(e)$$

It should be noted that S_{11} is unaffected by any termination but S_{22} and $S_{12}S_{21}$ are affected by the reciprocal of the termination reflection coefficient.

5:4.6 The Short/OffsetShort/Open Circuit Correction Method

This is the case when:

$$\Gamma_1 = 1\angle 180^\circ \; ; \qquad \Gamma_2 = 1\angle 180^\circ \; ; \qquad \Gamma_3 = 1\angle 0^\circ$$

From Equation 5.19

$$S_{11} = \frac{\rho_1\rho_2(1-e^{-2\rho_2}) - \rho_2\rho_3(\Gamma_3 + e^{-2\rho_2}) + \rho_3\rho_1(\Gamma_3 e^{-2\rho_2} + e^{-2\rho_2})}{\rho_1(e^{-2\rho_2}+\Gamma_3) - \rho_2(\Gamma_3 e^{-2\rho_2} + e^{-2\rho_2}) + \rho_3\Gamma_3(e^{-2\rho_2}-1)} \quad \ldots\ldots \quad 5.19(f)$$

From equation 5.20

$$S_{22} = \frac{S_{11} - \rho_1 + e^{2\rho_2}(\rho_2 - S_{11})}{\rho_1 - \rho_2} \quad \ldots\ldots \quad 5.20(f)$$

From equation 5.21

$$S_{12}S_{21} = (S_{11} - P_1)(1 + S_{22}) \quad \ldots\ldots \quad 5.21(f)$$

From equation 5.22

$$\Gamma = \frac{P_m - S_{11}}{S_{22}P_m + S_{12}S_{21} - S_{11}S_{22}} \quad \ldots\ldots \quad 5.22(f)$$

This is the method devised by Shurmer (Ref. 5.20) Practical measurements using this system (Ref 5.23 have shown the corrected results to be highly dependent on the accuracy of the open circuit termination.

5:5 The Four Termination Correction Methods

5:5.1

These four termination correctionmethods were invented to overcome some of the difficulties associated with the three termination correction methods. The chief problems associated with the three termination correction methods are:-

(a) Difficulty in specifying calibration lengths.

(b) Difficulty in defining the calibration termination.

(c) Changing the position of the measurement plane.

(d) Constructional problems.

5:5.1.1 Difficulty in Specifying Calibration Lengths

In the case of air co-axial line and wave guide systems, electrical line lengths can be accurately specified. However, when dielectric filled co-axial lines, waveguides and particularly microstrip are used, the dielectric medium may not be homogenous. Furthermore, because of dispersion effects, the electrical length specified at one frequency may be different from that at another frequency. The ideal solution would be to find some method of determining the propagation properties (total attenuation loss and phase change) of the line at each frequency.

5:5.1.2 Difficulty in Defining the Calibration Terminations

It has already been mentioned in Section 5:4 that because of difficulty in specifying the calibration terminations, these are generally limited to short circuits, open circuits and matched loads. The short circuit presents little difficulty for co-axial lines and waveguides as the losses associated with electrical conductivity are minimal. The effective plane of an open circuit termination is difficult to determine especially in microstrip. Furthermore, for certain calibration procedures, (Sections 5:4.4 and 5:4.5) the corrected accuracy may be seriously impaired if the open circuit is not correctly defined. The difficulty associated with producing a perfect matched load are well known and need no further comment. An ideal solution would be a method which was independent of the calibration termination.

5:5.1.3 Changing the Position of the Measurement Plane

In the measurement of some components, e.g., capacitors, inductors etc., it is frequently desired to alter the plane of measurement to determine the actual component value of the item at its place of origin instead of its value transformed by a length of transmission line. This change of the measurement plane can be carried out by using equation 5.23. However, the electrical length must be accurately known at the frequency concerned.

5:5.1.4 Construction Problems

Difficulty is often encountered in the construction of short circuits in microstrip especially when the line is terminated away from the edge of the substrate. This problem is compounded when brittle substrates such as sapphire, quartz, glass etc., are used. Some "Shattering" experiences were encountered when holes had to be drilled to construct short-circuits. A solution independent of the calibration termination would avoid these problems.

5:5.2 The Four Termination Correction Methods

This method was invented and initially submitted to "Electronic Letters" on 11th February, 1976 (Reference 5.21). The calibration procedure requires the construction of four test pieces. All test pieces must have identical terminations, identical transitions to the network analyser terminals and identical transmission lines (except for length) connecting the transitions and the terminations. The transitions and transmission lines (Z_{o2} in figure 5.8) must also be identical to that used for connecting the device to be measured to the network analyser terminals. It follows that all the transmission lines used will have identical attenuation constants, identical phase constants and identical characteristic impedances at each measurement frequency but none of these values need be known at this stage.

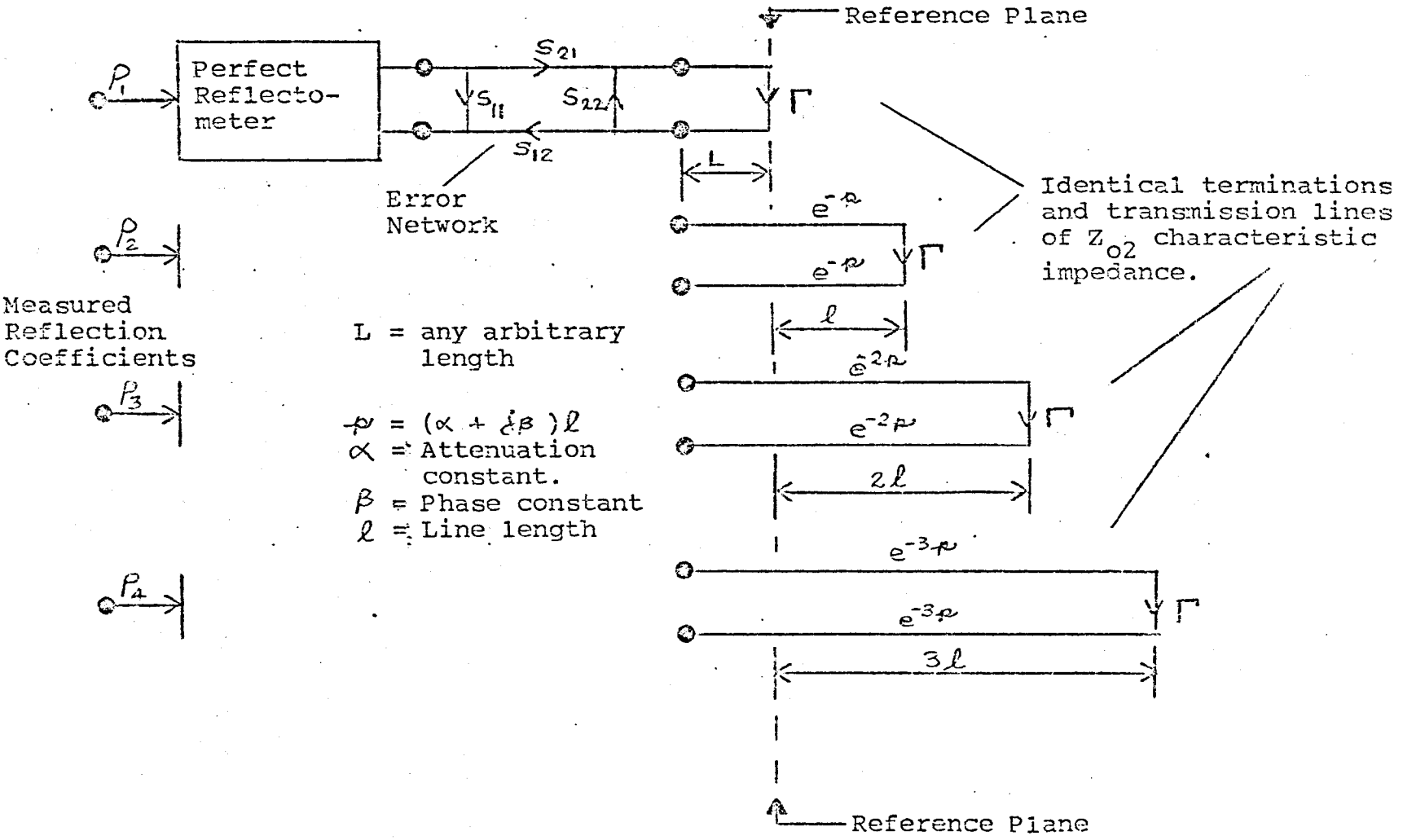

FIGURE 5.8 SIGNAL FLOW GRAPH OF THE FOUR TERMINATION CORRECTION METHOD

The physical lengths of the uniform transmission lines used in the test pieces must be "L", "$L+\ell$", "$L+2\ell$", "$L+3\ell$", where "L" and "ℓ" are constants but the value of "L" need not be known.

For calibration purposes, each test piece is connected to the network analyser terminals and measured. From these measurements, it is possible to calculate the total attenuation and phase change of the line length "ℓ". To derive the scattering parameters of the error network, it is necessary to know the complex reflection coefficient of each test piece. No difficulty exists if the termination is a short circuit. However, if the termination is unknown, e.g., an imperfect open circuit, then its stray immittance must be found. This can be obtained by placing a short circuit across the reference plane (Fig 5.8) and making an additional (fifth) measurement. Then by using the information from all the calibration measurements and equations 5.28, 5.31, 5.32 and 5.35, it will be possible to calculate the scattering parameters of the error network. This information may then be utilized for the correction methods of Section 5:4.2.

If the line impedance of the test pieces is not that of the reflectometer, the corrected reflection coefficient derived will be that normalized to the line impedance of the test peices. This is of course, the established custom used with non-TEM waveguides where a unique definition of impedance does not exist. Hence this method is applicable even when the measured device is embedded in a line impedance other than that of the reflectometer system.

The signal flow graphs of figure 5.8 yield:-

$$P_1 = S_{11} + \frac{S_{12}S_{21}\Gamma}{1 - S_{22}\Gamma} \quad \ldots\ldots \quad 5.24$$

$$P_2 = S_{11} + \frac{S_{12}S_{21}\Gamma e^{-2p}}{1 - S_{22}\Gamma e^{-2p}} \quad \ldots\ldots \quad 5.25$$

$$P_3 = S_{11} + \frac{S_{12}S_{21}\Gamma e^{-4p}}{1 - S_{22}\Gamma e^{-4p}} \quad \ldots\ldots \quad 5.26$$

$$P_4 = S_{11} + \frac{S_{12}S_{21}\Gamma e^{-6p}}{1 - S_{22}\Gamma e^{-6p}} \quad \ldots\ldots \quad 5.27$$

The mathematical basis for these correction systems have been derived by the author in reference 5.23 which is included in this thesis as Appendix 12.2.
Only the results of this paper will be repeated here.

$$\Gamma\left\{2\cosh^2 2\rho(-P_1P_3+P_1P_4+P_2P_3-P_2P_4)+\cosh 2\rho(P_1P_2-P_1P_4-P_2P_3+P_3P_4)\right.$$
$$\left.+(-P_1P_2+2P_1P_3-P_1P_4-P_2P_3-P_3P_4+2P_2P_4)\right\} \quad \ldots\ldots \quad 5.28$$

Hence, provided $\Gamma \neq 0$, a solution of the quadratic equation i.e., $\cosh 2\rho$ is possible. Furthermore, "ρ" may be resolved into its real and quadrate parts to yield the total line attenuation and phase change. In addition, if the physical length of the line "ℓ" is known or measured, the effective dielectric constant may be calculated.

Let one root of the quadratic equation of 5.28 be denoted by $(\mu + j\nu)$ where "μ" and "ν" are real numbers. Writing $\cosh 2\rho$ in its exponential form will result in

$$e^{4\rho} - 2e^{2\rho}(\mu + j\nu) + 1 = 0 \quad \ldots\ldots \quad 5.29$$

If one root of the quadratic of equation 5.29 is denoted by $(x + jy)$, then

$$e^{2\rho} = e^{2\alpha\ell}\,\underline{/2\beta\ell} = \sqrt{x^2+y^2}\,\underline{/\tan^{-1}(y/x)} \quad \ldots\ldots \quad 5.30$$

Hence,

$$2\alpha\ell = \ln\sqrt{x^2+y^2} \quad \text{Nepers} \quad \ldots\ldots \quad 5.31$$

$$2\beta\ell = \tan^{-1}(y/x) \quad \text{Radians} \quad \ldots\ldots \quad 5.32$$

If the reflection coefficient Γ of the test pieces are known, then equations 5.31 and 5.32 may be used in conjunction with the measured parameters P_1, P_2, P_3 (equations 5.24, 5.25 and 5.26) to solve the scattering parameters of the error network (equations 5.19, 5.20 and 5.21). Measurement correction can then be applied to an unknown device as detailed in Section 5:3.

If the reflection coefficients, Γ, of the test pieces are unknown, then it must be found either from tables (Section 5:4.4) or by measurement and/or calculation. The procedure used is detailed in Section 5:6.

5:6 The Evaluation of the Reflection Coefficient of the Test Pieces

Research into this problem was initially started because of the difficulty of producing good short circuits in microstrip. It had been obvious for some time that correction (Section 5:4.4) using open circuits with their inherently simple construction is especially desirable in microstrip. However, previous attempts (Ref 5.19) at calculating the stray immittances were not sufficiently accurate.

In this procedure, the reflection coefficient ($\Gamma = e^{(\Omega + j\phi)}$) of the test pieces is obtained by an additional (fifth) measurement. This additional measurement, P_5 is that made when a short circuit termination is placed at the reference plane shown in figure 5.8.

From equation 5.19, 5.20 and 5.21, it is readily deduced that provided

(a) S_{11} is unaffected by the type of termination

(b) $$S_{22} = e^{-(\Omega + j\phi)} S_{22}' \quad \ldots\ldots \quad 5.33$$

where $$S_{22}' = \frac{\left[e^{2P_2} (P_2 - S_{11}) + S_{11} - P_1 \right]}{P_2 - P_1} \quad \ldots\ldots \quad 5.33a$$

(c) $$S_{12}S_{21} = e^{-(\Omega + j\phi)} S_{12}S_{21}' \quad \ldots\ldots \quad 5.34$$

where $$S_{12}S_{21}' = (P_1 - S_{11})(1 - S_{22}') \quad \ldots\ldots \quad 5.34a$$

From the fifth measurement

$$\rho_5 = S_{11} + \frac{S_{12}S_{21}\,1\angle 180^\circ}{1 - S_{22}\,1\angle 180^\circ}$$

$$= S_{11} - \frac{S_{12}S_{21}'\,e^{-(\Omega+j\phi)}}{1 + S_{22}'e^{-(\Omega+j\phi)}}$$

$$= S_{11} - \frac{S_{12}S_{21}'}{e^{(\Omega+j\phi)} + S_{22}'}$$

Transposing,

$$e^{(\Omega+j\phi)} = \frac{S_{12}S_{21}'}{S_{11} - \rho_5} - S_{22}' \qquad \ldots\ldots \quad 5.35$$

Hence from equations 5.35, 5.34(a), 5.33(a) and 5.19, the real and quadrate parts of the reflection coefficient of the test pieces may be calculated. Subsequent experimental tests prove that this method is accurate to 1% of the published figures.

5:7 Conclusions

The information presented in this chapter is vitally important. Detailed mathematical arguements have been used to establish why it is possible to measure reflection coefficients correctly in spite of imperfect instruments. An error correction model has been derived in Section 5:1. The general theory regarding correction procedures has been extensively expounded in Sections 5:2 and 5:3. General formulae for calibration and correction using three calibration pieces have been derived for the first time, and applied to previously established special cases. Several new calibration procedures have been evolved in Section 5:4. Furthermore, some of the methods invented are now accepted as standard methods of correction.

The methods of Section 5:5 are exceptional methods in that they have shown how the attenuation constant, the phase constant, dispersion and even how the reflection coefficient of the test pieces may be obtained. Hitherto these properties have not been taken into account as these losses were not easily ascertained. Finally this theoretical analysis has established clearly that error correction procedures are possible without the use of expensive pre-calibrated test pieces.

* * * * * * * * * * *

5:8 References

5.1 Barlow, H and Cullen, A "Microwave Measurements - Constable & Co., London 1950

5.2 Adam, S.F. "Microwave Theory and Application" Prentice Hall, New York.

5.3 Sucher M and Fox J "Handbook of Microwave Measurements, Vols. 1, 2, 3 - Pergammon Press New York 1963.

5.4 Beatty, R.W. "Invariance of the Cross-Ratio Applied to Microwave Network Analysis" National Bureau of Standards. Boulder, Colorado, issued September 1972.

5.5 Bianco B and Parodi, M "Measurement of the Effective Relative Permittivities of Microstrip" Electronic Letters 1975, 11, pp 71-72.

5.6 Ajose, S, Matthews, N, Aitchison, C "Characterization of Co-Axial to Microstrip Connector Suitable for Evaluation of Microstrip 2-Ports" Electronic Letters Vol 12 No. 17 pp 430-431 August 1976.

5.7 Hewlett Packard Application Note 221 - Semi-Automatic Measurements using the 8401B Microwave Network Analyser and the 9825A Desk-Top Computer

5.8 Adams S. "A New Precision Automatic Microwave Measurement System" I.E.E. Trans. on Instrumentation and Measurement. Vol IM 17 No 4 Dec. 1968.

5.9 Hackborn, Richard "An Automatic Network Analyser System" Microwave Journal, Vol 11 No. 5 May1968.

5.10 Reich, Volker "Microstrip-Messingen mit Netzwerkanalysator" Nachrichten Technische Zeitung 1975, Heft 5 pp 255-259.

5.11 Shurmer, H.V., "Low-Level Programming for the On Line Correction of Microwave Measurements" The Radio and Electronic Engineer, August 1971 pp 357-364.

5.12 Twisleton, J.R.G., "Microwave Insertion Loss Measurements" I.E.E. Colloquium on R.F.Measurements on Solid State Devices, London 25th May 1971.

5.13 da Silva, E.F. and McPhun M.K. "Calibration of Microwave Network Analyser for Computer Corrected S Parameter Measurements" Electronic Letters 1973 9, pp 126-128.

5.14 Gould, J and Rhodes, G "Computer Correction for a Microwave network analyser without accurate frequency measurement" Electronic Letters 1973 9, pp 494-495.

5.15 Kwesah, A "Characterization of Integrated Bi-polar Transistors using Computer Aided Measurements and Optimisation" Ph.D Thesis - University of Warwick,Nov. 1976.

5.16 Warner, F. "Microwave Attenuation Measurement" 1977 Peter Peregrinus Ltd (I.E.E. Monograph Series 19).

5.17 Woods, D "Rigorous Derivation of Computer Corrected Network Analyser Calibration Equations" Electronic Letters 21 August 1975 Vol 11 No 17 pp 403-404.

5.18 Woods, D "Immittance Transformation using Precision Air-Dielectric Co-Axial lines and Connectors" Proc I.E.E. Vol 118 No 11, Nov 1971.

5.19 James, D.S. and Tse, S.H. "Microstrip End Effects" Electronic Letters 1972, 8 pp 46-47

5.20 Shurmer, H.V. "Calibration Procedure for Computer Corrected S Parameter of Devices Mounted in Microstrip" Electronic Letters 1973 9, pp 323-324.

5.21 Hills, T.D. "Private Communication dated 18.2.76" I.E.E. Reference R 1495.

5.22 Cox, T B.Sc. Final Year Project 1974 Engineering Department, University of Warwick.

5.23 da Silva, E.F. and McPhun, M.K. "Calibration of an Automatic Network Analyser using Transmission Lines of Unknown Characteristic Impedance, Loss and Dispersion" The Radio and Electronic Engineer Vol 48, No 5 May 1978 pp 227-234.

5.24 da Silva, E.F. and McPhun, M.K. "A Review of Network Analyser Calibration Techniques for One Port Measurements" Microwave Journal, June 1978.

* * * * * * * * * *

CHAPTER VI

MEASUREMENT EQUIPMENT (Software)

6:0 Introduction

Practical applications of the equations in Chapter V require long and tedious computations of complex numbers and a desk-top programmable calculator (Hewlett-Packard 9100A) was used in the initial stages. With this calculator, the calibrations for each frequency had to be keyed in manually and the answers were returned on a printed sheet.

Later, when measurement automation was introduced, the Hewlett Packard Calculator was replaced by the Rank Xerox Sigma 5 computer. Considerable difficulties were initially experienced in using this computer as the idiosyncracies of the computer-network analyser interface had to be learnt, and the large storage requirements of the programme made it feasible to use the computer only late at night. However, the many months spent producing the programme has been amply rewarded by the speed and the efficiency of the automated systems.

The computing programmes described in this chapter may be divided into two main categories:-

(a) Programmes for manual operation.
(b) Automated programmes.

The manual programmes will be fully described. Complete descriptions of the automated programmes are impractical because of the length of the programmes.

Figure 6.1

Picture of Hewlett Packard Programmable Calculator Medel 9100A

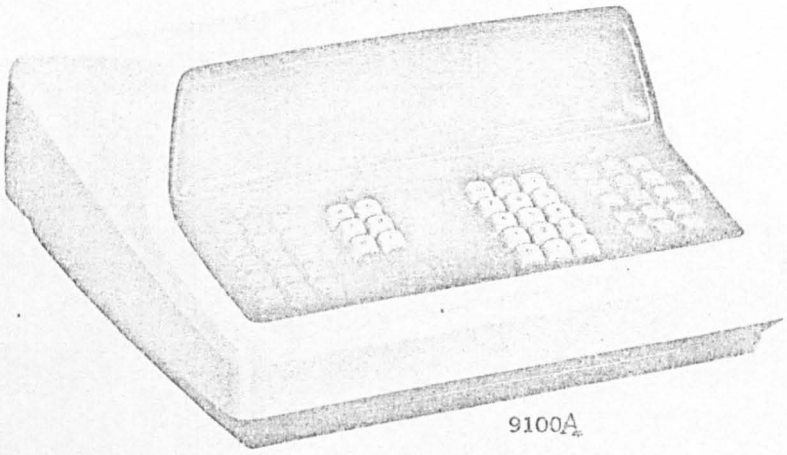

Printer mounted on calculator

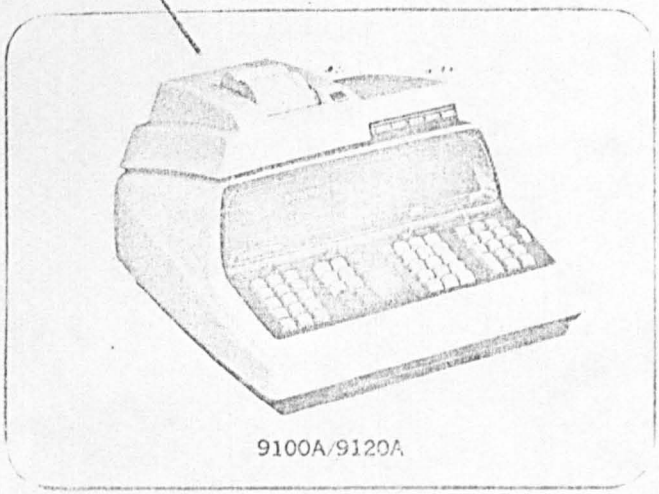

6:1 The Three Short Circuits Calculator Programme

Note: It is assumed that the reader is conversant with the calculator. If not please consult the manual (Ref 6.1).

The programme was written for use on the Hewlett Packard Programable Calculator 9100A (Fig 6.1). The programme accepts input data; calculates them according to the equations 5.19(b), 5.20(b), 5.21(b) and 5.22(b) speficied in Section 5:4.2; and prints the output data.

The calculator will accept two items of information at a time; one item must be put into its "x" register and the other must be put into its "y" register. In the display, the "y" register is situated above the "x" register. Each set of information contains two items of information. Five sets of input data must be read from the measuring instruments by the operator. This information must be hand fed into the calculator in the order specified in Table 6.1.

Table 6.1
Input Format

Set Order	"x" Register	"y" Register	Remarks
1	Blank	Freq. in GHz	Frequency of Operation
2	Magnitude	Angle/Degree	Measured Reflection Coefficient of 1st short circuit
3	Magnitude	Angle/Degree	Measured Reflection Coefficient of 2nd short circuit
4	Magnitude	Angle/Degree	Measured Reflection Coefficient of 3rd short circuit
5	Magnitude	Angle/Degree	Measured Reflection Coefficient of unknown device

The output data is printed out in the format shown in Table 6.2.

Table 6.2

Output Format

Set Order	"x" Register	"y" Register	Remarks
1	Magnitude	Angle/Degrees	Reflection Coefficient of 1st short circuit*
2	Magnitude	Angle/Degrees	Reflection Coefficient of 2nd short circuit*
3	Magnitude	Angle/Degrees	Reflection Coefficient of 3rd short circuit*
4	Magnitude	Angle/Degrees	S_{11} - Error Network Parameter
5	Magnitude	Angle/Degrees	S_{22} - Error Network Parameter
6	Magnitude	Angle/Degrees	$S_{12}S_{21}$ - Error Network Parameter
7	Magnitude	Angle/Degrees	Measured Reflection Coeff't of Unknown Device*
8	Magnitude	Angle/Degrees	Corrected Reflection Coeff't of unknown Device
9	Magnitude	Angle/Degrees	Actual Series Impedance (Polar Form)#
10	Real	Quadrate	Actual Series Impedance (Rectangular Form)#
11	L (mH) or	C (pF)	of Set 9; only one figure will be printed

* This data is merely printed out to ensure that a copy of the input data to the machine is retained.

With reference to a 50 Ω line system.

The programme is pre-recorded in machine language on Magnetic Cards (Hewlett Packard Type 5060-5919). Each magnetic card is approximately 93mm x 51mm in size and each card contains two standard programmes. Each standard programme will store 196 program steps of instructions but 14 steps are automatically lost within the machine whenever one storage register is used. If the machine is programmed correctly, it is possible to successively feed one standard programme set of instructions after another into the machine without destroying the information retained in the storage registers. THE FLOWCHART IS GIVEN ON THE NEXT PAGE.

Flow Chart of the Programme used on the HP9100A Calculator

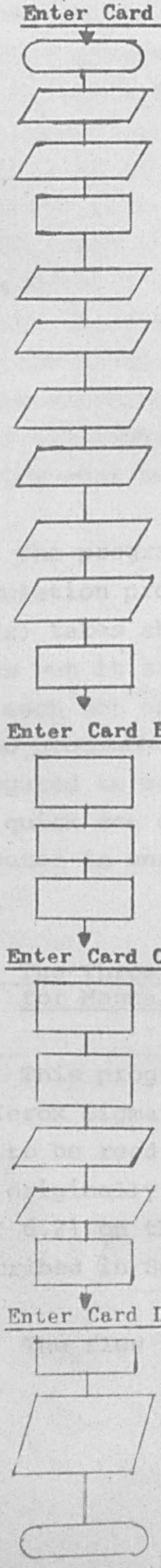

Enter Card A

Clears machine.

Input frequency data in GHz. Continue

Prints out frequency entered in GHz.

Calculates and stores the phase shift for the selected line length in register a. Generates a constant. Stop

Input 1st reflection coefficient. Continue.

Prints out 1st reflection coefficient and processes values for storage in register b. Stop

Input 2nd reflection coefficient. Continue.

Prints out 2nd reflection coefficient and processes values for storage in register c. Stop.

Input 3rd reflection coefficient. Continue.

Prints out 3rd reflection coefficient and processes values for storage in register d

Calculates 1st and 2nd terms of the numerator of S_{11} End.

Enter Card B Continue.

Calculates 3rd numerator term of S_{11} and stores the total numerator result in registers Z and 9.

Calculates the denominator of S_{11}

Calculates the total value of S_{11} and stores results in registers 9 and d. End.

Enter Card C Continue

Calculates S_{22} and stores the results in registers f and e.

Calculates $S_{12}S_{21}$ and stores the results in registers Y and b. Stop.

Input measured reflection coefficient. Continue.

Prints out measured reflection coeffcient.

Commences calculation to yield corrected reflection coefficient. End.

Enter Card D Continue

Continues calculations to yield corrected refl. coef.

Prints out reflection coefficient in polar form, its equivalent impedance referenced to 50 ohms in both polar and rectangular form, and its equivalent capacitance or inductance.

End.

Two magnetic cards (4 standard programmes) were utilized to produce the output data of Table 6.2. In spite of these standard programmes, there were still storage problems and this restricted the use of the programme to the case where there is an equal electrical length between the short circuit calibration pieces. The lengths are pre-set into the magnetic cards but it only takes a few seconds to alter this length. In the coded print-out of the complete programme given in Appendix 11.5 this length has been set for 6mm. To avoid errors, the coded programme print-out has been taken directly from the machine, but it can be easily decoded by reference to the decoding table also included in Appendix 11.5. The other restriction on the calculator is that its associated plotter must be disconnected.

The programme works satisfactorily and the complete calculation process (including the loading of the magnetic cards) takes about three minutes. This is slow in computer terms but it saves about half an hour of hand calculations for each set of measurements. With the advent of the automated programmes of the Sigma V Computer, this system is now relegated to manual measurements or to those cases where a few quick set of results are required when the Sigma V Computer is unavailable.

6:2 The Three Short Sigma V Programme for Manual Use

This programme was written for use in conjuction with theXerox Sigma V Computer. Data from the network-analyser has to be read and punched into data cards. The programme was originally used in the calculation of data for a paper (Ref 6.2) on the three short circuit correction method described in Section 5:4.2.

The flow chart for this programme is shown in Figure 6.2.

Figure 6.2

Flow Chart of 3-Shorts (Manual) Programme

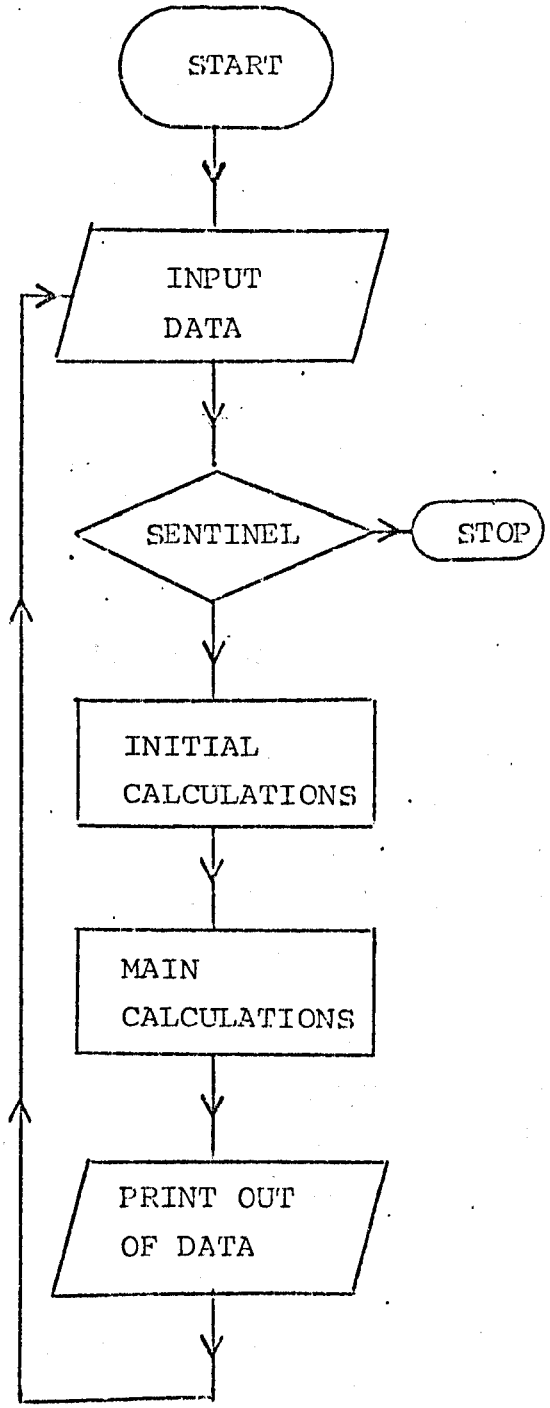

Initiate Fortran Programme

Reads Input Data which consists of frequency, magnitude & angle of Refl. Coef. of 1st, 2nd, 3rd Short, & Unknown

Sentinel to test input data, if data card is blank, programme stops.

Calculation of effective electrical lengths between short circuits.

Calculates Error Network Parameters and corrected reflection coefficient of the device under test.

Writes out input data and corrected reflection coefficient of unknown device.

Returns to read more data.

The programme is relatively short and is given in Appendix 11.6. By the alteration of two constants it may be modified for any offset length of short circuits.

The entire programme is punched on cards. This is useful as it is loaded onto the background system of the Sigma V, which means that results may virtually be obtained at any free interval between the top priority foreground programmes. Loading and running time is about two and a half minutes.

6:3 The Four Shorts Sigma V Programme for Manual Use

This programme was written for use on the Sigma V Computer for three main purposes:-

1: To calculate from the measured data of Section 5:5.2 the total attenuation and phase change of the equi-distant offset lines and then to use this result for the correction procedure of Section 5:4.2.

2: To form the basis of the calculation sub-routine for the automated programme.

3: To compare the results of the single precision (six significant figures) of the Sigma V computer against those obtained using double preceision (fifteen significant figures).

The flow-chart of this programme is shown in figure 6.3.

Figure 6.3

Flow-Chart of 4 Shorts (Manual) Programme

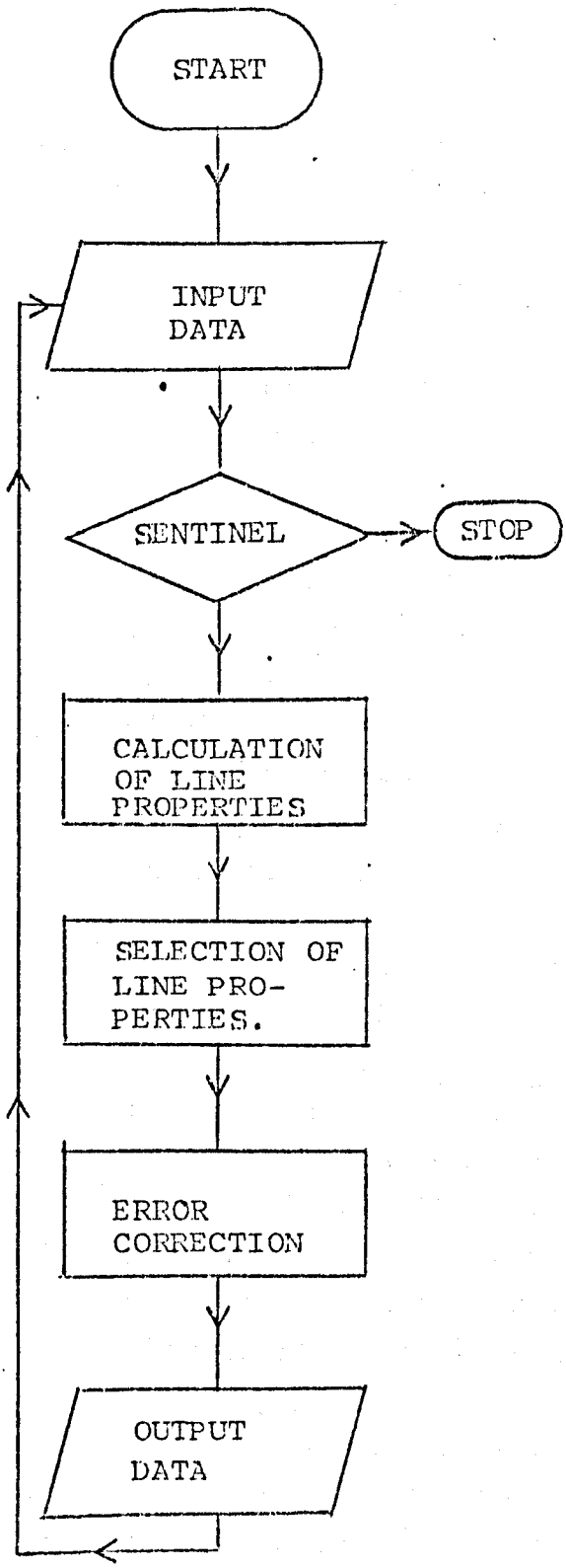

Initiates Fortran Programme

Reads input data which consists of 5 sets of refl. coefs; 4 calibration ones & one from the device under test

Sentinel to test input data; if data card is blank, programme stops

Calculates the total attenuation and phase of the transmission lines associated with the calibration pieces.

Selects the roots of the quadratic equation to obtain the correct values of the attenuation and phase of the offset lengths.

Calculates the network error parameters, and the corrected reflection coefficient of the device under test

Prints out both the input data and the corrected data.

6:3.1 The Four Shorts (Single Precision) Programme for Manual Use on the Sigma V Computer

The programme is listed in Appendix 11.7. The entire programme is punched on paper cards and is suitable for background use on the Sigma V Computer. Loading and running time is about three minutes. Additional sets of data require about one minute which is mostly printing time.

As this programme was to be incorporated in the automated programmes, it had to be thoroughly checked. This was carried out as follows:-

(a) Practical values of the error network parameters S_{11}, S_{22} and $S_{12}\ S_{21}$ were assumed. An electrical line length having practical attenuation and phase characteristics was also chosen.

(b) These chosen values were used in conjunction with theoretically perfect short circuits and a chosen reflection coefficient for the test piece to calculate ρ_1, ρ_2, ρ_3, ρ_4, ρ_5 the apparent reflection coefficients of the calibration and test pieces. These calculatins were carried out using a hand calculator (Hewlett Packard Model HP 21) which displays ten significant figures.

(c) These theoretical coefficients ρ_1, ρ_2, ρ_3, ρ_4, ρ_5 were fed into the Sigma V programme, and its resultant output values, i.e., S_{11}, $S_{12}\ S_{21}$, S_{22} and the corrected reflection coefficient of the test piece were compared against the values initially assumed for them. In all cases, the results agreed to within the fifth decimal place. This is extremely good as the Sigma V in single precision form only calculates up to six significant figures and rounding-off errors are bound to result.

Intermediate calculation values were also compared to ensure that the attenuation and phase change associated with the offset lengths were correct. This was made possible by temporary alteration of the output statements in the programme to provide the intermediate calculations.

The entire system was repeated for different sets of results to ensure that the first verification was not a coincidence.

Finally, in using this programme, the restrictions on the minimum offset lengths detailed in section 6.3 should be observed for minimal computational errors.

6:3.2 The Four Shorts (Double Precision) Programme for Manual use on the Sigma V Computer.

A correction programme for Section 5:5 carries out many mathematical operations on small numbers. The Sigma V computer calculates with only six digit accuracy when operated in the single precision mode. When operated in the double precision mode, the same computer calculates with a fifteen digit accuracy. In order to investigate whether "rounding off" errors would be troublesome, a double precision programme with a flow chart similar to that of figure 6.3 was written.

Practical values of error scattering parameters, offset line length attenuation and associated phase changes were assumed. These figures were fed into both the single precision and the double precision programmes. Both programmes were slightly modified for these purposes to print out intermediate results. The results obtained from both these programmes were compared with the initially assumed values. These results are tabulated on the next page.

Comparison of Single and Double Precision Programme Results

Total Electrical Offset Length (Forward) (and Return)	Item Compared	Assumed Values	Double Precision Calculated Values	Single Precision Calculated Values
0.25 λ (90°)	Attenuation (Neper/cm)	1.2000000000000 E-3	1.199999999999537 E-3	1.199079 E-3
	Phase (Radians)	1.68179512023926	1.68179512023926	1.68179
0.1111λ (40°)	Attenuation (nepers/cm)	1.20000000000000 E-3	1.199999999999537 E-3	1.186839 E-3
	Phase (Radians)	.747464358806610	.747464358806610	.747472
.02777λ (10°)	Attenuation (Nepers/cm)	1.20000000000000 E-3	1.200000000177164 E-3	3.248334 E-3
	Phase (Radians)	.186866044998169	.186866044998770	.200133

The main conclusions are:

(a) Computational error is small when the unit offset electrical length (forward and reflected path) is a quarter wavelength ($\lambda/4$) at the frequency of measurement. The unit offset length is defined as twice the electrical distance between any of the evenly spaced calibration pieces.

(b) Computation error begins to be troublesome in single precision mode when the unit offset electrical length (forward and reflected path) is $0.1111\lambda \simeq \lambda/10$ at the frequency of measurement.

Gross computational error occurs in the single precision mode when the unit electrical offset length (forward and return path) is 0.0277λ at the measurement frequency.

Hence, the restriction that the minimum unit offset electrical length (forward and return path) is greater than $\lambda/8$ must be applied whenever the single precision measurement programme for section 5:5 is used.

It has not been possible to incorporate double precision computation within the automated programmes due to computer storage problems. Hence, the restriction mentioned above also applies to the automated programme of Section 6:5.

The details of the double precision programme are included in Appendix 11.8. The programme is extremely useful for checking out suspect computational errors. It is also used for manual measurements when the Sigma V computer is unavailable for automatic measurements.

6:4 The Four Unknown/Reference Short Termination for Manual Use on the Sigma V Computer

This programme was written to check out the theories of Sections 5:4.4, 5:5.2 and 5:6 which are that:

(a) The unknown reflection coefficients of the calibration pieces can be calculated from the calibration measurements.

(b) The total attenuation and phase change of the offset lengths may be calculated.

(c) The results can be used for error calculation.

(d) To form the basis of a sub-routine for the automated programme.

The flow-chart for this programme is shown in figure 6.4.

Figure 6.4

Flow Chart of the 4 Unknown Terminations and a Reference Short (Manual) Programme

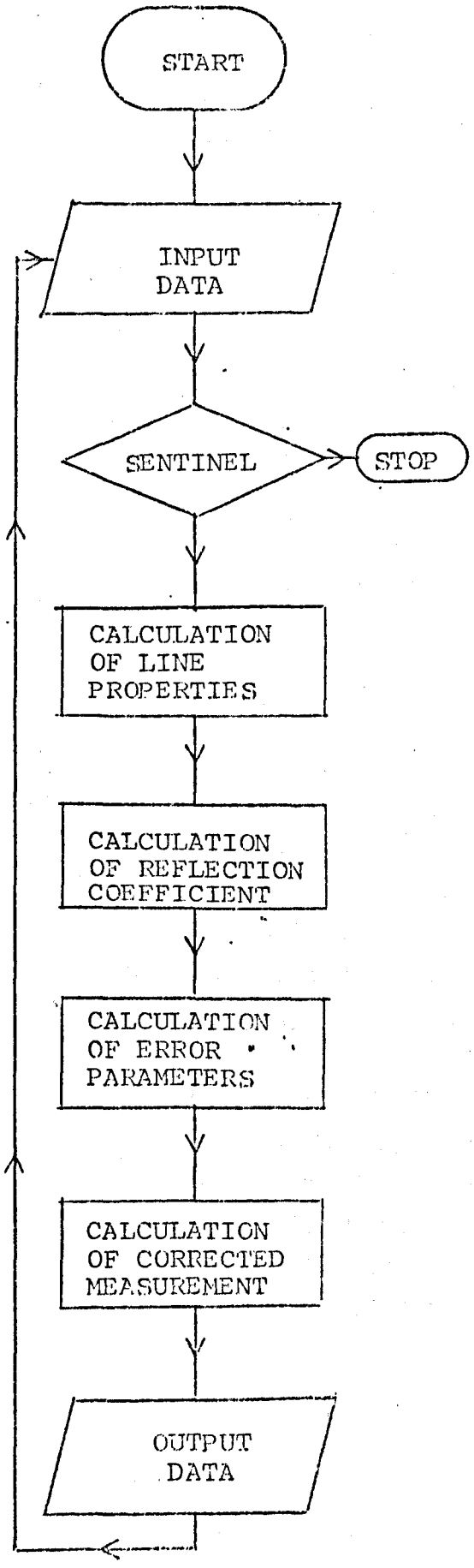

Initiates Fortran Programme

Reads 6 input data sets (4 'open', 1 short circuit) and one set from the device under test.

Sentinel to test input data; if data card is blank, programme stops.

Calculates and selects the correct total attenuation and phase of the offset lengths.

Calculates the reflection coefficient of the 'open' pieces to enable the error network to be found.

Calculates the error network parameters to enable correction to take place.

Calculates the corrected reflection coefficient of the device under test.

Prints out the input data, the line properties, reflection coefficient of the calibration pieces, and the corrected and uncorrected reflection coefficient of the device under test.

The programme is punched on cards and being relatively short (104 statements) it has been included in Appendix 11:9. As this programme is vitally important, it had to be thoroughly checked. This was carried out in the following manner:-

(1) Values based on practical results were chosen to produce the input data to the programme. These were:-

S_{11} = 0.04385706 $\angle 61.987010^{\circ}$

$S_{12}S_{21}$ = 0.9980757 $\angle 4.345090^{\circ}$

S_{22} = 0.04385706 $\angle 122.358430^{\circ}$

Γ = Unknown reflection coefficient of the calibration pieces

= 1.000 $\angle 5.400^{\circ}$

Γ_x = Reflection coefficient of the device

= 0.023900 $\angle -120.695702$

Frequency = 3 GHz (λ = 100mm in air)

Unit off-set Length = 10mm

(2) From the data in (1), the expected measured reflection coefficients, ρ_1, ρ_2, ρ_3, ρ_4, ρ_5 and ρ_m were calculated by using equations 5.24, 5.25, 5.26, 5.27, 5.24 and 5.24 respectively. Calculation was carried out using a ten digit hand calculator (Hewlett Packard Type HP21). The values obtained were:-

ρ_1 = 0.999998 $\angle 13.613013^{\circ}$

ρ_2 = 0.999999 $\angle -57.997191^{\circ}$

ρ_3 = 1.000000 $\angle -135.722251^{\circ}$

ρ_4 = 0.999999 $\angle 148.718243^{\circ}$

ρ_5 = 1.000000 $\angle 179.999855^{\circ}$

ρ_m = 0.020000 $\angle 60.000000^{\circ}$

(3) The values obtained in (2) were then fed into the computer programme. Provided no "rounding off" errors have occurred, the results produced by the programme should agree with the original data in (1). A comparison table is given below:-

Item Compared	Assumed Data (See Para.1)	Calculated Data (See Para. 3)
S_{11}	$0.04385706 \angle 61.987010^{\circ}$	$0.043931 \angle 61.909840^{\circ}$
$S_{12}S_{21}$	$0.9980757 \angle 4.345090^{\circ}$	$0.998071 \angle 4.348839^{\circ}$
S_{22}	$0.04385706 \angle 122.35843^{\circ}$	$0.043929 \angle 122.438152^{\circ}$
Attenuation	1.00000	0.999999
Phase	72°	71.9982°
(Calibration) (Refl. Coeff)	$1.000000 \angle 5.400000^{\circ}$	$0.999999 \angle 5.390873$
(Device) (Refl. Coeff)	$0.023900 \angle -120.695702$	$0.023972 \angle -120.845939$

The following conclusions were drawn:-

(1) The computer programme is correct.

(2) Slight rounding-off errors occur. This is inevitable with six-digit computation. It was not possible with this or with the other arithmetical cases tried to ascertain how the "rounding-off" errors could be proportioned between the manual calculator and the computer. However, computational accuracy to within 0.0001 has been achieved.

(3) The idea that a reference short circuit measurement could be used to calculate the reflection coefficient of the unknown calibration terminations was confirmed arithmetically.

(4) Finally, all the points mentioned in the early part of Section 6:4,(a), (b), (c) and (d) have been verified.

6:5 The Automated Computer Correction Programme

The main purpose of the automated programmes is to enable computer corrected measurements over a wide frequency band to be made quickly and accurately. Two programmes were used

(a) The Four Shorts/Five Termination Programme.
(b) The Three Shorts & Allied Correction Programme.

The items discussed in this section are applicable to both programmes. Items peculiar to a particular programme will be identified by reference to the programme concerned.

6:5.1 Basic Principles

The automated programme initially developed by Duckett (reference 6.7) was used as a starting point, and new calculation storage and display sub-routines were written and inserted by the author. Sections of the inter-active control structures were also modified.

When on-line computer-correction is used, sets of reflection coefficient measurements using the appropriate calibration pieces are made at fixed frequencies within the band of interest. The number of measurement sets made is determined by the number of calibration pieces used. Each set of measurements is stored within the computer. The device to be measured is then connected and a further set of reflection coefficient measurements at the same fixed frequencies are made and stored within the computer. When the correctedmeasurement results are required, the computer withdraws from store the information required, calculates and prints out all the measured and corrected sets of measurements. Subsequent measurement of other devices at the same fixed frequencies may be made without further calibration. Facilities are also provided within the

programme for graphical displays on a video display unit of the measured reflection coefficients in either polar or co-ordinate forms.

Additional facilities are also provided for over twenty features. These include data storage on external tape, repetition of readings etc.

The programmes may be examined more closely by reference to the photograph of the measuring equipment (Fig.3.2) and the diagram showing the inter-face between the measurement equipment and the computer, (Fig 6.5). Flow-charts of the programmes may be found in figures 6.6 and 6.7. Only the main features of the programme will be discussed. Verbatim listing of the programmes will not be given because of length; for example, the five termination programme involves one-thousand two-hundred and sixty-eight (1,268) Fortran statements and two-hundred andseventy-nine (279) machine code instructions making a total of 1,547 statements.

The main functions of the programme are:-

(1) To prompt the operator into following the correct calibration and measurement procedure (Section 6:5.2).

(2) To calculate, step, and control the frequency of the signal generator within the desired frequency band. (Section 6:5.3).

(3) To measure, average, store and calculate the data obtained. (Section 6:5.4).

(4) To reproduce the results graphically on the video display unit, to print-out the results on the line printer, and if desired to store measured data on a separate data tape for later use. (Section 6:5.5).

(5) To permit the use of supplementary tasks such as measuring line attenuation and phase changes, to allow repetition of some measurements to correct for errors during calibration etc. (Section 6:5.6).

Figure 6.5

Block Diagram of the Computer Corrected Microwave Analyser System

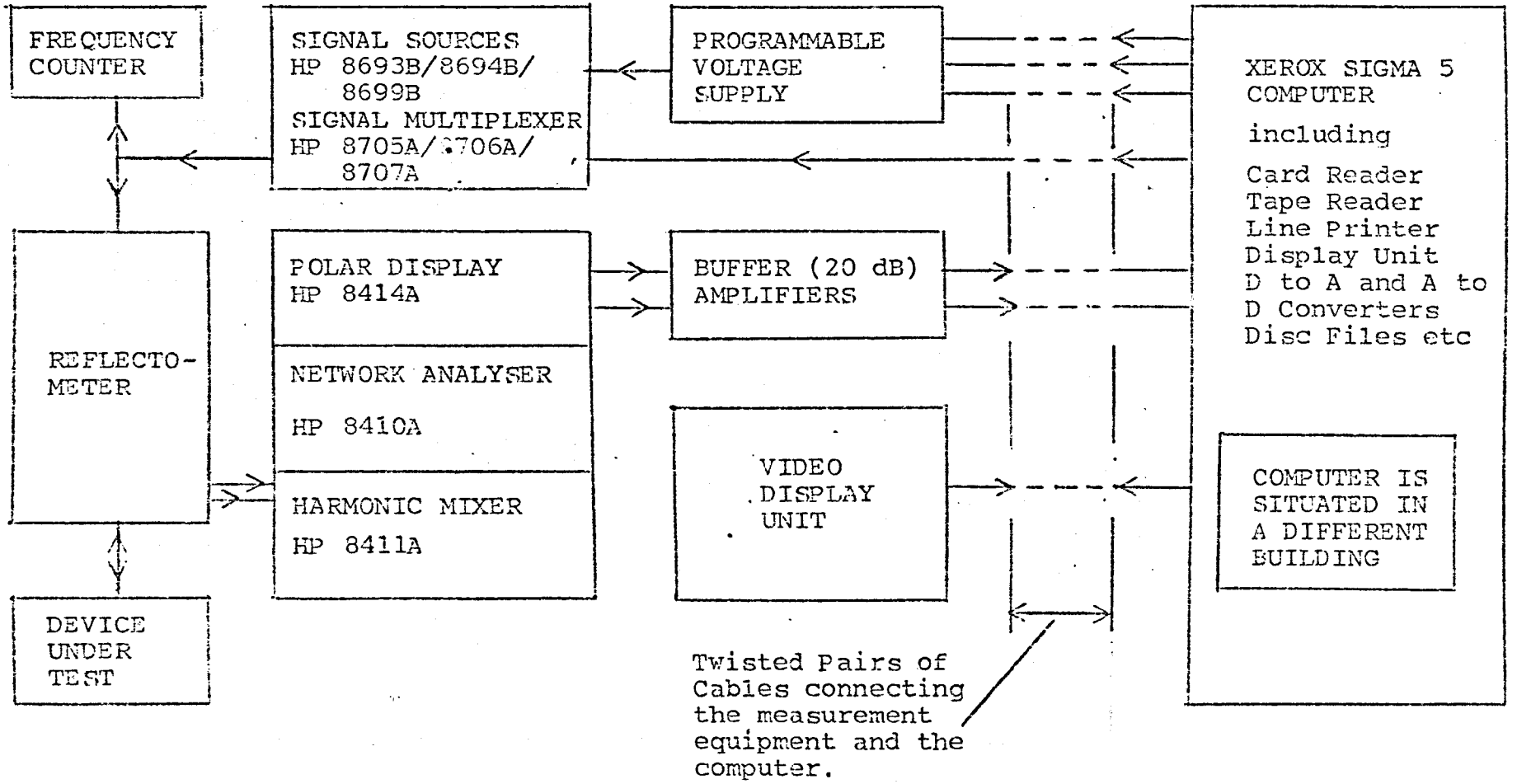

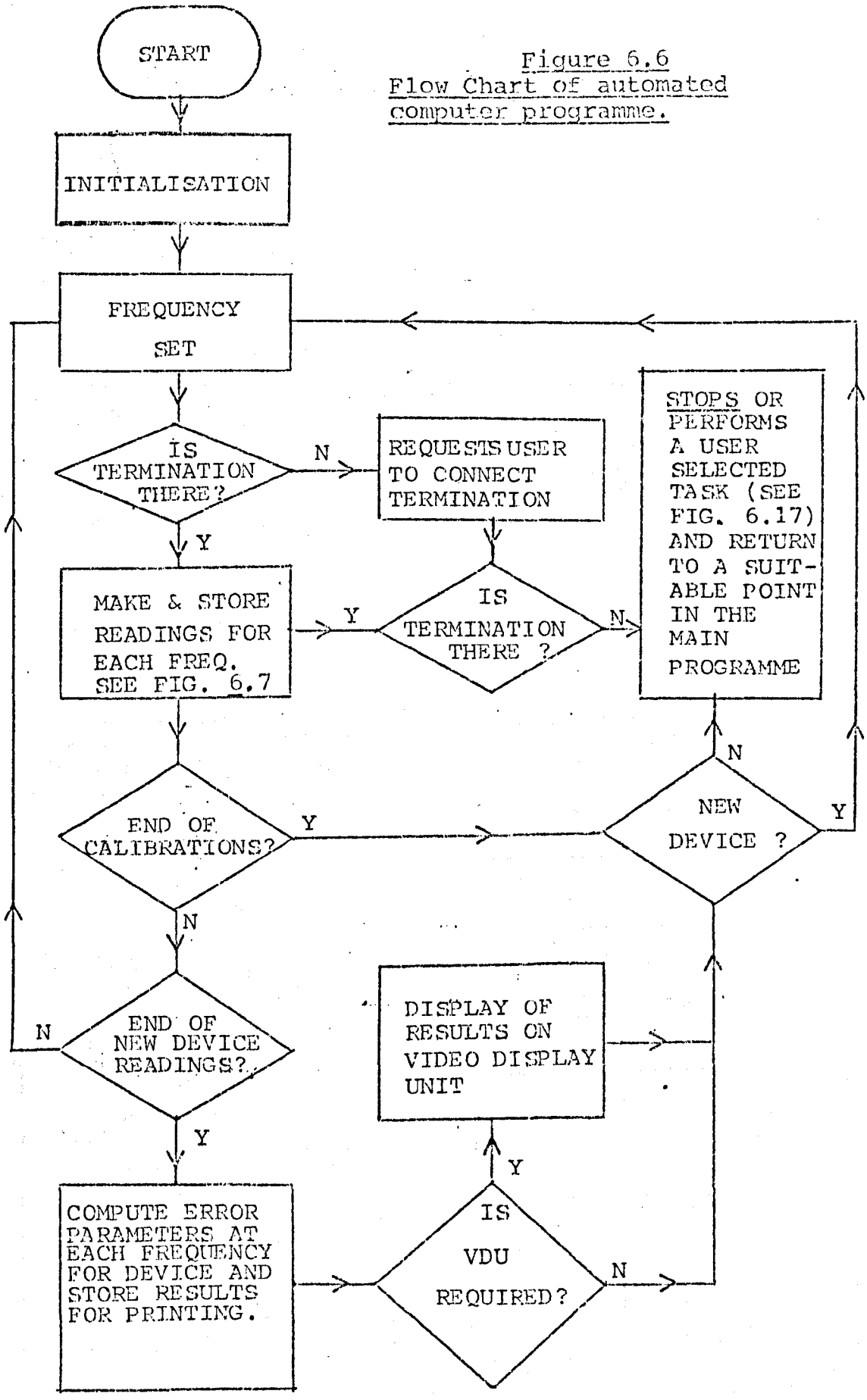

Figure 6.6
Flow Chart of automated computer programme.

Figure 6.7
Details of Frequency Storage Procedure and Signal Measurement.

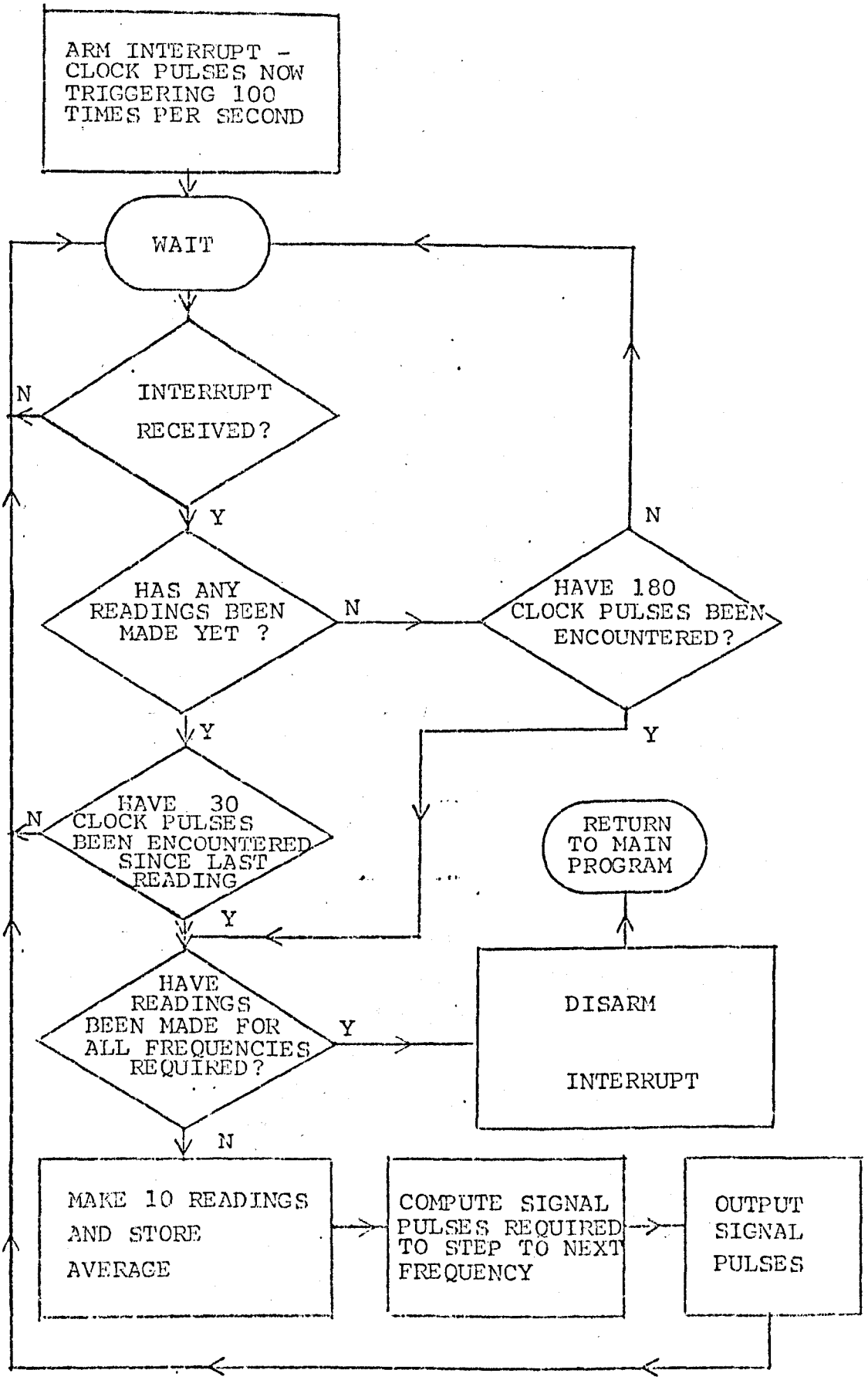

6:5.2 Interface Between Operator and Computer

Communications between the operator and the computer is carried out via a graphics terminal (Video Display Unit (VDU) with an input keyboard) situated remotely from the computer. A typical question and answer routine is shown in figures 6.8(a) and 6.8(b).

Upon receipt of the appropriate operator command, the VDU prints out the first five lines of figure 6.8(a). Initialisation in the programme refers to the measurement frequency bandwidth required and to the number of measurement steps required. The option to use an external data tape to store all the measurement data is also given. If the external data tape is desired, the computer will search the tape until it finds the last stored data position. For this particular case, the display indicates that 37 data sets have been stored. The next data set to be stored will be indicated as Test 38 (See figure 6.8(b)).

The amplifiers referred to in the programme are the two 20dB voltage amplifiers inserted between the network analyser and the remotely sited computer. When these amplifiers are used, the computer must be informed.

The programme then presents two options either (a) the standard calibration using 4 short circuits (figures 6.8(a) or (b) the non-standard calibration using 4 unknown terminations and a reference short circuit (figures 6.9(a) and 6.9(b). The above mentioned figures are photo-copies of the video display. Most of the remainder of the display is devoted to the initialisation procedure. The "no. of points per reading = 10" "Timing Interval (N* 0.01 sec). N = 30" indicates that the average of 10 readings is taken at each frequency step and that the interval between each reading is 0.3 seconds. The next three lines indicate to the computer what instruments are in use.

Figure 6.8(a)

Communications between Operator and Computer

```
REFLECTION COEFFICIENT MEASUREMENT CORRECTION

USING 4 SHORTS OR 4 UNKNOWN TERMINATIONS AND A REFERENCE SHORT
VERSION 6UL2/R2
J-BAND FACILITIES INCLUDED
INITIALISATION REQUIRED ? TYPE Y OR N >YES
USE OF DATA TAPE REQUIRED ? TYPE Y OR N >YES
DATA TAPE LOADED :   37
ARE AMPLIFIERS IN USE ? TYPE Y OR N ?YES
INPUT TYPE COAX ONLY

STANDARD CALIBRATION USES SHORT CIRCUITS ONLY

NONSTANDARD CALIBRATION USES 4 UNKNOWN TERMINATIONS AND A REFERENCE SHORT

STANDARD CALIBRATION REQUIRED ? (TYPE Y OR NO) ?YES
JOYSTICK IS NOT IN USE.
NO. OF POINTS PER READING =10
TIMING INTERVAL ( N*0.01 SEC). N=30
INPUTS TAKEN FROM POLAR DISPLAY OR PHASE GAIN UNIT ?
TYPE LOG,LIN,OR POL ?*? POL
CENTRE BEAM WHILE TYPING ANY CHARACTER P
MAXIMUM FREQUENCY (GHZ) = 6
MINIMUM FREQUENCY (GHZ) = 4
NO. OF POINTS = 21
SWITCH TOLEC RESET TO 3V.
MINIMUM FREQUENCY SET UP
CORRECTION TO FREQ. IN MHZ = 0
```

Figure 6.8(b)

Communications between the Operator and Computer

```
K=1   CONNECT CALIBRATION 1      >YES
K=2   CONNECT CALIBRATION 2      >YES
K=3   CONNECT CALIBRATION 3      >YES
K=4   CONNECT CALIBRATION 4      >YES

NEW DEVICE ? >YES
TYPE DEVICE IDENTIFICATION & TERMINATE WITH CR
TEST 38
K=6   CONNECT DEVICE             >YES

IS VDU DISPLAY REQUIRED ? <TYPE Y OR N>
```

Figure 6.9(a) Communications between Operator and Computer

```
REFLECTION COEFFICIENT MEASUREMENT CORRECTION

USING 4 SHORTS OR 4 UNKNOWN TERMINATIONS AND A REFERENCE SHORT
VERSION OULZ/R2
J-BAND FACILITIES INCLUDED
INITIALISATION REQUIRED ? TYPE Y OR N >YES
USE OF DATA TAPE REQUIRED ? TYPE Y OR N >YES
DATA TAPE LOADED :   38
ARE AMPLIFIERS IN USE ? TYPE Y OR N ?YES
INPUT TYPE COAX ONLY

STANDARD CALIBRATION USES SHORT CIRCUITS ONLY

NONSTANDARD CALIBRATION USES 4 UNKNOWN TERMINATIONS AND A REFERENCE SHORT

STANDARD CALIBRATION REQUIRED ? (TYPE Y OR NO) ?NO
JOYSTICK IS NOT IN USE.
NO. OF POINTS PER READING =10
TIMING INTERVAL ( N*0.01 SEC). N=30
INPUTS TAKEN FROM POLAR DISPLAY OR PHASE GAIN UNIT ?
TYPE LOG,LIN,OR POL ??? POL
CENTRE BEAM WHILE TYPING ANY CHARACTER P
MAXIMUM FREQUENCY (GHZ) = 8
MINIMUM FREQUENCY (GHZ) = 6
NO. OF POINTS = 31
SWITCH TOLEC RESET TO 3V.
MINIMUM FREQUENCY SET UP
CORRECTION TO FREQ. IN MHZ = 0
```

Figure 6.9(b) Communications between the Operator and the Computer

```
K=1    CONNECT CALIBRATION 1       >YES
K=2    CONNECT CALIBRATION 2       >YES
K=3    CONNECT CALIBRATION 3       >YES
K=4    CONNECT CALIBRATION 4       >YES
K=5    CONNECT REFERENCE SHORT     >YES

NEW DEVICE ?  >YES
TYPE DEVICE IDENTIFICATION & TERMINATE WITH CR
TRIAL OF 10/10/77
K=6    CONNECT DEVICE              >YES

IS VDU DISPLAY REQUIRED ? (TYPE Y OR N)!
```

For this particular case, the minimum and maximum frequencies have been chosen to be 4 and 6 GHz respectively and measurements will be carried out at 21 frequencies evenly spaced between 4 and 6 GHz. A facility for adjusting the initial starting frequency to the correct value is also incorporated in this particular case, no frequency correction was considered necessary.

No explanation will be given for figures 6.8(b) and 6.9(b) as they are considered to be self-explanatory.

6:5.3 The Control of the Signal Frequency

To control the signal frequency, two signals are required, one to select the desired R.F. Oscillator Unit and the other to alter the voltage controlling the frequency of the chosen oscillator. There are three R.F. sweep oscillators with the signal source unit and the desired oscillator is selected by means of a direct voltage which is interpreted as a 4 bit binary word by the Control Unit (HP 8706A).

The direct voltage controlling the frequency is obtained from an electronically programmable voltage power supply which is in its turn controlled by the computer. A voltage range of 0 volts to 73 volts is required from the power supply to control the entire frequency range of each oscillator. The resolution of this voltage is controlled in increments of 1 millivolt by each voltage pulse from the computer and these are supplied at the rate of 30,000 pulses per second. The particular voltage level to provide a given frequency at any stage of calibration or testing is determined by the data stored and calculated within the computer.

When the maximum frequency (GHz), the minimum frequency (GHz) and the number of frequencies for measurement are specified (Fig. 6.8(a)), the computer calculates

the number of pulses required for the minimum frequency, the number of pulses required for each increment in frequency and the number ofpulses required for the maximum frequency. It commences by selecting the appropriate sweep oscillator calibration table and displaying what it considers to be the minimum frequency. The operator is at liberty to alter this frequency if it does not agree with that shown on the frequency counter. The computer receives the additional instructions and will alter the minimum frequency to suit the operator. It also stores the new number of required clock pulses as that required for the minimum frequency and re-adjusts the necessary frequency stepping procedure described earlier.

Two other important points must be mentioned here. When the oscillator frequency is altered a small amount of waiting time is required for the frequency to stabilize. The amount of waiting time built into the programme is one second and this is incorporated in the flow-diagram of 6.7. In addition to this, 300 milliseconds is normally allowed between each of ten readings carried out at any one frequency to nullify the effects of noise voltage transients etc. The operator has the choice of altering the timing interval between measurements by calling up the pertinent sub-routine (Section 6:5.6).

6:5.4 Measurement, Storage and Calculation of Data

The programme incorporates facilities for accepting the non-identical output voltages from two different display units, namely, the phase gain indicator unit (HP 8413A) and the polar display unit (HP 8414A). The phase gain unit provides input information in polar co-ordinates i.e., magnitude either in linear form (0 to 1 volt max) or in decibels (50 mV/dB) and phase 10 mV per degree). The polar display unit provides linear outputs ($\pm$ 10v Max) in the form of rectangular co-ordinates. The computer must be informed as to which display unit is used. In most cases,

the polar display unit is invariably used because (a) it provides a better signal to noise ratio to the computer especially after the 20dB buffer amplifiers and (b) it provides an instant display of any instrument malfunction during measurement.

It was mentioned briefly in Section 6:5.3 that ten reflection coefficient measurements are taken at any one frequency to minimise the effects of noise transients etc. These readings are put into a temporary storage register, averaged and only the final result is put into the main data storage. The other readings are discarded.

Calculations are carried out in a sub-routine called "Calc" (Not shown). This sub-routine features several "IF" statements to determine whether the standard calibration or non-standard calibration calculation procedure is required. If the non-standard procedure (i.e., 4 unknown terminations and a reference short) is used, then the unknown termination will also have to be calculated. The attenuation and phase properties of the transmisiion lines used in the calibration procedures are calculated in both cases and are available in the printed results.

The error parameters and the corrected reflection coefficient of the device under test are also calculated in this sub-routine.

All the above data, calibration and measured results can also be stored on an external data tape. This procedure allows:-

(a) An almost unlimited set of measurements to be performed and stored.

(b) Measured data to be readily available without recourse to the measuring equipment.

(c) There is no photo-copying facilities allied to the video display unit in the measurements laboratory but one is available in the computer room situated some distance away. The ability to recall measured data on the video display unit in the computer room permits easy photo-copying of measured results.

Figure 6.10 Communications between the Operator and the Computer (Displays)

```
DISPLAY REQUIRED ?
AM  AMPLITUDE VS FREQUENCY
PH  PHASE VS FREQUENCY
PO  POLAR PLOT
NO  NONE - LEAVE DISPLAY SEQUENCE
PLOT ? !>NONE
DATA TO BE DUMPED ON TAPE ? <TYPE Y OR N> !YES
READINGS DUMPED AS FILE NO.   38

NEW DEVICE ? >YES
TYPE DEVICE IDENTIFICATION & TERMINATE WITH CR
2ND TRIAL 3B
K=G   CONNECT DEVICE                >YES

IS VDU DISPLAY REQUIRED ? <TYPE Y OR N>?
```

6:5.5 Reproduction of Results

Facilities are provided for three types of graphical display of the results on the video display unit. The provision for entry into the display sub-routine is made available automatically at the end of each device measurement (Fig. 6.9(b)) by the query "Is VDU Display Required? (Type Y or N)". The operator then has the choice of three displays (see Figure 6.10). Typical photo-copies of some of the graphical plots for a short circuit are given in Figure 6.11 (Amplitude vs Frequency), Fig. 6.12 (Phase vs Frequency) and Fig. 6.13 (Polar Display). In all cases, the points joined by a line are the uncorrected values; the corrected values are denoted by separate symbols. The above-mentioned figures are actual size photo copies of the display which is a convenient scale for most applications. However, expansion facilities for both the abscissa and ordinate scales are provided if desired. This facility may be obtained by answering the query "MAX X = " in the bottom left hand corner of each display. For example in the measurement of a matched load (Fig. 6.14) the difference between the corrected and the uncorrected reflection coefficient was found to be impractically small for full-scale display and it was decided to expand the ordinate scale to produce a meaningful graph. This was carried out by the following sequence:

"MAX	X	=	"	6	CR (Carriage Return)
"MIN	X	=	"	4	CR "
"MAX	Y	=	"	.1	CR "
"MIN	Y	=	"	0	CR "

The first two replies designate the frequency bandwidth to be displayed whilst the last two replies set the amplitude range required. The result is the graph of Figure 6.14.

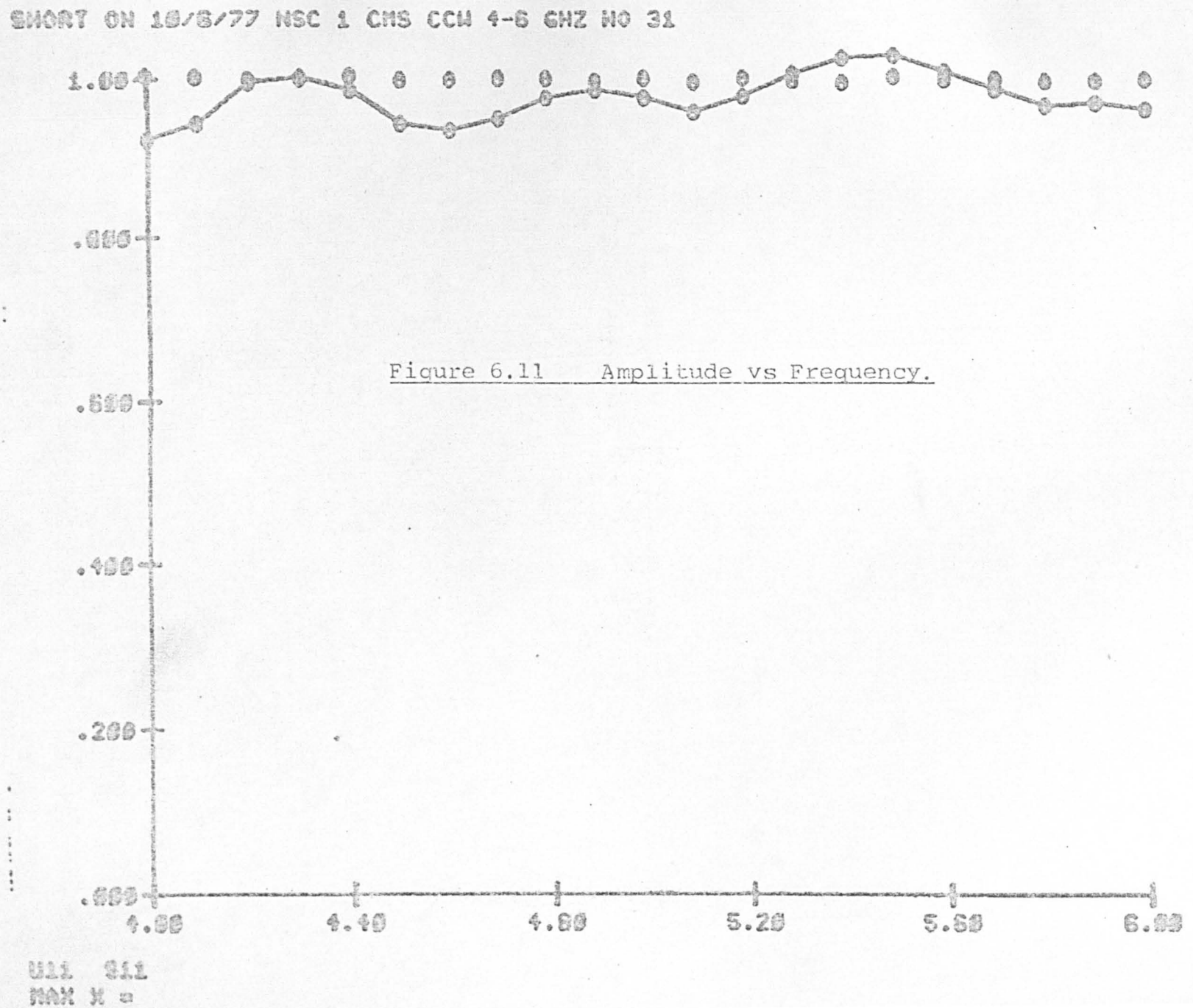

Figure 6.11 Amplitude vs Frequency.

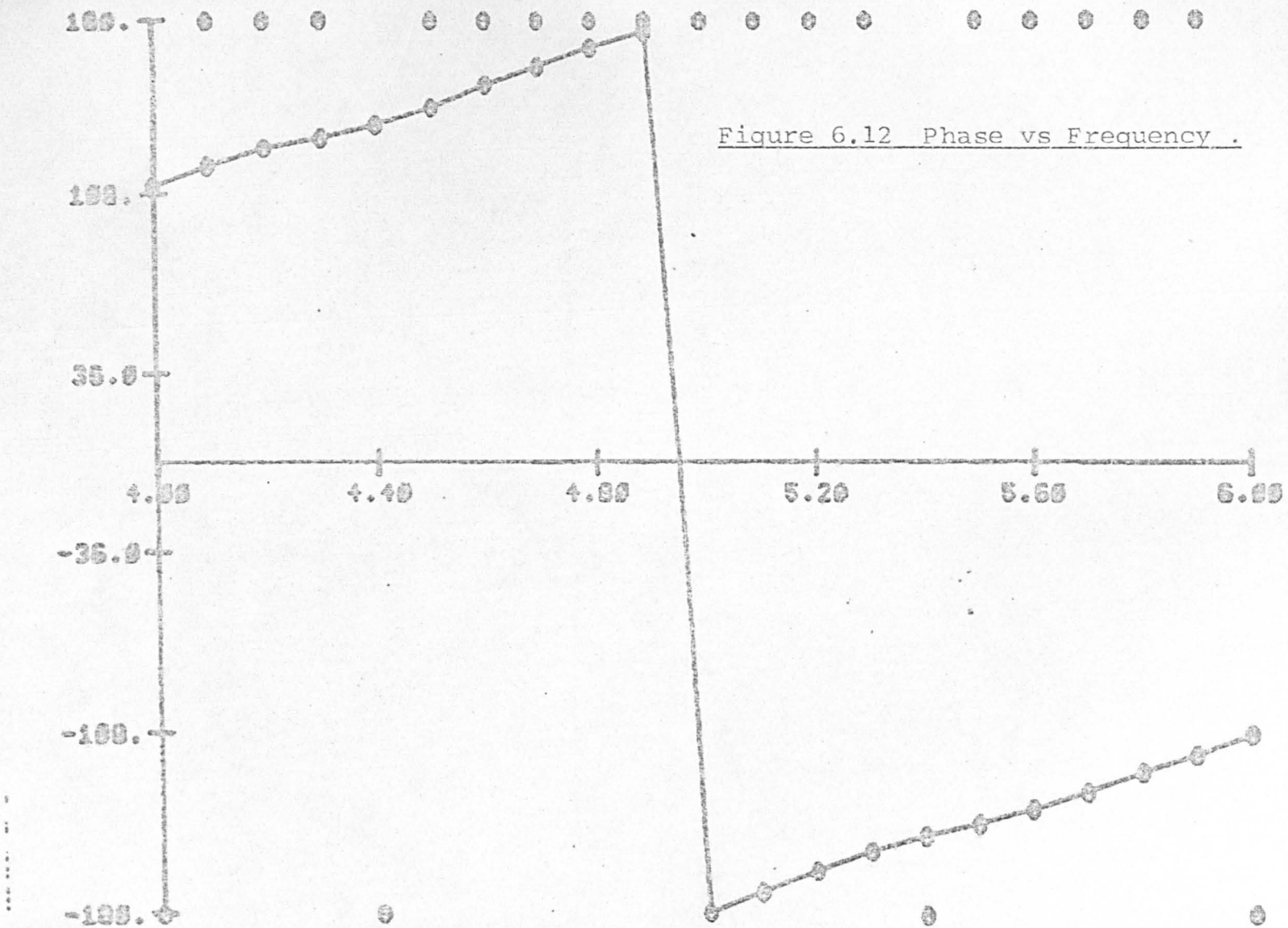

Figure 6.12 Phase vs Frequency .

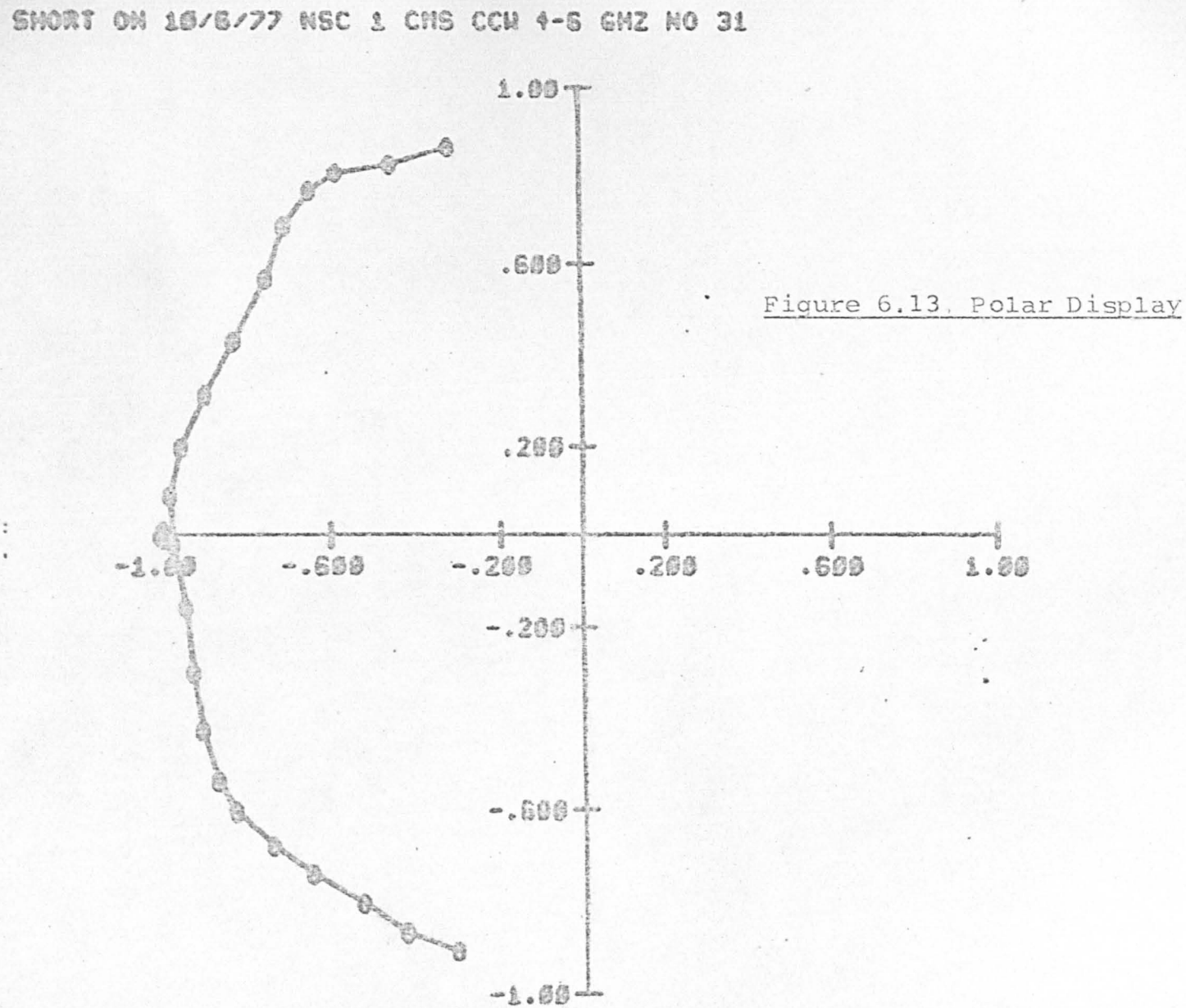

Figure 6.13. Polar Display

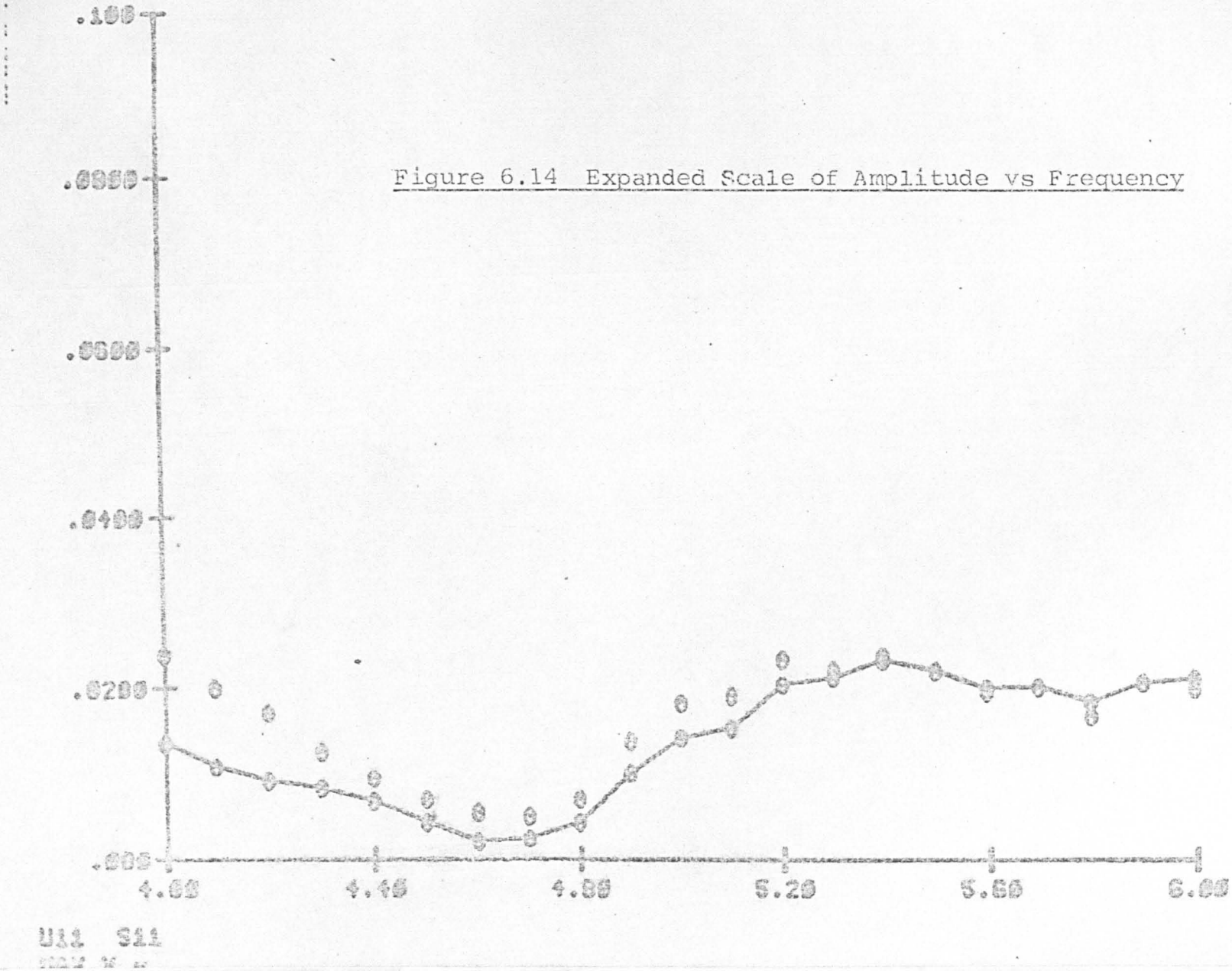

Figure 6.14 Expanded Scale of Amplitude vs Frequency

MATCH LOAD ON 10/6/77 4-6 GHZ NSC 1 CMS CCW NO 29

FREQUENCY GHZ	CALIBRATION 1 AMPLT	CALIBRATION 1 PHASE	CALIBRATION 2 AMPLT	CALIBRATION 2 PHASE	CALIBRATION 3 AMPLT	CALIBRATION 3 PHASE	CALIBRATION 4 AMPLT	CALIBRATION 4 PHASE	REF. SHORT AMPLT	REF. SHORT PHASE	UNCRT DEVICE AMPLT	UNCRT DEVICE PHASE	ONE LINE LENGTH NEPERS	ONE LINE LENGTH DEGREES
4.000	.973	-79.5	.998	-176.1	.968	86.9	1.002	-7.8	.918	110.6	.014	-1.7	.01	47.91
4.100	.938	-74.2	.963	-173.2	.934	87.6	.966	-9.6	.941	119.4	.011	-.4	.01	49.16
4.200	.914	-66.6	.936	-168.4	.905	90.2	.937	-9.6	.996	126.4	.009	5.1	.01	50.46
4.300	.899	-57.5	.921	-162.3	.891	93.9	.920	-7.9	1.003	130.5	.008	13.2	.01	51.72
4.400	.936	-48.7	.952	-156.5	.921	97.8	.948	-6.3	.982	136.1	.007	26.6	.01	52.96
4.500	.969	-42.8	.982	-152.9	.949	99.1	.979	-7.5	.943	143.3	.004	24.6	.00	54.14
4.600	.971	-37.5	.984	-149.9	.952	99.6	.987	-9.3	.935	152.9	.002	33.6	.00	55.31
4.700	.956	-31.8	.960	-146.6	.930	100.7	.961	-11.2	.948	161.0	.003	177.7	.00	56.58
4.800	.936	-24.7	.935	-141.9	.910	103.0	.932	-11.0	.974	168.6	.004	-151.0	.00	57.73
4.900	.938	-16.8	.934	-136.5	.911	106.3	.936	-9.9	.989	175.1	.010	-125.8	.00	58.85
5.000	.959	-9.5	.952	-131.3	.935	108.8	.960	-10.3	.975	-178.7	.014	-113.6	.00	60.13
5.100	.986	-4.4	.971	-128.3	.951	109.5	.973	-12.0	.961	-170.2	.015	-102.2	.00	61.26
5.200	.977	1.1	.959	-125.2	.947	111.0	.973	-13.4	.976	-161.8	.020	-90.4	.00	62.39
5.300	.962	8.0	.943	-120.4	.930	112.6	.955	-14.1	1.008	-154.4	.021	-77.9	.00	63.68
5.400	.951	15.6	.924	-115.2	.913	116.7	.938	-12.4	1.032	-148.3	.023	-68.5	.00	64.61
5.500	.961	24.0	.940	-108.7	.932	119.6	.958	-11.9	1.026	-143.5	.022	-66.8	.00	65.98
5.600	.994	30.4	.968	-104.6	.963	122.6	.989	-11.5	1.009	-137.6	.020	-57.8	.00	66.91
5.700	1.018	36.2	.992	-100.5	.993	122.6	1.020	-13.8	.987	-131.2	.020	-57.0	.00	68.34
5.800	1.008	41.0	.983	-97.9	.981	123.8	1.006	-15.0	.967	-123.3	.018	-52.1	.00	69.30
5.900	1.006	47.1	.983	-94.2	.985	124.3	1.006	-16.9	.972	-116.4	.021	-55.2	.00	70.67
6.000	.974	52.5	.957	-91.0	.957	126.0	.977	-17.6	.961	-108.9	.021	-53.7	.00	71.66

FREQUENCY GHZ	REF COEFF REAL	REF COEFF IMAG	REF COEFF AMP	REF COEFF DB	REF COEFF PHASE	VSWR
4.000	-.003	.022	.024	-32.507	109.3	1.049
4.100	-.004	.020	.020	-34.008	100.2	1.041
4.200	-.001	.017	.017	-35.383	94.6	1.035
4.300	-.001	.013	.013	-37.999	92.8	1.026
4.400	.001	.010	.010	-40.392	85.2	1.019
4.500	-.000	.007	.007	-42.985	90.5	1.014
4.600	-.002	.005	.006	-45.097	116.1	1.011
4.700	-.005	.002	.005	-45.879	155.0	1.010
4.800	-.006	-.004	.007	-42.931	-149.5	1.014
4.900	-.009	-.011	.014	-37.231	-129.5	1.028
5.000	-.011	-.015	.018	-34.881	-125.9	1.037
5.100	-.011	-.015	.019	-34.433	-125.9	1.039
5.200	-.011	-.021	.023	-32.720	-117.3	1.047
5.300	-.011	-.019	.022	-32.184	-121.0	1.045
5.400	-.009	-.022	.024	-32.534	-112.5	1.048
5.500	-.012	-.018	.022	-33.195	-124.4	1.045
5.600	-.008	-.018	.020	-34.163	-115.5	1.040
5.700	-.015	-.013	.020	-33.979	-138.6	1.041
5.800	-.012	-.012	.017	-35.483	-135.8	1.034
5.900	-.017	-.012	.021	-33.745	-146.0	1.042
6.000	-.016	-.012	.020	-34.015	-143.3	1.041

FIGURE 6.15

DATA SHEET OF
PRINTED RESULTS

The data sheet produced by the line printer at the end of each measurement is shown in figure 6.15. The information presented is fairly comprehensive and includes:

(a) The frequency of measurement.

(b) The reflection coefficients of all the calibration measurements.

(c) The reflection coefficient of the device under test.

(d) The total one-way attenuation and phase of the incremental length of line between the calibration pieces.

(e) The corrected reflection coefficient of the device under test given in the lower rectangular data block. This is given in rectangular co-ordinates (columns 2 & 3) polar co-ordinates (cols 4, 5, 6) and in VSWR relative to a 50 ohm line.

6:5.6 Supplementary Tasks

The programme has facilities for various supplementary tasks. These are listed in detail in figure 6.16. Entry into these sub-routines are only permitted at certain points in the programme. These points are obtained by typing "No" to any of the following questions displayed on the video display unit.

(a) Connect Calibration 1? - No
(b) Connect Calibration 2? - No
(c) Connect Calibration 3? - No
(d) Connect Calibration 4? - No
(e) Connect Device ? - No
(f) Is display required ? - No
(g) Display Required ? - No
(h) New Device ? - No

This will result in the following sentence:

"Task? (Type LI for list of Options)!!"

Figure 6.16 List of Supplementary Tasks

```
< OPTIONS - TWO LETTER KEYS REQUIRED
LI   LIST OPTIONS                ZE   RESTART PROGRAM
DG   RESTART CALIBRATION         RE   REPEAT LAST READING
SK   RESET K (SEE BELOW)         ND   GO TO NEW DEVICE
CA   CALCULATE                   PR   PRINT
DI   ENTER DISPLAY               DU   DUMP READINGS
UD   UNDUMP READINGS             ST   RELEASE PROGRAM
CO   INSERT COMMENT              CE   CENTRE BEAM
AM   RESET AMPLIFIERS            IN   RESET INPUT TYPE
WA   WAVEGUIDE OR COAX           CL   DEFINE CALIB PIECES
JO   JOYSTICK SWITCH             FR   RESET FREQ RANGE
MF   CORRECT MIN FREQ            NO   RESET NO. POINTS
TI   RESET TIMING INT            TF   UPDATE TAPE FORMAT
DC   DISC FILE CLEAR


SETTINGS FOR K IN SK OPTION
K=1    CONNECT SHORT CIRCUIT
K=2    CONNECT OFFSET SHORT 1
K=3    CONNECT OFFSET SHORT 2
K=4    CONNECT OFFSET SHORT 3
K=5
K=6    CONNECT DEVICE

TASK ? (TYPE LI FOR LIST OF OPTIONS)  !!
```

At this stage, the operator is free to select the tasks listed by typing the key code listed and terminating with a carriage return (CR). Alternatively if the key codes cannot be remembered then typing LI will result in the display of figure 6.16 and any of the procedures listed may be selected by typing in the appropriate key code.

The programme is terminated by typing "ST" at the task entry point.

Finally, when this programme is used, the restriction mentioned in Section 6:3 should be observed.

6:6 The Automated Programme for the Three Short Circuits Correction Method

This programme operates in a similar manner to that described for the 5 termination programme except for the following points:-

(a) All lines are assumed to be lossless.
(b) All the electrical offset lengths must be stated.
(c) All calibration terminations must be known.

A typical operating format is shown in Figure 6.17 and a typical line printer data sheet can be seen in Figure 6.18.

The programme also incorporates two other correction systems (Ref. 6.5 and 6.6). These are useful when the cross-checking of measurements are required. This programme was written by Stoneman (Ref. 6.3). Other than providing the derivations for the three shorts correction procedure, no credit is claimed for the writing of this programme.

Figure 6.17 Operating Format for the Three Shorts Automated Programme

```
 REFLECTION COEFFICIENT MEASUREMENT CORRECTION

USING MATCHED LOAD WITH SHORT OR OPEN CIRCUIT
OR SHORT AND OPEN CIRCUITS
VERSION OVL2/R2
J-BAND FACILITIES INCLUDED
INITIALISATION REQUIRED ? TYPE Y OR N >YES
USE OF DATA TAPE REQUIRED ? TYPE Y OR N >NO
ARE AMPLIFIERS IN USE ? TYPE Y OR N !YES
INPUT TYPE COAX ONLY

STANDARD CALIBRATION USES SLIDING LOAD, SHORT AND OFFSET SHORT.
STANDARD CALIBRATION REQUIRED ? (TYPE Y OR NO) !NO
CALIBRATION WITH MATCHED LOAD REQUIRED ? (TYPE Y OR N) !NO
CALIBRATION PIECE 1 IS SHORT CIRCUIT.
CALIB. PIECE 2 IS OFFSET SHORT.
CALIB. PIECE 3 CAN BE OPEN CIRCUIT OR OFFSET SHORT.

CALIB PIECE 2: LENGTH OF OFFSET SHORT (CM) =   4
CALIB PIECE 3 ? (TYPE OP OR OF) !!OFFSET
LENGTH OF OFFSET SHORT (CM) = 2
JOYSTICK IS NOT IN USE.
NO. OF POINTS PER READING =10
TIMING INTERVAL ( N*0.01 SEC). N=30
INPUTS TAKEN FROM POLAR DISPLAY OR PHASE GAIN UNIT ?
TYPE LOG,LIN,OR POL !!! POL
CENTRE BEAM WHILE TYPING ANY CHARACTER Y
MAXIMUM FREQUENCY (GHZ) = 4
MINIMUM FREQUENCY (GHZ) = 2
NO. OF POINTS = 21
SWITCH TOLEC RESET TO 3U.
MINIMUM FREQUENCY SET UP
CORRECTION TO FREQ. IN MHZ =
```

310 MATCHED LOAD ON 2/7/77 4-6 GHZ S/.46/1.16

FREQUENCY GHZ	K=1 AMP	K=1 PHASE	K=2 AMP	K=2 PHASE	K=3 AMP	K=3 PHASE	K=4 AMP	K=4 PHASE	K=5 AMP	K=5 PHASE	K=6 DEVICE AMP	K=6 DEVICE PHASE
4.000	.965	178.6	.965	134.6	1.001	64.3	.000	.0	.000	.0	.015	54.4
4.100	.986	179.7	.994	133.5	1.015	59.0	.000	.0	.000	.0	.012	51.7
4.200	1.035	178.9	1.029	130.3	.996	53.6	.000	.0	.000	.0	.011	51.3
4.300	1.036	175.9	.994	126.0	.940	50.9	.000	.0	.000	.0	.011	50.1
4.400	1.022	174.7	.962	125.2	.941	50.9	.000	.0	.000	.0	.009	45.8
4.500	.970	174.8	.940	126.8	.961	49.0	.000	.0	.000	.0	.007	45.3
4.600	.947	176.8	.936	126.8	.980	46.4	.000	.0	.000	.0	.006	42.7
4.700	.968	177.4	.966	125.2	.995	41.2	.000	.0	.000	.0	.003	38.3
4.800	.992	178.2	.979	123.7	.971	37.8	.000	.0	.000	.0	.001	-56.4
4.900	1.009	177.1	.975	121.5	.963	35.2	.000	.0	.000	.0	.005	-121.9
5.000	.983	176.6	.951	121.5	.959	33.3	.000	.0	.000	.0	.008	-107.9
5.100	.974	178.4	.954	121.4	.990	30.5	.000	.0	.000	.0	.013	-99.2
5.200	.985	179.0	.982	120.7	1.000	25.5	.000	.0	.000	.0	.015	-91.7
5.300	1.019	-179.6	1.016	119.8	.991	21.7	.000	.0	.000	.0	.017	-91.2
5.400	1.045	179.1	1.002	115.0	.973	19.1	.000	.0	.000	.0	.018	-89.9
5.500	1.049	177.1	.975	112.2	.966	17.7	.000	.0	.000	.0	.019	-88.4
5.600	1.031	175.1	.967	111.9	.988	14.9	.000	.0	.000	.0	.017	-87.8
5.700	1.008	175.3	.952	110.5	1.018	12.1	.000	.0	.000	.0	.016	-92.3
5.800	.990	175.2	.963	108.9	1.007	7.6	.000	.0	.000	.0	.015	-100.1
5.900	.999	175.0	.968	108.3	1.021	3.4	.000	.0	.000	.0	.015	-110.4
6.000	.984	175.3	.964	105.6	.985	.0	.000	.0	.000	.0	.013	-124.0

FREQUENCY GHZ	REF COEFF REAL	REF COEFF IMAG	REF COEFF AMP	REF COEFF DB	REF COEFF PHASE	VSWR
4.000	.003	.046	.046	-26.690	86.6	1.097
4.100	.004	.051	.051	-25.809	85.2	1.108
4.200	.010	.053	.054	-25.420	79.0	1.113
4.300	.007	.045	.046	-26.827	81.3	1.095
4.400	.002	.045	.045	-26.947	87.4	1.094
4.500	.020	.047	.051	-25.882	67.3	1.107
4.600	.005	.042	.042	-27.507	83.2	1.088
4.700	.004	.041	.041	-27.644	84.1	1.087
4.800	.003	.040	.040	-27.955	85.1	1.083
4.900	.001	.038	.038	-28.318	88.6	1.080
5.000	.011	.037	.039	-28.236	73.8	1.081
5.100	-.003	.036	.036	-28.933	94.6	1.074
5.200	.010	.035	.036	-28.756	74.8	1.076
5.300	.016	.034	.038	-28.483	64.1	1.078
5.400	-.006	.035	.035	-29.063	99.9	1.073
5.500	-.012	.034	.036	-28.941	109.9	1.074
5.600	.004	.034	.035	-29.211	84.0	1.072
5.700	-.014	.039	.042	-27.602	110.2	1.087
5.800	-.013	.030	.033	-29.650	113.3	1.068
5.900	-.006	.040	.040	-27.886	98.2	1.084
6.000	-.017	.033	.037	-28.613	117.4	1.077

FIGURE 6.18

DATA SHEET OF PRINTED RESULTS

6:7 Conclusions

Five manual and two automated computation programmes have been presented. These computer programmes form a very necessary and important part of the research programme to verify the theory experimentally. Of these programmes, great difficulty was experienced in writing the automated five Termination Programme. As this programme was unfunded, computer programming assistance was not available and considerable time and effort had to be invested in gaining the familiarity with the computer hardware needed for this type of work.

* * * * * * * * * * *

6:8 References

6.1 Hewlett Packard Co., Page Mill Road, Palo Alto, California, "Hewlett-Packard Calculator Model 9100A Operating and Programming".

6.2 da Silva, E.F. and McPhun, M.K. "Calibration of Microwave Network Analyser for Computer Corrected S Parameter Measurements" Electronic Letters 1972, 9, pp 126-128.

6.3 Shurmer, H.V., Luxton, H., Hosseini, N. and Katie A Stoneman "the Application of an On-Line Computer to Microwave Measurement" IMEKO VII - 10-14 May 1976 (London).

6.4 Hewlett Packard /Network Analyser Data Sheet" Model 8410A issued 1st July 1967.

6.5 Adams, S.F. "A New Precision Automatic Measurement System" I.E.E.E. Trans. 1968, IM 17, pp 308-313.

6.6 Shurmer, H.V., "Calibration Procedure for Computer Corrected S Parameter Characterisation of Devices Mounted in Microstrip" Electronic Letters 1973, 9, pp 323-324.

6.7 Ducket, J. "Private Communications" Computer Programmer, Department of Engineering, University of Warwick.

* * * * * * * * * * *

CHAPTER VII

The FABRICATION of TEST and CALIBRATION PIECES

7:0 Introduction

The theory of the new measurement systems have been described in Chapter V. The associated computer programmes (software) for calculating the required correction results have been explained in Chapter VI. This chapter provides details of the construction of the calibration pieces used to verify the theory of the previous two chapters.

It was obvious in the initial conception of these calibration pieces that any design conceived must incorporate the following vitally important properties:-

(a) Electrical and mechanical stability in use.

(b) Uniformity in reproduction.

(c) Ease of construction (economy).

(d) Easy interface with the measuring instruments.

After much thought, it was decided to construct the majority of these calibration pieces in air coaxial line using APC-7 connectors for the following reasons:-

(a) The characteristic impedance of a precision air coaxial line can be accurately defined.

(b) APC-7 connectors are known to be electrically stable and provide more consistent VSWR's.

(c) The mechanical dimensions of these connectors are held within tolerances of $\pm$ 0.0025 m.m.

(d) Inner and Outer conductors with dimensions and tolerances identical to that of the APC-7 connectors are available and may be purchased separately to permit easier fabrication of precision air-coaxial lines.

(e) Various transitions, e.g., co-axial to micro-strip etc., are available.

(f) Easy interface with the measurement reflect-meters whose ports are also connected with APC-7 connectors.

(g) Easy machining of the inner and outer conductors due to their physical dimensions.

7:1 General Details of the Calibration Standards

This section describes the points common to the coaxial calibration standards. Particular details of the individual standards will be described in later sections (7:2; 7:3 & 7:4).

7:11 Choice of Offset Lengths

The choice of offset lengths within the calibration pieces is important for the following reasons:-

(a) At a particular frequency of measurement the offset lengths must not be chosen so that the calibration reflection coefficients measured are Γ/θ , $\Gamma/\theta+2\pi$, $\Gamma/\theta+2n\pi$ etc., where n is any interger. For, if this were the case, then the error network cannot be solved.

(b) The offset lengths should be chosen to produce large calibration reflection coefficient angles differences to minimise the inaccuracies involved in specifying offset lengths. For example if the ability to measure a mechanical length is limited to $\pm$ 0.01mm , then choosing an offset length of 0.1mm is obviously unwise for a $\pm$ 10% uncertainty would be involved in specifying the offset length.

(c) For maximum accuracy in locating the virtual centre of a Smith Chart, the calibration reflection coefficients should be spaced 120° for any three termination calibration method (sections 5:4) and 90° for any four termination method (Section 5:5).

(d) Unneccessary mechanical difficulties would arise in maintaining the concentricity of the inner conductor if the offset lengths were made too long. Support by bead etc., is not favoured as discontinuities albeit small, will be produced unnecessarily. Furthermore, errors inaccurately specifying the electrical length of the offset, especially with changes in frequencies, could result.

In view of the above considerations, tables 7.1 and 7.2 were constructed to permit a more detailed study of optimum offset length. Each table contains seven sets of "preferred" offset lengths. Set 1 to 6 are chosen for optimum offset lengths for a particular frequency. For example, Set 1 is chosen for optimum operation at 12 GHz. Similarly, Sets 2, 3, 4, 5 and 6 are chosen for operation at 10, 8, 6, 4 and 2 GHz respectively.

From these Tables it is clear that if the ideal electrical offset length Sets are to be chosen, then many Sets will be required. This is obviously financially unacceptable and a compromise had to be made into choosing one set of calibration pieces for the short circuit measurements and one Set for open circuit measurements.

Table 7.1

($C = 3 \times 10^{11}$ mm/s)

3 Termination Measurements

Offset Length (mm)	Effective Phase Change (Degrees)					
	2GHz	4GHz	6GHz	8GHz	10GHz	12GHz
Set 1						
4.167	20.0	40.0	60.0	80.0	100.0	120.0
8.333	40.0	80.0	120.0	160.0	200.0	240.0
Set 2						
5.000	24.0	48.0	72.0	96.0	120.0	144.0
10.000	48.0	96.0	144.0	192.0	240.0	288.0
Set 3						
6.250	30.0	60.0	90.0	120.0	150.0	180.0
12.500	60.0	120.0	180.0	240.0	300.0	360.0
Set 4						
8.333	40.0	80.0	120.0	160.0	200.0	240.0
16.667	80.0	160.0	240.0	320.0	400.0	480.0
Set 5						
12.500	60.0	120.0	180.0	240.0	300.0	360.0
25.000	120.0	240.0	360.0	480.0	600.0	720.0
Set 6						
25.000	120.0	240.0	360.0	480.0	600.0	720.0
50.000	240.0	480.0	720.0	960.0	1200.0	1440.0
Set 7						
4.670	22.4	44.8	67.2	89.7	112.1	134.5
9.340	44.8	89.7	134.5	179.3	224.2	269.0

Table 7.2
($C = 3 \times 10^{11}$ mm/s)
4 Termination Measurements

Offset Length (mm)	Effective Phase Change (Degrees)					
	2GHz	4GHz	6GHz	8GHz	10GHz	12GHz
Set 1						
3.125	15.0	30.0	45.0	60,0	75.0	90.0
6.250	30.0	60.0	90.0	120.0	150.0	180.0
9.375	45.0	90.0	135.0	180.0	225.0	270.0
Set 2						
3.750	18.0	36.0	54.0	72.0	90.0	108.0
7.500	36.0	72.0	108.0	144.0	180.0	216.0
11.250	54.0	108.0	162.0	216.0	270.0	324.0
Set 3						
4.688	22.5	45.0	67.5	90.0	112.5	135.0
9.376	45.0	90.0	135.0	180.0	225.0	270.0
14.064	67.5	135.0	202.5	270.0	337.5	405.0
Set 4						
6.250	30.0	60.0	90.0	120.0	150.0	180.0
12.500	60.0	120.0	180.0	240.0	300.0	360.0
18.750	90.0	180.0	270.0	360.0	450.0	540.0
Set 5						
9.375	45.0	90.0	135.0	180.0	225.0	270.0
18.750	90.0	180.0	270.0	360.0	450.0	540.0
28.125	135.0	270.0	405.0	540.0	675.0	810.0
Set 6						
18.750	90.0	180.0	270.0	360.0	450.0	540.0
37.500	180.0	360.0	540.0	720.0	900.0	1080.0
56.250	270.0	540.0	810.0	1080.0	1350.0	1620.0
Set 7						
4.670	22.4	44.8	67.2	89.7	112.1	134.5
9.340	44.8	89.7	134.5	179.3	224.2	269.0
14.010	67.2	134.5	201.7	269.0	336.2	403.5

The short circuit set constructed is that shown in Set 7 of Table 7.2 manely 4.67mm, 9.34mm and 14.01mm. The open circuit calibration set chosen were 4.83mm, 14.83mm, 24.83mm and 34.83mm. These are obviously not the Eelectrical ideals" but were chosen as a compromise between the conflicting electrical and mechanical requirements

7:2 The 7mm Short Circuit Co-axial Calibration Pieces

Photo copies of these short circuits are shown in Figure 7.1. The machine drawings relating to their construction are shown in Figures 7.2 and 7.4 to 7.7. These were designed by the author.

Figure 7.1

Photograph of the Short Circuit Calibration Pieces

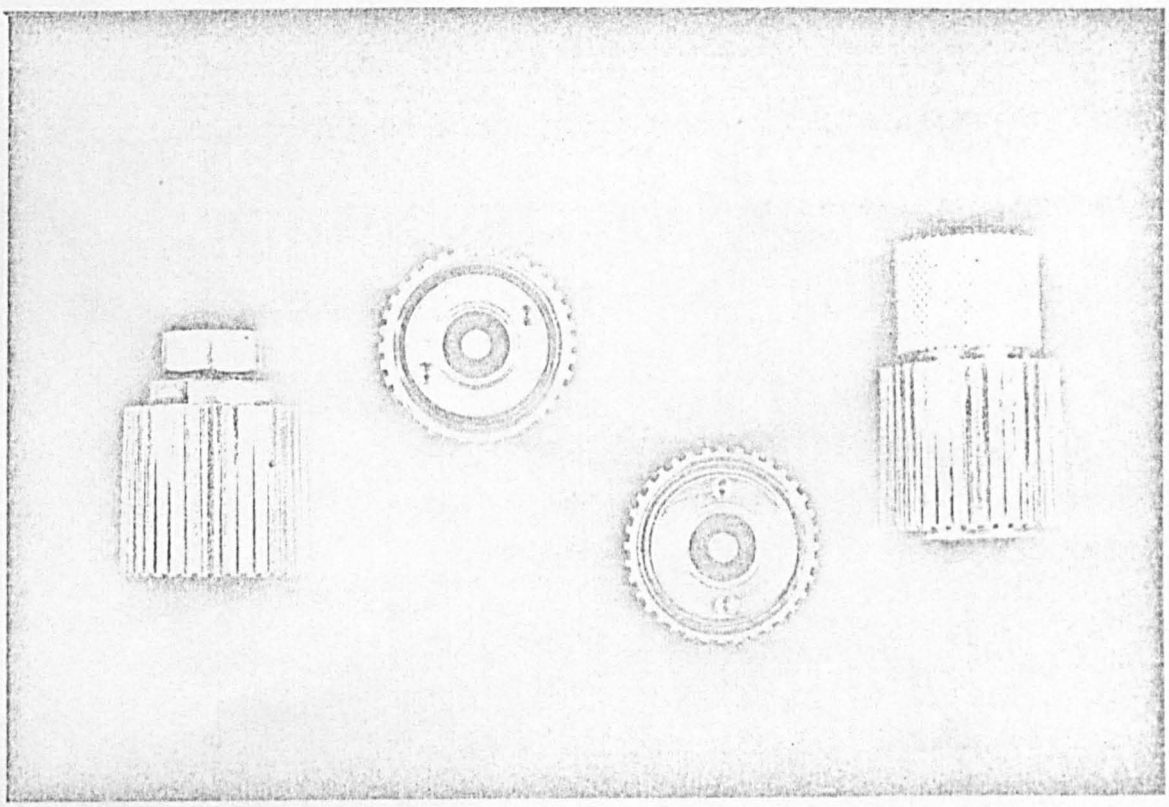

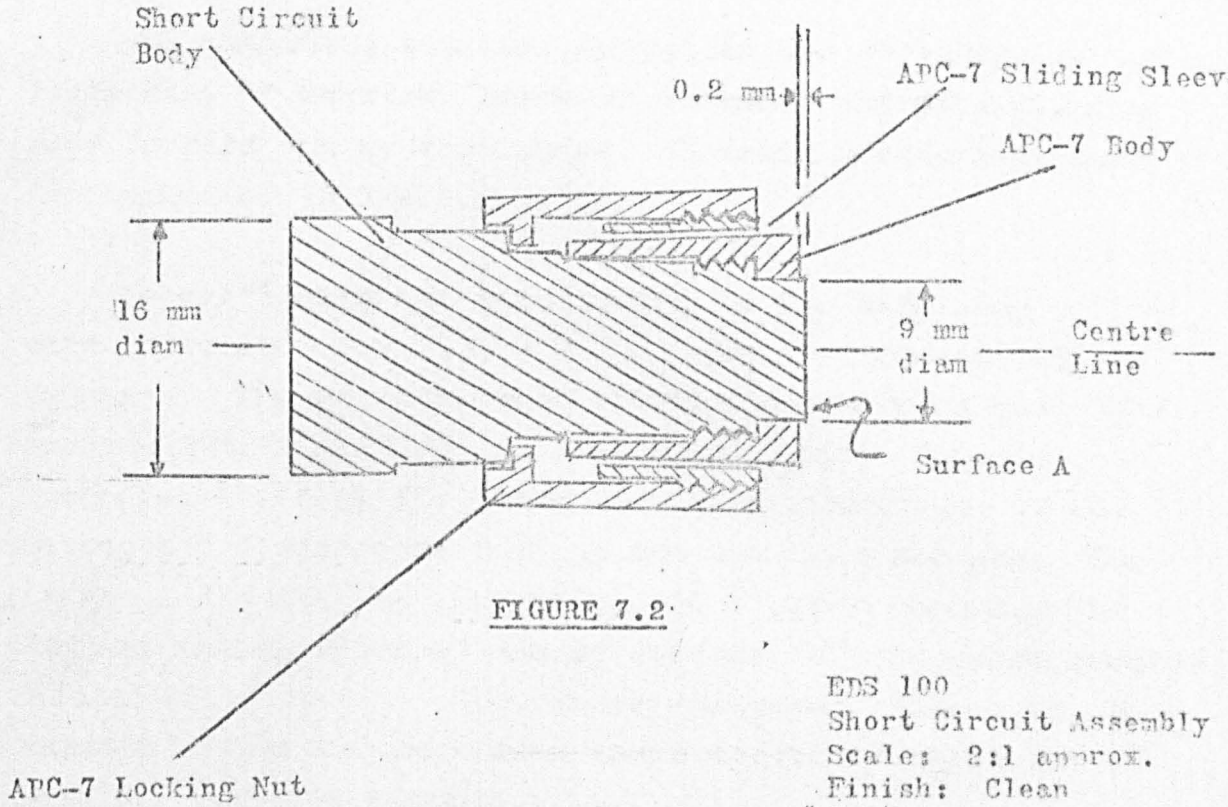

FIGURE 7.2

EDS 100
Short Circuit Assembly
Scale: 2:1 approx.
Finish: Clean
Tolerances: ----
Date: 1st July, 1974

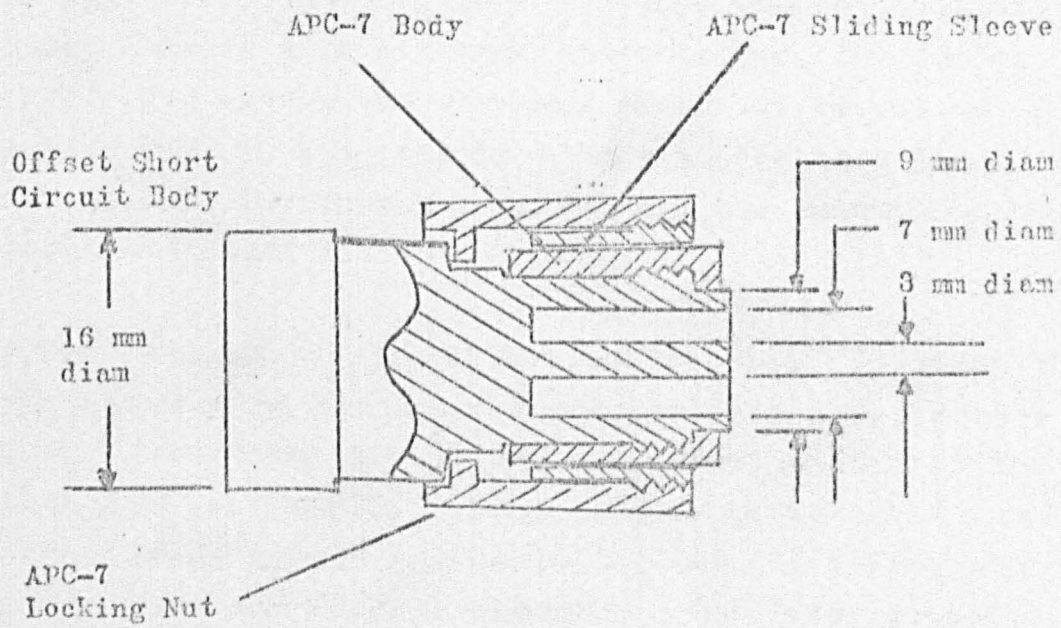

FIGURE 7.3

EDS 101
Offset Short Circuit Assembly.
Scale: 2:1 approx
Finish: Clean
Tolerances: -------
Date 2nd, July, 1974

The machining was carried out in the workshops of the University of Warwick. General Assembly and gold plating were carried out by the author. Details for gold plating are explained in Section 7:5.

No difficulty was experienced in the machining of the short circuit block Figure 7.2 as extreme accuracy is not required. The critical part of this assembly is that the surface "A"(Figure 7.2) is completely flat. This is essential for both the inner and outer conductors of the mating APC 7 connector butt up against this surface. The internal diameter of the mating APC 7 outer conductor is 7mm and the diameter of 9mm of surface "A" allows an annulus contact width of 1mm. Good inner conductor contact is assured by the spring loaded inner conductor mechanism. (Ref 2 - Amphenol Patent).

For the construction of the offset short circuits, it was initally proposed that the construction of Figure 7.3 should apply with the provision that the offset line length be counter bored with a hollow reamer. This method proved to be impractical because such a reamer was not available. SEcondly even if such a reamer was obtained, the lathes available for use in the workshop could not be relied upon to hold a turning diameter to within a tolerance $\pm$ 0.0025mm. An alternative design was required and the assembly produced is shown in Figure 7.4.

The assembly of figure 7.4 has two main features. The larger diameter of the inner conductor (Fig 7.5) is held to 3.04 $\pm$ 0.00254mm (Ref 3) and the outer conductor (Fig 7.6) to 7$\pm$ 0.00038mm (Ref 3). Concentricity between the inner and outer conductors were ensured by careful boring of the plug (Fig 7.6) and careful assembly. The inner conductor, plug and outer conductor assembly was then gold plated.

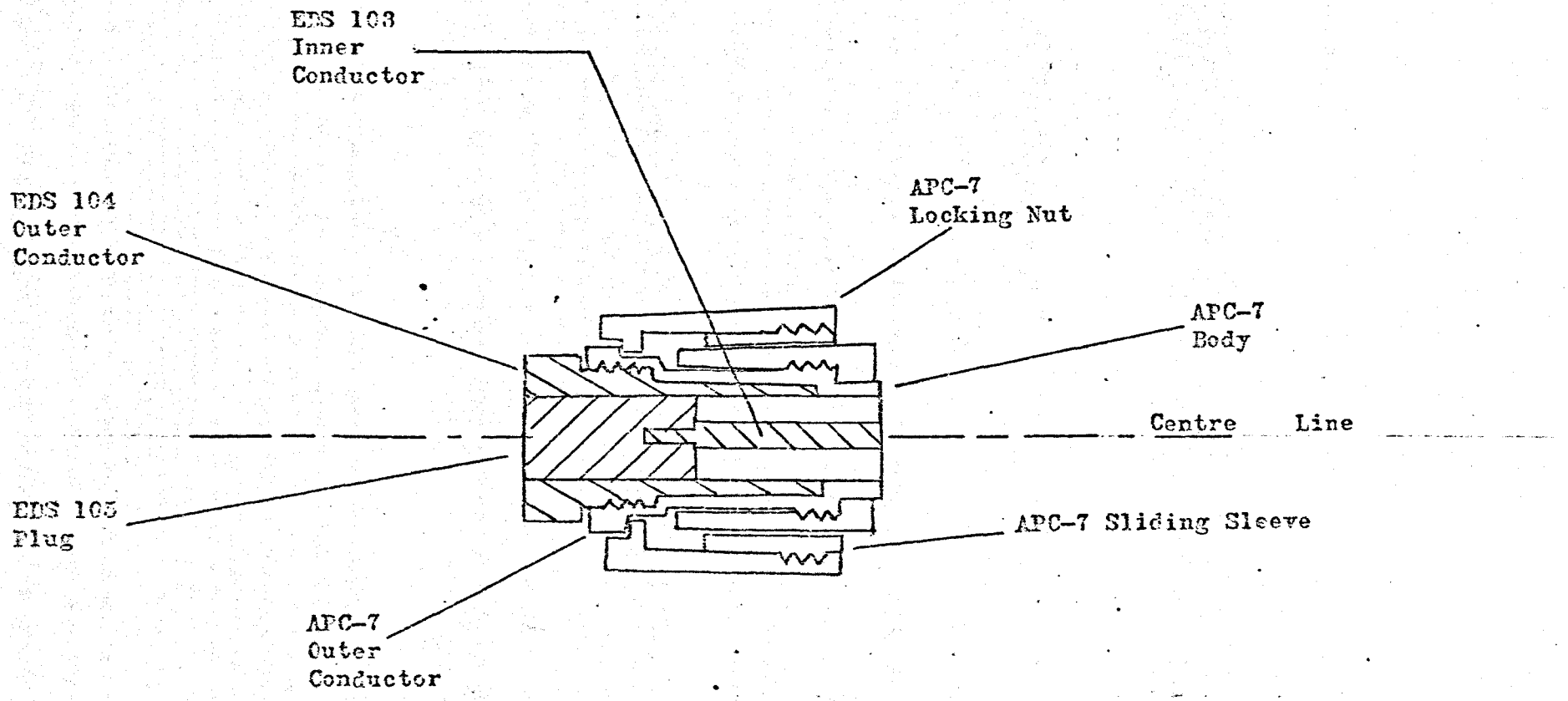

FIGURE 7.4

Remarks: The materials used for EDS 103-5 are made from Amphenol Precision Rod 131-2026 and Tube 131-2027. The three items are soft soldered together at the edges. The assembly is then plated before being fully assembled.

EDS 102
Offset Short Circuit
Assembly. (Beadless)
Scale: 2:1 approx
Finish: Clear
Tolerances: ----
Date: 4th July, 1974

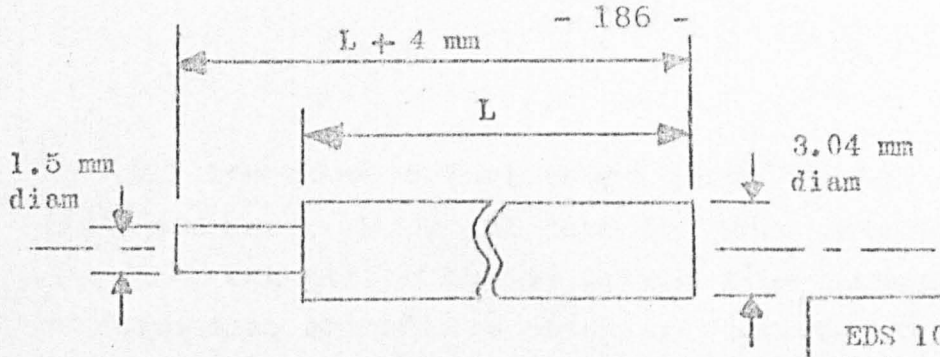

Assembly	Length (L)
A	4.67
B	9.34
C	14.01

FIGURE 7.5

EDS 103 Inner Conductor
Matl: Amphenol 131-2026
Finish: Clean, no burrs
Size: 4:1
Dimensions: millimetres
Tolerances: Lengths ± 0.025
Diams ± 0.013

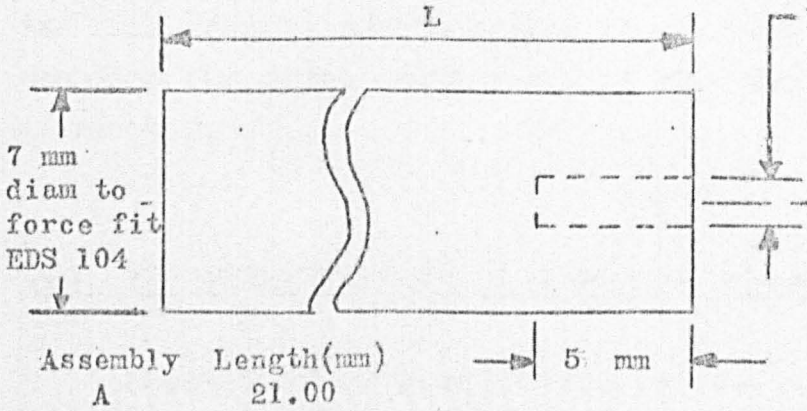

Assembly	Length(mm)
A	21.00
B	16.33
C	11.66

FIGURE 7.6

EDS 105 Plug
Matl: Copper
Finish: Clean, no burrs
Size: 4:1
Dimensions: millimetres
Tolerances: Lengths ± 0.025
Diams ± 0.013

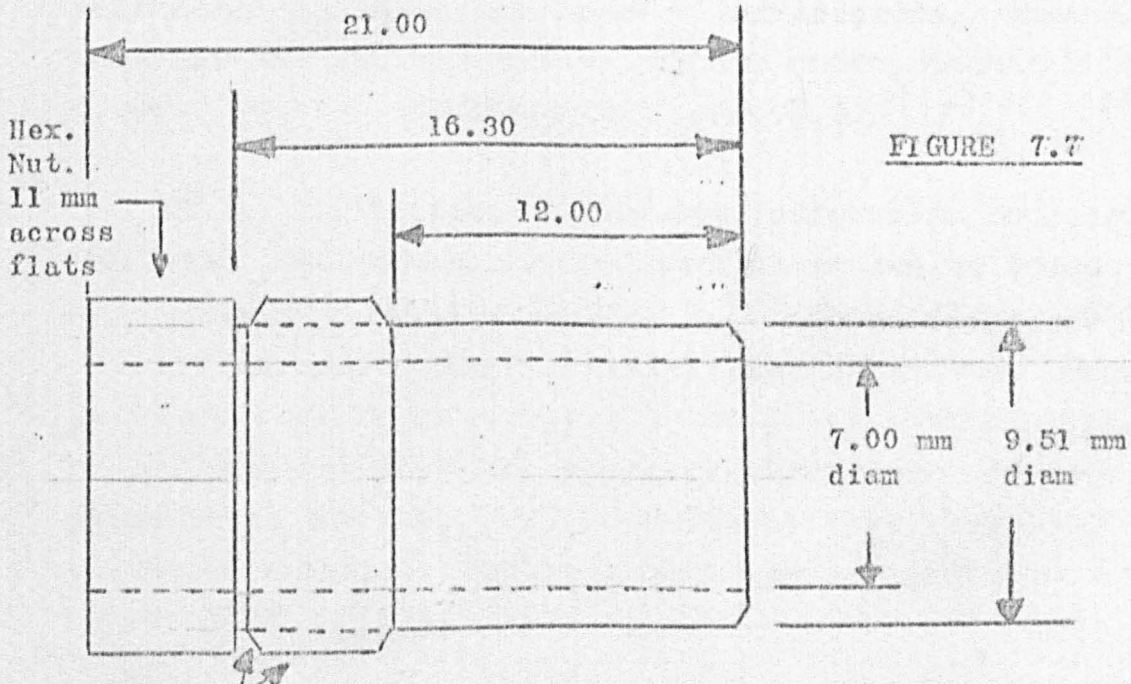

FIGURE 7.7

EDS 104 Outer Conductor
Matl: Amphenol 131-2027
Finish: Clean, no burrs
Size: 4:1
Dimensions: millimetres*
Tolerances: Lengths ± 0.025
Diams ± 0.013
DATE: 5th July, 1974

*unless stated otherwise.

All the above offset short circuits were constructed in this manner. They all have the same external dimensions (Fig 7.4) but differ in the offset line lengths by the corresponding assemblies shown in figures 7.5 and 7.6.

The offset length of 4.67mm was decided by ease of construction because the distance between the end of the inner conductor and the surface of the bead on an APC 7 connector is 4.67mm. Hence, if the first offset were set to this length, good electrical contact can be made between the outer conductors of the short circuit and the connector.

7:3 3mm Short Circuit Calibration Pieces

Shortly after publication of the paper (Ref 7.4) on the three short circuit calibration methods, one of my colleagues, A. Kwesah (Ref 7.5) decided to use the above method for measuring the input impedance of transistors. Discussions were carried out between us and the short circuit calibration pieces evolved are shown in Figure 7.8.

These calibration pieces are designed to be used with 3mm (OSM) connectors. Details of these can be found in most R.F. connector catalogues (Ref 7.6. These dielectric filled coaxial connectors have a nominal characteristic impedance of 50 ohms which is produced by an inner conductor diameter of 1.270mm and an outer conductor whose internal diameter is 3mm (nominal). The dielectric used is poly-tetrafluorethylene (Teflon) which has an effective dielectric constant of 2.1 (Ref 7.7).

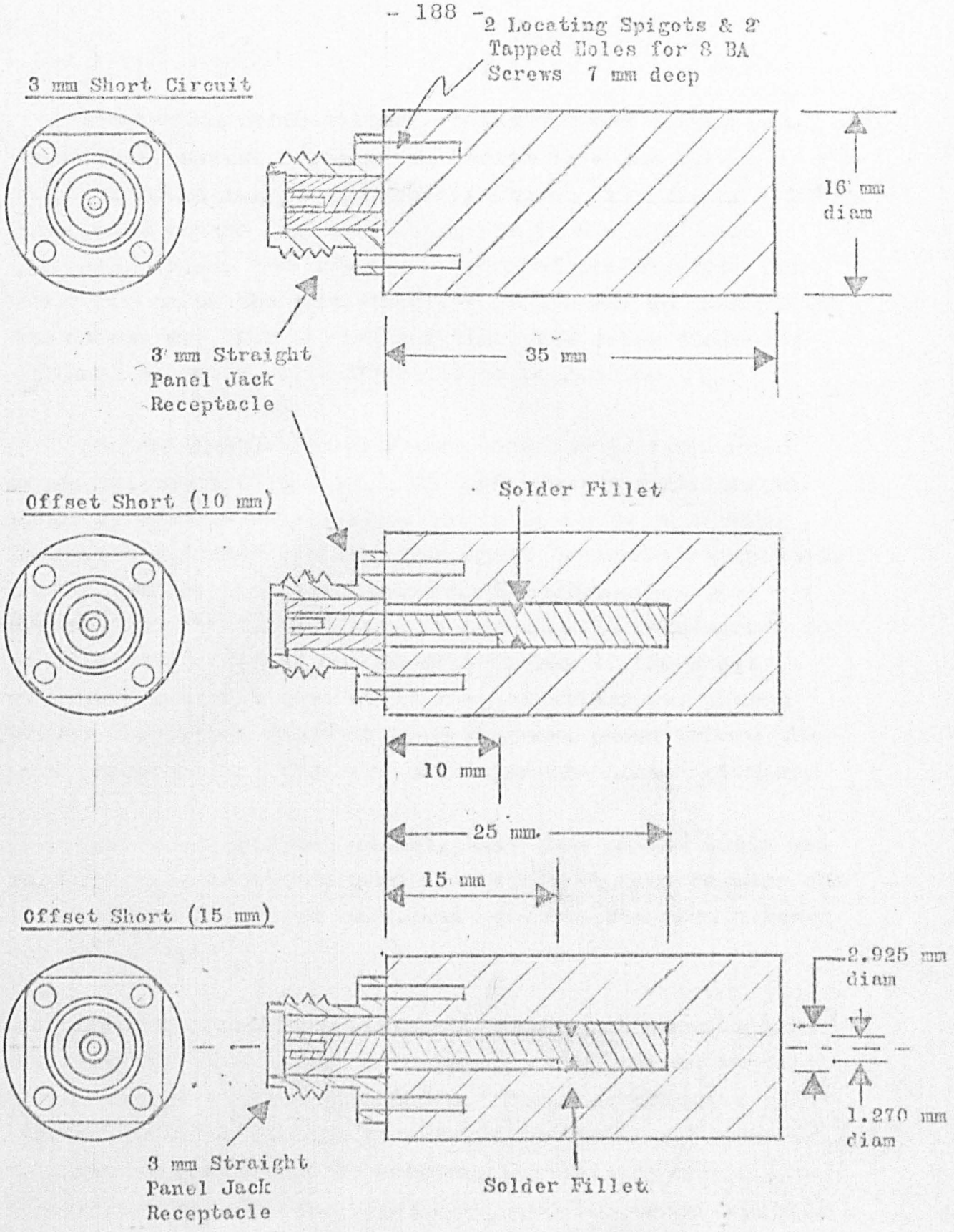

Material: Brass
Finish: Clean and Gold Plated
Scale: 2: 1 approximately.

Figure 7.8 3 mm Calibration Pieces

After much deliberation, it was decided not to construct the offset coaxial lines using teflon as a dielectric as the offset lengths must be accurately known. Air filled coaxial lines were chosen instead. In order to minimise the discontinuities, the inner conductor of the air line was chosen to be of the same diameter (1.270 mm) as that of the 3mm connector. For a 50 Ω air line, the outer conductor internal diameter was calculated to be 2.925mm.

The calibration pieces were constructed from solid brass cylinders (Fig 7.8). The cylinders for the offset short circuit standards were centrally bored to a depth of 25mm with a 2.90mm reamer. The inner conductors were lathe turned from solid brass pieces to the dimensions shown in Figure 7.8. The inners were constructed in this manner to minimise the high current density losses at the short circuit points. A concentric ring of solder was placed around the larger diameter of each inner piece before they were inserted into the bore-holder of the brass cylinders.

The brass cylinder assembly was then heated until the solder flowed to ensure good electrical contact between the inner and outer. Each completed assembly was then cleaned and gold plated.

The 3mm connectors (straight panel jack receptacles) were ground and polished to present a flat mating surface to the brass cylinder assemblies. Two diametrically opposed locating spigots were fixed to the brass cylinder to minimise concentricity problems between the two pieces. Finally two 8 BA brass screws were used to ensure reliable contact between the connector and the calibrating pieces.

These short circuits have worked remarkably well. Excellent repeatibility of measurements carried out using these calibration pieces have been reported by Kwesah (Ref 7.5).

7:4 Construction of the Open Circuit and Reference Short Co-axial Calibration Standards

Photo copies of these standards are shown in Figure 7.9. The assembly drawings of the open circuit standards and the reference short circuit standards are given in Figures 7.10 and 7.13 respectively. Detailed drawings are given in Figures 7.11 and 7.12 for the open circuits and Figures 7.14, 7.15 and 7.16 show details for the reference short circuits

Figure 7.9

Photograph of the Three Open Circuit Pieces

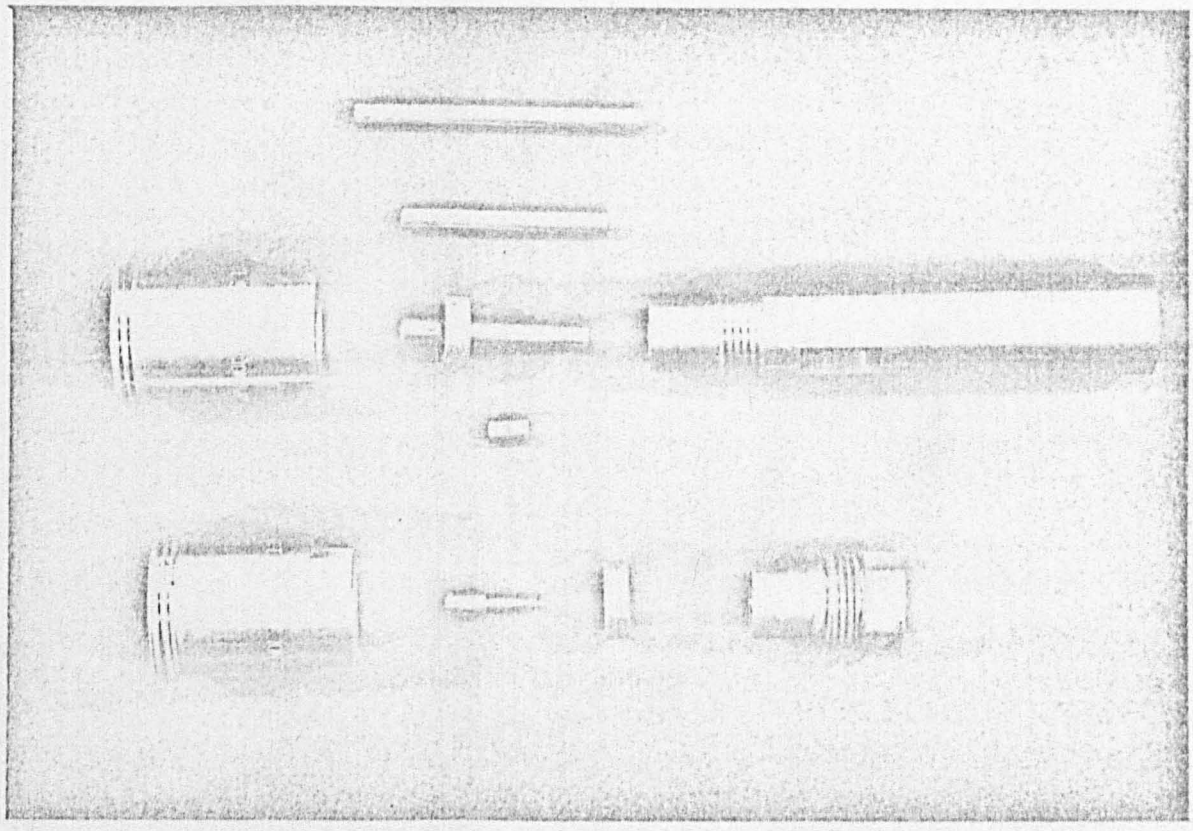

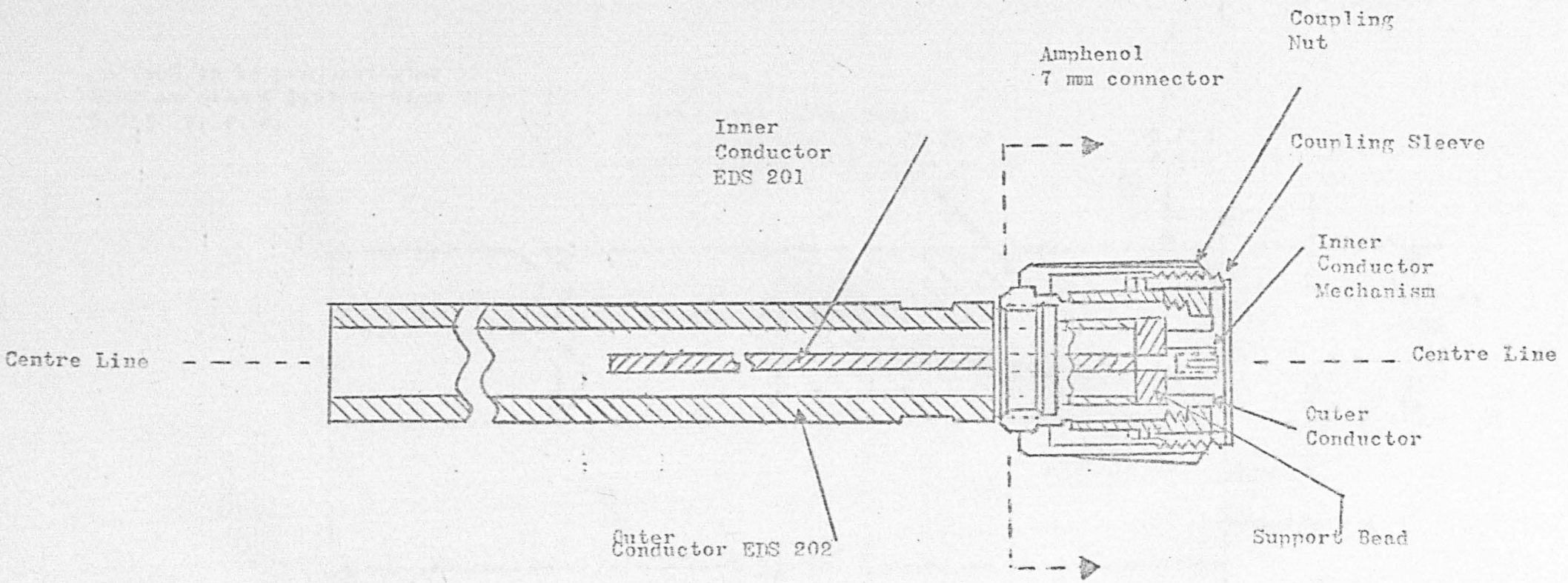

FIGURE 7.10

EDS 200
Assembly Drawing
Calibration Piece (Open Circuit)
Scale: Not to scale
Date 15/8/77
Notes: Amphenol 7 mm connector
to be supplied.

Surface A to be perpendicular to 3.04 mm diam & 1.54 mm diam with 0.013 T. I. R.

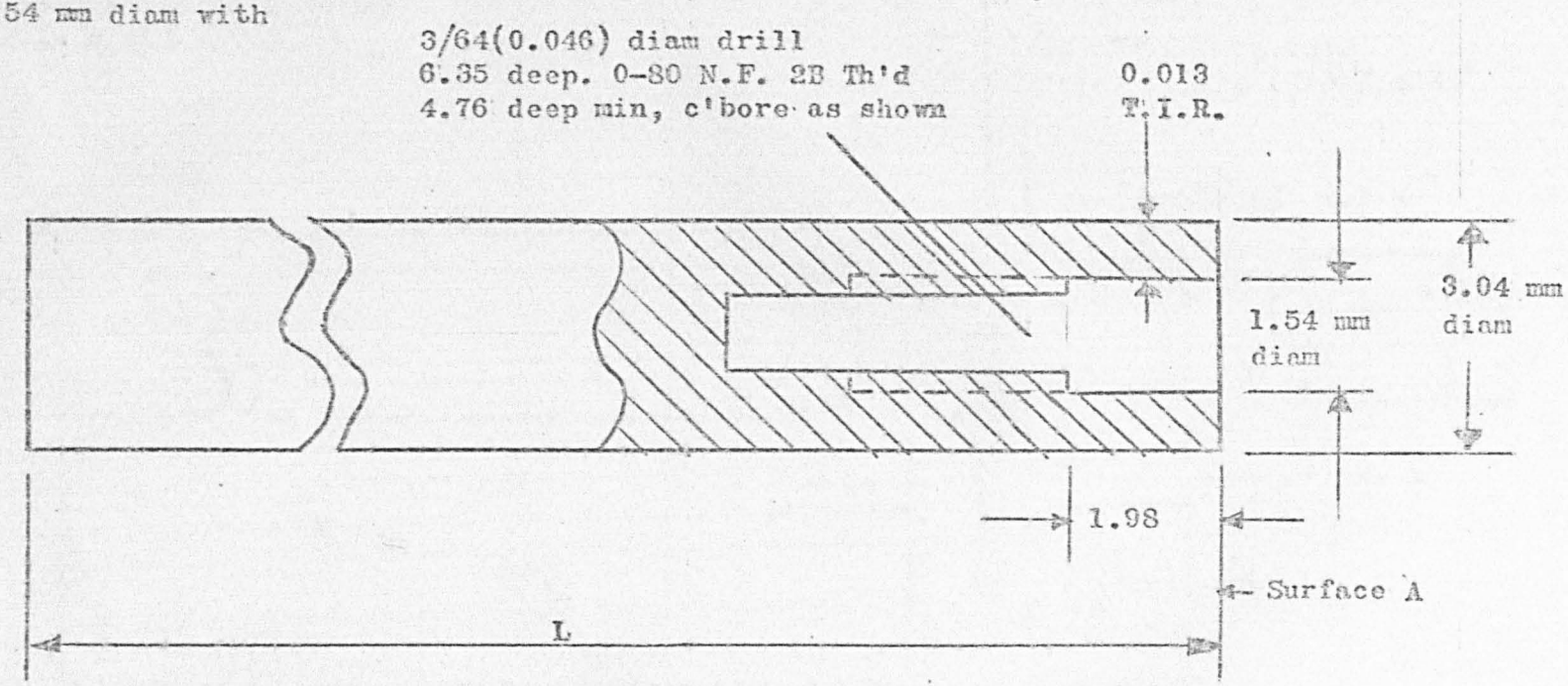

Assembly	L (mm)
A	4.83
B	14.83
C	24.83
D	34.83

FIGURE 7.11

EDS 201 INNER CONDUCTOR

Material: Amphenol Inner Rod 131-2026 (supplied)

Finish: Clean, no burrs.

Size: 10:1

Tolerance: Lengths ± 0.025
Centres ± 0.013

Dimensions: mm unless otherwise stated.

Date: 15/8/77

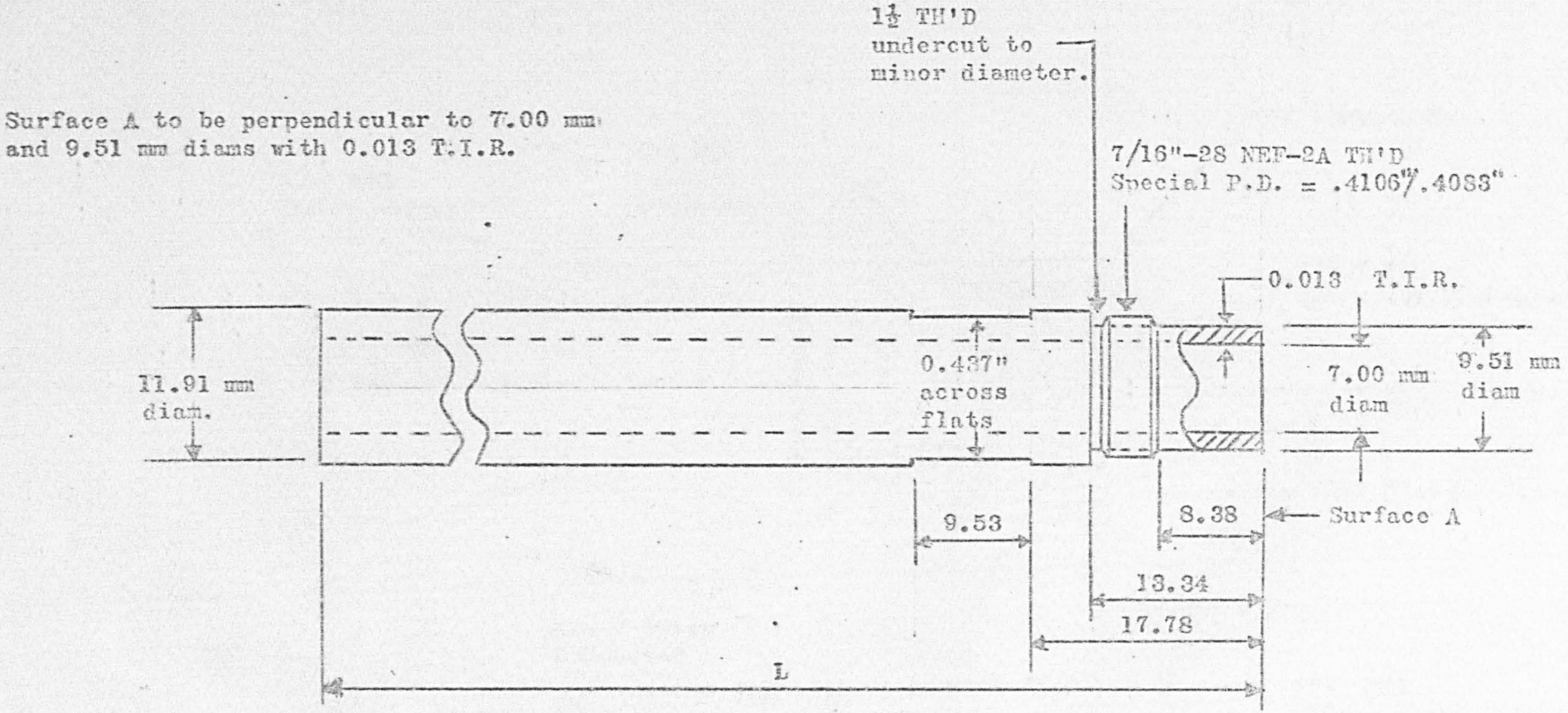

Assembly	L (mm)
A	30.00
B	40.00
C	50.00
D	60.00

FIGURE 7.12

EDS 202
Outer Conductor.Assembly.
Matl: Amphenol Outer
Conductor 131-2027
(supplied)
Size: 2:1
Tolerances: Lengths ± 0.025
Centres ± 0.013
Dimensions: mm unless stated
otherwise.
Date: 15th August, 1977

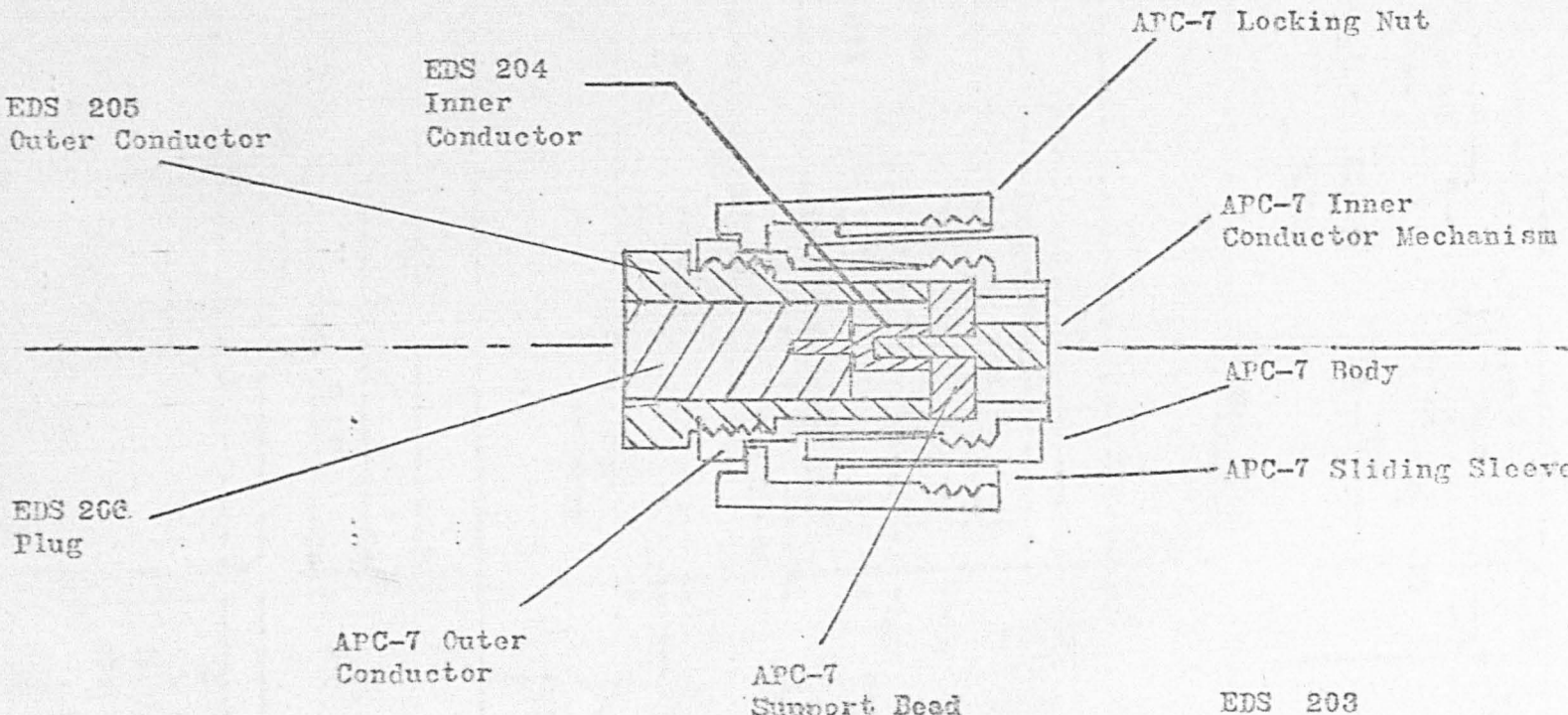

FIGURE 7.13

EDS 203
Offset Short Circuit Assembly
Scale: 2:1 approx
Finish: Clean
Tolerances: ------
Date: 15th August, 1977

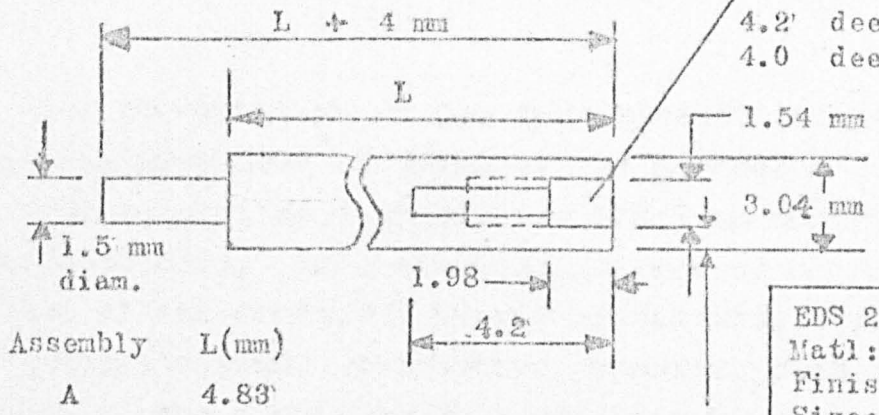

Assembly	L(mm)
A	4.83

FIGURE 7.14

EDS 204 Inner Conductor
Matl: Amphenol 131-2026
Finish: Clean, no burrs
Size: 4:1
Dimensions: mm unless stated otherwise.
Tolerances: Lengths ± 0.025
Diams ± 0.013

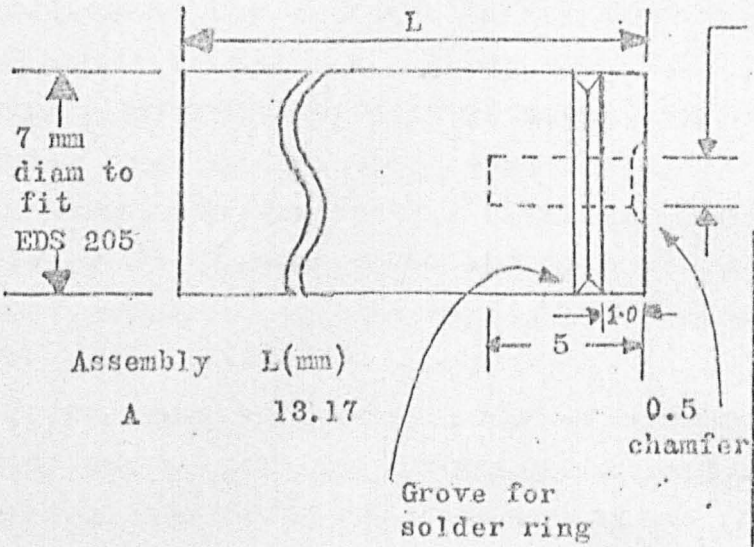

Nominal Diam 1.5 mm
To force fit 1.5 diam of EDS 204 Inner Conductor

Assembly	L(mm)
A	13.17

FIGURE 7.15

EDS 206 Plug
Matl: Copper
Finish: Clean, no burrs
Size 4:1
Dimensions: millimetres
Tolerances: Lengths ± 0.025
Diams ± 0.013
Date: 16/8/77

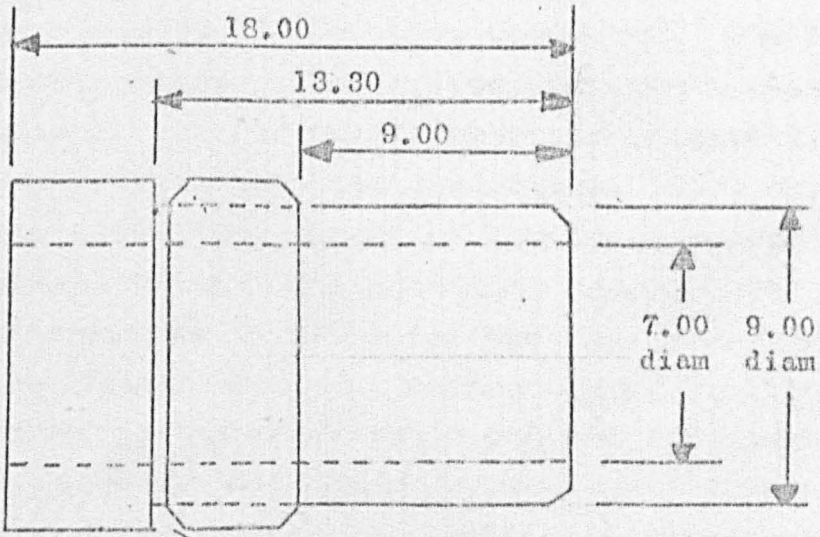

Hex. Nut 11 mm across flats

7/16" 28 NEF 2A Th'd
Special P.D. - .4106"/.4083" 1½ Th'd undercut to minor diam

FIGURE 7.16

EDS 205 Outer Conductor
Matl: Amphenol 131-2027
Finish: Clean, no burrs
Size: 4:1
Dimensions: mm unless stated otherwise.
Tolerances: Lengths ± 0.025
Diams ± 0.013
Date: 16/8/77

The construction of the open circuit calibration standards have been dictated by the necessity to retain the standard support bead within the APC 7 to centralize the inner conductor. Insulative supports were not used at the far end of the conductor to retain uniformity within the precision air line. Conductive supports, such as a short circuit placed a quarter of a wavelength away were rejected because these would immediately make the calibration pieces narrow frequency band devices. It was realized that supporting the inner at one end only will cause concentricity problems at the unsupported end (far end) between the inner and outer conductors. Adams (Ref 7.1) has given some figures relating to this problem. In practice, the concentricity problem has not proved to be troublesome. This is believed to be due to the fact that the near end is rigidly held by the support bead and that it is centralized by the inner conductor of the mating APC 7 connector.

In order to minimize the effects of the supporting bead, and to provide sufficient thread length for a rigid support, the first open circuit plane (Fig 7.11 Ass A) was placed 4.83mm away from the far surface of the support bead which is a physical length of 7.67mm (14.01 electrical) from the contact edge of the inner conductor. The other reference planes are spaced apart at 10mm increments (Ass B, C and D of Figure 7.9). The outer conductor (Figure 7.10) was originally drawn for four assemblies. Each outer was meant to exceed the length of the inner conductor by approximately 16mm thus providing nearly 100dB of evanescent mode attenuation at 12GHz for the TM_{01} mode. A later costing exercise showed that this method was prohibitive and it was decided to use a common outer and APC 7 connector and to change the inner conductors as desired. This method has not proved to be particularly troublesome but does require more computer time during calibration because of the longer time required for changing the calibration pieces.

The reference short circuit was constructed using the principles derived for both the short circuits (Section 7:2) and the open circuits described in this section. The short circuit plane has been placed 4.83mm away from the far side of the support bead to coincide with the plane of the first open circuit calibration standard.

Hence, all measurements are referenced to a plane 4.83mm away from the far side of the support bead (i.e., 14.01mm electrical) from the contact edge of the inner conductor.

7:5 Fabrication of Microstrip Circuits

The fabrication of the microstrip pieces were carried out on the premises. The general principles are well known (Refs 7.8 to 7.18) but as the majority of the items were fabricated by the author using non-commercial equipment developed within the University, a brief resume of the methods used will be mentioned. The main fabrication processes are shown in Figure 7.17.

Figure 7.17
Main Fabrication Processes of Microstrip

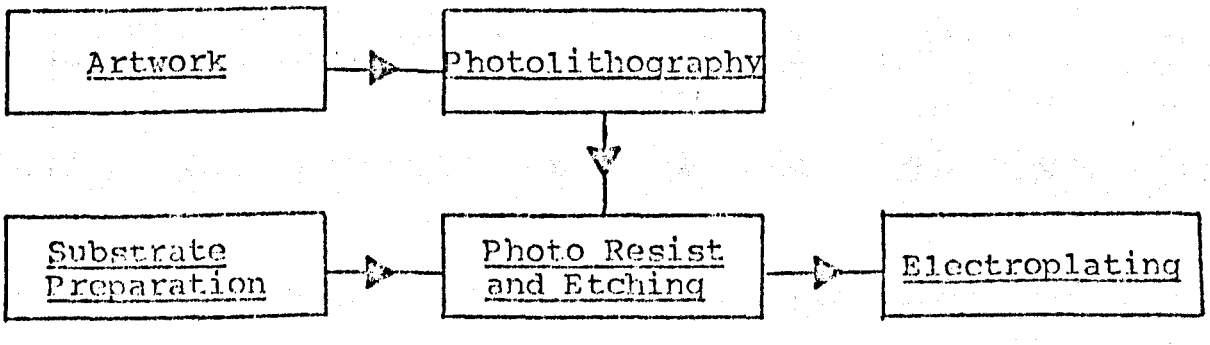

7:5.1 Maskmaking

The desired artwork was drawn on "Cut N Strip" film using a co-ordinatograph with a sharp cutting blade. "Cut N Strip" film may be described as a teflon transparent sheet film with a thin reddish (strip away) plastic film attached to it. The film is claimed by the manufacturers to be

FIGURE 7.18 THE PHOTOGRAPHIC ROOM

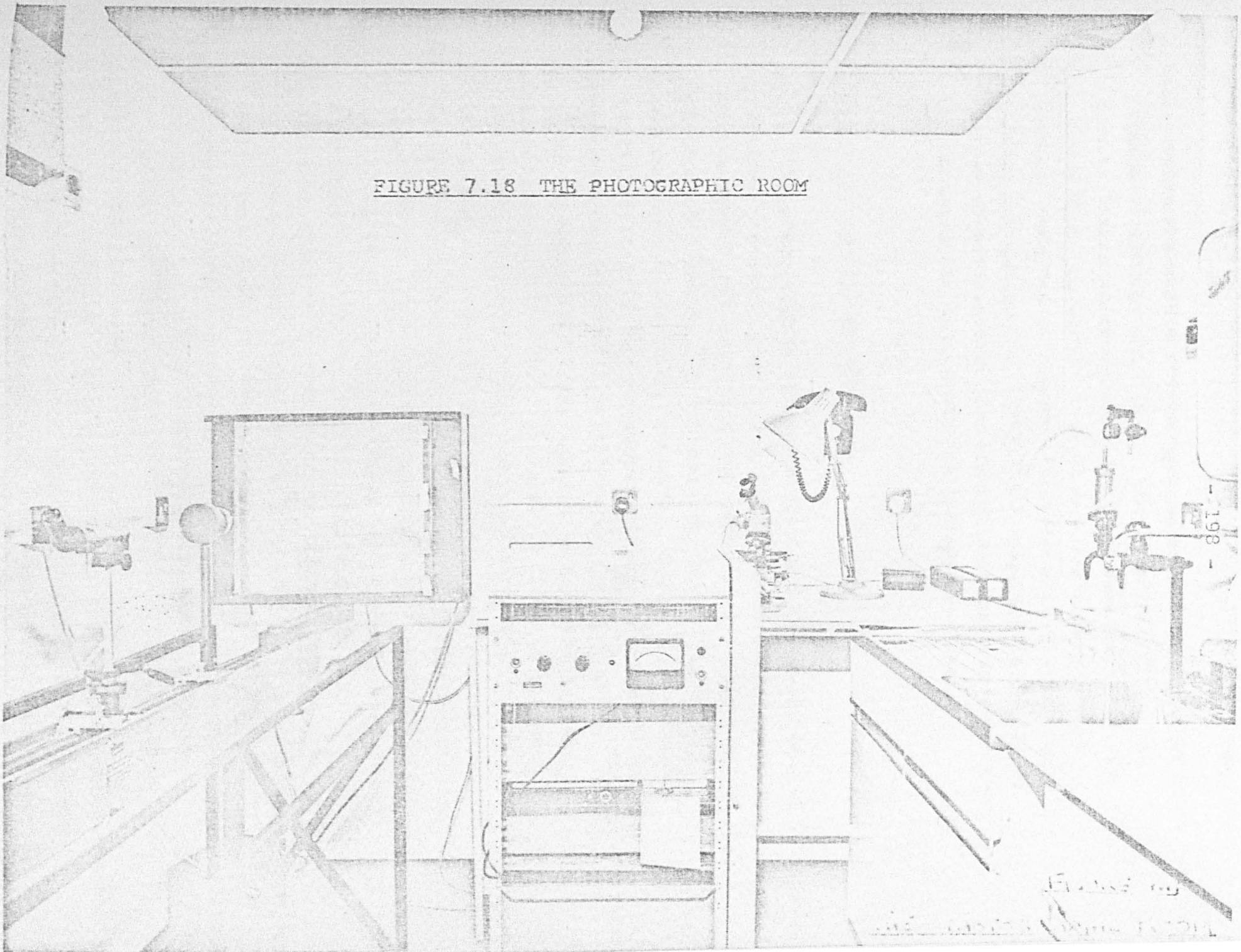

dimensionally stable and to provide excellent contrast for subsequent photographic work. The coordinatograph has vernier scales which permit accurate positioning of the cutting blade to within ± 0.01mm. The drawings were normally made ten or twenty times the actual size required so that any cutting or stripping irregularities would be reduced significantly. The masked produced was taken into the photographic laboratory for photo-reduction.

7:5.2 Photo-lithography

The photographic equipment used was developed on the premises. Kelland (Ref 7.15) did the preliminary work and Michie (Ref 7.16) finalised the system. A picture of the photographic laboratory is shown in Figure 7.18. The photographic bench is on the left; the wash basin and general film development equipment is on the right. All photographic equipment is attached to a rigid beam suspended by springs from a main frame to minimise building vibrations. The back lit artwork is fixed to one end of the beam. The simple box camera and the focussing microscope has slide attachments to permit movement along the beam. Various lenses may be used with the camera body. Dimensionally stable photographic plates are attached to the other end of the camera by a vacuum chuck. No shutter is provided within the camera. Exposure is controlled by exposing the film to back lighting emanating from behind the artwork. Size reduction is carried out by moving the camera body along the bench until the desired image on a dummy photo plate is obtained. The same image is also examined by a travelling microscope to ensure sharp focussing. Focussing and aperature control is carried out by adjustments within the lens used.

Exposure time usually between 8-30 seconds was varied to suit the reduction size and the Kodak high resolution plates used (Ref 7.11). Development time was rigidly controlled and was carried out according to the following:-

Process	Solution	Time (Gentle Agitation)
Developer	1 part Kodak DG10 to 6 parts de-ionized water.	6 minutes
Stop Bath	3 parts Glacial Acetic Acid to 8 parts de-ionized water	45 seconds
Rinse	De-ionized Water	1 minute
Fixer	130 gms of Kodak Unifix Powder per litre of de-ionized water	8 minutes
Rinse	De-ionized water	1 minute
Hypo-Clear	61 gms of Kodak Hyop Clear Powder dissolved in 2.25 litres of de-ionized water	10 minutes
Rinse	De-ionized water	20 minutes

7:5.3 Substrate Preparation

Two main types of substrates were used, metal deposited substrates, e.g., alumina, and sapphire substrates. In the case of the latter, metallic deposition was carried out using vacuum evaporation. The equipment used was the Edwards/Birvac Model TA-150. A close-up view of the evaporation chamber with the bell jar removed is shown in figure 7.19. The method of using this unit has been substantially described (Ref 7.8, 7.17 and 7.18) and only a resume of the preparation and vacuum deposition of the substrates will be given:-

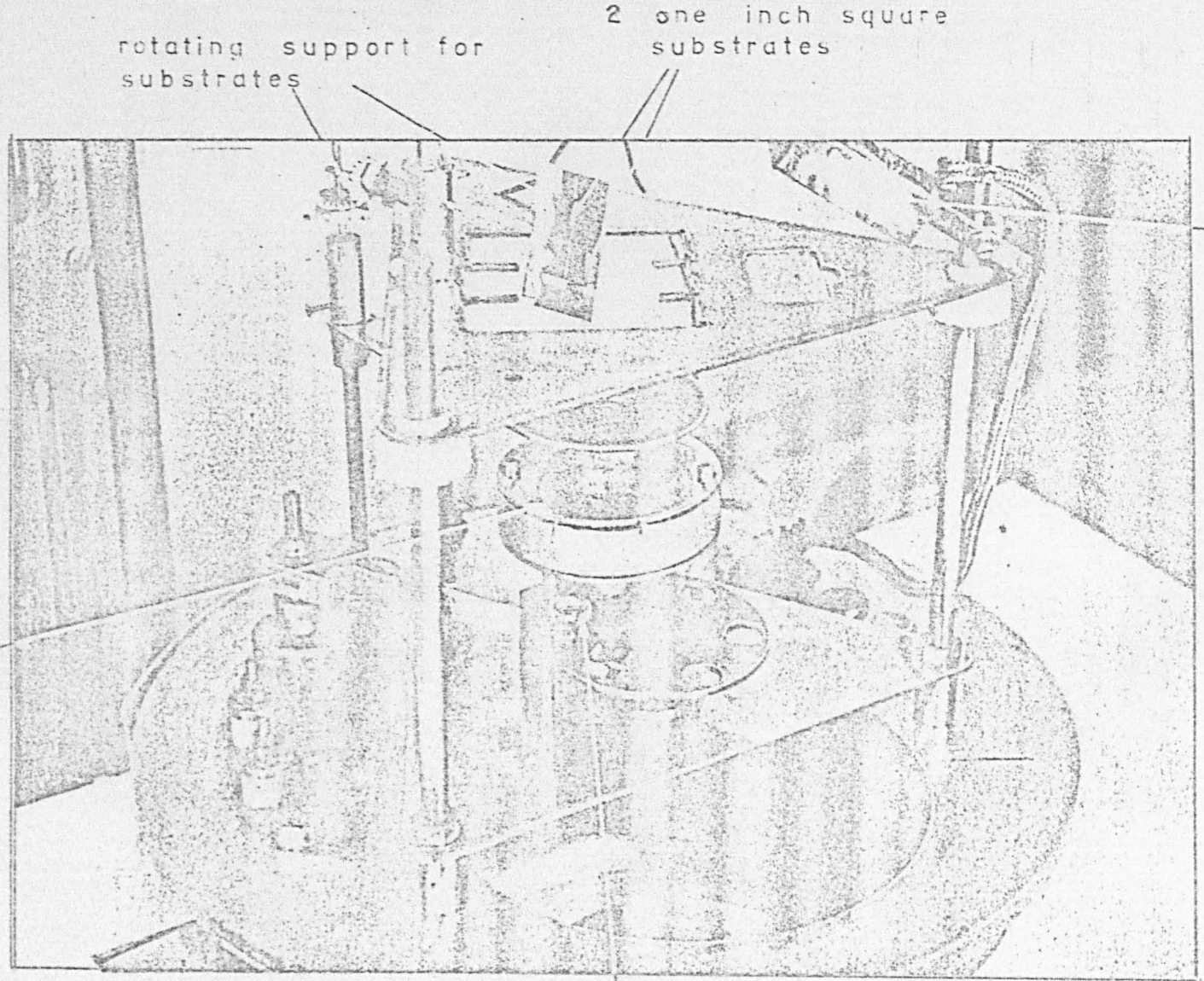

FIGURE 7.19

EVAPORATION FACILITIES

(a) First Wash : Substrates washed in a solution of 5cc teepol and 100 cc de-ionized water in an ultra-sonic bath for 3 minutes (Fig 7.20).

(b) Second Wash : Same as First Wash.

(c) Third Wash : Substrate washed in 100cc of carbon tetrachloride for three minutes in ultrasonic bath.

(d) Fourth Wash : Substrate washed in 100 cc of Isopropanol in ultrasonic bath.

(e) Substrate dried in oven at 70^{o}c for five minutes.

(f) Substrate placed in vacuum chamber, Birvac TA-150.

(g) System evacuated to 0.1 torr.

(h) System heated to 150^{o}c for fifteen minutes of outgassing.

(i) Heater switched off, but glow cleaning applied at 1Kv for ten minutes.

(j) Filament current switched on at 25 Amps and left for five minutes.

(k) Nichrome heated and allowed to deposit on target shield for two minutes. This is to minimise any nichrome oxide on the substrate later.

(l) Nichrome deposited on substrate for 60 seconds. Target voltage was set to 2.5Kv, recorded current was 25mA. Pressure was 5×10^{-5} Torr; thickness of deposition about 400 Angstroms.

(m) Copper heated and allowed to deposit on target sheild for two minutes. This is to minimise the deposition of copper oxide on the substrate later.

(n) Copper deposited for twenty minutes with target voltage set at 3Kv. Recorded current was 65 mA. Thickness of deposition about 1 micron.

(o) System left to cool. After thirty minutes, air was allowed in by the bleeder value. If the substrate was not desired immediately, it was stored in the vacuum until required.

(p) Removal from the vacuum chamber was immediately followed with photoresist coating to minimise oxidation.

7:5.4 Photoresist Application and Etching

Two types of photoresist were used, the negative type Kodak Thin Film Resist (KTFR) and the positive type resist, Shipley AZ 111. The negative resist was used when it was desired that all image parts exposed to ultra-violet light would be washed away in the developer. The positive resist was used when it was desired that all the parts not exposed to ultra-violet light would be washed away in the developer.

In both cases, the method of application is the same. K.F.T.R. is applied with a syringe fitted with a negative resist filter (Millipore Type AAWP 01300-A), Shipley AZ 111 is applied with a syringe fitted with a positive resist filter (Millipore Type UHWP 01300-A). The equipment used for this work is shown in figure 7.20.

The substrate was vacuum held on a rotating spinner. A thin layer of resist was allowed to flow over the substrate, which was then spun at 3000 rpm for 20 seconds. A second coat of resist was similarly applied and spun. Pre-etch baking time was 10 minutes at 70°c. Exposure time was 3 minutes followed by development in KFTR developer for the Kodak type and Shipley AZ 303 for the positive resist. Post-developing baking time was 10 minutes at 70°c.

The copper etch used was a solution of ferric chloride prepared by mixing 80 gms of ferric chloride with 400cc of water. Etching was by gentle agitation and the complete etching time was about 20 seconds. The substrate was immediately removed and washed as soon as the nichrome layer underneath was visible. The nichrome etching solution was prepared from 40gms of potassium ferrocynide, 10gms of sodium hydroxide dissolved in a solution of deionized water to make a solution of 200cc. The solution was used at 50°c. This solution weakens with time and should be discarded within seven days. In practice, it was noted that even after 3 days, the etching qualities were impaired. Electroplating was then used to the required thickness.

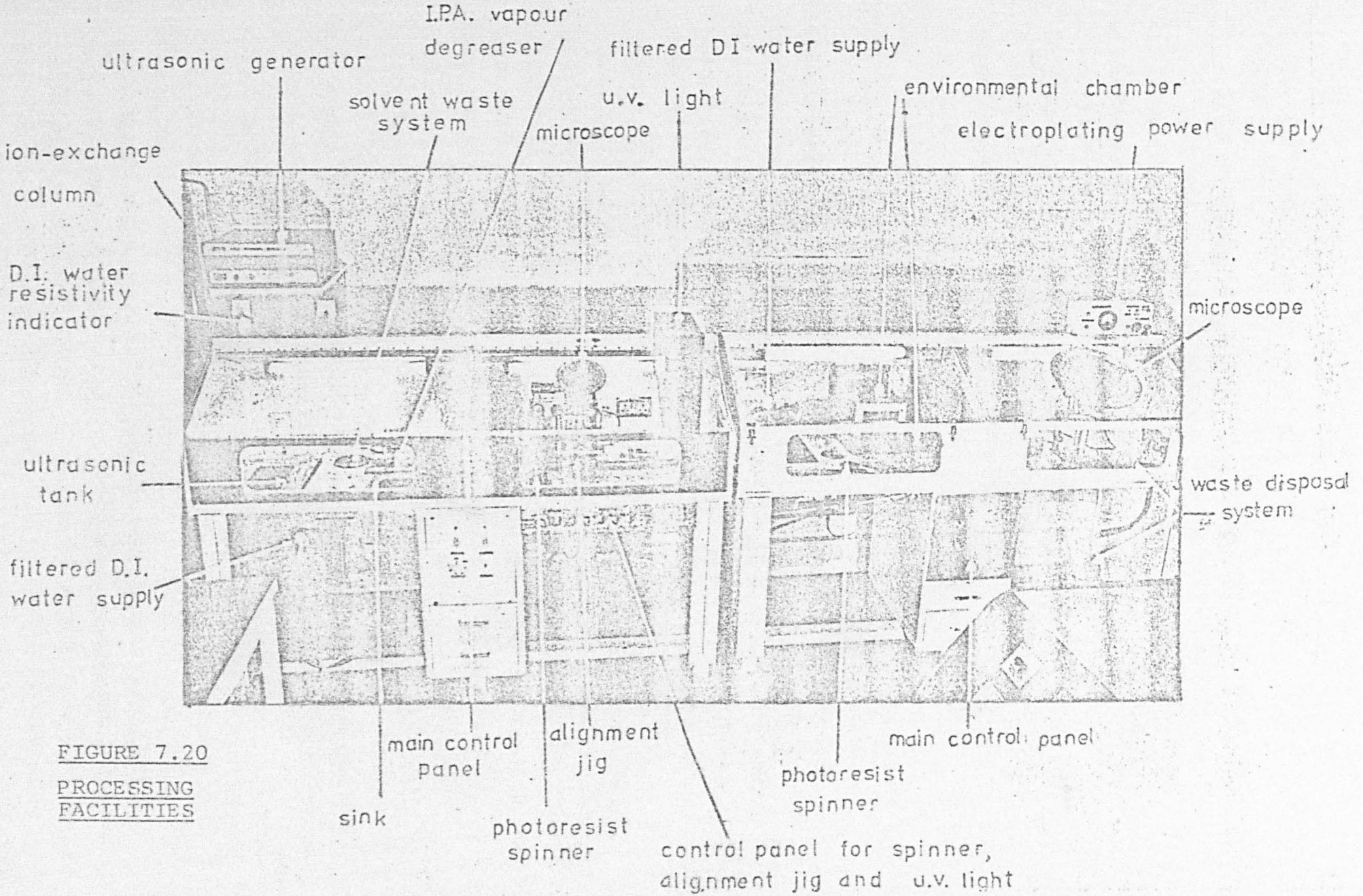

FIGURE 7.20

PROCESSING FACILITIES

7:5.5 Electroplating

Most of the plating techniques came from (Refs 7.13, 7.14, 1.16 and 7.18). The book by Raub and Mueller is excellent on fundamentals and helped considerably towards understanding the other references. Graehme (Ref 7.18) is particularly good and goes into considerable detail on thin and thick film plating. Although copper plating was achieved fairly easily, considerable difficulty was experienced in plating after etching. This was finally traced to photoresist contamination and a cleaning process had to be derived.

After the etching of the chrome film; the remaining photoresist was removed; KFTR by a spray of carbon tetrachloride; Shipley AZ 111 by a spray of Acetone. Both actions were followed by a spray of Isopropanol. By this time, the copper surface was well and truly oxidised and had to be once again acid dipped. Various solutions of nitric and hydrochloric acid dips were tried. The one finally decided upon was a 20% of sulphuric acid used for a 20 seconds dip. The substrate was then immediately connected to the plating bath. A solution of copper sulphate and dilute sulphuric acid was used as the plating electrolyte. The solution was made by dissolving 850gms of copper sulphate in a weak solution of dilute sulphuric acid made from mixing 198 gms of concentrated sulphuric acid mixed with 9 litres of deionized water. The age-old precaution of always adding acid to water was adopted in preparing the solution. The current used was 300 ma per square centimetre of plating surface.

Copper plating was followed by a gold flash using a gold plating solution, a commercial product called Transtherm Solution made by PMO Chemicals Limited. This solution must be maintained at 65°c during plating. The solution is used undiluted. Removal from the gold plating bath must be followed immediately by a dip in Isopropanol

followed by immediate drying with compressed air to provide a shiny gold finish. The current used was 100 ma per square centimetre of plating surface.

7:6 Conclusions

This chapter has explained and described in detail the construction of the calibration and test peices used in the system. Considerable effort was expended in trying to produce theoretically perfect calibration standards. Whilst not all of these aims have proved practicable, the majority and vital principles have been achieved.

The consistency of the various standards have also been verified by Kwesah (Ref 7.5) and Hosseini (Ref 7.20).

* * * * * * * * * * *

7:7 References

7.1 Adams S.F., "A New Precision Automatic Measurement System" I.E.E.E. Trans. 1968, IM17 pp 308-313.

7.2 Amphenol Catalogue Sheets "Series 131 - Precision 7mm Connectors" Microwave Product Date Directory 1973.

7.3 Amphenol Specification Sheets on Outer Conductor Tubing 131-2027 and Conductor Rod 131 - 2026.

7.4 da Silva E.F. & McPhun M. "Calibration Microwave Network Analyser for Computer Corrected S-Parameter Measurements" Electronic Letters 9, pp 126-128, March 1973.

7.5 Kwesah A, "Characterization of Integrated Bi-polar Transistors using Computer Aided Measurements and Optimisation" Chapter 4 Ph.D Thesis. University of Warwick 1976.

7.6 "Microwave Engineers' Technical and Buyers Guide Handbook" 1970 Edition published by Microwave Journal, Horizon House, Dedham, Ma.

7.7 Military Standards. P-19468 on Plastics published by the Joint Armed Services. U.S.A.

7.8 Maissel L.I. and Glang M.M. "Handbook of Thin Film Technology" Mc Graw Hill, New York 1970.

7.9 Keuffel & Esser Publication "Uses of Stabiline 'Cut N Strip' Film Data Sheet 1964.

7.10 Kodak Publication "An Introduction to Photofabrication using Kodak Photosensitive Resists" Kodak Publication Book No. P79.

7.11 Kodak Publication "Kodak High Resolution Plate" Data Sheet.

7.12 Chemical Processes Ltd., "12/LS Resist Stripper" Data Sheet by Chemical Processes Ltd., Chidburgh, Suffolk.

7.13 W. Canning & Co. Ltd., "Handbook on Electroplating" Birmingham, 20th Edition, Jan. 1966.

7.14 Raub E. and Mueller K "Fundamentals of Metal Deposition" Elsevier Publishing Co. 1967.

7.15 Keeland G "The Commissioning of a Reduction Camera" University of Warwick; Internal Report 1969.

7.16 Michie D, "Microwave Integrated Circuits; Preparation of and Measurement Techniques for Overlay Capacitor" Ph.D Thesis, University of Warwick, 1978.

7.17 da Silva E.F., "Inductors as Lumped Elements in Microwave Integrated Circuits" M.Sc Thesis University of Warwick, 1971.

7.18 Pender R.S., "Thin Film Microelectronics" I.E.E. Students' Quarterly Journal, September 1970 pp 153-157.

7.19 Graehme A., "Electroplating Engineering Handbook" Rheinhold Book Co. 1969.

7.20 Hosseini, N.M., "The Application of Computer Aided Design to Microstrip Circuits" Ph.D Thesis, University of Warwick, July 1977.

* * * * * * * * * * *

CHAPTER VIII

PRACTICAL PROBLEMS IN COMPUTER CORRECTED MEASUREMENTS

8:0 Introduction

The main purpose of this chapter is to examine the problems which are encountered when theoretical ideas are applied to practical problems. A brief survey of the complete measurement equipment is initially made. This is followed by a more detailed review of the polar display unit to establish the principles by which the magnitude and phase components of the reflection coefficient are detected. The problems associated with non-linearity in the amplifiers are also analysed and the solution used to overcome this problem is explained.

Tests are then carried out to establish the viability of the equipment for computer corrected measurements. These are followed by further tests to confirm that both manual and automated corrections have been satisfactorily achieved.

8:1 A Brief Review of the Measurement Equipment

A block diagram of the measurement equipment is shown in figure 8.1 and a detailed block diagram of the polar display unit is shown in figure 8.2. These are based on the manufacturer's information (reference 8.1).

Figure 8.1

Main Block Diagram of the Measurement System

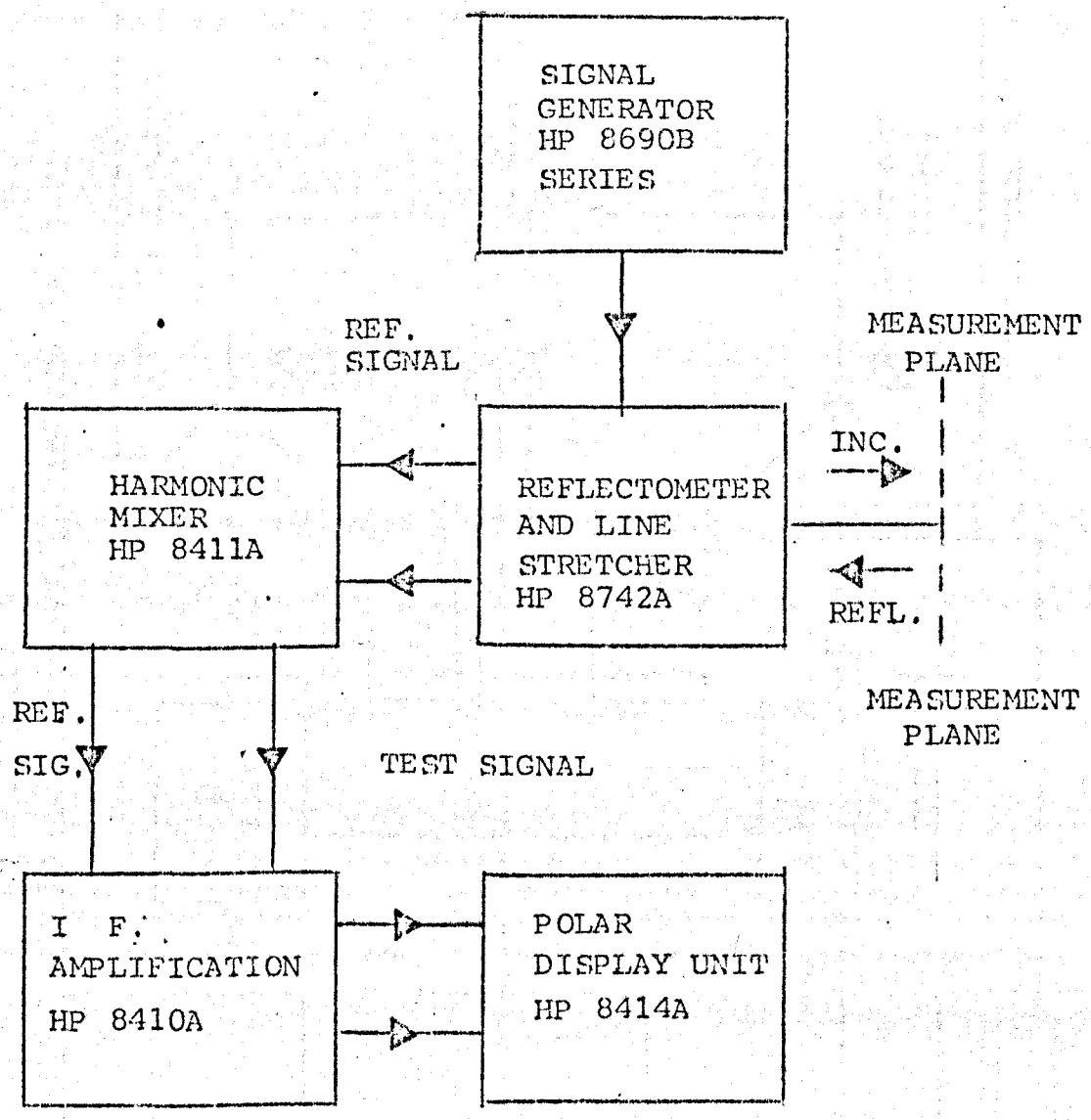

Figure 8.2

Overall Block Diagram of Polar Display (HP8414A)

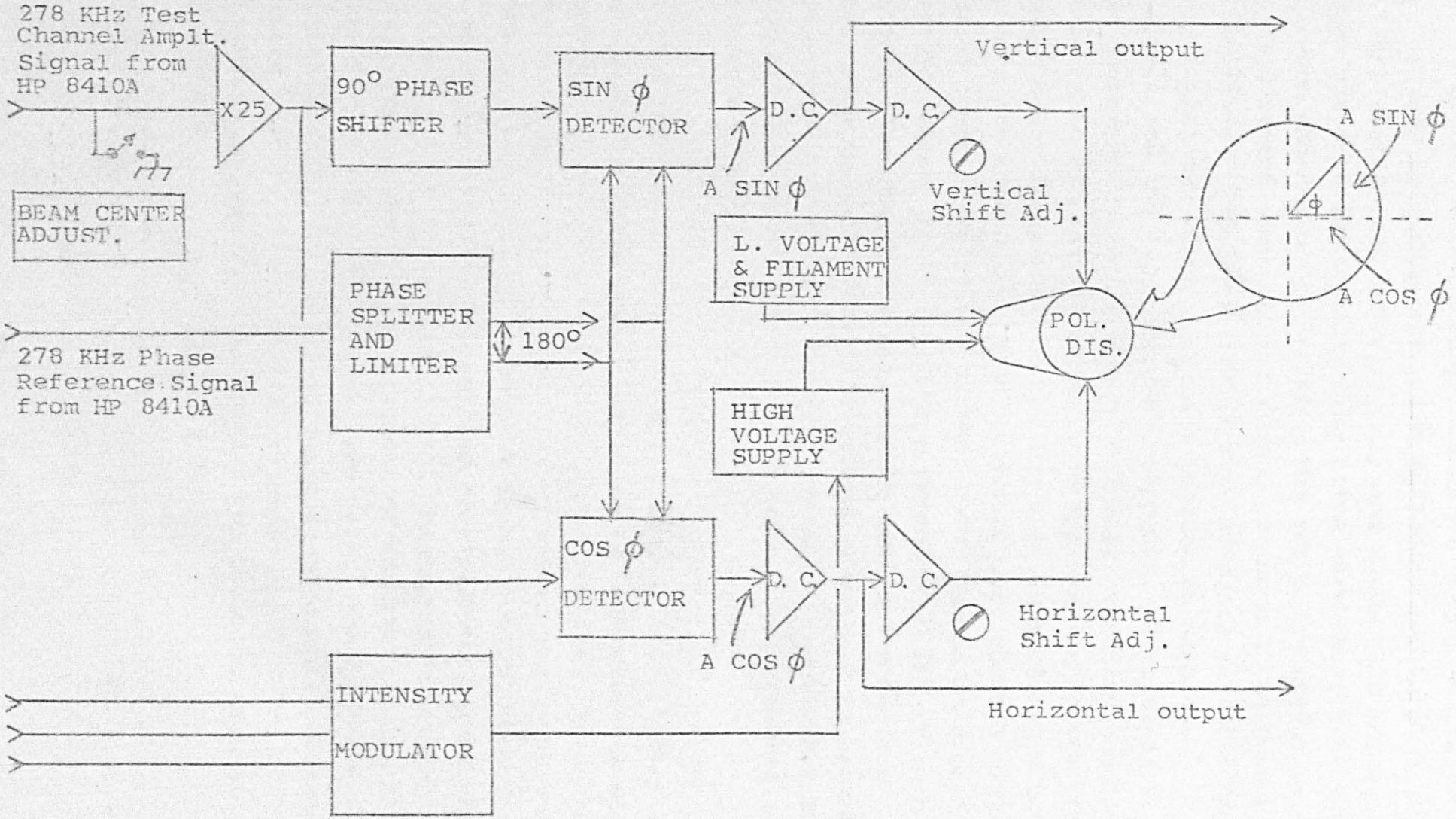

In figure 8.1, the output from the signal generator is fed into the reflectometer. The reflectometer samples the incident signal (reference signal) and feeds this reference signal via a variable delay line (line stretcher) into the reference channel of the mixer. The reflected signal from the measurement plane is fed into a co-channel (test channel) of the mixer. The line stretcher is normally adjusted in use, so that the electrical path lengths in both the reference and the test channels are equal. Both signals are down converted to 20.278 MHz (1st I.F.), amplified, and down converted to 278 KHz (2nd I.F.) for application to the polar display unit (figure 8.2). The 1st I.F. amplifiers in both channels are controlled by an automatic gain control system sampled from the reference channel. Any change in signal generator output level is equally compensated for in both channels. Thus the ratio between the test and reference signal remains unaltered. The reference channel is provided with a phase control and the test channel is provided with an amplitude control. Both these controls are situated within the main I.F. unit (HP8410A).

The block diagram of the polar display unit (figure 8.2) is particularly interesting for it shows the processes of phase detecting. It is important to notice that the phase reference signal is amplitude limited before phase detection commences. This has the effect of theoretically rendering the detection circuits insensitive to amplitude errors when the limiter is working efficiently. Practical confirmation of this was obtained by measurement of the phase angle of a short circuit for a given amplitude gain. The gain control was then altered and the phase angle re-measured. Results obtained in this manner showed the phase angle to be independent of the amplitude signal for large reflection coefficients.

8:2 Sources of Errors in Automatic Network Analyser

Hands, (reference 8.2), Woods (references 8.3 and 8.4), Adams (references 8.5 and 8.6), Ridella (references 8.7 and 8.8) and Warner (reference 8.9) are some of the authors who have investigated sources of errors in automatic network analysers. Warner has issued a comprehensive list. This is included below:-

(a) Instability i.e., the inability to produce identical results for the same measurement.

(b) Noise.

(c) Non-infinite directivity in the couplers.

(d) Imperfect matching at the test point.

(e) Departures from identical tracking in the test and reference channels.

(f) Leakage between the two channels.

(g) Imperfections in calibration standards such as incorrect dimensions of the connectors, contact resistances, errors in offset length specifications etc.

(h) Imperfections in instrumentation such as frequency and power level non-linearities, gain and phase drifts in the I.F. amplifiers, detectors, attenuator and display circuits.

(i) Quantatization errors, such as errors in the analogue to digital conversions, rounding off errors in computation etc.

8:2.1 The Instability (Non-repetitive) Problem

It has already been shown in Chapter V that the measured reflection coefficient, ρ is related to the true reflection coefficient Γ, by a system bilinear transformation of the $\rho = \frac{A\Gamma + B}{C\Gamma + D}$ where A, B, C, and D are complex constants. Furthermore, it was also shown that by making a set of calibrations, the complex constants can be solved mathematically and hence yield the the true reflection coefficient.

This mathematical solution is only possible if the four complex constants remain invariant throughout the set of measurement, i.e., the entire measurement system from the calibration standards to the computer output terminals must be stable. If this is not the case, then computer correction is not possible. Hence, it is essential that tests are carried out to ascertain whether the equipment is suitable for computer correction.

The method used to verify the stability of the system was the repetitive measurement of the same calibration piece twenty times.

The conditions of measurement were:-

(a) The same test piece (short circuit) was disconnected and re-connected for each measurement.

(b) The frequency was selected by the computer for each measurement. Hence any errors introduced by frequency drifts etc., were included.

(c) The measurement result is that taken from the print-out from the computer. Hence quantatization errors, etc., were included.

(d) The amplitude gain was deliberately set to present reflection coefficients less than unity to ensure that amplifier limiting would be minimal. A full discussion will be given in Section 8:3.

The results of the measurements carried out at 6 GHz are tabulated in figure 8.3.

Figure 8.3

Table of Repetative Measurements

Measured Reflection Coefficients		Measured Reflection Coefficients	
Amplitude	Degrees	Amplitude	Degrees
0.928	175.6	0.919	176.2
0.928	175.6	0.925	177.1
0.925	175.4	0.919	175.5
0.933	175.5	0.919	175.6
0.925	175.5	0.915	175.5
0.922	175.5	0.916	175.2
0.921	175.8	0.915	175.3
0.923	175.8	0.915	175.0
0.923	176.0	0.915	175.0
0.921	175.9	0.938	177.1

From the table shown in figure 8.3 the following were calculated.

Mean Amplitude = 0.9223
Standard Deviation of Mean Amplitude = 0.00617
∴ Standard Deviation 0.67%
Mean Phase (Degrees) = 175.705°
Standard Deviation of Mean Phase = 0.5633°
∴ Standard Deviation 0.32%

In the results calculated above, the amplitude and the phase have been calculated as if the numbers are two independent quantities. The basis for this treatment has been discussed in Section 8.1.

The final conclusion from the above measurements was that although the measurement system was not perfectly stable, it did appear that computer correction was a possibility.

8.3 Practical Difficulties in Measuring Large Reflection Coefficients; Amplifier Limiting Problems

In the measurement system used, the Hewlett Packard Reflectometer System is situated some distance away from the computer. The signal lines connecting the two pieces of equipment are subject to noise-pick-up etc. To improve the signal to noise ratio, the two outputs ($\pm$ 10 volts Max)

of the polar display are applied to two external 20dB amplifiers before application to the signal lines. Ideally if a reflection coefficient of unity is set to produce maximum output, then no limiting of the external amplifiers will result. Unfortunately in practice, due to errors in the measurement equipment, it is possible to measure apparent reflection coefficients greater than unity. When this occurs some limiting of the external amplifier occurs. To avoid this the amplifier gain setting with the Hewlett Packard equipment is reduced by approximately 1-2dB so that a reflection coefficient of unity is presented to the computer terminals as slightly less than unity $\sim$ 0.9. If this multiplication factor is denoted by k then any measured reflection coefficient, ρ_m, presented to the computer terminals become ρ'_m and the following relationship applies

$$\rho'_m = k \rho_m \qquad \ldots\ldots \quad 8.1$$

To ascertain the effect of the above on the error network scattering parameters and the final corrected results, the following analysis was used:

8:3.1 Modification of Error Scattering Parameters

S_{11};

From equation 5.19,

$$S_{11} = \frac{\rho_1\rho_2(\Gamma_2\Gamma_3 e^{-2\rho_2} - \Gamma_1\Gamma_3) - \rho_2\rho_3(\Gamma_1\Gamma_2 e^{2(\rho_3-\rho_2)} - \Gamma_1\Gamma_3) - \rho_3\rho_1(\Gamma_2\Gamma_3 e^{-2\rho_2} - \Gamma_1\Gamma_2 e^{2(\rho_3-\rho_2)})}{\rho_1(\Gamma_1\Gamma_2 e^{2(\rho_3-\rho_2)} - \Gamma_1\Gamma_3) + \rho_2(\Gamma_2\Gamma_3 e^{-2\rho_2} - \Gamma_1\Gamma_3 e^{2(\rho_3-\rho_2)}) + \rho_3(\Gamma_1\Gamma_3 - \Gamma_2\Gamma_3 e^{-2\rho_2})}$$

and using equation 8.1 and defining S_{11}'' as the new modified value of S_{11}

$$S_{11}'' = \frac{k^2\rho_1\rho_2(\Gamma_2\Gamma_3 e^{-2\rho_2} - \Gamma_1\Gamma_3) - k^2\rho_2\rho_3(\Gamma_1\Gamma_2 e^{-2(\rho_3-\rho_2)} - \Gamma_1\Gamma_3) - k^2\rho_3\rho_1(\Gamma_2\Gamma_3 e^{-2\rho_2} - \Gamma_1\Gamma_2 e^{2(\rho_3-\rho_2)})}{k\rho_1(\Gamma_1\Gamma_2 e^{2(\rho_3-\rho_2)} - \Gamma_1\Gamma_3) + k\rho_2(\Gamma_2\Gamma_3 e^{-2\rho_2} - \Gamma_1\Gamma_3 e^{2(\rho_3-\rho_2)}) + k\rho_3(\Gamma_1\Gamma_3 - \Gamma_2\Gamma_3 e^{-2\rho_2})}$$

Hence the conclusion is

$$S_{11}'' = k S_{11} \qquad \ldots\ldots \quad 8.2$$

S_{22};

From equation 5.20,

$$S_{22} = \frac{\Gamma_1 e^{2\rho_2}(\rho_2 - S_{11}) + \Gamma_2(S_{11} - \rho_1)}{\Gamma_1 \Gamma_2 (\rho_2 - \rho_1)}$$

Using equations 8.1 and 8.2 and defining S_{22}'' as the new modified value of S_{22}

$$S_{22}'' = \frac{\Gamma_1 e^{2\rho_2} k(\rho_2 - S_{11}) + \Gamma_2 k(S_{11} - \rho_1)}{k\Gamma_1 \Gamma_2 (\rho_2 - \rho_1)}$$

The conclusion is that $S_{22}'' = S_{22}$ 8.3

$\therefore$ S_{22} is unaffected by the multiplication factor k.

$S_{12}S_{21}$;

From equation 5.21,

$$S_{12}S_{21} = \frac{(\rho_1 - S_{11})(1 - S_{22}\Gamma)}{\Gamma_1}$$

Using equations 8.1, 8.2 and 8.3 and defining $S_{12}S_{21}''$ as the new modified value of $S_{12}S_{21}$,

$$S_{12}S_{21}'' = \frac{k(\rho_1 - S_{11})(1 - S_{22}\Gamma)}{\Gamma_1}$$

$$\therefore \quad S_{12}S_{21}'' = k(S_{12}S_{21}) \quad ..... \quad 8.4$$

$\therefore$ $S_{12}S_{21}$ is affected by the multiplication factor k.

The Corrected Reflection Γ

From equation 5.22

$$\Gamma = \frac{\rho_m - S_{11}}{S_{22}\rho_m + S_{12}S_{21} - S_{11}S_{22}}$$

Using equations 8.4, 8.5, 8.6 and 8.7 and defining Γ'' as the modified value of Γ ,

$$\Gamma'' = \frac{k\rho_m - kS_{11}}{kS_{22}\rho_m + kS_{12}S_{21} - kS_{11}S_{22}}$$

$$\therefore \quad \Gamma'' = \Gamma \quad ..... \quad 8.5$$

The conclusion is that the corrected reflection coefficient result is unaffected by the multiplication factor "k".

The result of equation 8.5 can be cross-checked by recalling the invariance of the cross-ratio of the bilinear transformation of equation 5.7

$$\frac{(P_1 - P_2)(P_3 - P_4)}{(P_2 - P_3)(P_4 - P_1)} = \frac{(\Gamma_1 - \Gamma_2)(\Gamma_3 - \Gamma_4)}{(\Gamma_2 - \Gamma_3)(\Gamma_4 - \Gamma_1)}$$

and using equation 8.1 again, it is seen that "k" has no effect on the corrected result.

8:3.2 The Effect of the Multiplication Factor "k" on Line Propagation Properties

From equation 5.28 which is repeated here

$$\Gamma \{2\cosh^2 2p(-P_1P_3 + P_1P_4 + P_2P_3 - P_2P_4) + \cosh 2p(P_1P_2 - P_1P_4 - P_2P_3 + P_3P_4) + (-P_1P_2 + 2P_1P_3 - P_1P_4 - P_2P_3 + 2P_2P_4)\} = 0$$

it is clear that the multiplication factor "k" has no effect on the results for the propagation properties of a line.

8:4 Preliminary Computer Corrected Measurements

8:4.1 A Manual Correction Test

One of the earliest tests carried out to check the effectiveness of computer correction was the measurement of a test piece (coaxial termination) through three different transitions. The corrected reflection coefficient results would be identical in all three cases as the same test piece was measured. Vastly different results would have pointed to errors in the system. The success of these corrections were ultimately published by the author (reference 8.10) and this is included as Appendix 12:1 in this thesis. However as many details of the practical measurements had to be deleted in the publication, they will be provided here.

The measurements were carried out using 7mm air coaxial lines and short circuits. The method of correction chosen was the three shorts method of section 5:4.2 using the correction programme of section 6:2. The test piece chosen was a Hewlett Packard Type 909A coaxial termination. All calibration and test pieces were fitted with APC7 connectors. At the time of verification, suitable one piece off-set short circuits were not available and they were constructed by using a standard Hewlett Packard Coaxial Air Lines (Type 11566A - 10.25 cms and Type 11567A - 20.25 cms) terminated with a coaxial short circuit (Hewlett Packard Type 11565A).

The three sets of calibrations and measurements were carried out using:-

(a) Set 1; consisted of connecting the calibration pieces directly to the network analyser for measurement correction.

(b) Set 2; the network analyser was connected to a pair of 3mm (OSM) to 7mm (APC 7) adaptors back-to-back. Hence the reference plane was transferred to the 7mm side of the final 3mm to 7mm adapter. All calibrations and measurements were then made referenced to the new plane.

(c) Set 3; the network analyser was connected to a pair of 7mm (APC 7) to General Radio Adapters (GR874) connected back-to-back, thus transferring the measurement reference plane to the end of the APC 7 side of the final GR874 connector. The same calibration pieces and coaxial terminations were used for measurement.

The results of the three sets of measurements are given in Table 1 of Appendix 12:1. From this table, it was concluded that the corrected results could be contained within a circle corresponding to $|\Gamma| = 0.0035$. Hence the measurement system was considered to be sufficiently stable and an automated computerized system was worth producing.

The above information was subsequently used by Gould and Rhodes (reference 8.11) for further experimental work. It should also be noted that Gould and Rhodes reported that their results compared most favourably with the results produced above i.e., all their measured reflected coefficients were within an error circle of 0.0033. Some of the other authors which have since acknowledged the paper are Woods (reference 8.3), Shurmer (reference 8.12), Hosseini (reference 8.13), Menzel (reference 8.14) and Warner (reference 8.9).

8:4.2 An Automated Correction Test

One of the earliest automated measurements carried out on the three short circuit correction method of Section 5:4.2 was reported by Kwesah (reference 8.15). Kwesah's results were obtained using the 3mm short circuit calibration pieces described in figure 7.8 of section 7:3. For his test piece, Kwesah used a Tek Wave thin film chip resistor (Type 20-01320-50) whose nominal value was $50\Omega \pm 2\%$. His measurements were made in the 1 to 8 GHz band.

Kwesah's results for the 2-4 GHz band are given in figures 8.4, 8.5, 8.6 and 8.7. Attempts at combining his results onto one graph were unsuccessful because of the closeness of his results. Hence Kwesah's independent work has also shown that the three short circuit correction method is a good one.

8:5 Conclusions

This chapter has shown how the theory derived and developed in the earlier chapters may be applied practically. A brief review of the equipment for computer correction was carried out in section 8:2.1. A full mathematical treatment has also been presented to show how the effects of amplifier limiting may be minimised.

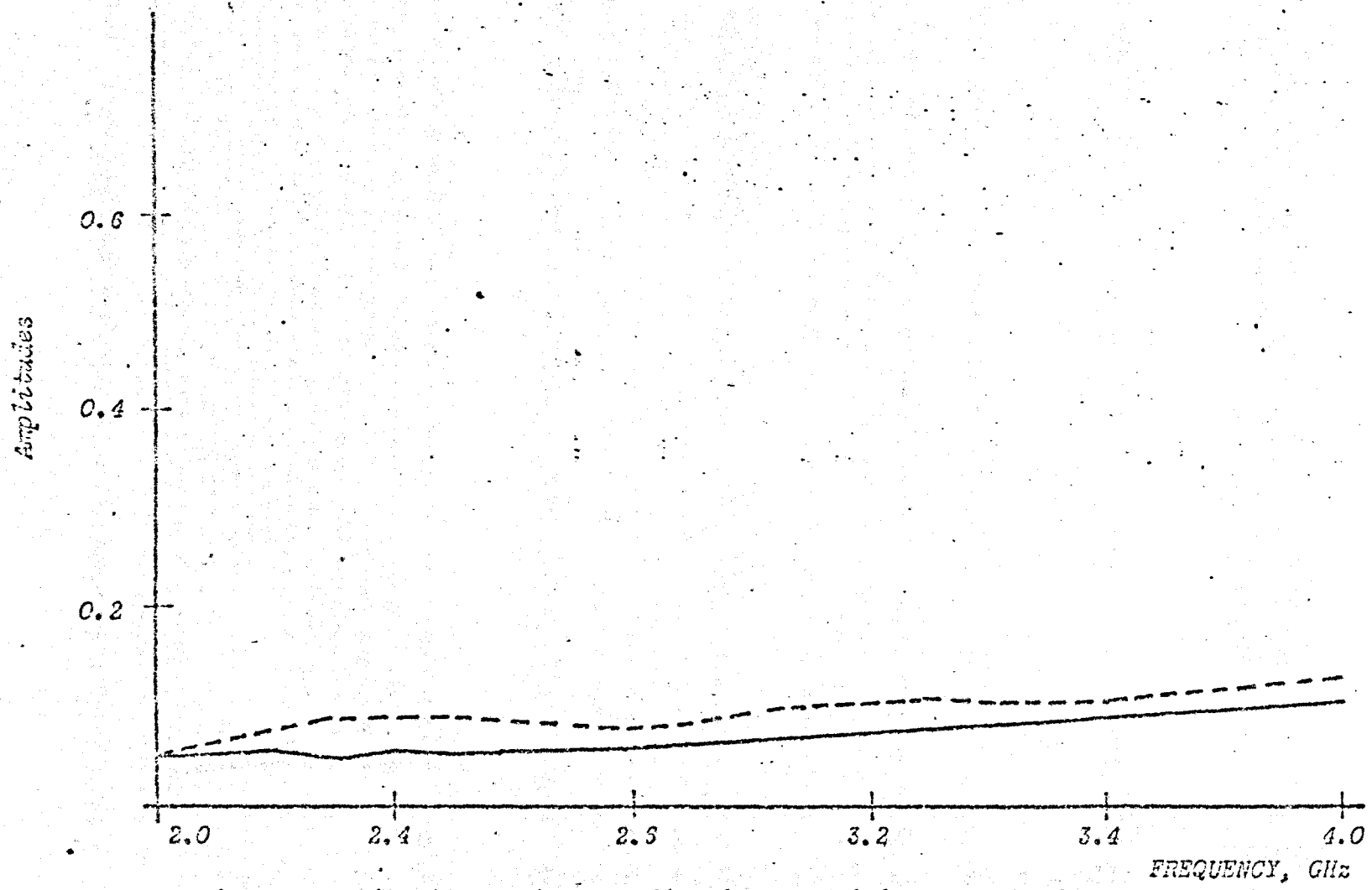

Fig. 8.4 Thin-Film Resistor Reflection Coefficient Amplitudes
---- (Uncorrected)
—— (Corrected)

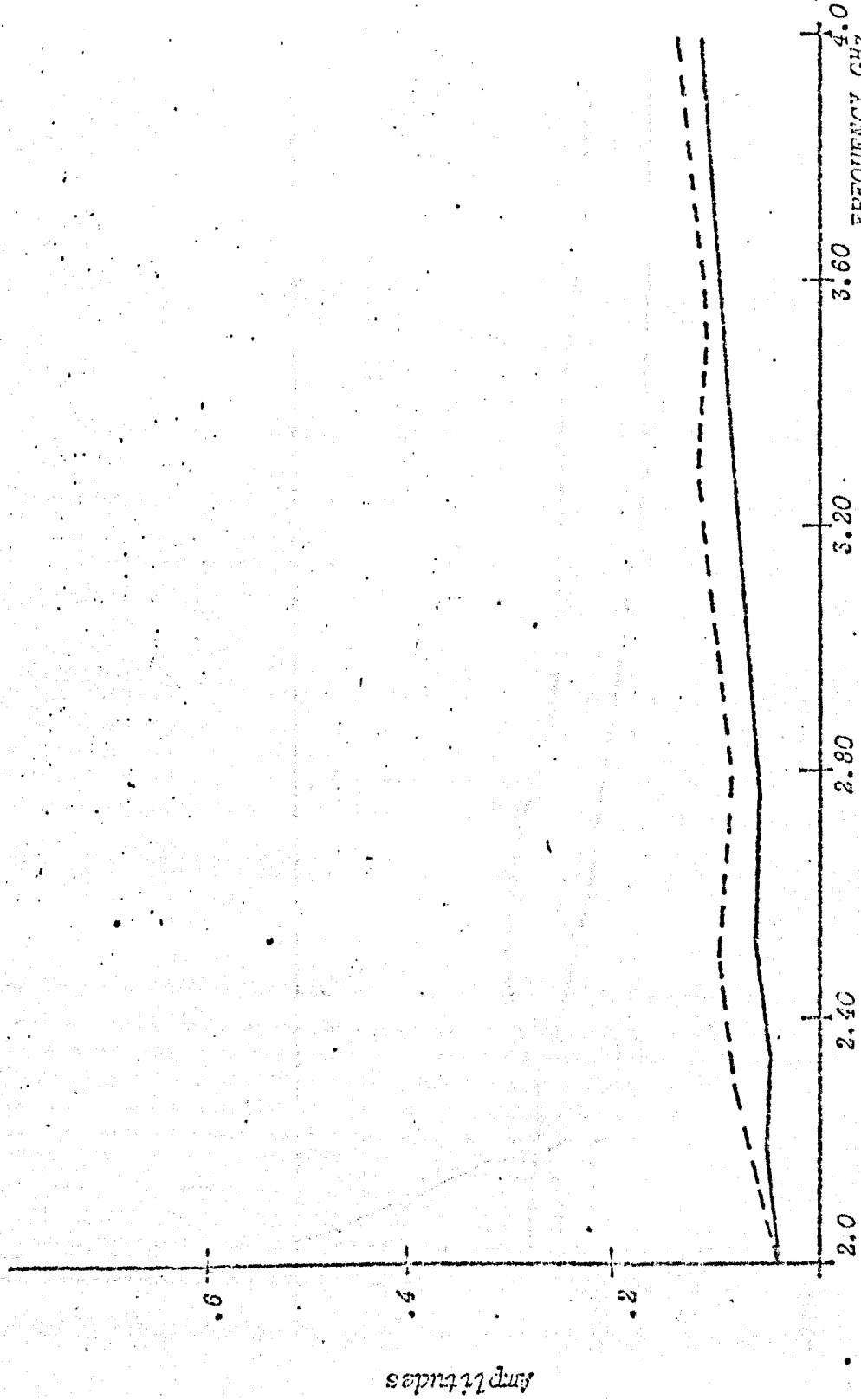

Fig. 8.5 The Repeatability of the Reflection Coefficient Amplitudes
--- (Uncorrected)
—— (Corrected)

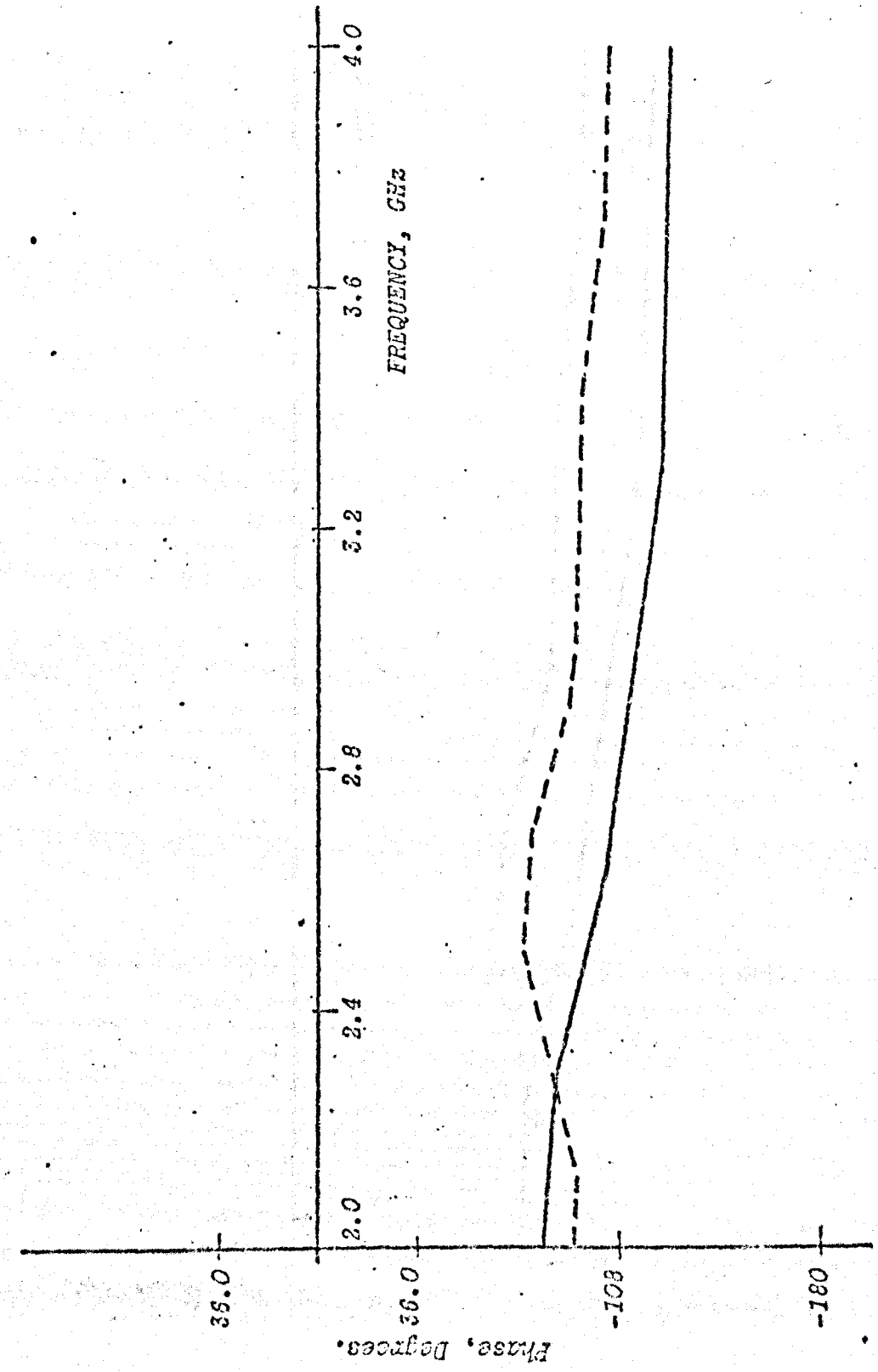

Fig. 8.6 Thin-Film Resistor Reflection Coefficient phases
---- (Uncorrected)
—— (Corrected)

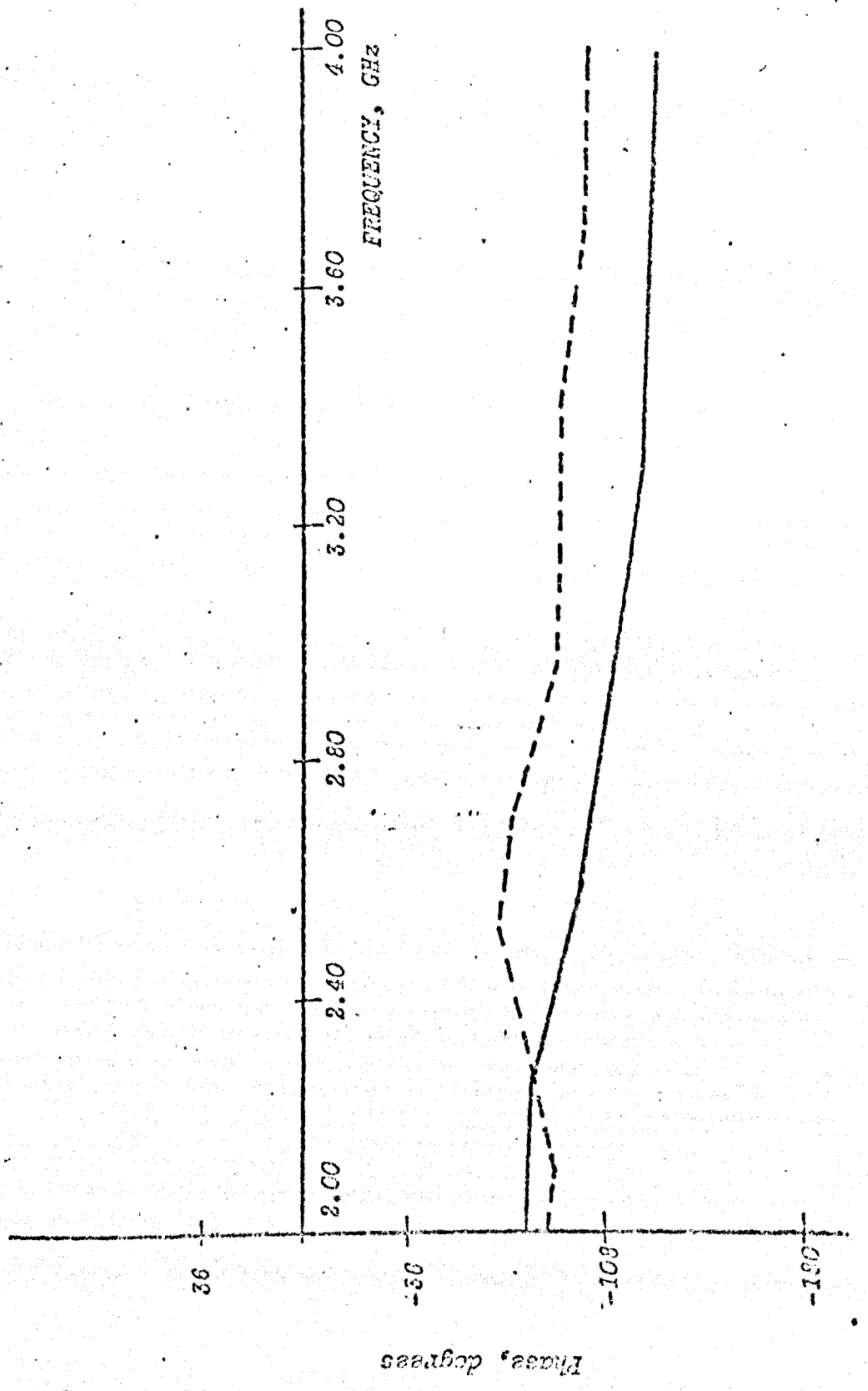

Fig. 3.7 The Repeatability of the Reflection Coefficient Phase
---- (Uncorrected)
—— (Corrected)

Two methods, one manual and the other automatic, to prove the feasibility of the three short circuit correction system have been presented. Finally, results obtained independently by another researcher are produced to show that this correction system works very well.

* * * * * * * * * * *

References

8.1 Hewlett Packard; "Microwave Network Analyser Applications" Application Report AN 117-1, Palo Alto, California.

8.2 Hand, B.P; "Developing Accuracy Specifications for Automatic Network Analyser" Hewlett Packard Journal, Feb 1970, No 21, pp 16-19.

8.3 Woods, D; "Rigorous Derivation of Computer Corrected Network Analyser Calibration Equations" Electronics Letters, 1975, 11, pp 403-405.

8.4 Wood, D; "Re-appraisal of Computer-Corrected Network Analyser Design and Calibration" Proc. I.E.E. Vol 124 No 3, March 1977 pp 205-211.

8.5 Adams, S; "A New Precision Automatic Microwave Measurement System" I.E.E.E. Trans 1968, IM-17 pp 308-313.

8.6 Adams, S; "Automatic Network Measurements" Proc I.E.E.E. Vol 66, No 4 April 1978, pp 384-391.

8.7 Ridella, S; "Computerized Microwave Measurements Accuracy Analysis" Proceedings of the European Microwave Conference, Paper B34, 1973.

8.8 Ridella, S; "Computerized Reflection Measurements C.P.E.M. Digest 1973, pp 51-53.

8.9 Warner, F; "Microwave Attenuation Measurements" (I.E.E. Monograph 19) Peter Peregrinus Ltd 1977 pp 208.

8.10 da Silva, E.F. and McPhun, M.K. "Calibration of a Microwave Network Analyser for Computer Corrected "S" Parameter Measurements" Electronics Letters, March 1973, 9, pp 126-128.

8.11 Gould, J.W. and Rhodes, G.M; "Computer Correction of a Microwave Network Analyser without Accurate Frequency Measurement" Electronics Letters 1973, No 9, pp 494-495.

8.12 Shurmer, H.V: "Calibration Procedure for Computer-Corrected S Parameter Characterization of Devices Mounted in Microstrip" Electronics Letters 1973, 9, pp 323-324.

8.13 Hosseini, N; "Optimisation Methods for Microwave Circuits" Ph.D Thesis, University of Warwick 1977.

8.14 Menzel, W: "Network Analyser Reflection Measurements of Microstrip Circuits not Requiring exactly reproducible Coaxial to Microstrip Transitions" Electronics Letters, 8 July 1976, Vol 12, No 14 pp 351-353.

8.15 Kwesah, A; "Characterization of Integrated Bipolar Transistors using Computer Aided Measurements and Optimisation" Ph.D Thesis, University of Warwick, 1976.

* * * * * * * * * *

CHAPTER IX

RESULTS OF MEASUREMENTS (including accuracy) USING THE NEW REFLECTION COEFFICIENT CORRECTION MEASUREMENT SYSTEMS

9:0 Introduction

No attempt will be made in this chapter to present all the data measured for reasons of space; only a cross-section of the measured data will be presented. The data shown will include measurements of matched loads, offset short circuits, short circuits etc., using the three new measurement correction systems of sections 5:4.2, (three short circuits) and 5:5 (the four and five termination methods).

Data will also be presented to show how the corrected measurements tend to vary with calibration errors such as errors resulting from specifying the incorrect offset lengths. Comparisons are also made between the corrected measurements on a coaxial load using the new reflection reflection correction systems of section 5:5 and that of the older and more established system (short/offset short/matched load) of section 5:4.3.

Finally data pertaining to measurement accuracies is provided in sections 9:7 and 9:8.

9:1 Measurement Results Using the Three Short Circuit Correction Methods of Section 5:4.2

9:1.1 Measurement of a Short Circuit

A short circuit, an offset short circuit of length 3.0mm and another offset short circuit of length 4.6mm was used as calibration devices to computer correct the refelction coefficient of a short circuit. The results are shown in figures 9.1 to 9.3. The calibration and device measurements were carried out bearing in mind the practical considerations mentioned in section 8:3 i.e., calibration and measured values were taken with reduced gains on the network analyser.

Figure 9.1 shows a polar display of the reflection coefficient for the frequency range 4-6 GHz. A glance on the polar display will quickly reveal whether good correction has been achieved. However, because in this case both the measured and corrected sets of values are virtually superimposed upon themselves, the display is not particularly useful for identifying a particular result against a particular frequency. To overcome this problem, alternative graphs have been provided. Firugre 9.2 is a graphical display of the reflection coefficient amplitude vs frequency. This graph shows clearly the measured and corrected reflection coefficient for a particular frequency. Figure 9.3 is similar except that instead of amplitude, the angle has been plotted against frequency. From these graphs, it can be seen that measurement correction has been successfully carried out. A print-out sheet relating to the foregoing measurements is given in figure 9.4. In this table, columns k = 1; k = 2; k = 3 are the calibration measurements. Columns k = 4 and k = 5 are not related to this set of measurements at all. They have been left in the programme store from other correction systems. [The print out subroutine is common to the different calibration systems]. Column k = 6 is themeasured (uncorrected) value of the device. The corrected set of values is given in the lower set of columns, where the results are first given in rectangular co-ordinates and then in polar co-ordinates.

From the foregoing, it is clear that very good correction has been achieved.

TEST 10S/SC

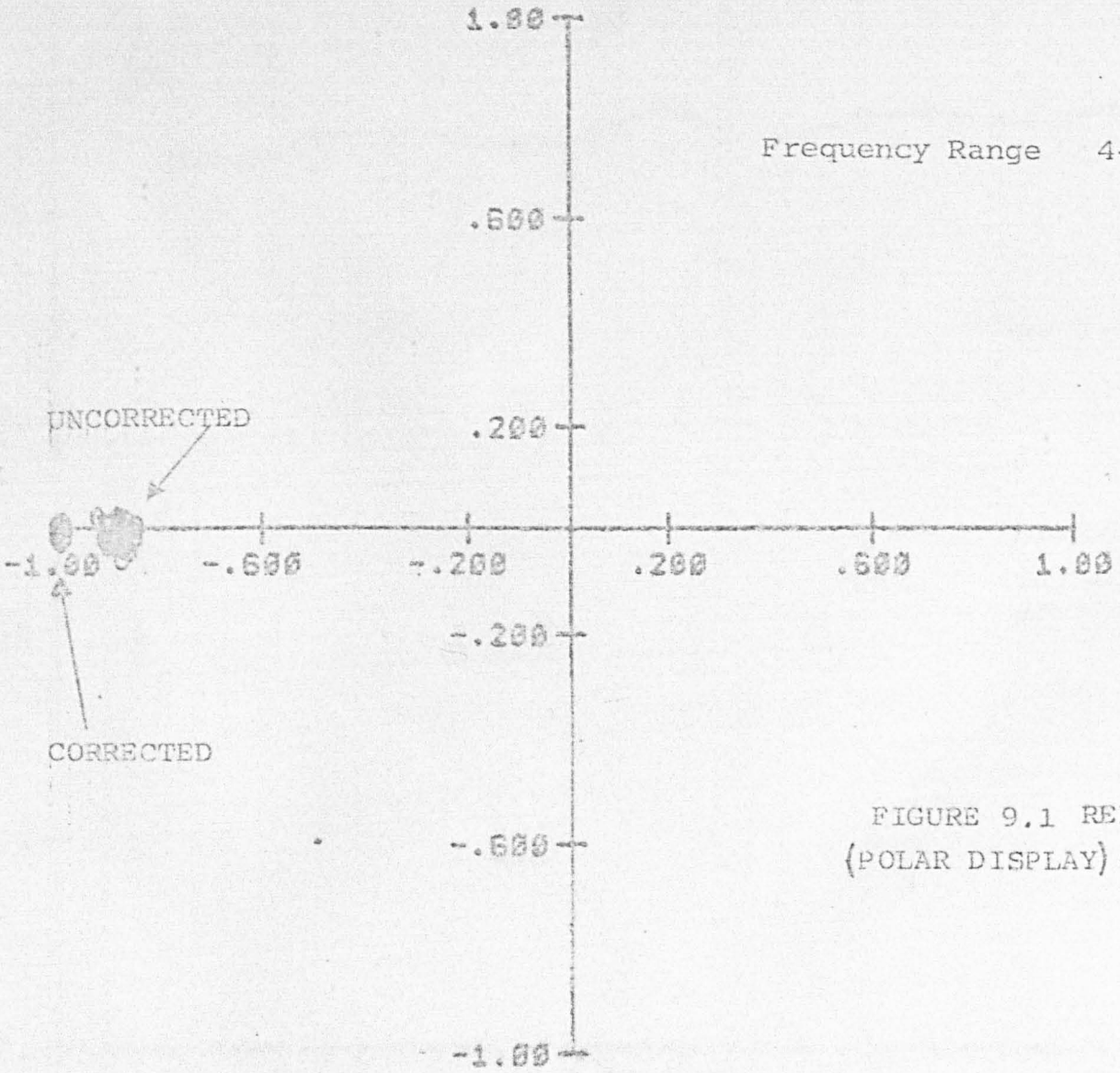

Frequency Range 4-6 GHz

FIGURE 9.1 REFLECTION COEFFICIENT (POLAR DISPLAY) OF SHORT CIRCUIT

U11 S11
MAX X =

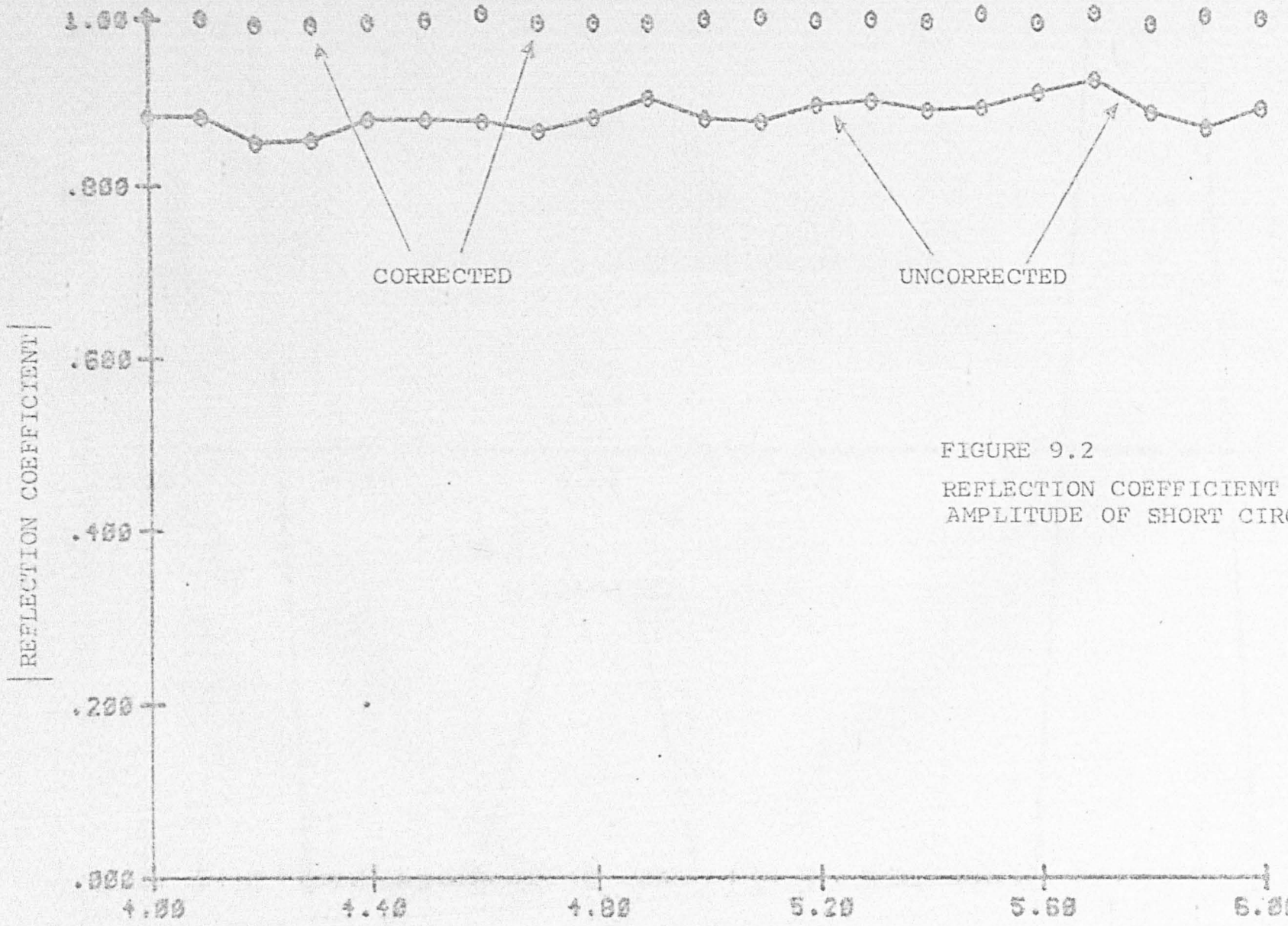

FIGURE 9.2

REFLECTION COEFFICIENT
AMPLITUDE OF SHORT CIRCUIT

TEST 105/SC

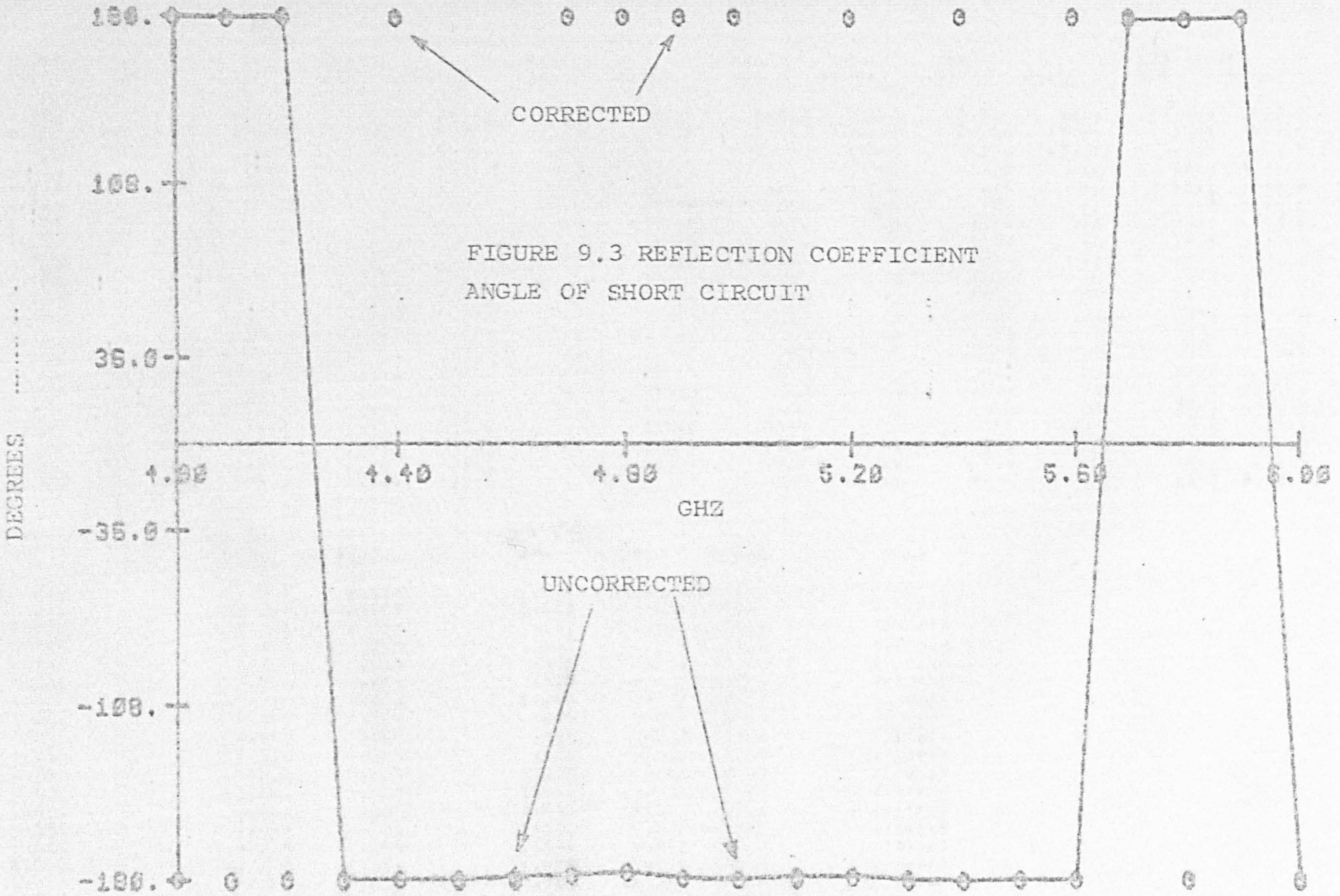

FIGURE 9.3 REFLECTION COEFFICIENT
ANGLE OF SHORT CIRCUIT

U11 S11
MAX X =

TEST 105/SC

FIGURE 9.4 CORRECTIONS OF A SHORT CIRCUIT USING THE 3 SHORT CIRCUITS METHOD

FREQUENCY GHZ	K=1 AMP	PHASE	K=2 AMP	PHASE	K=3 AMP	PHASE	K=4 AMP	PHASE	K=5 AMP	PHASE	K=6 DEVICE AMP	PHASE
4.000	.879	178.7	.870	151.0	.865	134.0	1.111	134.9	1.110	134.9	.881	179.7
4.100	.879	178.5	.865	149.3	.864	132.9	1.111	134.9	1.110	134.8	.881	178.9
4.200	.855	178.9	.841	149.6	.841	132.6	1.108	134.9	1.109	134.8	.850	179.5
4.300	.859	-179.2	.854	149.7	.859	132.3	.000	.0	.000	.0	.853	-179.0
4.400	.881	-178.3	.870	148.5	.863	129.9	.000	.0	.000	.0	.877	-179.0
4.500	.877	-179.1	.869	147.9	.851	128.8	.000	.0	.000	.0	.877	-178.9
4.600	.870	-178.3	.856	147.3	.850	129.0	.000	.0	.000	.0	.876	-178.0
4.700	.868	-177.5	.857	147.9	.851	128.2	.000	.0	.000	.0	.864	-177.5
4.800	.886	-176.1	.883	146.7	.870	126.9	.000	.0	.000	.0	.881	-176.3
4.900	.903	-178.2	.881	145.0	.862	123.7	.000	.0	.000	.0	.904	-178.3
5.000	.880	-178.8	.865	143.5	.847	123.4	.000	.0	.000	.0	.879	-179.1
5.100	.872	-178.3	.869	143.7	.859	122.3	.000	.0	.000	.0	.875	-177.6
5.200	.897	-177.4	.886	142.0	.878	120.9	.000	.0	.000	.0	.896	-178.1
5.300	.901	-179.5	.884	140.5	.864	117.7	.000	.0	.000	.0	.901	-179.2
5.400	.892	-179.7	.866	139.1	.855	117.9	.000	.0	.000	.0	.890	-180.0
5.500	.895	-179.9	.874	139.2	.866	116.3	.000	.0	.000	.0	.892	-179.1
5.600	.916	-178.9	.895	137.2	.894	114.6	.000	.0	.000	.0	.911	-179.0
5.700	.918	178.7	.887	135.2	.859	112.2	.000	.0	.000	.0	.926	178.5
5.800	.890	177.6	.848	135.5	.841	112.6	.000	.0	.000	.0	.886	178.3
5.900	.865	179.5	.851	136.0	.840	113.8	.000	.0	.000	.0	.868	178.8
6.000	.890	179.3	.875	136.0	.873	111.7	.000	.0	.000	.0	.891	-179.6

FREQUENCY GHZ	REF COEFF REAL	IMAG	REF COEFF AMP	DB	PHASE	VSWR
4.000	-1.002	-.020	1.002	.015	-178.8	*******
4.100	-1.002	-.007	1.002	.014	-179.6	*******
4.200	-.992	-.011	.992	-.070	-179.4	*******
4.300	-.993	-.003	.993	-.062	-179.8	*******
4.400	-.996	.013	.996	-.038	179.3	*******
4.500	-.999	-.004	.999	-.005	-179.8	*******
4.600	-1.007	-.005	1.007	.058	-179.7	*******
4.700	-.995	.000	.995	-.041	180.0	*******
4.800	-.996	.004	.996	-.038	179.8	*******
4.900	-.996	.002	.996	-.039	179.9	*******
5.000	-1.000	.004	1.000	.001	179.8	*******
5.100	-1.004	-.012	1.004	.033	-179.3	*******
5.200	-.999	.011	1.000	-.004	179.4	*******
5.300	-1.000	-.006	1.000	.001	-179.7	*******
5.400	-.998	.005	.998	-.016	179.7	*******
5.500	-1.008	-.014	1.008	.068	-179.2	*******
5.600	-.996	.002	.996	-.034	179.9	*******
5.700	-1.008	.004	1.008	.067	179.8	*******
5.800	-.995	-.012	.995	-.045	-179.3	*******
5.900	-1.003	.011	1.004	.030	179.4	*******
6.000	-1.001	-.020	1.001	.010	-178.9	*******

9:1.2 Measurement of a Matched Load

The corrected reflection coefficient measurement of a matched load will not be given here because the results of such a measurement by Kwesah (reference 8.15) have already been included in figures 8.4 to 8.7 of section 8:4.2. Kwesah has reported excellent results.

9:1.3 Errors in Correction

From reports by other authors (references 8.11 and 8.15) and by comparative measurements with other reflection coefficient systems (references 9.1 and 9.3) the correction system appears to function satisfactorily. However, for good correction, it is essential that the additional phase changes associated with the offset short circuits are accurately known. This is easily specified in coaxial air lines but trouble can be experienced with microstrip lines etc. In order to investigate this problem, a termination was constructed and correction was carried out using the true offset lengths of 4.6mm and 11.6mm. False correction was then calculated using the same measured data but with $\pm$ 2% errors in the offset lengths. The results of such measurements are shown in figure 9.5. From this graph, it is clear that the necessity for accurate offset phase shift specifications are most important. It should also be noted that signal frequency drift during measurement is tantamount to additional phase shift error. Further information on errors in calibration standards may be obtained from reference 9.1 which is included as appendix 12.3.

9:2 Measurements Results Using the Four Short Circuits Correction Method of Section 5:5

9:2.1 Measurement of a Sliding Load Termination

The reflection coefficient amplitude measurement of one position of a sliding load is shown in figure 9.6. The measurement was made using a sliding load short circuit coaxial line to produce the four short circuit calibrations.

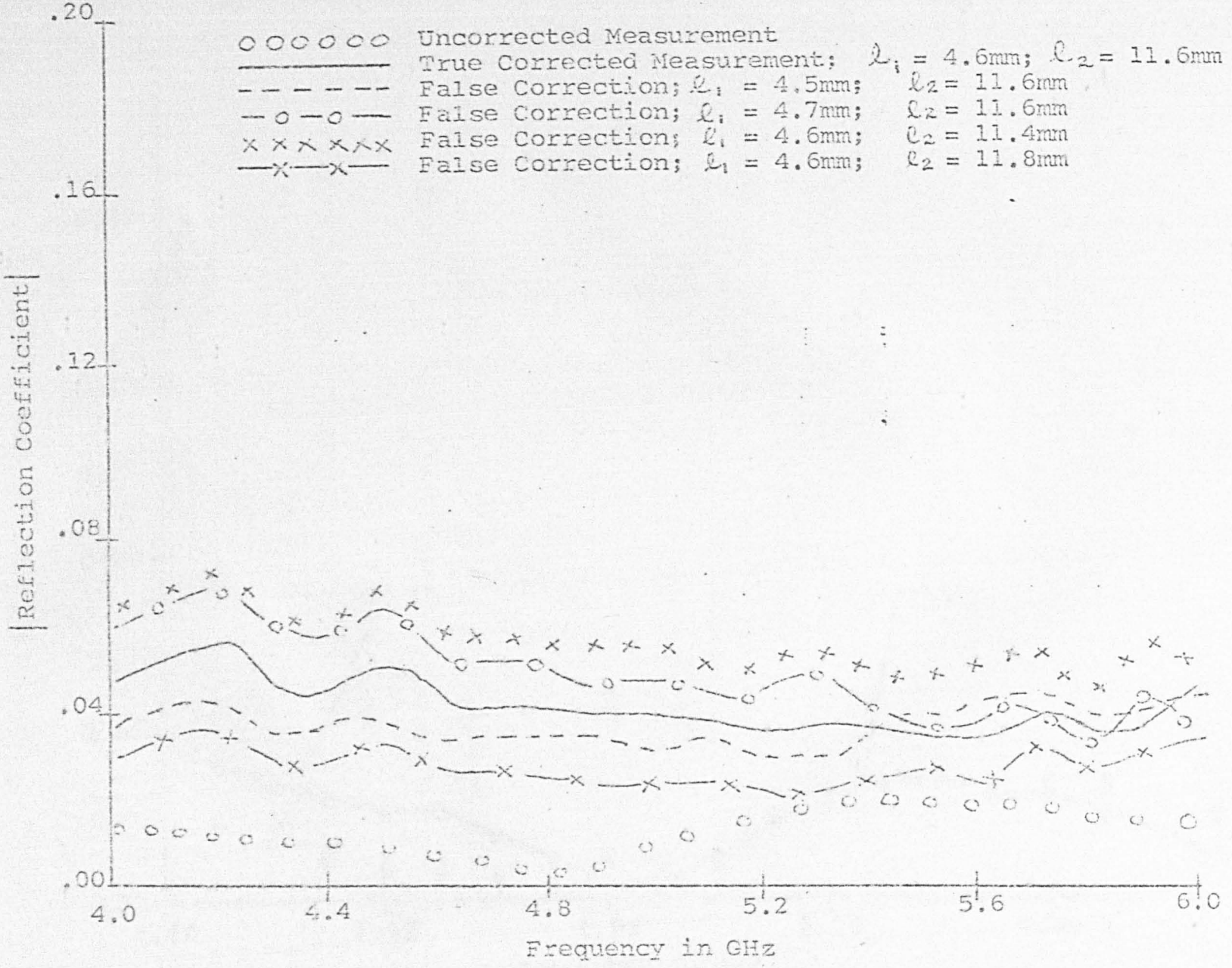

FIGURE 9.5 MEASUREMENT OF A TERMINATION
(COMPUTED CORRECTION USING THREE SHORT CIRCUITS)

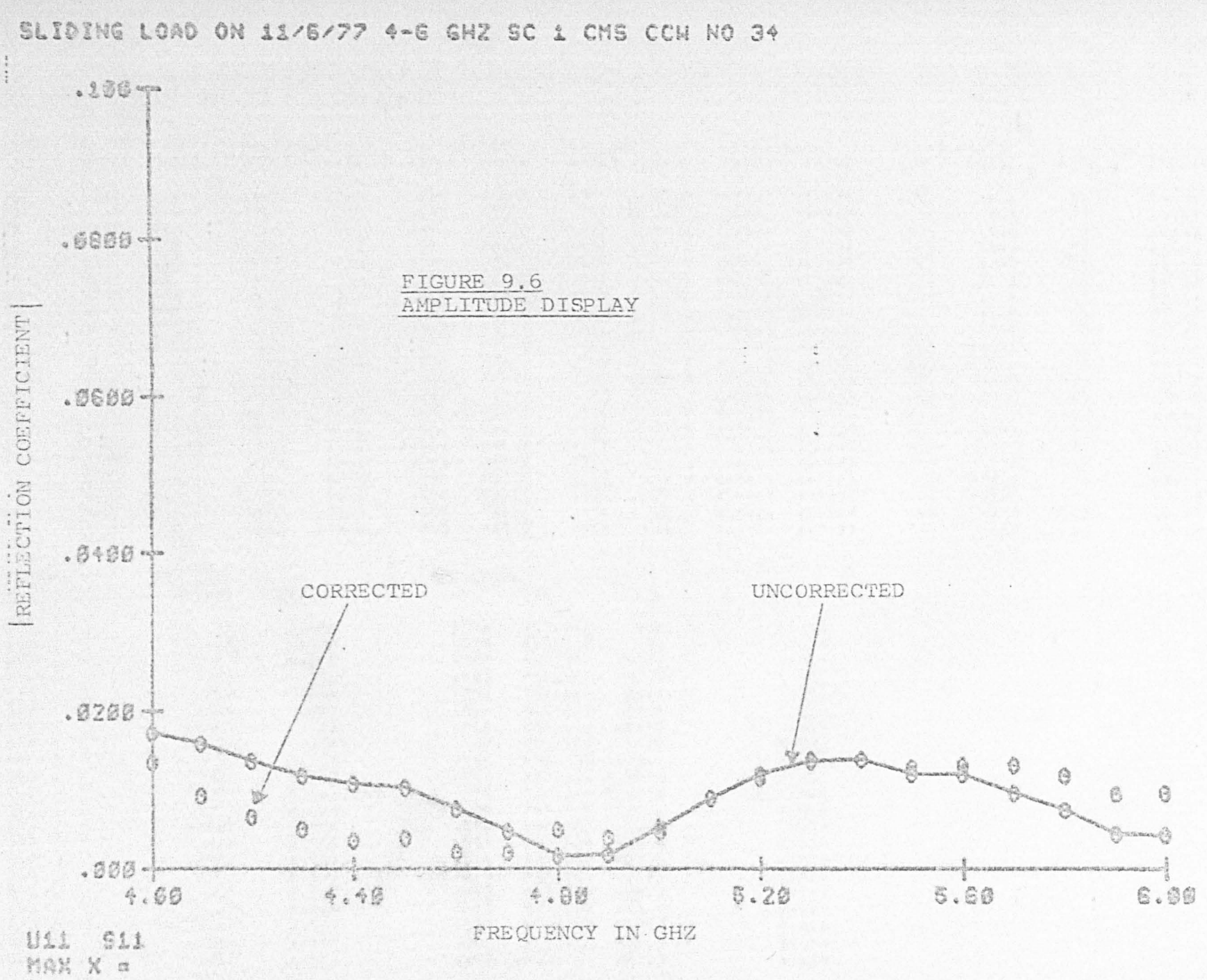

FIGURE 9.6
AMPLITUDE DISPLAY

FIGURE 9.7 CORRECTIONS OF A SLIDING LOAD USING THE 4 SHORT CIRCUIT METHOD

SLIDING LOAD ON 11/6/77 4-6 GHZ GC 1 CMS CCW N6 34

FREQUENCY GHZ	CALIBRATION 1 AMPLT	CALIBRATION 1 PHASE	CALIBRATION 2 AMPLT	CALIBRATION 2 PHASE	CALIBRATION 3 AMPLT	CALIBRATION 3 PHASE	CALIBRATION 4 AMPLT	CALIBRATION 4 PHASE	REF. SHORT AMPLT	REF. SHORT PHASE	UNCRT DEVICE AMPLT	UNCRT DEVICE PHASE	ONE LINE LENGTH NEPERS	ONE LINE LENGTH DEGREES
4.000	.912	111.8	.941	15.3	.913	-80.8	.934	-177.3	######	######	.017	2.2	.00	48.23
4.100	.935	120.3	.959	21.0	.933	-77.0	.954	-176.2	######	######	.016	4.9	.00	49.54
4.200	.989	127.4	1.008	25.1	.981	-75.2	1.005	-176.6	######	######	.014	6.6	.00	50.80
4.300	.995	131.4	1.009	26.8	.984	-76.0	1.006	-179.7	######	######	.012	11.4	.00	51.96
4.400	.979	137.2	.989	30.0	.964	-75.0	.985	179.0	######	######	.011	19.7	.00	53.12
4.500	.937	144.2	.942	34.7	.921	-72.6	.942	178.7	######	######	.010	20.1	.00	54.33
4.600	.931	153.6	.930	41.7	.912	-67.8	.932	-179.0	######	######	.008	44.4	.00	55.50
4.700	.943	161.6	.939	47.2	.923	-64.5	.943	-178.0	######	######	.005	49.9	.00	56.64
4.800	.966	169.2	.958	52.5	.946	-61.4	.960	-177.5	######	######	.002	67.0	.00	57.83
4.900	.980	175.8	.965	56.8	.957	-59.6	.973	-178.0	######	######	.002	-130.0	.00	58.98
5.000	.969	-178.2	.951	60.9	.950	-58.4	.964	-179.0	######	######	.005	-111.1	.00	60.14
5.100	.947	-169.7	.931	66.8	.930	-54.5	.944	-177.8	######	######	.009	-86.9	.00	61.32
5.200	.961	-161.1	.939	73.3	.946	-50.3	.957	-176.2	######	######	.012	-73.2	.00	62.48
5.300	.992	-153.7	.970	78.5	.977	-47.4	.991	-175.8	######	######	.014	-69.3	.00	63.64
5.400	1.017	-147.6	.991	82.5	1.001	-46.1	1.015	-176.9	######	######	.014	-55.1	.00	64.84
5.500	1.016	-142.9	.995	84.7	1.004	-46.2	1.018	-179.4	######	######	.012	-44.8	.00	66.02
5.600	.993	-137.1	.969	88.1	.983	-45.2	.996	179.1	######	######	.012	-32.5	.00	67.21
5.700	.968	-130.4	.943	92.8	.964	-43.5	.976	178.5	######	######	.010	-23.5	.00	68.47
5.800	.945	-122.4	.928	98.6	.945	-39.9	.957	179.4	######	######	.008	-28.9	.00	69.63
5.900	.951	-115.5	.936	103.1	.952	-38.3	.962	178.9	######	######	.005	-3.3	.00	70.89
6.000	.939	-108.3	.926	107.9	.940	-36.3	.950	178.9	######	######	.004	-.7	.00	72.13

FREQUENCY GHZ	REF COEFF REAL	REF COEFF IMAG	REF COEFF AMP	REF COEFF DB	REF COEFF PHASE	VSWR
4.000	.013	.002	.014	-37.341	7.6	1.028
4.100	.009	.000	.009	-40.572	.4	1.019
4.200	.007	-.001	.007	-43.394	-8.8	1.014
4.300	.005	.000	.005	-45.468	3.8	1.011
4.400	.003	.002	.004	-48.627	29.3	1.007
4.500	.004	.002	.004	-47.712	27.4	1.008
4.600	-.001	.002	.002	-53.047	106.5	1.004
4.700	-.002	.001	.002	-53.130	148.4	1.004
4.800	-.005	.000	.005	-45.939	179.0	1.010
4.900	-.004	-.002	.004	-47.714	-154.6	1.008
5.000	-.002	-.004	.005	-46.300	-112.0	1.010
5.100	-.002	-.009	.009	-40.849	-105.0	1.018
5.200	-.001	-.012	.012	-38.670	-93.8	1.024
5.300	-.002	-.014	.014	-37.094	-97.0	1.028
5.400	.002	-.014	.014	-37.109	-80.1	1.028
5.500	.003	-.013	.013	-37.811	-77.8	1.026
5.600	.005	-.012	.013	-37.547	-68.3	1.027
5.700	.005	-.012	.013	-37.552	-66.0	1.027
5.800	.002	-.012	.012	-38.508	-82.2	1.024
5.900	.004	-.009	.010	-40.405	-64.2	1.019
6.000	.005	-.009	.010	-40.201	-61.7	1.020

The physical spacing between each calibration was 1 centimetre. A print out which gives details of the calibration, measured and corrected values is shown in figure 9.7. This print out differs from that of figure 9.4 for it contains additional information not shown in the graphical displays. These are the attenuation and phase change asscciated with the evenly spaced lengths between the calibration pieces. For a 1 cm length of good air coaxial line, the attenuation is as expected, practically zero.

Comparisons between the theoretical and measured electrical offset lengths yield the table below:-

Frequency GHz	Electrical Length (Degrees)		Percentage Discrepancy
	Theoretical	Measured/Calculated	
4	48	48.23	0.48%
5	60	60.14	0.23%
6	72	72.13	0.18%

The discrepancies are due to inaccuracies in (a) manual setting of the 10mm offsets; (b) setting the frequency of measurement; (c) computational errors. The discrepancies are greatest when the electrical length is shortest. The reasons for these computational errors have been extensively discussed in section 6:3.

It should be noted that this programme can be used to measure the attenuation and phase change associated with short lengths of line, e.g., microstrip. The effective dielectric constant of such a line may also be ascertained if the physical length of the line is known.

9:2.2 Measurement of a Short Circuit

In normal measurements carried out on a network analyser, the electrical lengths of the reference and test channel are set to be equal. Hence, the reflection coefficients of a good short circuit can be expected to hover around the $1 \angle 180^{\circ}$ point on a polar display as the measurement frequency is altered.

If the electrical lengths of the reflection and test channels are not equal, then the angle of the measured reflection coefficients would appear to alter with frequency on the polar display. A good computer correction scheme should resolve these apparent discrepancies and produce corrected results to prove that the device is in fact a short circuit and all its reflection coefficient valves should cluster about the $1\angle 180^{o}$ point.

This effect is very clearly demonstrated in figures 9.8, 9.9, and 9.10 where a short circuit measured with the above-stated conditions is shown to be a short circuit after computer correction.

9:3 Measurement Results Using the Four Unknown Terminations and Reference Short Method of Section 5:5

9:31 Measurement of an Attenuator Terminated by a Short Circuit

One of the preliminary checks carried out on this correction technique was the measurement of a 10dB attenuator terminated by a short circuit. If the VSWR of the attenuator is temporarily ignored and if one assumes the short circuit to be perfect, then a return loss of 20 dB (VSWR 1.22) can be expected. In practice this would not be so because of the input and output match of the attenuator and also because of slight variations in the attenuator loss. However, such a set of measurements does provide a crude but effective approximation. The results of such a corrected measurement are shown in figure 9.11. The correction was carried out using the calibration pieces described in section 7:4. It is easily seen that the corrected results tend to behave as predicted.

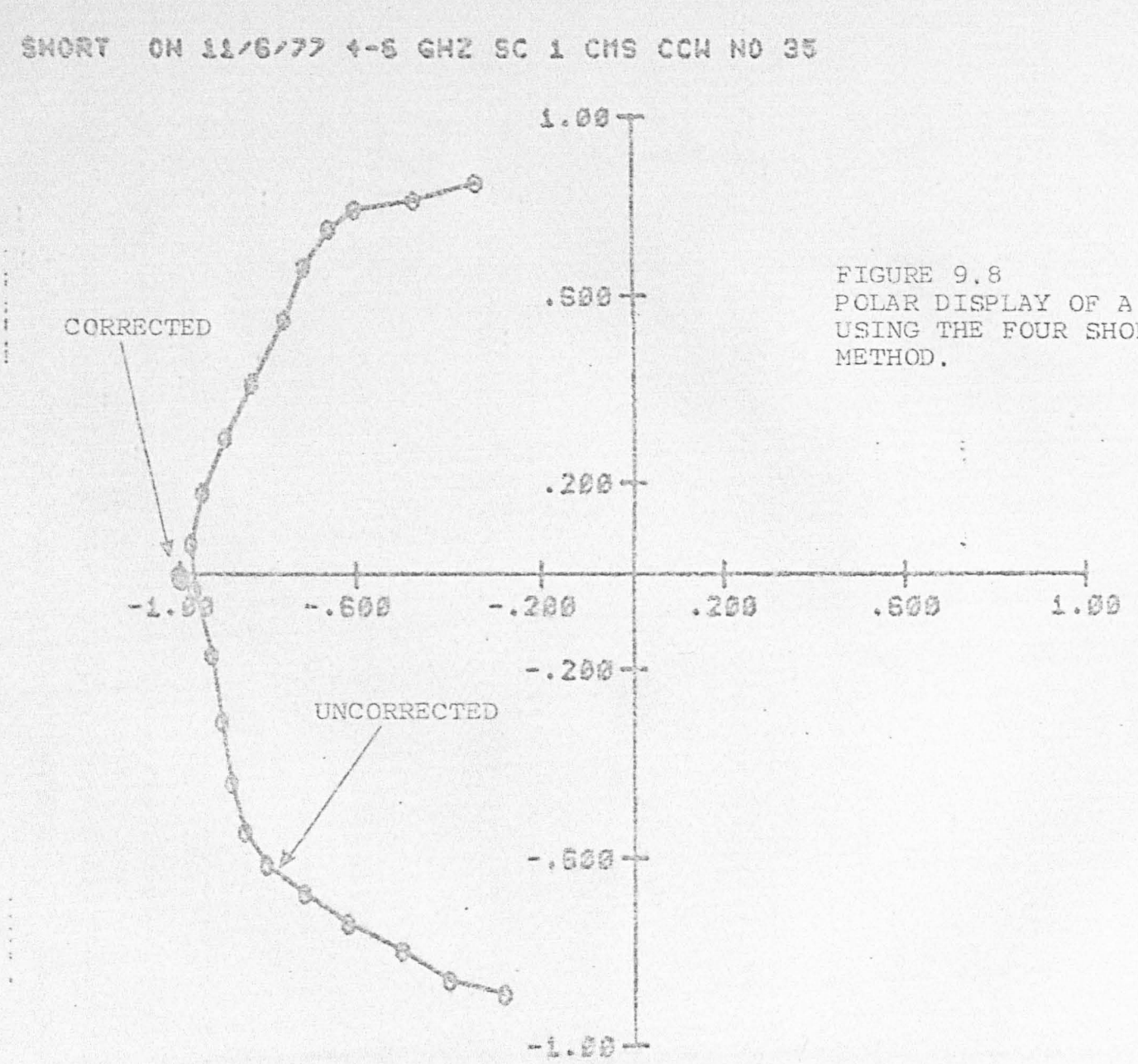

FIGURE 9.8
POLAR DISPLAY OF A SHORT CIRCUIT
USING THE FOUR SHORT CIRCUIT CORRECTION
METHOD.

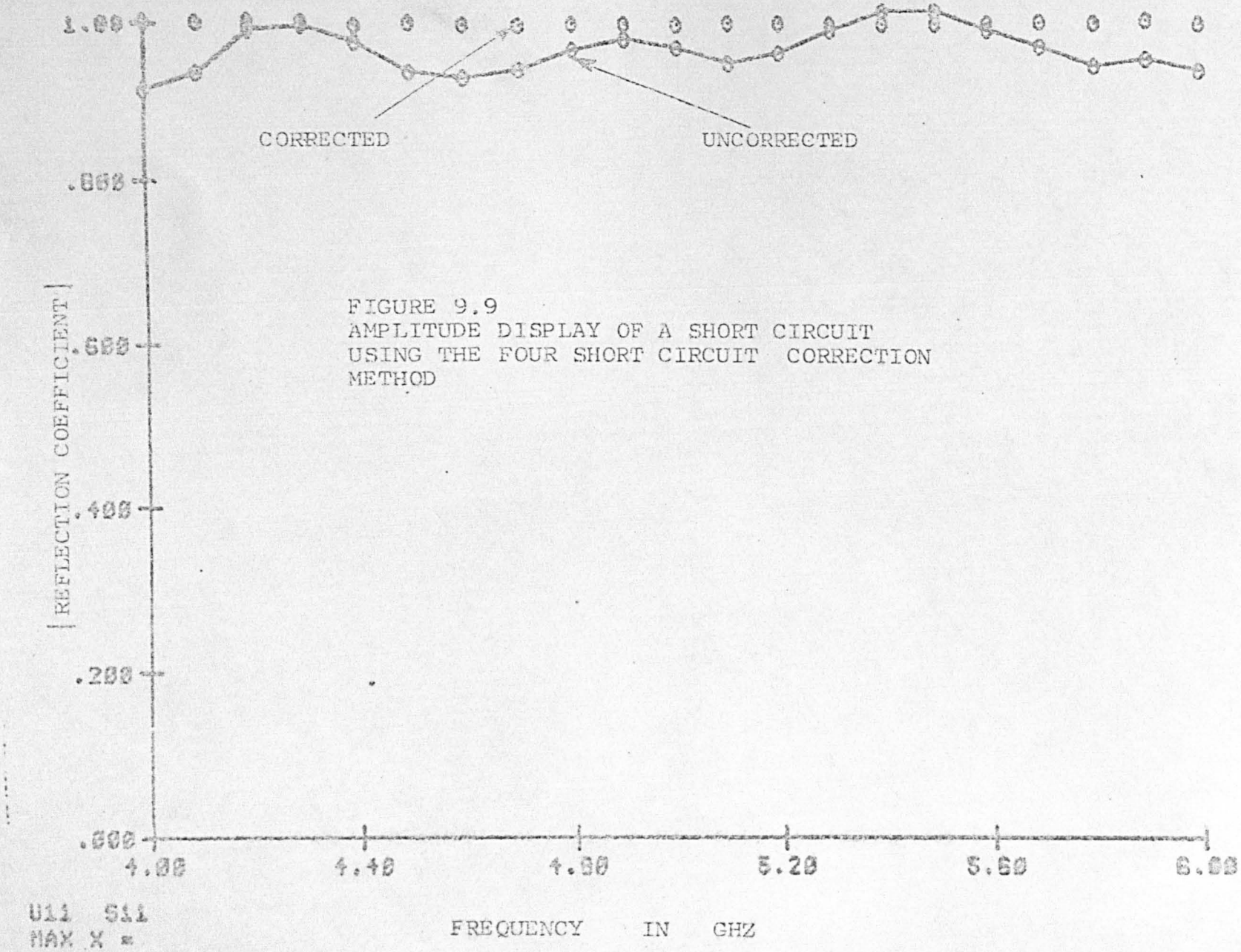

FIGURE 9.9
AMPLITUDE DISPLAY OF A SHORT CIRCUIT
USING THE FOUR SHORT CIRCUIT CORRECTION
METHOD

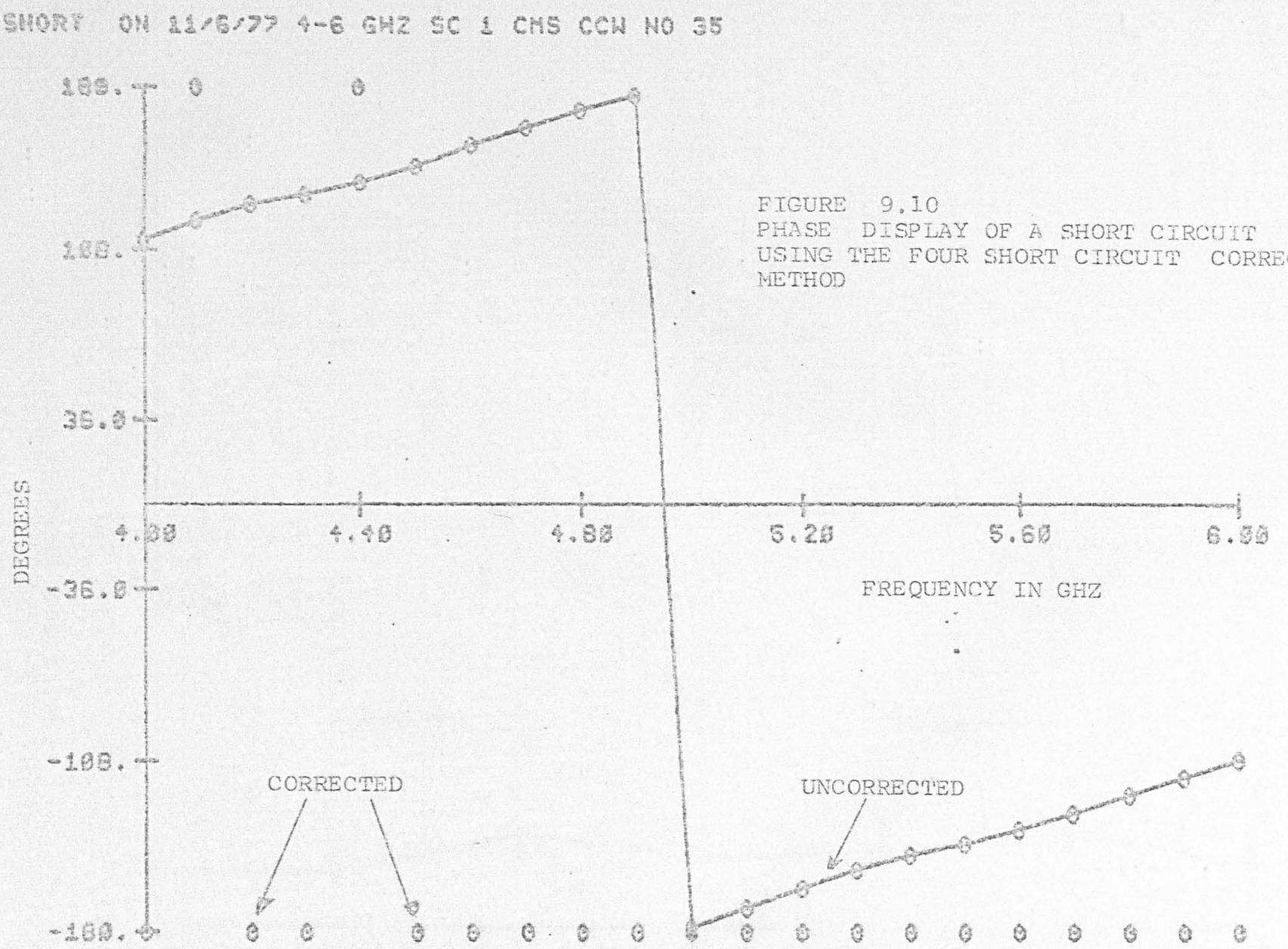

FIGURE 9.10
PHASE DISPLAY OF A SHORT CIRCUIT
USING THE FOUR SHORT CIRCUIT CORRECTION
METHOD

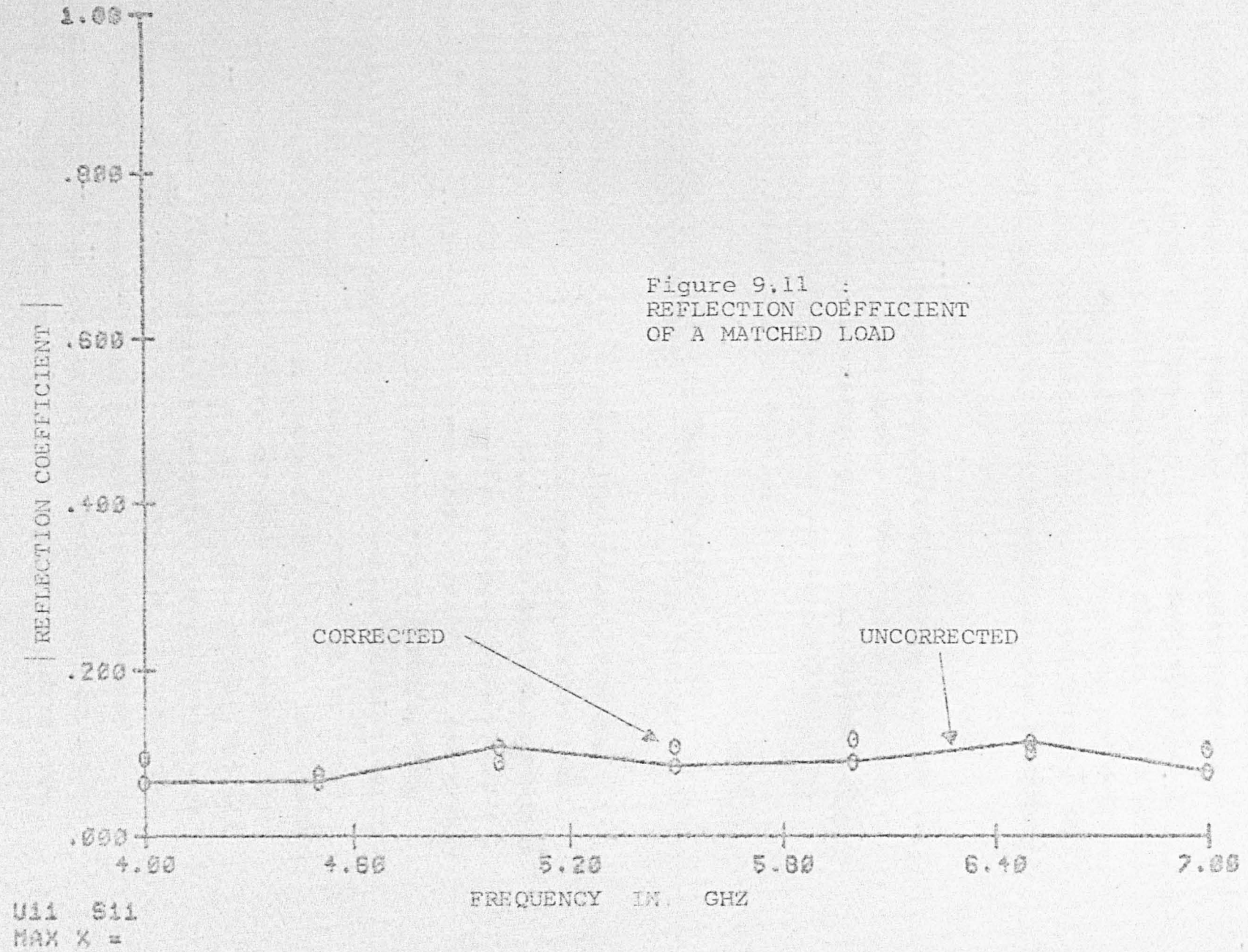

Figure 9.11 :
REFLECTION COEFFICIENT
OF A MATCHED LOAD

9:3.2 Measurement of a Short Circuit

The measurement results carried out on a short circuit using this method and the calibration pieces of section 7:4 is shown in figure 9.12. The table of results associated with it can be found in figure 9.13. The main difference between this table and that described for figure 9.7 is that an additional set of calibration figures has been added to the print out under the Reference Short Circuit Column. The corrected results are particularly consistent with frequency.

Note:

The information given in figure 9.13 may be used in conjunction with the computer programme of Appendix 11:9 to calculate the admittance of the unknown termination. The theoretical work for this calculation has been referred to in Section 5:6.

9:4 Comparison of Results Using Different Correction Techniques

To provide a means of comparison between the new correction methods and an older and more established one (reference 9.3 and section 5:4.3), it was decided to measure a matched termination. The results of these measurements are shown in figure 9.14. Apart from a small initial cross-over, it can be seen that the short/offset short/sliding load and the Three Short Circuit Correction Method results agree very closely. The results obtained by the Four Evenly Spaced Short Circuits Method and the Four Termination/Reference Short Circuit Method are also very similar. It might be argued that there is a slight discrepancy between the former set (3 termination methods) and the latter set of measurement. However, it should be borne in mind that the former set assumes that lossless lines are used in the calibrations whilst the latter set takes line attenuation into account, therefore identical results should not be expected.

FIGURE 9.12

POLAR DISPLAY OF A
SHORT CIRCUIT (4-7 GHZ)

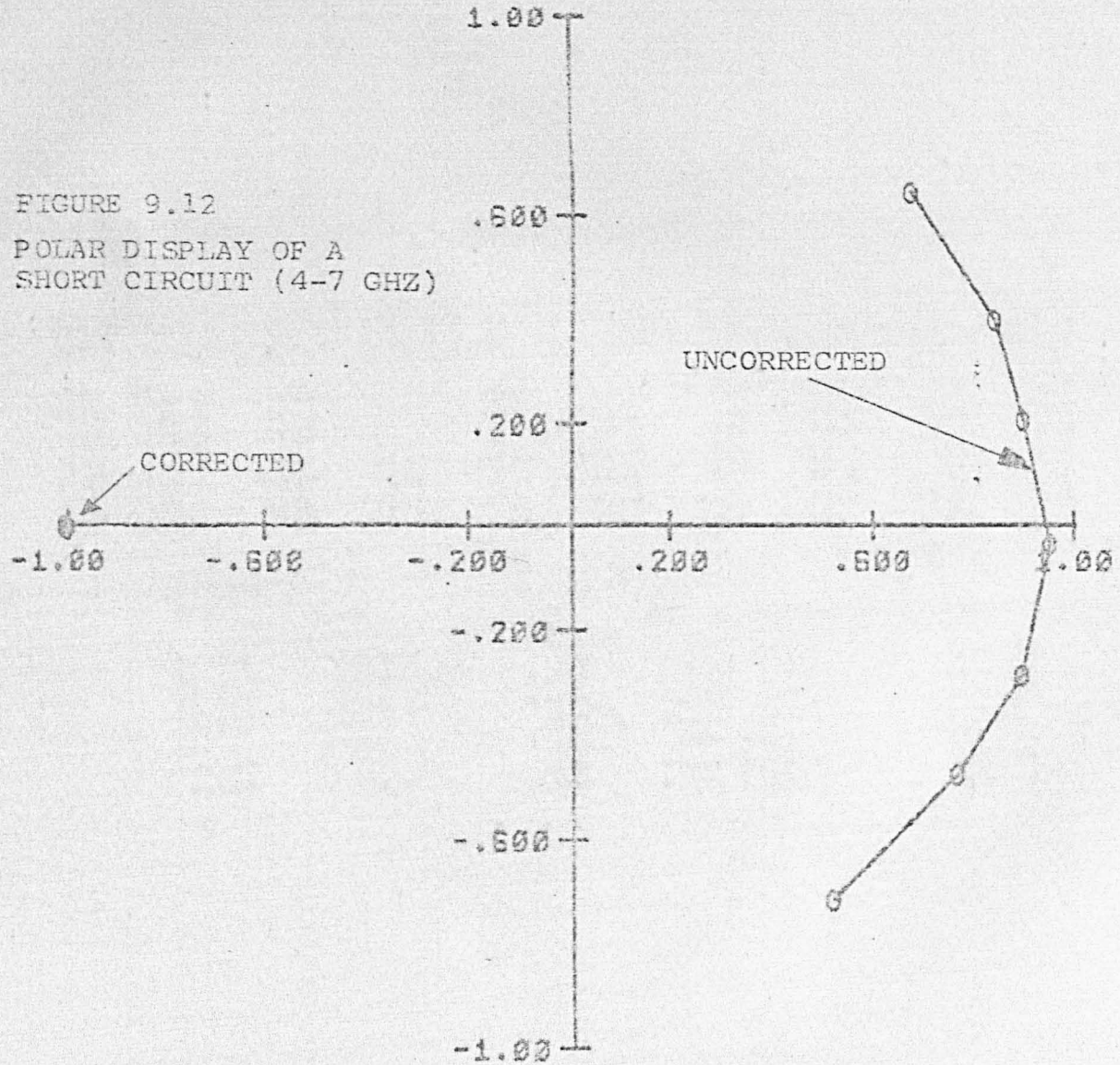

U11 S11
MAX X =

FIGURE 9.13 CORRECTIONS OF A SHORT CIRCUIT USING 4 TERMINATIONS & A REF. SHORT CIRCUIT

NSC9

FREQUENCY GHZ	CALIBRATION 1 AMPLT	CALIBRATION 1 PHASE	CALIBRATION 2 AMPLT	CALIBRATION 2 PHASE	CALIBRATION 3 AMPLT	CALIBRATION 3 PHASE	CALIBRATION 4 AMPLT	CALIBRATION 4 PHASE	REF. SHORT AMPLT	REF. SHORT PHASE	UNCRT DEVICE AMPLT	UNCRT DEVICE PHASE	ONE LINE LENGTH NEPERS	ONE LINE LENGTH DEGREES
4.000	.906	-144.0	.910	119.9	.944	23.3	.889	-71.3	.938	43.3	.937	43.5	.01	47.75
4.500	.911	-160.0	.904	87.3	.920	-17.7	.892	-124.3	.933	25.3	.936	25.3	.01	54.27
5.000	.917	-177.6	.909	58.9	.857	-55.0	.921	-178.2	.923	13.0	.923	12.9	.00	60.10
5.500	.931	163.1	.971	31.0	.889	-98.1	.922	125.7	.953	-2.1	.953	-2.2	.01	66.05
6.000	.931	143.9	.963	4.6	.911	-144.1	.945	72.2	.937	-17.8	.941	-17.8	.00	72.37
6.500	.898	129.2	.918	-21.1	.921	173.2	.917	23.3	.903	-32.1	.902	-32.0	.00	78.77
7.000	.912	113.2	.899	-55.7	.913	137.1	.906	-29.1	.885	-54.2	.884	-54.1	.00	83.69

FREQUENCY GHZ	REF COEFF REAL	REF COEFF IMAG	REF COEFF AMP	REF COEFF DB	REF COEFF PHASE	VSWR
4.000	-1.000	-.003	1.000	-.004	-179.8	*******
4.500	-1.004	.001	1.004	.032	179.9	*******
5.000	-1.000	.001	1.000	-.002	180.0	*******
5.500	-.999	.001	.999	-.005	180.0	*******
6.000	-1.004	-.000	1.004	.036	-180.0	*******
6.500	-.999	-.002	.999	-.008	-179.9	*******
7.000	-.999	-.001	.999	-.006	-180.0	*******

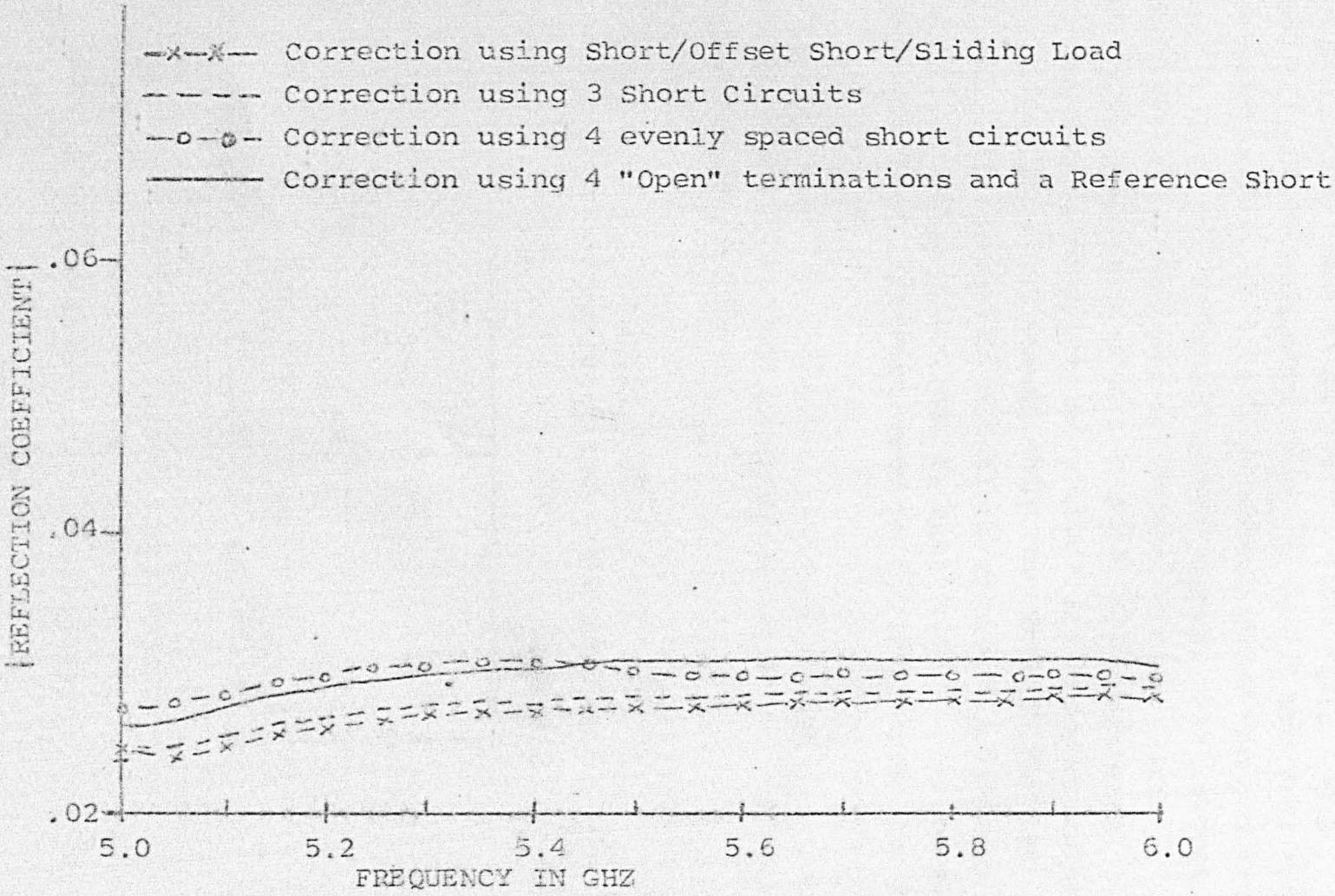

Figure 9.14 Comparision of Corrections using Four Different Methods for the measurement of the same termination(matched load).

Many more sets of reflection coefficient measurements using the other correction techniques are given in a paper (reference 9.1) published by the author. This publication is included in Appendix 12:3.

9:5 Accuracy of Measurements

Several authors such as Hand (reference 9.2), Adams (reference 9.3 and 9.4) Ridella (references 9.5 and 9.6) and Woods (references 9.7 and 9.8) have investigated the problems ofaccuracy in computer corrected measurements. Each author has placed particular emphasis on several errors. Hand (Reference 9.2) has made a detailed study of errors with particular reference to noise, gain error and the particular errors in the calibration standards on the Hewlett Packard 8542A system. This system is a transmission and reflection measuring system and is not directly applicable to the measuring system used here. However, some of his principles can be used.

Consider the signal flow graph of an idealized reflectometer system (figure 9.15):

Figure 9.15
Flow Chart of an Idealized Reflectometer

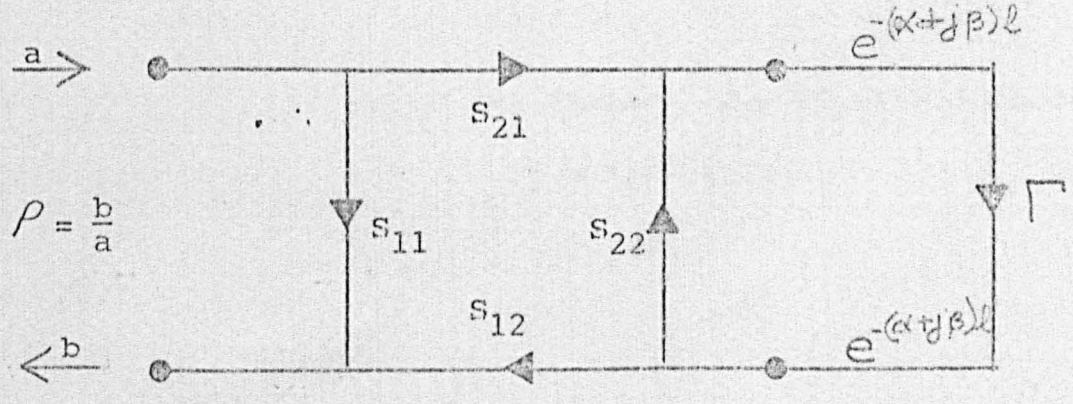

It can easily be seen that for a directly connected calibration piece ($\ell = 0$)

$$\rho_1 = S_{11} + \frac{S_{12}S_{21}\Gamma}{1 - S_{22}\Gamma} \quad \ldots\ldots \quad 9.1$$

Consider now the case when there is gain error (ε_g) noise error (ε_n) and reflection coefficient error (ε_Γ), and using the suffix 1 to denote the errors for equation 9.1, the new reflection coefficient becomes:-

$$\rho_1' = (1+\varepsilon_{g1})\left[S_{11} + \frac{S_{12}S_{21}(\Gamma+\varepsilon_{\Gamma 1})}{1-S_{22}(\Gamma+\varepsilon_{\Gamma 1})} + \varepsilon_{n1}\right]$$

..... 9.1(a)

For the idealized case of an offset calibration piece, it can be seen from the flow chart that

$$\rho_2 = S_{11} + \frac{S_{12}S_{21}\Gamma_2 e^{-2(\alpha+j\beta)l_2}}{1-S_{22}\Gamma_2 e^{-2(\alpha+j\beta)l_2}}$$

..... 9.2

and for the non-idealized case, taking gain, noise, reflection coefficient errors and the additional errors of offset lengths (ε_2) equation 9.2 becomes:-

$$\rho_2' = (1+\varepsilon_{g2})\left[S_{11} + \frac{S_{12}S_{21}(\Gamma_2+\varepsilon_{\Gamma 2})e^{-2(\alpha+j\beta)(l_2+\varepsilon_{l2})}}{1-S_{22}(\Gamma_2+\varepsilon_{\Gamma 2})e^{-2(\alpha+j\beta)(l_2+\varepsilon_{l2})}} + \varepsilon_{n2}\right]$$

..... 9.2(a)

Similarly for the third calibration the idealized case is:

$$\rho_3 = S_{11} + \frac{S_{12}S_{21}\Gamma_3 e^{-2(\alpha+j\beta)l_3}}{1-S_{22}\Gamma_3 e^{-2(\alpha+j\beta)l_3}}$$

..... 9.3

and for the non-idealized case it is:

$$\rho_3' = (1+\varepsilon_{g3})\left[S_{11} + \frac{S_{12}S_{21}(\Gamma_3+\varepsilon_{\Gamma 3})e^{-2(\alpha+j\beta)(l_3+\varepsilon_{l3})}}{1-S_{22}(\Gamma_3+\varepsilon_{\Gamma 3})e^{-2(\alpha+j\beta)(l_3+\varepsilon_{l3})}} + \varepsilon_{n3}\right]$$

..... 9.3(a)

In the measurement of the device under test, the idealized case is:

$$\rho_m = S_{11} + \frac{S_{12}S_{21}\Gamma_L}{1 - S_{22}\Gamma_L} \qquad \text{which results in}$$

$$\Gamma_L = \frac{\rho_m - S_{11}}{\rho_m S_{22} + S_{12}S_{21} - S_{11}S_{22}} \qquad \ldots\ldots \quad 9.4$$

and for the non-idealized case

$$\rho_m' = (1+\varepsilon_{gl})\left[S_{11} + \frac{S_{12}S_{21}\Gamma_L}{1 - S_{22}\Gamma_L} + \varepsilon_{nl}\right] \qquad \text{which results in}$$

$$\Gamma_L' = \frac{\frac{\rho_m'}{(1+\varepsilon_{al})} - S_{11} - \varepsilon_{nl}}{\left(\frac{S_{22}\rho_m'}{1+\varepsilon_{gl}}\right) + S_{12}S_{21} - S_{11}S_{22} - S_{22}\varepsilon_{nl}} \qquad \ldots\ldots \quad 9.4(a)$$

It is clear that the ideal error scattering parameters S_{11}, $S_{12}S_{21}$ and S_{22} will be derived from equations 9.1, 9.2 and 9.3. (Section 5:4). The non-idealized error scattering paramaters S_{11}', $S_{12}S_{21}'$ and S_{22}' are calculated from equations 9.1(a), 9.2(a) and 9.3(a). The computer is not aware of the idealized parameters. It can only substitute the non-idealized values, S_{11}', $S_{12}S_{21}'$, S_{22}' and ρ', into equation 9.4 to solve for the reflection coefficient. This will no doubt result in further error. If Γ_L'' is defined as the calculated erroneous reflection coefficient then equation 9.4(a) may be written as

$$\Gamma_L'' = \frac{\rho_m' - S_{11}'}{\rho_m' S_{22}' + S_{12}S_{21}' - S_{11}'S_{22}'} \qquad \ldots\ldots \quad 9.4(b)$$

which is really the calculated result when gain, noise, calibration termination error and offset errors are considered.

The problem is how to distinguish the calculated result Γ_L'' (calculated by equation 9.4(b) from the idealized one, Γ_L. A direct solution is not practical because accurate knowledge of the individual errors are not known. Hand (reference 9.2) who has full access to the manufacturer's data has pointed out that any attempt at a complete explicit solution is pointless since while the maximum magnitudes of the various terms may be known, their phases are in general quite

unpredictable. Hand also tried combining the random-phase errors with the root of the sum of the squares (RMS) values of amplitudes but finally decided on a statistical method of analysis.

His statistical method involved taking 'n' sets of calibration measurements (Hand does not specifically state what 'n' is but his released data seems to be based on 2 to 12 measurements). From these calibrations, he calculated the error parameters. He then assigned magnitudes, (based on production line limits) to the error parameters. The phase error limit was set between 0 and 2π radians and phase was selected by a computer driven random number generator. Selected values of the device to be measured were then inserted into his correction programme. The results obtained were then compared against his original input values and the difference noted. Hand described his device to be measured using four S parameters, i.e., S_{11}, S_{12}, S_{21}, S_{22}.

In his calculations S_{11} and S_{22} were made equal in phase and magnitude so that in effect there were 200 calculated values of the same quantity compared.

From these 200 values, 8 of the worst values were discarded, which meant that the remaining values had a probability of 192/200 or a 96% confidence level of being within a certain region whose outer limit was determined by the 9th worst value.

Hand claims that this procedure can be used to establish the limiting curves for the system or for that matter any degree of confidence level.

Adams' paper (reference 9.3) is extremely useful in that it does provide detailed error information on individual items such as contact resistance, eccentricity of coaxial line, connector mismatch error, etc., Adams also lists some errors on phase-locked systems which do not seem to be available elsewhere.

For reflection type measurements, Adams claims the calculated system uncertainty to be:-

Without a Phase Lock Source:

Magnitude of Uncertainty $= \pm[0.003 + 0.015\rho + 0.01\rho^2]$

Angle of Uncertainty $= \pm\left[0.5^\circ + \frac{\tan^{-1}0.003}{\rho} + 4\tan^{-1}(0.015\rho)\right]$

With a Phase Lock Source:

Magnitude of Uncertainty $= \pm[0.0015 + 0.005\rho + 0.003\rho^2]$

Angle of Uncertainty $= \pm\left[0.25^\circ + \frac{\tan^{-1}0.0015}{\rho} + 4\tan^{-1}(0.005\rho)\right]$

where $\rho = |\Gamma_L|$ and $|S_{11}| \ll \rho$ in the equations relating to angle error.

It is not known to which system the above figures apply. Adams does not give the information and neither does he indicate clearly as to how these figures were deduced or obtained.

Ridella (references 9.5 and 9.6) in addition to having given some equations (derivations not shown) for the calibration repeatibility, the measurement repeatibility etc., has reported the results obtained when various devices were measured on four different network analysers. However, Ridella reports that the error expressions which he has arrived at differ considerably from those of Adams (reference 9.3). He also points out that the error curves issued by Hewlett Packard have been modified very often over the years. This was also noted by the author when investigating hardware data in chapter 4 (section 4:3).

Woods (references 9.7 and 9.8) notes that the calibration procedure described by Hand(reference 9.2) overlooks the small impedance changes that occur when the reflection/transmission switches are changed over and Woods has suggested the use of three receiving channels instead of the present two to overcome this. Fortunately this problem does not exist in the measurement system used by the author because only reflection measurement is considered here.

Nevertheless, from the above paragraphs, it is clear that:

(a) Different opinions exist as to how the accuracy of an automatic network analyser should be specified.

(b) Detailed information on the errors of individual items are virtually unobtainable.

9:6 The Practical Aspects of Correction Accuracy

The prime purpose is to be able to determine the true reflection coefficient of a device and to be able to predict the accuracy of the measurement and its confidence level. Individual errors existing within the instruments are accepted and efforts to correct them will not be made for the re-design of the instruments is not intended here. However, it is vitally important that the bilinear transformation complex constants, A, B, C and D (representing instruement system errors) remain invariant during all the measurements, this has been discussed extensively in section 8:2.1.

In the case of correction systems using short and/or open circuits, many of the sources of errors mentioned in section 8:2 such as (b) to (h) are minimized because:

(a) The reflected or test signal is large ($|\Gamma| \simeq 1$) during calibration and tends to mask the effects of noise, leakage, non-infinite directivity etc.

(b) The magnitude of the reflected signals remain at similar levels throughout the calibration procedure and the working dynamic range of the amplifiers, detectors etc is reduced. This reduction is even more evident when the device to be measured also has a large reflection coefficient. The minimisation of non-linearity and limiting problems have also been discussed in detail in section 8:3.

9:6.1 Availability of Measurement Standards

Confirmation of measurement accuracy can be more easily ascertained if some accurately defined calibration standards, traceable to National Standards are available for comparative measurements. Ridella (references 9.5 and 9.6) was particularly fortunate in this respect for he had access to the use of four different network analysers in different countries and one of these analysers (Hewlett Packard in Geneva) was traceable to a National Standards Laboratory. For the work at Warwick University, such financial expenditure was impractical and considerable effort had to be made into acquiring some accurately defined standards. To begin with the use of existing "standards" within the laboratories of the University of Warwick were impractical for although some of the matched loads and offset short circuits had been calibrated at one time, there was no assurance that the calibration values were still valid.

Ideas introduced by Woods (reference 9.9) for the construction of immittance standards were also investigated but after examination of his equipment and seeking his advice, it was decided that the financial costs would be prohibitive.

The construction of test pieces whose electrical properties can be well defined has been suggested by Warner (reference 9.10) as a means of checking the correct operation of a network analyser system. This idea was seriously considered and led to the adoption of a modified Hewlett Packard APC7 Coaxial Short Circuit (Type 11565A) as the main measurement standard.

The main constructional features of this short circuit have been described in Chapter VII and detailed in figure 7.2.

From an inspection of figure 7.2, it is clear that the electrical contact required for a good short circuit is dependent on the contact area and conductivity of Surface A. This surface was examined more closely after dismantling the entire short circuit assembly. After Surface A had been cleaned and polished it was checked for surface roughness on the Tallysurf machine. The surface irregularities were less than 0.002mm. This surface was then re-cleaned again. Visual inspection of the surface revealed sufficient gold plating on the short circuit surface. Had this not been so, then re-plating would have been carried out.

The advantages of using such a device as the main calibration standard are:-

(a) The financial cost is minimal.

(b) The reflection coefficient can be accurately defined without expensive recourse to calibration laboratories.

(c) The APC-7 on the short circuit ensures minimal interface problems with its mating connector on the reflectometer.

9:7 General Procedure Used for Verifying System Accuracy

The general procedure adopted for assessing the accuracy of measurement was that of repeating many sets of measurements. For example, in corrected measurements involving the Three Short Circuit Correction Method of Section 5:4, one hundred sets of measurements of the same test piece was carried out. Each set of measurements involved:

(a) Repeating the same calibration procedure at the same frequency of interest using the same calibration standards.

(b) Measuring the same test piece after calibrating.

(c) Calculating the correct reflection coefficients.

The formulae of appendix 11:10 were used to calculate the mean value and to predict from tables the expected deviations from the mean at the required confidence levels. The results obtained from statistical tables were then compared against the known reflection coefficient of the test pieces to show the error of measurement.

9:7.1 Accuracy of Measurements Using the 3-Short Circuit Correction Method of Section 5:4.2 and the Computer Programme Described in Section 6:5.

For this assessment, one-hundred sets of measurements (calibration and test piece evaluation) were carried out. The test piece used was the modified Hewlett Packard Short Circuit described in section 9:6.1. The network analyser and its peripheral instruments (excluding the computer) were switched on for two hours prior to the commencement of measurements. The 1st and 2nd offset short circuits used in the calibrations had offset lengths of 3mm and 4.6mm respectively. The calibration and test pieces were spray cleaned after every ten sets of readings.

The measurements were carried out at 4GHz without the use of the phase lock system. Measurements were carried out continuously and required about 8 hours of computer time. To avoid prejudicing the results, shown in figure 9.16, no measurement was discarded. This has resulted in some particularly bad sets of measurements e.g., set 32, where the corrected reflection coefficient was calculated to be $0.975 \angle 183.0^{\circ}$. Analysis carried out later after examining the computer print-out revealed the third calibration reading to be at fault.

The results in figure 9.16 were processed by making the assumption that the magnitude and phase angles measured for large reflection coefficient are independent events. This has already been justified by the arguements of section 8.1. Next the magnitudes and phase angles (figures 9.17 and 9.18) were plotted and it was observed that the distribution was close to the normal error curve. By using equations 11.10.1, 11.10.3 and 11.10.5, the mean and the best estimate of the

Figure 9.16

Table of 100 Corrected Reflection Coefficient Measurements Taken at 4 GHz

No	Corrected Reflection Coefficient		No	Corrected Reflection Coefficient		No	Corrected Reflection Coefficient		No	Corrected Reflection Coefficient	
	Magni-tude	Phase (Deg)		Magn-tude	Phase (Deg)		Magni-tude	Phase (Deg)		Magni-tude	Phase (Deg)
1	.998	180.0	26	.995	180.1	51	1.003	179.9	76	1.001	179.3
2	1.000	179.8	27	1.002	180.0	52	.998	179.8	77	1.002	180.0
3	1.003	179.8	28	.996	179.4	53	1.001	180.0	78	1.000	179.9
4	.993	181.5	29	.982	182.5	54	1.001	180.4	79	1.004	180.2
5	1.004	180.5	30	.974	181.7	55	.998	179.0	80	.998	179.2
6	.994	180.3	31	1.002	179.9	56	.996	181.1	81	.998	180.1
7	.999	180.1	32	.975	183.0	57	1.009	180.4	82	1.003	180.3
8	1.009	178.8	33	.995	180.3	58	.998	180.5	83	.994	180.7
9	.993	180.8	34	1.001	180.3	59	.998	180.2	84	1.005	179.7
10	1.008	178.9	35	.995	180.7	60	.999	179.7	85	1.003	179.6
11	.997	179.8	36	1.000	180.8	61	1.009	180.7	86	1.009	180.1
12	.997	179.9	37	1.004	179.8	62	.979	181.6	87	.991	181.5
13	1.001	180.0	38	.995	180.7	63	.991	180.7	88	1.008	181.5
14	.996	180.4	39	.997	181.0	64	.999	179,8	89	1.000	180.2
15	.996	180.1	40	.997	180.8	65	.996	179.8	90	.998	180.1
16	.996	180.7	41	.996	180.9	66	1.012	179.2	91	1.007	179.9
17	.999	179.8	42	.998	180.4	67	.995	180.9	92	1.004	180.3
18	1.004	180.1	43	.997	180.2	68	.999	179.1	93	.992	181.2
19	1.007	179.7	44	1.005	180.1	69	1.000	180.2	94	.999	180.1
20	.994	180.7	45	1.004	180.1	70	1.006	180.8	95	.997	180.5
21	.991	179.1	46	.996	181.0	71	.999	179.8	96	.997	180.5
22	1.004	180.4	47	1.005	179.6	72	.992	179.5	97	.999	180.4
23	1.008	181.0	48	1.005	180.0	73	1.003	180.4	98	1.005	180.4
24	.999	180.4	49	.984	183.8	74	.997	179.9	99	.994	180.7
25	1.000	180.0	50	1.005	180.4	75	.998	180.1	100	1.005	179.0

FIGURE 9.17 RELATIVE FREQUENCY OCCURENCE OF THE MAGNITUDE OF THE REFLECTION COEFFICIENT

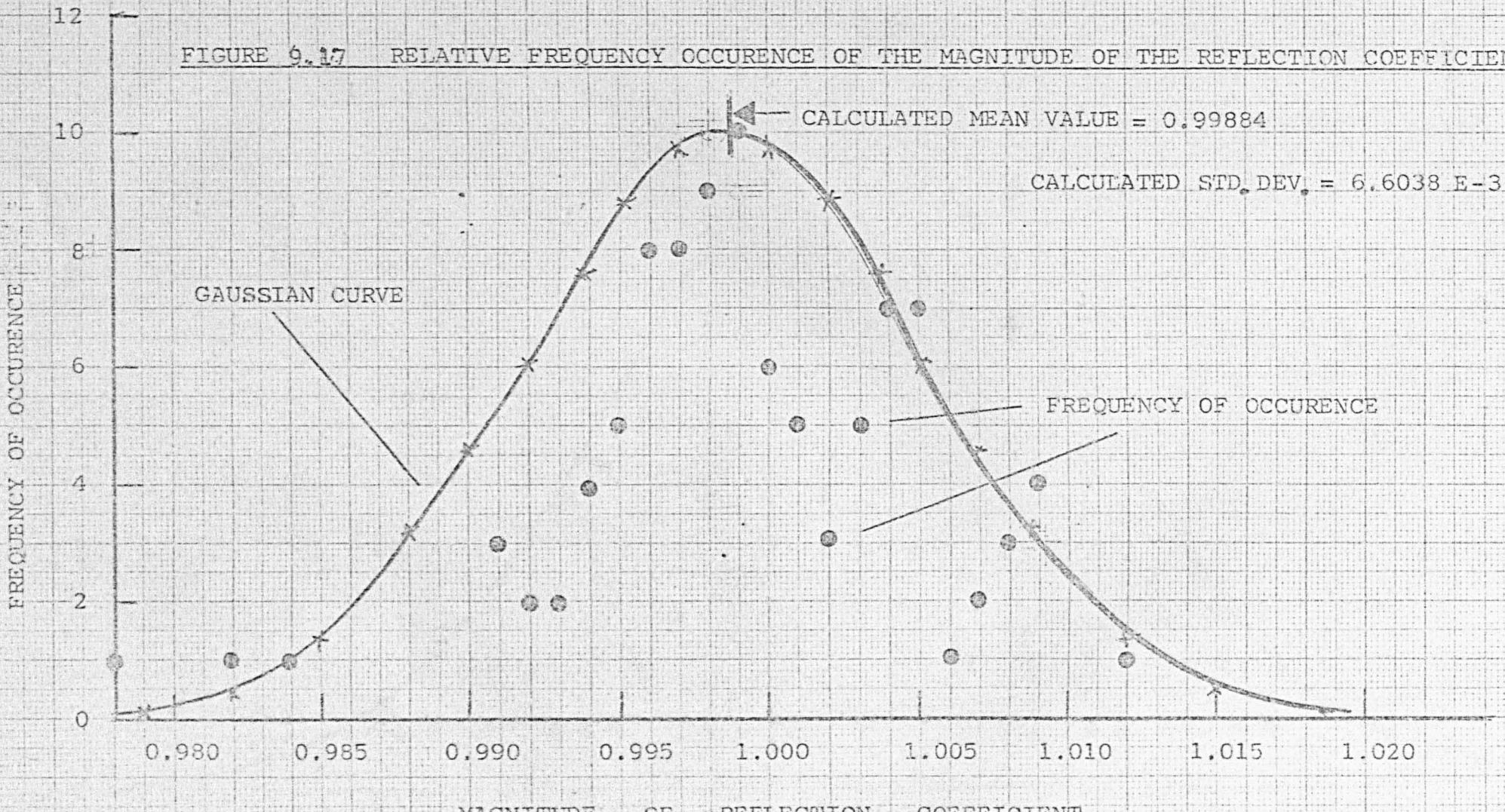

FIGURE 9.18 RELATIVE FREQUENCY OCCURENCE OF THE PHASE OF THE REFLECTION COEFFICIENT

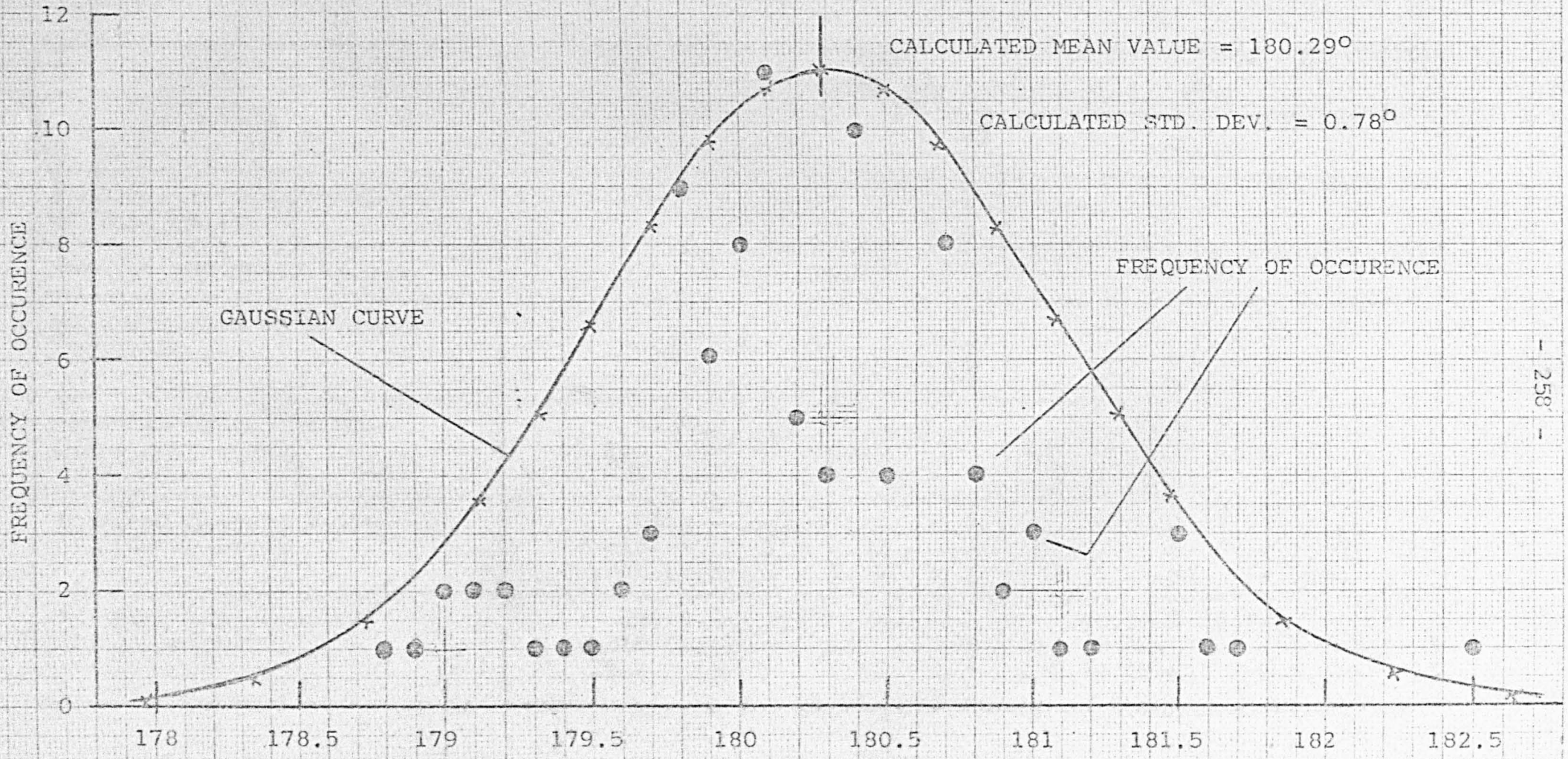

Figure 9.19

Reflection Coefficient Results with Confidence Levels for Measurements on a Short Circuit (based on 100 Measurements Using the Three Short-Circuit Correction Method)

Item	Reflection Coefficient at 4 GHz	
	Magnitude	Phase
True Reflection Coefficient of Test Device	1.000	180°
Mean of 100 Measurements	0.99884 $\simeq$ 0.999	180.29°
Best Estimate of Standard Deviation	6.6038 E-3	0.780°
Expected Range* for 90% Confidence Level	.9988 $\pm$ .0109 i.e. 1.010 (Max) or + 1.0% 0.988 (Min) - 1.2%	180.29 $\pm$ 1.287 i.e. 181.57 (Max) or + .87% 179.00 (Min) - .55%
Expected Range* for 95% Confidence Level	.9988 $\pm$ .0129 i.e. 1.012 (Max) or + 1.2% .986 (Min) - 1.4%	180.29 $\pm$ 1.529 i.e. 181.81 (Max) or + 1.00% 178.76 (Min) - .69%
Expected Range* for 99% Confidence Level	.9988 $\pm$ .0170 i.e. 1.016 (Max) or + 1.6% .982 (Min) - 1.8%	180.29 $\pm$ 2.013 182.30 (Max) or + 1.28% 178.28 (Min) - 0.95%

*Calculated by means of statistical table (Table 1 of Reference 3 in Appendix 11:3)
All percentage ranges are relative to 1 $\angle 180^{\circ}$

standard deviation was calculated. These values were then used in conjunction with Table 1 of Reference 3 of Appendix 11:10 to produce the table shown in figure 9.19. From this table it is seen that measurement accuracy to within $\pm$ 1.4% with a 95% confidence level can be obtained. For a 99% level, accuracy to $\pm$ 1.8% is attainable.

9:7.1.2 Measured Accuracies of the Means

The measured accuracies of the means of the magnitude and phase are of course better than these values. Using equations 11.10.9 and 11.10.10 of Appendix 11:1, i.e.

$$X = X_m \pm S_m \quad \text{where} \quad S_m = \frac{s_m}{\sqrt{n}}$$

the following table (figure 9.19(a)) may be constructed.

Figure 9.19a

Accuracy of the Mean Measurements Obtained from Figure 9.19

Confidence Level	Measured Means (100 Measurements)	
	Magnitude*	Phase* (degrees)
90%	.99993 (Max) or -.01 % .99775 (Min) -.22 %	180.419 (Max) or +.233% 180.161 (Min) +.090%
95%	1.0001 (Max) or +.013% .99755 (Min) -.25 %	180.443 (Max) or +.246% 180.137 (Min) +.076%
99%	1.0005 (Max) or +.05 % .99714 (Min) -.29 %	180.491 (Max) or +.273% 180.089 (Min) +.049%

*Referred to 1 $\angle 180^\circ$

From figure 9.19a, it is seen that the means of the magnitude and phase angles of the test piece (reference short circuit) at 4GHz have been measured with a confidence level of 99% to within 0.3% of the true value.

9:7.2 Accuracy of Measurements Using the 4 Short Circuit Correction Method of Section 5:5 and the Computer Programme Described in Section 6:5

The procedure used for determining the accuracy of the 4 Short Circuit Correction Method was similar to that carried out for the Three Short Circuit System (Section 9:7.1) except that 20 measurements per frequency were carried out. The results obtained at 4 GHz are shown in figures 9.20 and 9.21 respectively. For this number of measurements, the application of statistical theory is valid only when the measurement is a stationary statistical process i.e., the repeated results are consistent. The test used to determine this is similar to that described by Warner (reference 9.10). For this test, the 20 corrected measurements of figure 9.20 were divided into two groups of 10 each. The mean values, $\overline{x}_1$, and $\overline{x}_2$, and the variances $\sigma_1'^2$ and $\sigma_2'^2$ of the magnitudes of each group was calculated. The variances were then used in the Snedcor's F Test (Variance Ratio Test) which is defined as:

$$F = \frac{\text{Greater Estimate of the Variance of one Measurement Group}}{\text{Lesser Estimate of the Variance of Other Measurement Group}}$$

From table 6 of reference 11:10.3, it was noted that for $n = 10$, and for the variance to be considered steady then $F \leq 3.18$ (5% level of variance ratio).

The means, $\overline{x}_1$ and $\overline{x}_2$ were also tested using the Student 't' test, i.e,

$$t = \frac{\text{Error in Mean}}{\text{Standard Error of Mean}} = \frac{\sqrt{10}\,\left|\overline{x}_1 - \overline{x}_2\right|}{\sqrt{\sigma_1'^2 + \sigma_2'^2}}$$

For a 5% probability curve $t \leq 2.1$. This information was obtained from table 4 of reference 3 of Appendix 11:10.

Figure 9.20

Corrected Reflected Coefficients Obtained at 4 GHz Using the Four Short Circuit Correction Method of Section 5:5

No	Corrected Reflection Coefficient at 4 GHz		No	Corrected Reflection Coefficient at 4 GHz	
	Magnitude	Phase (Deg)		Magnitude	Phase (Deg)
1	.990	180.7	11	1.006	179.4
2	.990	181.0	12	.993	181.5
3	.997	180.4	13	1.007	179.5
4	.999	179.9	14	.991	180.8
5	.994	180.6	15	1.007	178.8
6	.995	181.0	16	.999	179.3
7	.999	180.9	17	1.000	179.9
8	1.000	179.9	18	.997	180.0
9	1.006	178.9	19	1.001	179.9
10	.999	180.3	20	.995	180.8

Figure 9.21

Correction Reflection Coefficients Obtained at 6 GHz Using the Four Short Circuit Correction Method of Section 5:5

No.	Corrected Reflection Coefficient at 6 GHz		No.	Corrected Reflection Coefficient at 6 GHz	
	Magnitude	Phase (Deg)		Magnitude	Phase (Deg)
1	1.009	180.0	11	.993	178.5
2	1.006	179.8	12	1.000	180.1
3	1.001	180.2	13	1.001	180.1
4	.992	180.0	14	1.000	180.1
5	1.003	181.2	15	1.002	179.8
6	1.001	180.2	16	.999	180.0
7	.999	180.1	17	.999	180.0
8	.999	179.8	18	1.000	180.0
9	.999	179.8	19	1.000	180.0
10	1.007	181.0	20	.987	179.1

The same procedure was adopted for processing the measurements on phase.

The following table was produced:

Item (4 Short Circuit Method used at 4GHz)	Magnitude		Phase	
	Calculated	Allowed	Calculated	Allowed
Ratio Test (F)	1.40	3.18	1.46	3.18
Mean Test (t)	1.13	2.1	0.99	2.1

From these results, it is seen that the measurement data is of a stationary statistical nature. Hence the use of twenty measurements is justified.

The analyses for these measurements are given in figures 9.22 and 9.23. It should be noted that the correction for small samples (20 measurements) have been made to the statistical data.

For the 4 GHz set of measurements, it is seen that measurement accuracies of about $\pm$ 1% with a confidence level of 95% can be achieved with one measurement.

Similar results have also been obtained for the set of measurements carried out at 6 GHz.

Figure 9.22

Analysis of Results Obtained in Figure 9.20

(Four Short Circuit Correction Method)

Item	Reflection Coefficient at 4 GHz	
	Magnitude	Phase (degrees)
True Reflection Coefficient of Test Device	1.000	180^{o}
Mean of 20 Measurements	0.99825	180.2
Best Estimate of Standard Deviation	0.0053693	0.72475
Expected Range*for 90% Confidence Level	.99825 $\pm$ 9.23519 E-3 i.e., 1.007 (Max) or + 0.7% 0.989 (Min) - 1.1%	180.2 $\pm$ 1.24657 i.e., 181.45 (Max) or + 0.80% 178.95 (Min) - 0.58%
Expected Range* for 95% Confidence Level	.99825 $\pm$ 1.12218 E-2 1.009 (Max) or + 0.9% 0.987 (Min) - 1.1%	180.2 $\pm$ 1.51472 i.e., 181.71 (Max) or + 0.95% 178.68 (Min) - 0.73%
Expected Range*for 99% Confidence Level	.99825 $\pm$ 1.53025 E-2 1.013 (Max) or + 1.3% 0.982 (Min) - 1.8%	180.2 $\pm$ 2.06553 i.e., 182.26 (Max) or + 1.25% 178.13 (Min) - 1.04%

* Calculated by means of statistical tables (Table 4 or Reference 3 in Appendix 11:3). All percentage figures are relative to 1 $\angle 180^{o}$.

Figure 9.23

Analysis of the Results of Figure 9.21

(Four Short Circuit Correction Method)

Item	Reflection Coefficient at 6 GHz	
	Magnitude	Phase (Degrees)
True Reflection Coefficient of Test Device	1.000	180.00°
Mean of 20 Measurements	0.99985	179.985
Best Estimate of Standard Deviation	0.0049659	.0550860
Expected Range* for 90% Confidence Levels	.099985 $\pm$ 8.54134 E-3 i.e. 1.008 (Max) or + 0.8% 0.991 (Min) - .9%	179.985 $\pm$ .94747. i.e. 180.93 (Max) or + .51% 179.04 (Min) - .53%
Expected Range* for 95% Confidence Levels	0.99985 $\pm$ 1.03787 E-2 i.e. 1.010 (Max) or + 1% 0.989 (Min) -1.1%	179.985 $\pm$ 1.51297 i.e. 181.14 (Max) or + .63% 178.83 (Min) - .55%
Expected Range* for 99% Confidence Levels	0.99985 $\pm$ 1.41528 E-2 1.014 (Max) or + 1.4% 0.985 (Min) - 1.5%	179.985 $\pm$ 1.56995 i.e. 181.55 (Max) or + .86% 178.42 (Min) - .87%

* Calculated by means of statistical tables (Table 4 of Reference 3 in Appendix 11:3)
All percentage figures are relative to 1 /180°

If the procedure outlined in Section 9:7.1.2 is adopted the following tables (figures 9.22a and 9.23a) result:

Figure 9.22a

Accuracy of the Mean Measurement obtained from Figure 9.22

Confidence Level	Measured Means (20 Measurements)	
	Magnitude*	Phase*
90%	1.0003 (Max) or + .03% .9962 (Min) - .38%	180.478 (Max) or + .26% 179.921 (Min) - .04%
95%	1.0007 (Max) or + .07% .9957 (Min) - .43%	180.538 (Max) or + .29% 179.861 (Min) - .08%
99%	1.0016 (Max) or + .16 .9948 (Min) - .52	180.661 (Max) or + .37% 179.738 (,in) - 0.15%

* Referenced to 1 $\angle 180^{\circ}$

From Figure 9.22a, it is seen that the means of the magnitude and phase angle of the test piece (reference short circuit) at 4 GHz have been obtained with a confidence level of 99% to within 0.5% and 0.2% respectively of the true value.

Figure 9.23a

Accuracy of the Mean Measurements obtained from Figure 9.23

Confidence Level	Measured Means (20 Measurements)	
	Magnitude*	Phase*
90%	1.0017 (Max) or + .17% 0.9979 (Min) - .2%	180.20 (Max) or + .11% 179.77 (Min) - .13%
95%	1.002 (Max) or + .2% 0.997 (Min - .3%	180.24 (Max) or + .13% 179.73 (Min) - .15%
99%	1.003 (Max) + .3% 0.9966 (Min) - .4%	180.34 (Max) or + .18% 179.63 (Min) - .21%

* Referenced to 1 $\angle 180^{\circ}$

From figure 9.23a, it is seen that the means of the magnitude and the phase angle of the test piece (reference short circuit) at 6GHz have been obtained with a confidence level of 99% to within 0.4% and 0.2% respectively of the true value.

9:7.3 Accuracy of Measurements Using the 4 Unknown Terminations and a Reference Short Circuit Correction Method of Section 5:5 and the Computer Programme of Section 6:5

Twenty sets of calibrations (4 open circuits and 1 reference short) were used for this method. The results of the measurements obtained are shown in figures 9.24 and 9.25. The tests mentioned in section 9:7.2 to determine the validity of the statistical data at 4 GHz yielded the following results:

Item (4 Unknown Terminations) (and a Reference Short)	Magnitude		Phase	
	Calculated	Allowed	Calculated	Allowed
Variance Ratio Test (F)	1.99	3.18	1.79	3.18
Mean Test (t)	0.14	2.1	0.19	2.1

From the above table, it was decided that a statistical treatment of the data was valid.

The analyses for these measurements are shown in figures 9.26 and 9.27. At 4 GHz, it is seen that measurement accuracies to within $\pm$ 1.3% with a confidence level of 95% are obtained for the 6 GHz set of measurements.

If the procedure outlined in section 9:7.1.2 is adopted, the following tables (figures 9.26a and 9.27a) result:

Figure 9.26a

Accuracy of the Mean Measurements Obtained from Figure 9.26

Confidence Level	Measured Means (20 Measurements)	
	Magnitude*	Phase*
90%	1.0003 (Max) or + .03% 0.996 (Min) - .4%	180.48 (Max) or + .27% 179.92 (Max - .04%
95%	1.0008 (Max) or + .08% 0.9957 (Min) - .43%	180.54 (Max) or + .30% 179.86 (Min) - .07%
99%	1.0017 (Max) or + .17% 0.9948 (Min) - .52%	180.66 (Max) or + .37% 179.74 (Min) - .14%

* Referenced to 1 $\angle 180^{\circ}$

Figure 9.24

Corrected Reflection Coefficients Obtained at 4 GHz Using the Four Unknown Terminations and a Reference Short Circuit Correction Method of Section 5.5

No	Corrected Reflection Coefficient at 4 GHz		No	Corrected Reflection Coefficient at 4 GHz	
	Magnitude	Phase (Deg)		Magnitude	Phase (Deg)
1	1.002	180.1	11	1.007	178.5
2	1.001	180.0	12	.998	179.9
3	1.003	180.0	13	1.009	178.7
4	1.002	179.9	14	1.000	180.3
5	.998	179.9	15	.999	180.1
6	.999	180.1	16	1.000	180.2
7	1.007	178.5	17	1.002	180.1
8	1.003	180.0	18	.999	180.1
9	1.000	180.2	19	1.003	180.0
10	.999	180.0	20	.999	180.3

Figure 9.25

Corrected Reflection Coefficients Obtained at 6 GHz Using the Four Unknown Terminations and a Reference Short Circuit Correction of Section 5.5

No	Corrected Reflection Coefficient at 4 GHz		No	Corrected Reflection Coefficient at 4 GHz	
	Magnitude	Phase (Deg)		Magnitude	Phase (Deg)
1	.991	180.2	11	1.014	182.0
2	1.009	180.0	12	.995	179.4
3	1.003	180.2	13	.996	178.9
4	1.007	181.1	14	1.006	180.6
5	.995	179.4	15	1.003	180.0
6	1.003	180.0	16	1.004	180.0
7	1.004	180.0	17	.991	180.2
8	1.001	180.1	18	.999	179.9
9	1.004	180.0	19	1.003	180.0
10	.999	179.9	20	1.006	180.6

Figure 9.26

Analysis of the Results Obtained in Figure 9.24

(4 Open Circuits/Reference Short Correction Method)

Item	Reflection Coefficient at 4 GHz	
	Magnitude	Phase (Degrees)
True Reflection Coefficient of Test Device	1.000	180.0
Mean of 20 Measurements	0.99825	180.2
Best Estimate of Standard Deviation	5.369259 E-3	0.72475
Expected Range* for 90% Confidence Level	0.99825 ± 9.23512 E-3 i.e. 1.007 (Max) or + 0.7% 0.989 (Min) - 1.1%	180.2 ± 1.24657 i.e. 181.45 (Max) or + .80% 178.95 (Min) - .58%
Expected Range* for 95% Confidence Level	0.99825 ± 1.12217 E-2 i.e. 1.009 (Max) or + 0.9% 0.987 (Min) - 1.3%	180.2 ± 1.51472 i.e. 181.72 (Max) or + .95% 178.68 (Min) - .73%
Expected Range* for 99% Confidence Level	0.99825 ± 1.53023 E-2 i.e. 1.014 (Max) or + 1.4% 0.982 (Min) - 1.8%	180.2 ± 2.06553 i.e. 182.27 (Max) or + 1.26% 178.13 (Min) - 1.04%

* Calculated by means of Statistical Tables (Table 4 of Reference 3 in Appendix 11:3)

All percentage figures are relative to 1 $\angle 180^{\circ}$

Figure 9.27

Analysis of the Results Obtained in Figure 9.25
(4 Open Circuits/Reference Short Correction Method)

Item	Reflection Coefficient at 6 GHz	
	Magnitude	Phase (Degrees)
True Reflection Coefficient of Test Device	1.000	180.00^{o}
Mean of 20 Measurements	0.99985	179.985
Best Estimate of Standard Deviation	4.96593 E-3	0.55086
Expected Range* for 90% Confidence Level	.99985 $\pm$ 8.54141 E-3 i.e. 1.008 (Max) or + .8% .991 (Min) - .9%	179.985 $\pm$ .94748 i.e. 180.93 (Max) or + .52% 179.04 (Min) - .53%
Expected Range* for 95% Confidence Level	.99985 $\pm$ 1.03788 E-2 i.e. 1.010 (Max) or + 1.0% .989 (Min) - 1.1%	179.985 $\pm$ 1.15129 i.e. 181.14 (Max) or + .63% 178.83 (Min) - .65%
Expected Range* for 99% Confidence Level	.99985 $\pm$ 1.41529 E-2 i.e. 1.014 (Max) or + 1.4% .985 (Min) - 1.5%	179.985 $\pm$ 1.56995 i.e. 181.55 (Max) or + .86% 178.41 (Min) - .88%

* Calculated by means of Statistical Tables (Table 4 of Reference 3 in Appendix 11:3)

All percentage figures are relative to 1 $\angle 180^{o}$

From figure 9.26a, it is seen that the means of the magnitude and the phase angle of the test piece (reference short circuit) at 4 GHz have been obtained with a confidence level of 99% to within 0.5% and 0.2% respectively of the true value for twenty measurements.

Figure 9.27a

Accuracy of the Mean Mesaurements Obtained from Figure 9.27

Confidence Level	Measured Means (20 Measurements)	
	Magnitude*	Phase*
90%	1.0018 (Max) or + .2% .9979 (Min) - .2%	180.20 (Max) or + .11% 179.77 (Min) - .13%
95%	1.0002 (Max) or + .2% .9975 (Min) - .3%	180.24 (Max) or + .13% 179.73 (Min) - .15%
99%	1.0030 (Max) or + .3% .9967 (Min) - .4%	180.34 (Max) or + .18% 179.63 (Min) - .2%

* Referenced to 1 $\angle 180^{\circ}$

From figure 9.27a, it is seen that the means of the magnitude and the phase angle of the test piece (reference short circuit) at 6 GHz have been obtained with a confidence level of 99% to within 0.4% and 0.2% respectively of the true value.

9:8 Comparison of Results for the Three New Types of Measurements

In section 9:7.1, the measurement conclusions were based on 100 sets of measurements. In sections 9:7.2 and 9:7.3 the measurement conclusions were each based on 20 sets of measurements. In order to provide a similar basis for comparison, the first 20 sets of the results (figure 9.16) of the Three Short Circuit Correction Method were analysed and its results are shown in figure 9.28. Thus three different sets of data, each obtained by a different correction method but each based on 20 sets of measurements at 4 GHz could be used for comparison.

Figure 9.28

The Analysis of 20 Measurements Carried Out at 4 GHz using the Three Short Circuit Correction Method of Section 5:4.2. The Twenty Measurements used are those of Figure 9.16 No.1 to No.20

Item	Reflection Coefficient at 4 GHz	
	Magnitude	Phase (Degrees)
True Reflection Coefficient of Test Device	1.000	180.00^{o}
Mean of 20 Measurements	0.9994	180.085
Best Estimate of Standard Deviation	4.97784 E-3	0.61411
Expected Range* for 90% Confidence Level	0.9994 $\pm$ 8.56189 E-3 i.e. 1.008 (Max) or + .8% .991 (Min) - .9%	180.085 $\pm$ 1.05626 i.e. 181.14 (Max) or + .63% 179.03 (Min) - .54%
Expected Range* for 95% Confidence Level	0.9994 $\pm$ 1.04036 E-2 i.e. 1.010 (Max) or + 1.0% 0.989 (Min) - 1.1%	180.085 $\pm$ 1.28349 i.e. 181.37 (Max) or + .76% 178.80 (Min) - .66%
Expected Range* for 99% Confidence Level	0.9994 $\pm$ 1.41868 E-2 i.e. 1.014 (Max) or + 1.4% 0.985 (Min) - 1.5%	180.085 $\pm$ 1.75021 i.e. 181.84 (Max) or + 1.02% 178.33 (Min) - .93%

*Calculated by means of Statistical Tables (Table 4 of Reference 3 in Appendix 11:3)

All percentage figures are relative to 1 $\angle 180^{o}$

To provide comparison at a different frequency e.g., 6 GHz, further data based on 20 sets of measurements using the Three Short Circuit Correction Method had to be obtained. The results of these measurements are shown in figure 9.29 and the analysed data is given in figure 9.30. Hence this information in conjunction with the data of figure 9.23 and 9.27 could be used as a basis for comparison at 6 GHz.

9:8.1 Comparison of Results at 4 GHz

The information presented in figure 9.31 has been extracted from figures 9.22, 9.26 and 9.28. The results of these measurements have been based on the corrected reflection coefficient measurements (20 sets for each method) of a specially prepared coaxial short circuit.

The conclusions are:-

1: From the best estimate of the standard deviation, it is seen that there is very little difference in the precision of measurement for three different correction systems. The reader should not be misled by the fact that the three short circuit correction method appears marginally better than the other two methods in Figure 9.31. Referral back to figure 9.19 will show that the best estimates for the standard deviations based on 100 measurements are 0.00660 and 0.780 ^{o} for the magnitude and phase angle respectively. These figures are slightly worse than the data presented for the three short circuit correction method in figure 9.31, even though they come from the same statistical data.

2: It should also be noted that the conclusions of (1) are based on the fact that the lines losses associated with the offset short circuits are zero. If this is not the case, then the three short circuit correction method should be used with caution.

Figure 9.29

Corrected Reflection Coefficients Obtained at 6 GHz Using the Three Short Circuit Correction Method of Section 5:4.2

No	Corrected Reflection Coefficient at 6 GHz		No	Corrected Reflection Coefficient at 6 GHz	
	Magnitude	Phase (Deg)		Magnitude	Phase (Deg)
1	1.000	178.8	11	.994	181.4
2	1.006	180.4	12	1.002	178.9
3	1.001	179.9	13	1.010	180.4
4	.999	180.2	14	1.000	179.9
5	.997	178.6	15	1.009	179.9
6	1.004	180.8	16	.998	179.2
7	1.000	181.0	17	1.002	180.1
8	1.001	179.2	18	.998	180.1
9	1.002	179.5	19	.997	180.4
10	.990	179.2	20	.992	179.7

Figure 9.30

Analysis of the Results of Figure 9.29

Item	Reflection Coefficient at 6 GHz	
	Magnitude	Phase (Degrees)
True Reflection Coefficient of Test Device	1.000	180.00
Mean of 20 Measurements	1.001	179.88
Best Estimate of Standard Deviation	4.99368 E-3	0.752259
Expected Range* for 90% Confidence Level	1.0001 ± 8.589E-3 i.e. 1.0087 (Max) or + 0.87% .9915 (Min) - .85%	179.88 ± 1.2939 i.e. 181.17 (Max) or + .65% 178.58 (Min) - .79%
Expected Range* for 95% Confidence Level	1.0001 ± 1.04368E-2 i.e. 1.010 (Max) or + 1.0% .990 (Min) - 1.0%	179.88 ± 1.5722 i.e. 181.45 (Max) or + .80% 178.31 (Min) - .94%
Expected Range* for 99% Confidence Level	1.0001 ± 1.4232E-2 i.e. 1.014 (Max) or + 1.4% .985 (Min) - 1.5%	179.88 ± 2.1439 i.e. 182.02 (Max) or + 1.12% 177.74 (Min) - 1.25%

* Calculated by means of Statistical Table (Table 4 of Reference 3 in Appendix 11:3)

All percentage figures are relative to 1 $\angle 180^{\circ}$

Figure 9.31

Comparison of the Three New Types of Correction Methods
Based on 20 Measurements of a Short Circuit at 4 GHz

Item	3 Short Circuit Correction Method		4 Short Circuit Correction Method		4 Unknown Terminations and a Reference Short Circuit Correction Method	
	Magnitude	Phase (Deg)	Magnitude	Phase (Deg)	Magnitude	Phase (Deg)
Best Estimate of Standard Deviation	0.0049778	0.61411	.0053693	0.72475	.0053692	0.72475
90% Confidence Level	.999 + .8% - .9%	180.1 + .63% - .54%	.998 + .7% - 1.1%	180.2 + .80% - .58%	.998 + .7% - 1.1%	180.2 + .80% - .58%
95% Confidence Level	.999 + 1% - 1.1%	180.1 + .76% - .66%	.998 + .9% - 1.1%	180.2 + .95% - .73%	.998 + .9% - 1.3%	180.2 + .95% - .73%
99% Confidence Level	.999 + 1.4% - 1.5%	180.1 + 1.02% - .93%	.998 + 1.3% - 1.8%	180.2 + 1.25% - 1.04%	.998 + 1.4% - 1.8%	180.2 + 1.26% - 1.04%

3: If an accuracy to within 1% is desired with a confidence level of 99%, it appears that the mean of three repeated measurements would suffice.

4: If an accuracy to within 0.5% is desired with a 99% confidence level, then the mean of ten repeated measurements should be taken.

9:82 Comparison of Results at 6 GHz

The information printed in figure 9.32 has been extracted from figures 9.23, 9.27 and 9.30. The results of these measurements have been based on the reflection coefficient measurements (20 sets) of a specially prepared coaxial short circuit.

The conclusions are:-

1: From the best estimate of the standard deviations, it is seen that there is still very little difference in the precision of measurement for the magnitudes of the three different correction systems. However, there is now a larger phase deviation with the three short circuit correction system. This is because the offset calibration electrical lengths in this programme are calculated from the product of the physical offset lengths and frequency. Hence, any frequency drift would appear to be more significant.

2: There is still a remarkable degree of similarity between the results for the Four Short Circuit and the Four Unknown Termination/Reference Short Circuit Correction methods.

3: An accuracy to within 1% with a confidence level of 99% appears possible by taking the mean of three measurements for all the correction methods.

4: An accuracy to within 0.5% with a confidence level of 99% appears possible by taking the mean of ten measurements for all the correction methods.

Figure 9.32

Comparison of the Three New Types of Measurements
Based on 20 Measurements of a Short Circuit at 6GHz

Item	3 Short Circuit Correction Method		4 Short Circuit Correction Method		4 Unknown Terminations and a Reference Short Circuit Correction Method	
	Magnitude	Phase (Deg)	Magnitude	Phase (Deg)	Magnitude	Phase (Deg)
Best Estimate of Standard Deviation	0.0049936	0.7522	0.0049659	0.55086	0.0049659	0.55086
90% Confidence Level	1.000 + .87% − 0.85%	179.9 + .65% − .79%	.999 + .8% − .9%	179.9 + .51% − .53%	.999 + .8% − .9%	179.8 + .52% − .53%
95% Confidence Level	1.000 + 1.0% − 1.0%	179.9 + .80% − .94%	.999 + 1.0% − 1.1%	179.9 + .63% − .65%	.999 + 1.0% − 1.1%	179.8 + .63% − .65%
99% Confidence Level	1.000 + 1.4% − 1.5%	179.9 + 1.12% − 1.25%	.999 + 1.4% − 1.5%	179.9 + .86% − .87%	.999 + 1.4% − 1.5%	179.8 + .86% − .88%

9:9 Conclusions

This lengthy but none-the-less very important chapter has verified experimentally the theoretical ideas developed in the early chapters of the thesis. The first half of this chapter has shown the various graphical plots and the print-out result sheets which may be obtained when corrected measurements are made.

The second half of this chapter has been devoted to obtaining, comparing and interpreting the statistical data amassed. Considerable time and effort had to be devoted to carrying out these all important tasks for without them, one would always be in doubt as to the degree of accuracies which can be obtained when these correction methods are used. Direct comparison with measurements carried out by other methods e.g., the Short/Off Short/Sliding Load/Method (section 5:4.3) have not been included because there is no assurance that such a method (Section 5:4.3) is perfect. However, graphical comparisons and some measurement errors have been included by the author in a published paper (reference 9.1).

The general conclusions from the measurement of the test piece indicate that accuracies to within 1% with confidence levels of 99% are possible with 3 measurements and that accuracies to 0.5% with confidence levels of 99% are possible with 10 measurements. These conclusions apply to any of the new correction systems.

* * * * * * * * * * *

References

9.1 da Silva, E.F. and McPhun, M.K. "Calibration Techniques for One Port Measurements" Microwave Journal, June 1978 pp 97-100.

9.2 Hand, B.P. "Developing Accuracy Specifications for Automatic Network Analysers" Hewlett Packard Journal, February 1970, No 21 pp 16-19.

9.3 Adams, S.F. "A New Precision Automatic Microwave Measurement System" I.E.E.E. Trans. 1968, IM-17 pp 308-313.

9.4 Adams, S.F. "Automatic Network Measurements" Proc. I.E.E.E. Vol 66, No 4 April 1978, Pp 384-391.

9.5 Ridella, S "Computerized Microwave Measurements Accuracy Analysis" Proceedings of the European Microwave Conference, Paper B34, 1973.

9.6 Ridella, S "Computerized Reflection Measurements" C.P.E.M. Digest 1973, pp 51-53.

9.7 Woods, D. "Rigorous Derivation of Computer Corrected Network Analyser Calibration Equations" Electronic Letters, 1975, 11 pp 403-405.

9.8 Woods, D. "Re-Appraisal of Computer-Corrected Network Analyser Design and Calibration" Proc. I.E.E. Vol. 124, No 3, March 1977, pp 205-211.

9.9 Woods, D. "Immittance Transformation Using Precision Air-Dielectric Coaxial Lines and Connectors" Proc. I.E.E. Vol 118, No 11 Nov 1971 pp 1667-1673.

9.10 Warner, F. "Microwave Attenuation Measurements" (I.E.E. Monograph 19) Peter Peregrinus Ltd., London 1977.

* * * * * * * * * *

CHAPTER X

CONCLUSIONS OF THE THESIS

10:0 Final Review

The information presented in this thesis is the accumulation of several years of research work directed towards producing a system for the rapid and accurate measurement of immittances over a wide frequency bandwidth. The project was commenced by carrying out a survey of the existing rapid wideband measuring techniques. (See Chapter I). This survey resulted in the selection of the reflectometer as the desired measurement system. A thorough understanding of the principle of reflectometry was then considered essential and considerable theoretical work was carried out in Chapter II. This work was mainly directed to establishing the desirable and undesirable properties of reflectometers. The principle of computer corrected reflectometry, i.e., accepting the defects of the reflectometer hardware and correcting these defects by calculation (software) was established in this chapter.

Knowledge of the peripheral equipment associated with the reflectometer is considered essential and a brief description of the equipment used was presented in Chapter III. Measurement equipment is seldom perfect and the reflectometer method of measurement is no exception, and an extensive review of these errors were carried out in Chapter IV.

The establishment of a bilinear transformation relationship between the measured reflection coefficient and that of the device being measured led to the development of the new calibration and correction procedures described extensively in Chapter V. The use of computer corrected systems required

considerable computation, and the development of the computer programmes described in Chapter VI was inevitable as manual calculations were found to be impractical. Considerable effort was devoted to investigating computational errors. The limits of accuracy associated with the use of single and double precision numbers in the correction programmes was also established. The development of the automated programmes were particularly time consuming as the length of these programmes required the use of computer overlay programming techniques to reduce the storage requirements within the computer.

Considerable effort was also put into the design of the calibration standards for the various correction methods. These standards (described in Chapter VII) have been proven to be electrically and mechanically stable. They have also been fabricated without much difficulty.

Initial tests to determine the suitability of the equipment for computer corrected measurements were carried out in Chapter VIII. The first half of Chapter IX has been devoted to the presentation of a cross section of measurements carried out using the three new correction methods. The second half of Chapter IX has been devoted to a very extensive discussion of the measurement accuracy of the new correction methods. These accuracy conclusions are summarized in Sections 10:1.1, 10:.1.2 and 10:1.3.

10:1 Achievement of Objective

The objective of this thesis has been to research for an accurate and rapid means of measuring lumped components over wide bandwidths at microwave frequencies.

This objective has been fulfilled by the invention and publication of three new computer correction network analyser methods for the rapid and accurate measurement of immittances. These methods were construed theoretically and have been

proven by experimental measurements. Automated measurement procedures for these correction systems have also been developed.

The new correction systems have been called:-

1: The Three Short Circuit Correction Method.

2: The Four Short Circuit Correction Method.

3: The Four Unknown Termination/Reference Short Circuit Correction Method.

10:1.1 The Three Short Circuit Correction Method

This method was invented because previous to this method there was no rapid and accurate means of measuring immittances in confined spaces over wide frequency bandwidths. Two manual computer programmes (Appendices 11:5 and 11:6) and one automated programme have been produced for this correction system.

The results obtained with this correction method for the measurement of a reference test piece (short circuit) are given in figure 10.1.

The results (section 9:7.1) have been based on a normal gaussian distribution of 100 measurements and have been determined for a confidence level of 99%. Statistical data based on the table above indicate that:-

(i) The mean of 3 measurements will produce an accuracy to within $\pm$ 1%.

(ii) The mean of 10 measurements will produce an accuracy to within $\pm$ 0.5%.

Frequency GHz	Measured Reflection Coefficient		Theoretical Reflection Coefficient	
	Magnitude	Phase (Degrees)	Magnitude	Phase (Degrees)
4	.999 $\pm$ 1.419E-2 or* .999 $^{+1.4\%}_{-1.5\%}$	180.09 $\pm$ 1.750 or* 180.09 $^{+1.2\%}_{-.93\%}$	1.000	180^{o}
6	1.000 $\pm$ 1.423E-2 or* 1.000 $^{+1.4\%}_{-1.5\%}$	179.88 $\pm$ 2.144 or* 179.88 $^{+1.12\%}_{-1.25\%}$	1.000	180^{o}

*Referenced to $1 \angle 180^{o}$; The improvement in accuracy is approximately 5 times that quoted by Hewlett Packard (See Section 4.7)

Figure 10.1

Measurement Results for the Reference Short Circuit Using the Three Short Circuit Correction Measurement

10:1.2 The Four Short Circuit Correction Method

This method was invented to overcome the difficulty of specifying accurate offset lengths in microstrip.

Two manual computer programmes (Appendices 11:7 and 11:8) and an automated programme have been written for this correction system. Two sets of calibration pieces (sections 7:2 and 7:3) have been constructed for this correction method.

The results obtained with this method for the measurement of a reference test piece (short circuit) are given in figure 10.2.

The results (section 9:7.2) have been based on a normal error curve corrected for a small sample distribution of 20 measurements and determined for a confidence level of 99%.

Statistical data based on the table above indicate that:

(i) The mean of 3 measurements would produce an accuracy to within $\pm$ 1%.

(ii) The mean of 10 measurements would produce an accuracy to within $\pm$ 0.5%.

10:1.3 The Four Unknown Termination/Reference Short Circuit Correction Method

This method was invented to overcome the difficulty of producing short circuits for calibrations within a microstrip environment.

One manual computer programme (Appendix 11:9) and an automated programme have been written for this correction system. One set of calibration pieces (Section 7:4) have been constructed for this correction system.

Frequency GHz	Measured Reflection Coefficient		Theoretical Reflection Coefficient	
	Magnitude	Phase (Degrees)	Magnitude	Phase (Degrees)
4	.998 $\pm$ 1.530E-2 or* .998 $^{+\ 1.3\%}_{-\ 1.8\%}$	180.2 $\pm$ 2.06 or* 180.2 $^{+1.25}_{-1.04}$	1.000	180°
6	.999 $\pm$ 1.415E-2 or* .999 $^{+\ 1.4\%}_{-\ 1.5\%}$	179.99 $\pm$ 1.57 or* 179.99 $^{+\ .86\%}_{-\ .88\%}$	1.000	180°

* Referenced to $1\ \angle 180^{\circ}$; The improvement in accuracy is approximately 5 times that quoted by Hewlett Packard. (See Section 4.7)

Figure 10.2

Measurement Results for the Reference Short Circuit Using the Four Short Circuit Correction Method

The results obtained with this method for the measurement of a reference test piece (short circuit) are given in figure 10.3.

The results (Section 9:7.3) have been based on a normal error curve corrected for a small sample distribution of 20 measurements and determined for a 99% confidence level.

Statistical data based on the above table indicate that:

(i) The mean of 3 measurements of the test piece will produce an accuracy to within $\pm$ 1%.

(ii) The mean of 10 measurements of the test piece will produce an accuracy to within $\pm$ 0.5%.

10:2 Final Conclusions

Comparison of the three new correction systems (section 9:7) have shown that the standard deviation of all these methods are similar. (However, it should be noted in this case, that the offset line propagation losses in the calibration standards in the case of the Three Short Circuit Correction Method were negligible).

For most practical cases, it is envisaged that the choice of the measurement system will be dictated more by the convenience of usage than by the accuracy requirements.

The Four Short Circuit and the Four Unknown Termination/Ref. Short Method should be used in measurement cases where the offset electrical lengths change with frequency (e.g., microstrip) and where offset line attenuation may be objectionable, or in any case where the propagation constant of the transmission medium is unknown.

Frequency GHz	Measured Reflection Coefficient		Theoretical Reflection Coefficient	
	Magnitude	Phase (Degrees)	Magnitude	Phase (Degrees)
4	.998 $\pm$ 1.530E-2 or* .998 $^{+\ 1.4\%}_{-\ 1.8\%}$	180.2 $\pm$ 2.065 or* 180.2 $^{+\ 1.26\%}_{-\ 1.04\%}$	1.000	180°
6	.998 $\pm$ 1.415 or* .998 $^{+\ 1.4\%}_{-\ 1.5\%}$	179.99 $\pm$ 2.065 or* 179.99 $^{+\ .86\%}_{-\ .88\%}$	1.000	180°

* Referenced to 1 $\angle 180^{\circ}$; The improvement in accuracy is approximately 5 times that quoted by Hewlett Packard. (See Section 4.7)

Figure 10.3

Measurement Results for the Reference Short Circuit Using the Four Unknown Terminations (Open Circuits) Reference Short Circuit Correction Method

If the frequency of measurement is not known precisely then more accurate measurements will also be achieved by using the last two named correction methods because these methods obtain their calibration offset electrical lengths by measurement. (The Three Short Circuit Correction Method depends on a knowledge of the frequency and the physical length to calculate its calibration offset lengths).

It is the author's belief that the Four Unknown Termination/Reference Short Circuit Method will prove to be the more versatile of the three new correction methods in practical measurements.

10:3 Future Work

Research work is never completed. In the case of the present equipment, considerable improvement in accuracy will be obtained when phase-locked signal generators are used in the measurement system. Reflectometers with wider bandwidths and greater directivities will also provide greater measurement versatility.

Improvements in operating economy will result with the replacement of the present computer by a microprocessor. One such system such as that developed by Crane (Reference 10.1) could be used to control the measurement equipment. Another success at eliminating the large computer have been carried out by Hewlett Packard (Reference 10.2). It is envisaged that future versions of the network analyser will incorporate microprocessors within the instrument casing and that computer correction facilities will be commonplace in such measurements.

New Methological Systems are constantly appearing to challenge the present ones. A typical example is the Six Port Reflectometer which has been described by Engen (References 10.3 and 10.4). This system has been claimed by Engen to be the alternative to the network analyser. Engen also claims that less complicated peripheral equipment is required and that instrument costs will be drastically reduced.

Authors such as Beatty (Reference 10.5), Adams (Reference 10.6) and Engen (Reference 10.7) publish periodic reviews of the state of microwave metrology. In the case of network analysers, the trend among these authors seem to indicate that future development work will be directed towards the simplification of measurement equipment to reduce costs, and that the subsequent deterioration in hardware performance will be compensated for by more extensive use of computational equipment such as microprocessors. If these authors are correct in their assumptions, then computer correction systems will be with us for many years.

* * * * * * * * * * *

References

10.1 Crane, F. "Private Discussion" University of Warwick, Coventry, England, 1977.

10.2 Hewlett Packard, "Semi Automatic Measurements Using the 8410B Microwave Network Analyser and the 9825A Desk-Top Computer" Application Note 221 - Palo Alto, California.

10.3 Engen, Glenn F. "The Six Port Reflectometer: An Alternative Network Analyser" I.E.E.E. Trans on Microwave Theory and Techniques Vol MTT-25, 12 Dec 1977. pp 1075-1080.

10.4 Engen, Glenn F "An Improved Circuit for Implementing the Six Port Technique of Microwave Measurements" I.E.E.E. Trans. on Microwave Theory and Techniques, Vol MTT-25, Dec. 1977. pp 1080-85.

10.5 Beatty, R.W. "Automatic Measurements of Network Parameters - A Survey" National Bureau of Standards, Boulder, Colorado, June 1st, 1976.

10.6 Adams, S. "Automatic Microwave Network Measurements" Proc. I.E.E.E. Vol 66, No 4 April, 1978. pp 384-391.

10.7 Engen, Glenn. "Advances in Microwave Science" Proc. I.E.E.E. Vol. 66, No. 4. April 1978. pp 374-383.

* * * * * * * * * *

APPENDIX 11:1

THE USEFULNESS OF THE BILINEAR TRANSFORMATION

The principle of bi-linear transformation applied to electro-magnetic fields is used extensively in this thesis. The purpose of this appendix is to justify its use and to clarify the fundamental postulates assumed in its use.

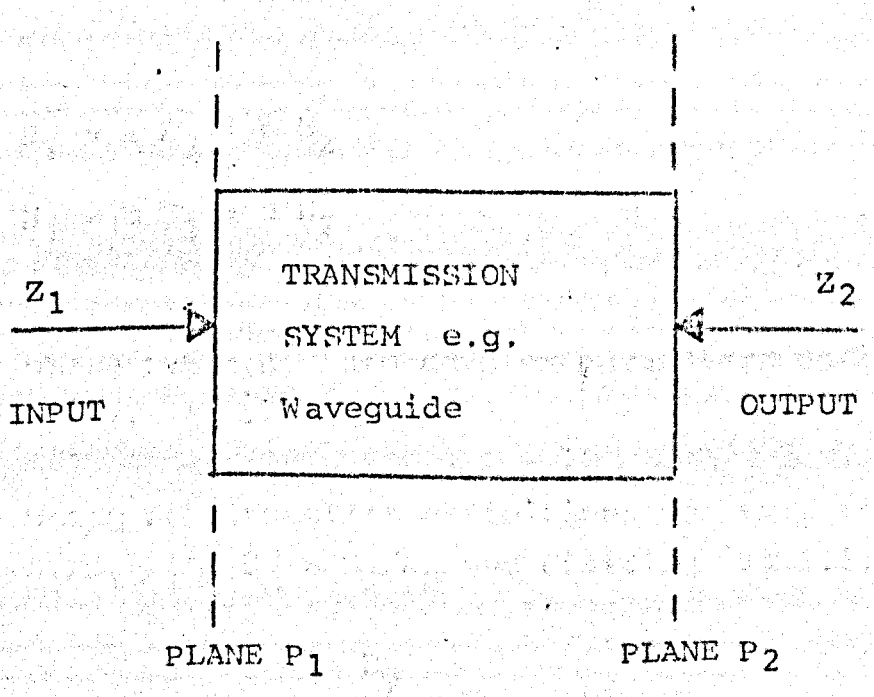

In the diagram above, the transmission system may contain any assortment of conductors, reactances, resistances, insulators etc., which need not be specified. However, these components do determine the electro-magnetic coupling between the input and output planes. Non-linear materials, i.e., those whose electro-magnetic properties depend on the strength of the electric or magnetic fields are excluded from the transmission system.

Two fundamental postulates are required

1: The field at the output is zero if the field at the input is zero (i.e., no internal source of electromagnetic energy other than that supplied from the input)

2: All field component vectors (E, H) add linearly in the region between reference planes P_1 and P_2. Hence a field (E_1, H_1) added to a field $(E_2\ H_2)$ produces a field (E_1+E_2, H_1+H_2).

Let the field components at planes P_1 and P_2 be represented by (E_1, H_1) and (E_2, H_2) respectively. Then from the usual two port theory

$$E_1 = a\,E_2 + b\,H_2 \qquad \ldots\ldots \quad (11.1.1)$$

$$H_1 = c\,E_2 + d\,H_2 \qquad \ldots\ldots \quad (11.1.2)$$

where a,b,c,d, are complex parameters defined in the normal way.

Using Schelkunoff's definitions for wave impedance, i.e., $Z_1 = E_1/H_1$ and $Z_2 = E_2/H_2$ and dividing (11.1.1) by (11.1.2)

$$\frac{E_1}{H_1} = Z_1 = \frac{a\,\frac{E_2}{H_2} + b}{c\,\frac{E_2}{H_2} + d} = \frac{a\,Z_2 + b}{c\,Z_2 + d}$$

or

$$Z_1 = \frac{a\,Z_2 + b}{c\,Z_2 + d} \qquad \ldots\ldots \quad (11.1.3)$$

Hence all transformations of impedances through transmission systems satisfying postulates 1 and 2 may be described in this manner which is called a bilinear transformation as it is a ratio of two linear equations.

Division of the numerator and denominator of the right-hand side of equation (11.1.3) by any of its constants e.g., d, will result in three new constants, a/d, b/d, c/d and unity. The left-hand side of the equation remains unchanged. It follows that with three sets of data, solution of the constants will result and the equivalent bilinear transformation between Z_1 and Z_2 can be ascertained.

Three other general properties of bilinear transformations should be noted here:-

1: It can easily be shown that if Z_1 is a bilinear transformation of Z_2 and vice-versa then,

$$Z_1 = \frac{a\,Z_2 + b}{c\,Z_2 + d} \quad \text{and} \quad Z_2 = \frac{-d\,Z_1 + b}{c\,Z_1 + a} \quad \ldots\ldots \quad (11.1.4)$$

2: If Z_1 is a bilinear transformation of Z_2 and Z_2 is a bilinear transformation of Z_3, i.e., let

$$Z_1 = \frac{a\,Z_2 + b}{c\,Z_2 + d} \quad \text{and} \quad Z_2 = \frac{AZ_3 + B}{CZ_3 + D},$$

then it follows that

$$Z_1 = \frac{a(AZ_3 + B) + b(CZ_3 + D)}{c(AZ_3 + B) + d(CZ_3 + D)}$$

$$Z_1 = \frac{(aA + bC)Z_3 + (aB + bD)}{(cA + cd)Z_3 + (cB + dD)} \quad \ldots\ldots \quad (11.1.5)$$

which means that two impedance bilinear transformations occuring in cascade can be replaced by a third bilinear transformation which satisfies the condition of the constituent bilinear transformations.

3: Any two port network described with the conventional impedance matrix of the form shown in (Fig 11.1) may be shown to be related by a bilinear transformation.

Figure 11.1

2-Port Impedance "Black Box"

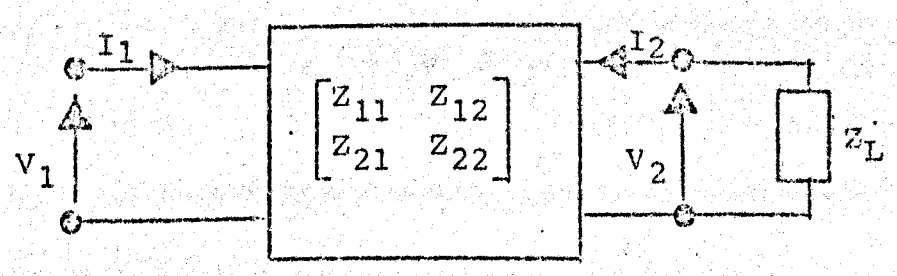

$$V_1 = Z_{11} I_1 + Z_{12} I_2 \quad \ldots\ldots \quad (11.1.6)$$

$$V_2 = Z_{21} I_1 + Z_{22} I_2 \quad \ldots\ldots \quad (11.1.7)$$

By inspection $V_2 = -I_2 Z_L$, and substituting in equation (11.1.7) results in

$$I_2 = \frac{-Z_{21} I_1}{Z_{22}+Z_L}$$

Substituting in equation (11.1.6) produces

$$V_1 = Z_{11} I_1 - \frac{Z_{12} Z_{21}}{Z_{22}+Z_L} I_1$$

and defining Z as $\frac{V_1}{I_1}$

$$Z = \frac{V_1}{I_1} = Z_{11} - \frac{Z_{12}Z_{21}}{Z_{22}+Z_L} = \frac{Z_{11}Z_L + (Z_{11}Z_{22} - Z_{12}Z_{21})}{Z_L + Z_{22}}$$

thus

$$Z = \frac{Z_{11}Z_L + (Z_{11}Z_{22} - Z_{12}Z_{21})}{Z_L + Z_{22}} = \frac{aZ_L + b}{cZ_L + d} \quad \ldots\ldots \quad (11.1.8)$$

where

$$a = Z_{11}; \quad b = (Z_{11}Z_{22} - Z_{12}Z_{21}) = \Delta Z$$

$$c = 1 \; ; \quad d = Z_{22}.$$

* * * * * * * * * * *

APPENDIX 11:2

BILINEAR TRANSFORMATIONS OF SCATTERING PARAMETERS

The purpose of this appendix is twofold:-

(a) to show the relationship between scattering parameters and bilinear transformations

(b) to note that two scattering bilinear transformations may be replaced by a single scattering bilinear transformation which satisfies the constituent bilinear transformations.

Scattering Coefficients of a 2 Port Network

a_1, a_2, and b_1, b_2 are defined as the incident and reflected waves into the two port network

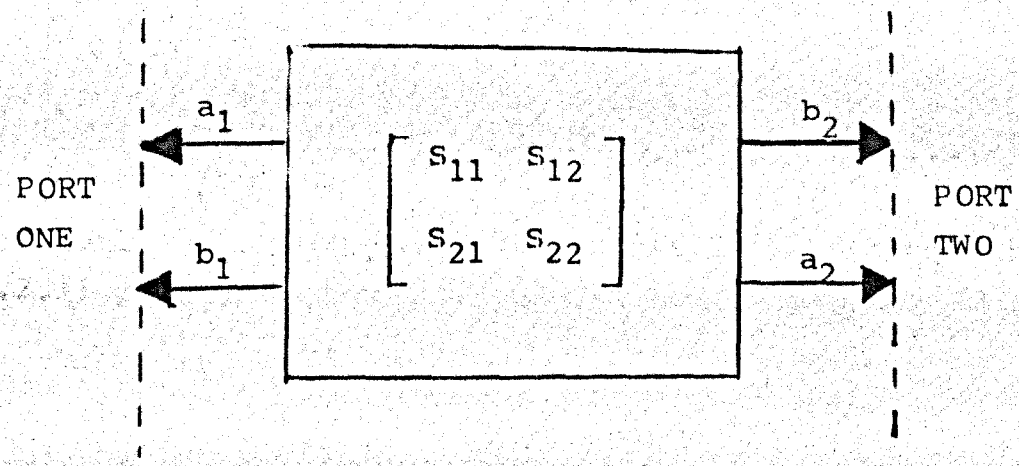

$$b_1 = a_1 S_{11} + a_2 S_{12} \quad \ldots\ldots \quad (11.2.1)$$

$$b_2 = a_1 S_{21} + a_2 S_{22} \quad \ldots\ldots \quad (11.2.2)$$

By definition, the reflection coefficient (Γ) is defined by

$$\Gamma = \frac{\text{Reflected Wave}}{\text{Incident Wave}}$$

Hence, the reflection coefficient (ρ) "looking " into the two port network is

$$\rho = \frac{b_1}{a_1} \quad \ldots\ldots \quad (11.2.3)$$

and the reflection coefficient (Γ_L) of the load terminating port 2 is

$$\Gamma_L = \frac{a_2}{b_2} \qquad \ldots\ldots \quad (11.2.4)$$

Substituting equation (11.2.4) into equation 11.2.2

$$b_2 = \frac{a_2}{\Gamma} = S_{21} a_1 + S_{22} a_2$$

$$a_2 \left(\frac{1}{\Gamma} - S_{22} \right) = S_{21} a_1$$

$$\frac{a_2}{a_1} = \frac{S_{21}}{\left(\frac{1}{\Gamma_L} - S_{22} \right)} = \frac{S_{21} \Gamma_L}{1 - S_{22} \Gamma_L} \qquad \ldots\ldots \quad (11.2.5)$$

Substituting equation (11.2.3) and (11.2.5) into equation (11.2.1) gives

$$b_1 = S_{11} a_1 + S_{12} a_2$$

$$\frac{b_1}{a_1} = \rho = S_{11} + \frac{S_{12} S_{21} \Gamma_L}{1 - S_{22} \Gamma_L} \qquad \ldots\ldots \quad (11.2.6)$$

or $$\rho = \frac{-(S_{11} S_{22} - S_{12} S_{21}) \Gamma_L + S_{11}}{-S_{22} \Gamma_L + 1}$$

or $$\rho = \frac{a \Gamma_L + b}{c \Gamma_L + d} \qquad \ldots\ldots \quad (11.2.7)$$

where

$$a = -(S_{11} S_{22} - S_{12} S_{21}) = -\Delta S \qquad \ldots\ldots \quad (11.2.7a)$$

$$b = S_{11} \qquad \ldots\ldots \quad (11.2.7b)$$

$$c = -S_{22} \qquad \ldots\ldots \quad (11.2.7c)$$

$$d = 1 \qquad \ldots\ldots \quad (11.2.7d)$$

Hence reflection coefficients between two measuring planes have also been shown to be related by a bilinear transformation.

Two Reflection Coefficient Bilinear Transformation in Cascade

Let the individual transformations be denoted by

$$\rho_1 = \frac{a\rho_2 + b}{c\rho_2 + d} \quad \text{and} \quad \rho_2 = \frac{A\rho_3 + B}{C\rho_3 + D}$$

then from equation 11.1.5

$$\rho_1 = \frac{(aA+bC)\rho_3 + (aB+bD)}{(cA+dC)\rho_3 + (cB+dD)} \qquad \ldots\ldots \quad (11.2.8)$$

which is another bilinear transformation.

Hence, it can be concluded that two reflection coefficient bilinear transformations in cascade can be replaced by a single bilinear transformation which satisfies the conditions of the constituent bilinear transformations.

A similar exercise may be used to show that three or more bilinear transformations in cascade may be reduced to that of a single bilinear transformation if and only if the constants of the constituent bilinear transformations are truly constant, i.e. they are unaffected by the act of cascading the additional networks.

* * * * * * * * * * *

APPENDIX 11:3

THE BILINEAR TRANSFORMATION OF A CIRCLE IN THE COMPLEX PLANE

The purpose of this appendix is to summarize the concepts necessary to establish the principles in the text. Much of this work has already been derived and published by Warner (reference 11.3.1), Barlow & Cullen (Reference 11.3.2) and Marton (Reference 11.3.3).

Consider a bilinear transformation of the form

$$\rho = \frac{a\Gamma + b}{c\Gamma + d} \qquad \ldots\ldots \quad (11.3.1)$$

where ρ represents transformation of points in the Γ plane and a, b, c and d are complex constants.

The transformation may be easily re-arranged in the form $\rho = \dfrac{a\Gamma + b + \frac{ad}{c} - \frac{ad}{c}}{c(\Gamma + d/c)}$

$$\rho = \frac{a}{c} + \left(\frac{bc - ad}{c^2}\right)\left(\frac{1}{\Gamma + d/c}\right) \qquad \ldots\ldots \quad (11.3.2)$$

Equation 11.3.2 shows that a bilinear transformation produces three distinct operations

1: An inversion term

2: A magnification and rotation term

3: A complexor displacement term

These will be considered in turn.

The Inversion Term

For a linear circular loci Γ , the inverse is always another circle provided only that the linear loci do not pass through the origin.

If Γ describes a circle of radius τ and centre a', then ρ describes a circle of radius σ and centre β as in figure 11.3.1

Figure 11.3.1
Inversion of a Circle

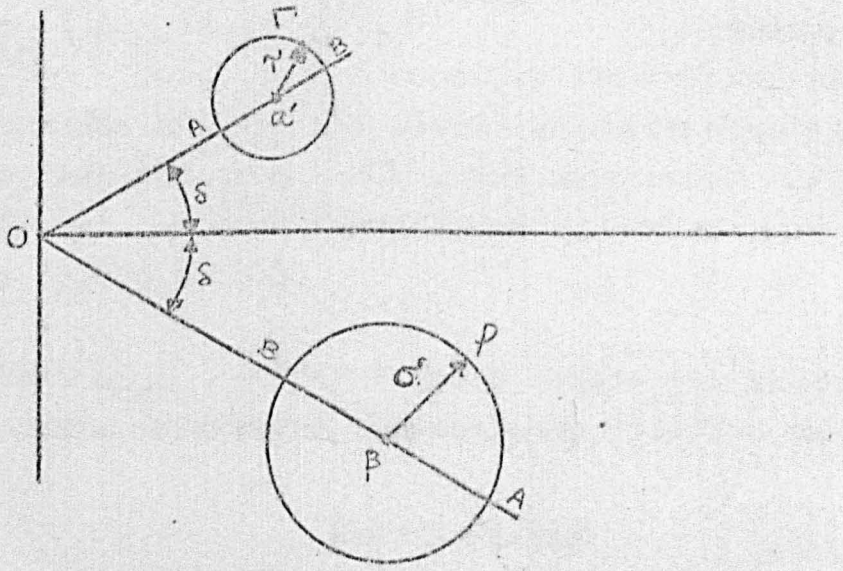

σ and β are shown by Barlow and Cullen (Ref 11.3.2) to be

$$\sigma = \left|\frac{bc-ad}{c^2}\right| \frac{\tau}{\left|a+\frac{d}{c}\right|^2 - \tau^2} \quad \ldots\ldots \quad (11.3.2)$$

and

$$\beta = \frac{a}{c} + \left\{\frac{bc-ad}{c^2}\right\}\left\{\frac{\left|a+\frac{d}{c}\right| e^{-j\delta}}{\left|a+\frac{d}{c}\right|^2 - \tau^2}\right\} \quad \ldots\ldots \quad (11.3.3)$$

Note in both cases the term $\left[\frac{bc-ad}{c^2}\right]$ is merely a magnification term.

The angular rate of change at the origin O of the produced circle ρ relative to the angular rate of change of Γ is not constant. This follows from the polar form

$$\rho\angle\theta_\rho = \frac{1}{|\Gamma| e^{j\theta_\rho} + \left|\frac{d}{c}\right| e^{j\theta_{d/c}}} \qquad \ldots\ldots \quad (11.3.4)$$

The modulus of the two rates of change only become equal when $\left|\frac{d}{c}\right| e^{j\theta_{d/c}} = 0$ and even then the direction of rotation is not the same for $\frac{1}{|\Gamma| e^{j\theta_\Gamma}} = \frac{1\, e^{-j\theta_\Gamma}}{|\Gamma|}$

The Magnification and Rotation Term

Let $\left(\frac{bc-ad}{c^2}\right) = |M|\, e^{j\theta_m}$. Multiplication by $|M| e^{j\theta_m}$ consists of a magnification of the amount which does not distort the circle but does magnify the distance from the origin O, and a rotation about the origin O of the magnified figure by the angle θ_m as shown in figure 11.3.2.

Note that the points A and B remain the maximum and minimam radial distances respectively from the origin O.

Figure 11.3.2
Magnification and Rotation by $|M| e^{j\theta_m}$

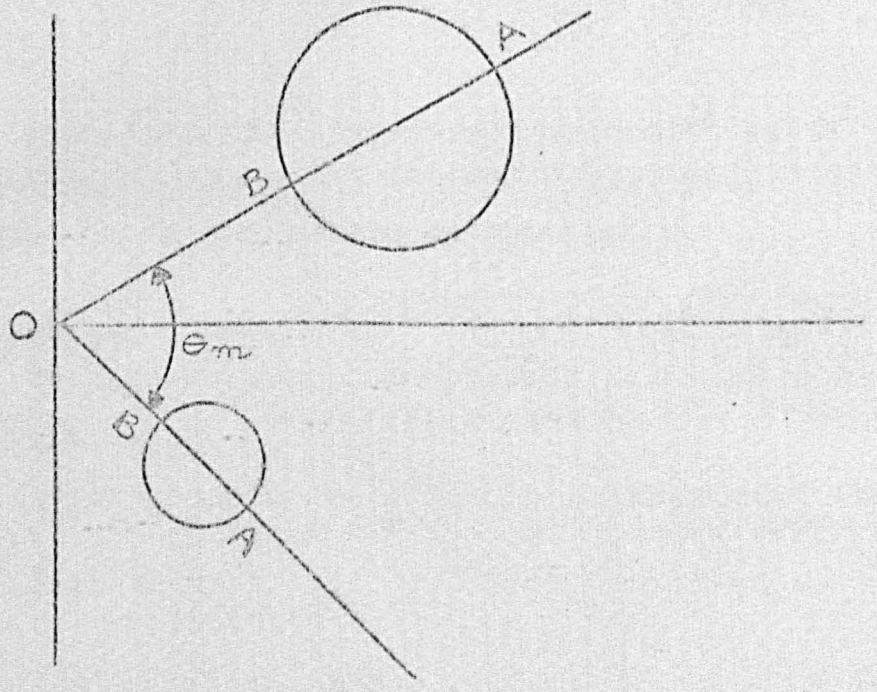

Displacement

Displacement by the complex $\left|\frac{a}{c}\right|$ amounts to a simple translation of the circle without rotation by a distance $\left|\frac{a}{c}\right|$ in the direction $\Theta\frac{a}{c}$ relative to the real axis as shown in figure 11.3.3

Figure 11.3.3
Displacement by $\left|\frac{a}{c}\right| e^{j\Theta\frac{a}{c}}$

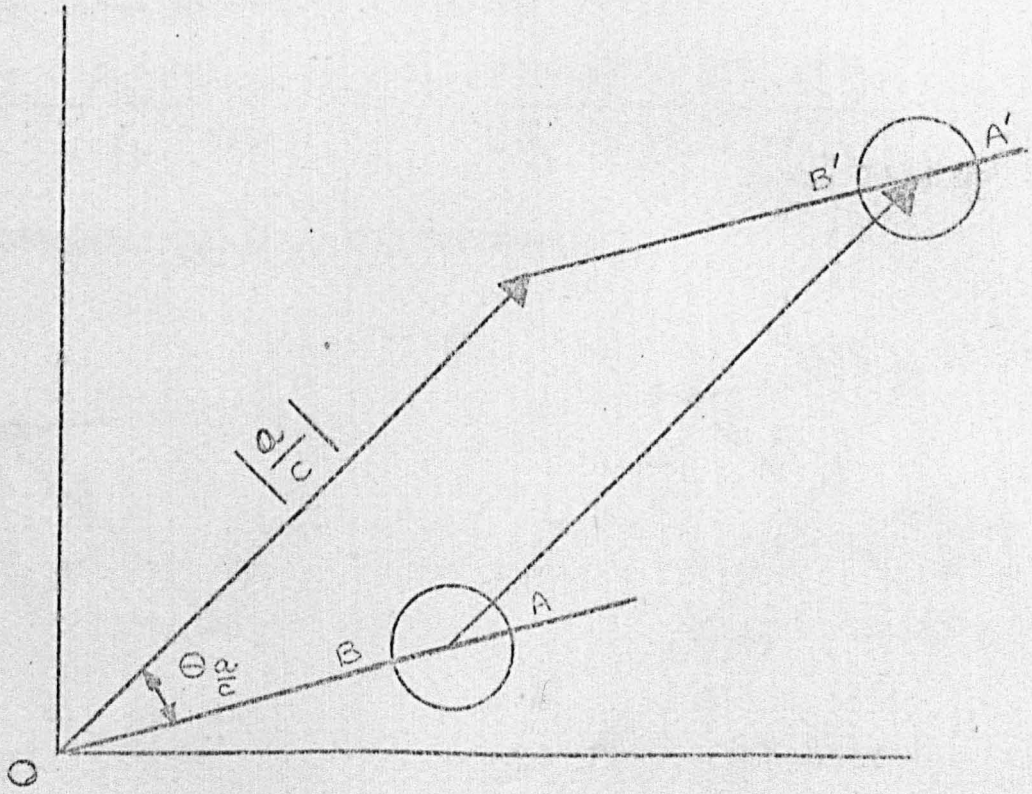

Note that the transformed points A′ and B′ are no longer the maximum and minimum radial distances from the origin O of the points on the circle.

References

11.3.1 Warner, F "Microwave Attenuation Measurement" I.E.E. Monograph Series 19. Peter Peregrinus Ltd., 1976.

11.3.2 Barlow H, & Cullen A, "Microwave Measurements Constable & Co Ltd., London 1950.

11.3.3 Morton, A.H. "Advanced Electrical Engineering Pitmans, 1971.

* * * * * * * * * * *

APPENDIX 11:4

THE INVARIANCE OF THE BILINEAR TRANSFORMATION CROSS-RATIO APPLIED TO MICROWAVE ANALYSIS

This principle is of great importance when it is desired to transfer four points, eg reflection coeffficients Γ_1, Γ_2, Γ_3, Γ_4 at a measurement plane, W , into four points eg, P_1, P_2, P_3, P_4 at another plane, Z . The relationship between these points is given by

$$\frac{(P_1 - P_2)(P_3 - P_4)}{(P_2 - P_3)(P_4 - P_1)} = \frac{(\Gamma_1 - \Gamma_2)(\Gamma_3 - \Gamma_4)}{(\Gamma_2 - \Gamma_3)(\Gamma_4 - \Gamma_1)} \quad \ldots\ldots 11.4.1$$

Consider the diagrams below:-

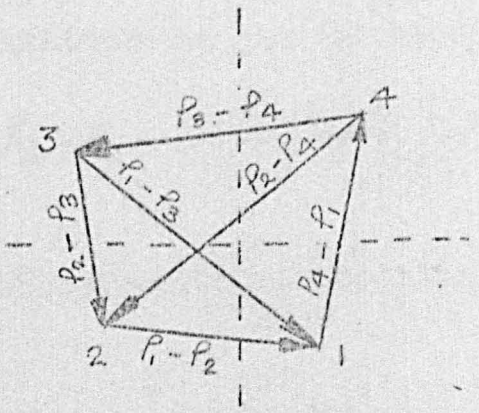

Z Plane

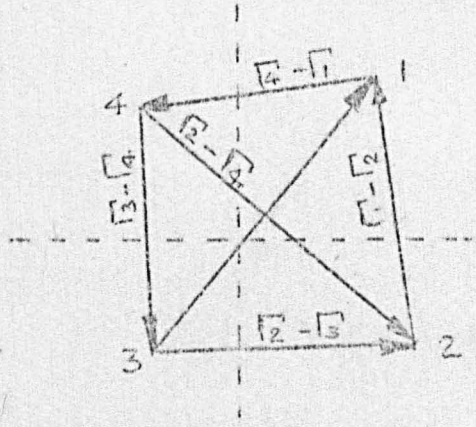

W Plane

In the diagrams above, each point, P, is related to Γ, by a bilinear transformation of the form

$$\rho = \frac{a\Gamma + b}{c\Gamma + d}$$

Hence,

$$\rho_1 - \rho_2 = \frac{a\Gamma_1 + b}{c\Gamma_1 + d} - \frac{a\Gamma_2 + b}{c\Gamma_2 + d}$$

$$= \frac{(a\Gamma_1 + b)(c\Gamma_2 + d) - (a\Gamma_2 + b)(c\Gamma_1 + d)}{(c\Gamma_1 + d)(c\Gamma_2 + d)}$$

$$= \frac{ac\Gamma_1\Gamma_2 + ad\Gamma_1 + bc\Gamma_2 + bd - ac\Gamma_1\Gamma_2 - ad\Gamma_2 - bc\Gamma_1 - bd}{(c\Gamma_1 + d)(c\Gamma_2 + d)}$$

$$\therefore \quad \rho_1 - \rho_2 = \frac{(ad - bc)(\Gamma_1 - \Gamma_2)}{(c\Gamma_1 + d)(c\Gamma_2 + d)} \qquad \ldots\ldots \quad (11.4.2)$$

Similarly it can be shown that

$$\rho_3 - \rho_4 = \frac{(ad - bc)(\Gamma_3 - \Gamma_4)}{(c\Gamma_3 + d)(c\Gamma_2 + d)} \qquad \ldots\ldots \quad (11.4.3)$$

$$\rho_2 - \rho_3 = \frac{(ad - bc)(\Gamma_2 - \Gamma_3)}{(c\Gamma_2 + d)(c\Gamma_3 + d)} \qquad \ldots\ldots \quad (11.4.4)$$

$$\rho_4 - \rho_1 = \frac{(ad - bc)(\Gamma_4 - \Gamma_1)}{(c\Gamma_4 + d)(c\Gamma_1 + d)} \qquad \ldots\ldots \quad (11.4.5)$$

Dividing equation 11.4.2 by equation 11.4.4

$$\frac{(\rho_1 - \rho_2)}{(\rho_2 - \rho_3)} = \frac{(ad - bc)(\Gamma_1 - \Gamma_2)(c\Gamma_2 + d)(c\Gamma_3 + d)}{(c\Gamma_1 + d)(c\Gamma_2 + d)(ad - bc)(\Gamma_2 - \Gamma_3)}$$

$$\therefore \quad \frac{(\rho_1 - \rho_2)}{(\rho_2 - \rho_3)} = \frac{(\Gamma_1 - \Gamma_2)(c\Gamma_3 + d)}{(\Gamma_2 - \Gamma_3)(c\Gamma_1 + d)} \qquad \ldots\ldots \quad (11.4.6)$$

Similarly dividing equation 11.4.3 by 11.4.5 gives,

$$\frac{(P_3 - P_4)}{(P_4 - P_1)} = \frac{(ad-bc)(\Gamma_3 - \Gamma_4)(c\Gamma_4 + d)(c\Gamma_1 + d)}{(c\Gamma_3 + d)(c\Gamma_4 + d)(ad-bc)(\Gamma_4 - \Gamma_1)}$$

$\therefore$

$$\frac{(P_3 - P_4)}{(P_4 - P_1)} = \frac{(\Gamma_3 - \Gamma_4)(c\Gamma_1 + d)}{(\Gamma_4 - \Gamma_1)(c\Gamma_3 + d)} \quad \ldots\ldots \quad (11.4.7)$$

Finally multiplying equations 11.4.6 and 11.4.7 together gives:

$$\frac{(P_1 - P_2)(P_3 - P_4)}{(P_2 - P_3)(P_4 - P_1)} = \frac{(\Gamma_1 - \Gamma_2)(\Gamma_3 - \Gamma_4)}{(\Gamma_2 - \Gamma_3)(\Gamma_4 - \Gamma_1)}$$

which is the desired result of equation 11.4.1.

* * * * * * * * * * *

APPENDIX 11:5

PROGRAMME FOR REFLECTION COEFFICIENT CORRECTION USING THE 3 SHORT CIRCUIT METHOD OF SECTION 5:4.2

This appendix provides the machine code programme for operation on the Hewlett Packard Programmable calculator HP9100B. The programme accepts the three short circuit calibration measurements in its polar form (modulus and angle in degrees). From this data, it calculates, stores and prints out the error correction network in polar form. The measured reflection coefficient is then entered in polar form and the corrected result is printed out as:-

(a) a reflection coefficient normalized to 50 Ω.
(b) as an impedance in polar form
(c) as an impedance in rectangular coordinates.

Due to the limited capacity of the machine the programme was written in four sections (2 magnetic cards) and was fed in sequentially as the calculations proceeded and additional storage became available. The lengths of the off-sets also had to be preset within the programme. However, the pre-set lengths can be easily altered.

To minimise the possibility of any typhographical errors, the programme is given directly from the actual print-out from the Hewlett Packard machine. This print-out uses numerical codes to represent the machine instructions. A conversion code is given in Table 11.5.1 to convert the numerical codes to the key or machine instructions.

TABLE 11:5.1

Key Code	Numeric Code	Key Code	Numeric Code
0	00	y → ( )	40
1	01	STOP	41
2	02	FMT	42
3	03	IF FLAG	43
4	04	GO TO ( )	44
5	05	PRINT	45
6	06	END	46
7	07	CONTINUE	47
8	10	IF X=Y	50
9	11	IF X<Y	52
e	12	IF X>Y	53
a	13	SET FLAG	54
b	14	|y|	55
f	15	π	56
c	16		
d	17		
CLEAR	20	Acc +	60
.	21	RCL	61
ROLL ↑	22	TO POLAR	62
x → ( )	23	ACC −	63
y ⇄ ( )	24	INT X	64
↓	25	LN X	65
Enter Exp.	26	TO RECT	66
↑	27	HYPER	67
x ⇄ y	30	SIN X	70
ROLL ↓	31	TAN X	71
CHG SIGN	32	ARC ▼	72
+	33	COS X	73
−	34	e^x	74
÷	35	LOG X	75
×	36	$\sqrt{x}$	76
CLEAR X	37		

Step	Code	
0.0	20	
0.1	41	
0.2	45	
0.3	27	
0.4	07	
0.5	21	✓
0.6	02	✓
0.7	00	✓
0.8	00	✓
0.9	00	✓
0.a	36	✓
0.b	40	✓
0.c	13	✓
0.d	03	✓
1.0	06	✓
1.1	00	✓
1.2	33	✓
1.3	17	✓
1.4	01	✓
1.5	26	✓
1.6	32	✓
1.7	11	✓
1.8	23	✓
1.9	15	✓
1.a	41	✓
1.b	45	✓
1.c	22	✓
1.d	15	✓
2.0	34	✓
2.1	31	✓
2.2	33	✓
3.3	17	✓
2.4	33	✓
2.5	40	✓
2.6	14	✓
2.7	41	✓
2.8	45	✓
2.9	22	✓
2.a	15	✓
2.b	34	✓
2.c	31	✓
2.d	33	✓

Step	Code	
3.0	17	✓
3.1	33	✓
3.2	40	✓
3.3	16	✓
3.4	41	✓
3.5	45	✓
3.6	45	✓
3.7	22	✓
3.8	15	✓
3.9	34	✓
3.a	31	✓
3.b	33	✓
3.c	17	✓
3.d	33	
4.0	40	
4.1	17	
4.2	61	
4.3	63	
4.4	13	
4.5	73	
4.6	62	
4.7	65	
4.8	60	
4.9	13	
4.a	27	
4.b	01	
4.c	65	
4.d	60	
5.0	17	
5.1	27	
5.2	64	
5.3	34	
5.4	30	
5.5	65	
5.6	60	
5.7	14	
5.8	27	
5.9	64	
5.a	34	
5.b	30	
5.c	65	
5.d	60	

Step	Code
6.0	00
6.1	27
6.2	02
6.3	65
6.4	60
5.5	61
6.6	63
6.7	74
6.8	66
6.9	22
6.a	40
6.b	11
6.c	14
6.d	30
7.0	14
7.1	64
7.2	34
7.3	30
7.4	65
7.5	60
7.6	16
7.7	30
7.8	16
7.9	64
7.a	34
7.b	30
7.c	65
7.d	60
8.0	61
8.1	63
8.2	74
8.3	66
8.4	31
8.5	34
8.6	24
8.7	11
8.8	31
8.9	30
8.a	34
8.b	47
8.c	47
8.d	46

Step	Code
0.0	47
0.1	16
0.2	27
0.3	64
0.4	34
0.5	30
0.6	65
0.7	60
0.8	17
0.9	30
0.a	17
0.b	64
0.c	34
0.d	30
1.0	65
1.1	60
1.2	02
1.3	30
1.4	13
1.5	36
1.5	01
1.7	65
1.8	60
1.9	61
1.a	63
1.b	74
1.c	66
1.d	32
2.0	22
2.1	33
2.2	24
2.3	11
2.4	30
2.5	22
2.6	34
2.7	14
2.8	27
2.9	64
2.a	34
2.b	30
2.c	66
2.d	60

Step	Code
3.0	16
3.1	30
3.2	16
3.3	64
3.4	34
3.5	30
3.6	66
3.7	63
3.8	61
3.9	63
3.a	62
3.b	65
3.c	60
3.d	13
4.0	30
4.1	13
4.2	33
4.3	01
4.4	65
4.5	60
4.6	61
4.7	63
4.6	74
4.9	66
4.a	60
4.b	16
4.c	30
4.d	16
5.0	64
5.1	34
5.2	30
5.3	66
5.4	63
5.5	17
5.6	30
5.7	17
5.8	64
5.9	34
5.a	30
5.b	66
5.c	60
5.d	61

Step	Code
6.0	63
6.1	62
6.2	65
6.3	63
6.4	24
6.5	11
6.6	25
6.7	62
6.8	65
6.9	60
6.a	61
6.b	63
6.c	74
6.d	45
7.0	66
7.1	23
7.2	17
7.3	40
7.4	11
7.5	60
7.6	16
7.7	27
7.8	64
7.9	34
7.a	30
7.b	66
7.c	63
7.d	61
8.0	63
8.1	62
8.2	65
8.3	60
8.4	13
8.5	27
8.6	33
8.7	01
8.8	65
8.9	60
8.a	47
8.b	47
8.c	47
8.d	46

Step	Code
0.0	47
0.1	61
0.2	63
0.3	74
0.4	66
0.5	63
0.6	14
0.7	27
0.8	64
0.9	34
0.a	30
0.b	66
0.c	63
0.d	17
1.0	27
1.1	24
1.2	11
1.3	40
1.4	17
1.5	60
1.6	61
1.7	63
1.8	62
1.9	65
1.a	60
1.b	14
1.c	27
1.d	64
2.0	34
2.1	30
2.2	66
2.3	27
2.4	24
2.5	16
2.6	25
2.7	27
2.8	64
2.9	34
2.a	30
2.b	66
2.c	31
2.d	34

Step	Code
3.0	16
3.1	22
3.2	34
3.3	31
3.4	62
3.5	66
3.6	63
3.7	61
3.8	63
3.9	74
3.a	45
3.b	66
3.c	60
3.d	23
4.0	16
4.1	00
4.2	27
4.3	01
4.4	60
4.5	61
4.6	63
4.7	62
4.8	65
4.9	60
4.a	14
4.b	30
4.c	14
4.d	64
5.0	34
5.1	30
5.2	66
5.3	24
5.4	11
5.5	40
5.6	14
5.7	34
5.8	30
5.9	24
5.a	11
5.b	31
5.c	24
5.d	17

Step	Code
6.0	32
6.1	30
6.2	33
6.3	30
6.4	22
6.5	62
6.6	65
6.7	60
6.8	61
6.9	63
6.a	74
6.b	45
6.c	45
6.d	24
7.0	14
7.1	30
7.2	24
7.3	11
7.4	30
7.5	31
7.6	63
7.7	41
7.8	45
7.9	66
7.a	60
7.b	61
7.c	63
7.d	62
8.0	65
8.1	63
8.2	24
8.3	11
8.4	30
8.5	24
8.6	14
8.7	65
8.8	60
8.9	61
8.a	63
8.b	74
8.c	47
8.d	46

Step	Code
0.0	47
0.1	66
0.2	60
0.3	17
0.4	27
0.5	16
0.6	60
0.7	61
0.8	63
0.9	62
0.a	65
0.b	63
0.c	13
0.d	27
1.0	07
1.1	21
1.2	02
1.3	00
1.4	00
1.5	00
1.6	00
1.7	35
1.8	27
1.9	61
1.a	63
1.b	74
1.c	45
1.d	45
2.0	66
2.1	60
2.2	23
2.3	17
2.4	40
2.5	16
2.6	00
2.7	30
2.8	01
2.9	60
2.a	61
2.b	63
2.c	62
2.d	22

Step	Code
3.0	23
3.1	14
3.2	05
3.3	00
3.4	36
3.5	17
3.6	24
3.7	16
3.8	63
3.9	00
3.a	30
3.b	01
3.c	60
3.d	61
4.0	63
4.1	62
4.2	65
4.3	63
4.4	25
4.5	16
4.6	65
4.7	60
4.8	61
4.9	63
4.a	74
4.b	45
4.c	66
4.d	45
5.0	23
5.1	17
5.2	40
5.3	16
5.4	00
5.5	52
5.6	07
5.7	10
5.8	50
5.9	07
5.a	10
5.b	47
5.c	47
5.d	47

Step	Code
6.0	47
6.1	01
6.2	30
6.3	35
6.4	14
6.5	35
6.6	56
6.7	35
6.8	02
6.9	35
6.a	47
6.b	47
6.c	47
6.d	47
7.0	47
7.1	00
7.2	44
7.3	10
7.4	06
7.5	47
7.6	47
7.7	47
7.8	14
7.9	35
7.a	02
7.b	35
7.c	56
7.d	35
8.0	47
8.1	47
8.2	47
8.3	47
8.4	47
8.5	00
8.6	45
8.7	45
8.8	45
8.9	46

APPENDIX 11:6

Manual Programme using Sigma V Computer for reflection coefficient correction using three short circuits.

```
EXTENDED FIV-F, VERSION B01
    1                 REAL KI1,KR1,KI2,KR2,KI3,KR3,KI4,KR4,KA4,KB4
    2                 REAL MAGMES, ANGMES
    3                 REAL MAGS11, ANGS11, MAGTMS, ANGTMS, MAGS22, ANGS22, MAGVAL,
    4                FANGVAL, FREQ
    5                 REAL F,OMEGA,PSI,THETA,WI,WR,XI,XR,KA1,KB1,KA2,KB2,KA3,KB3,OI,OR
    6                 COMPLEX A,B,C,D,K1,K2,K3,K4,W,X,S11,S21S12,S22,TVALUE
    7              100 CONTINUE
    8                 READ (105, 200) F,KA1,KB1,KA2,KB2,KA3,KB3,KA4,KB4
    9              200 FORMAT (9F)
   10                 IF(F .EQ. 0.0) STOP
   11                 A= CMPLX (1.0, 0.0)
   12                 OMEGA = 0.097808251 * F
   13                 PSI = 2.0 * OMEGA
   14                 THETA = 0.19561650 * F
   15                 OI = 1.0 * SIN (OMEGA)
   16                 OR = 1.0 * COS (OMEGA)
   17                 D = CMPLX (OR,OI)
   18                 WI = 1.0 * SIN(PSI)
   19                 WR = 1.0 * COS(PSI)
   20                 W =  CMPLX (WR,WI)
   21                 XI = 1.0 * SIN(THETA)
   22                 XR = 1.0 * COS(THETA)
   23                 X = CMPLX (XR, XI)
   24                 KB1 = KB1 * 3.1415926/180
   25                 KI1 = KA1 * SIN(KB1)
   26                 KR1 = KA1 * COS(KB1)
   27                 K1 = CMPLX (KR1, KI1)
   28                 KB2 = KB2 * 3.1415926/180
   29                 KI2 = KA2 * SIN(KB2)
   30                 KR2 = KA2 * COS(KB2)
   31                 K2 = CMPLX (KR2, KI2)
   32                 KB3 = KB3 * 3.1415926/180
   33                 KI3 = KA3 * SIN(KB3)
   34                 KR3 = KA3 * COS(KB3)
   35                 K3 = CMPLX (KR3, KI3)
   36                 KB4 = KB4 * 3.1415926/180
   37                 KI4 = KA4 * SIN(KB4)
   38                 KR4 = KA4 * COS(KB4)
   39                 K4 = CMPLX ( KR4, KI4)
   40                 B = K1*K2*(W-A)-K2*K3*(X-A)-K1*K3*(W-X)
   41                 C = (W-A)*(K2-K3)-(X-A)*(K2-K1)
   42                 S11 = B/C
   43                 S22 = (S11 - K1 + (K2 - S11)/W1/(K1 -K2)
   44                 S21S12 = (S11-K1)*(A+S22)
   45                 TVALUE = (K4 - S11)/(S22 + K4 + S21S12 - S11 * S22)
   46                 FREQ = F
   47                 MAGS11 = CABS (S11)
   48                 ANGS11 = 57.29578 * ATAN2(AIMAG(S11),REAL(S11))
   49                 MAGTMS = CABS (S21S12)
   50                 ANGTMS = 57.29578 * ATAN2(AIMAG(S21S12),REAL(S21S12))
   51                 MAGS22 = CABS (S22)
   52                 ANGS22 = 57.29578 * ATAN2(AIMAG(S22),REAL(S22))
   53                 MAGVAL = CABS (TVALUE)
   54                 ANGVAL = 57.29578 * ATAN2(AIMAG(TVALUE),REAL(TVALUE))
   55                 MAGMES = CABS(K4)
   56                 ANGMES=57.29578*ATAN2(AIMAG(K4),REAL(K4))
   57                 OUTPUT(108) FREQ, MAGS11, ANGS11, MAGTMS, ANGTMS, MAGS22,
   58                FANGS22, MAGVAL, ANGVAL
   59                 OUTPUT(108) MAGMES, ANGMES
   60                 OUTPUT(108) KA1,KB1,KA2,KB2,KA3,KB3,KA4,KB4
   61                 GO TO 100



   62                 STOP
   63                 END
```

APPENDIX 11:7

Manual Programme using Sigma V Computer for reflection coefficient correction using four short circuits.

```
21:27 APR 19,'77
!JOB  EFD
!FORTRANH LS,GO
    EXTENDED FIV-H, VERSION DC1
      1            C      THIS SINGLE PRECEISION PROGRAMME IS FOR 4 EVENLY SPACED SHORTS
      2                   IMPLICIT COMPLEX(S)
      3                   DIMENSION SI(5)
      4             100   CONTINUE
      5                   READ(105,200) A1,A2,A3,A4,A5,A6,A7,A8,A9,A10
      6             200   FORMAT (10F)
      7                   IF(A1*EQ*0*0) STOP
      8                   DATA PI/3*14159265358/
      9                   A2A = A2*PI/180*0
     10                   A1A = A1*COS(A2A)
     11                   A1B = A1*SIN(A2A)
     12                   SI(1) = CMPLX (A1A,A1B)
     13                   A4A = A4*PI/180*0
     14                   A3A = A3*COS(A4A)
     15                   A3B = A3*SIN(A4A)
     16                   SI(2) = CMPLX(A3A,A3B)
     17                   A6A = A6*PI/180*0
     18                   A5A = A5*COS(A6A)
     19                   A5B = A5*SIN(A6A)
     20                   SI(3) = CMPLX(A5A,A5B)
     21                   A8A = A8*PI/180*0
     22                   A7A = A7*COS(A8A)
     23                   A7B = A7*SIN(A8A)
     24                   SI(4) = CMPLX(A7A,A7B)
     25                   A10A = A10*PI/180*0
     26                   A9A = A9*COS(A10A)
     27                   A9B = A9 * SIN(A10A)
     28                   SI(5) = CMPLX(A9A,A9B)
     29                   SA=2*0*(SI(1)*SI(3)-SI(1)*SI(4)-SI(2)*SI(3)+SI(2)*SI(4))
     30                   SB = -SI(1)*SI(2)+SI(2)*SI(3)-SI(3)*SI(4)+SI(1)*SI(4)
     31                   SC=SI(1)*SI(2)-2*0*SI(1)*SI(3)+SI(1)*SI(4)+SI(2)*SI(3)
     32                  1 -2*0*SI(2)*SI(4)+SI(3)*SI(4)
     33                   SD= SB**2-4*0*SA*SC
     34                   SE10 = (-SB + CSQRT(SD))/(2*0*SA)
     35                   SE20 = (-SB -CSQRT(SD))/(2*0*SA)
     36                   SE11 = -2*0*SE10
     37                   SE21 = -2*0*SE20
     38                   SE30 = CMPLX(1*0,0*0)
     39                   SE12 = SE11**2 -4*0*SE30*SE30
     40                   SE22 = SE21**2-4*0*SE30*SE30
     41                   SE13 = (-SE11+CSQRT(SE12))/(2*0*SE30)
     42                   SE14=(-SE11-CSQRT(SE12))/(2*0*SE30)
     43                   SE23=(-SE21+CSQRT(SE22))/(2*0*SE30)
     44                   SE24=(-SE21-CSQRT(SE22))/(2*0*SE30)
     45                   PA = 180*0*ATAN2(AIMAG(SE13),REAL(SE13))/PI
     46                   PB = 180*0*ATAN2(AIMAG(SE14),REAL(SE14))/PI
     47                   PC=180*0*ATAN2(AIMAG(SE23),REAL(SE23))/PI
     48                   PD= 180*0*ATAN2(AIMAG(SE24),REAL(SE24))/PI
     49                   PHASE = 0*0
     50                   IF(PA*GT*1*0E-4*AND*PA*GE*PB*AND*PA*GE*PC*AND*PA*GE*PD)
     51                  1 PHASE = PA
     52                   IF(PB*GT*1*0E-4*AND*PB*GE*PA*AND*PB*GE*PC*AND*PB*GE*PD)
     53                  1 PHASE = PB
     54                   IF(PC*GT*1*0E-4*AND*PC*GE*PA*AND*PC*GE*PB*AND*PC*GE*PD)
     55                  1 PHASE = PC
     56                   IF(PD*GT*1*0E-4*AND*PD*GE*PA*AND*PD*GE*PB*AND*PD*GE*PC)
     57                  1 PHASE = PD
     58                   SE31 = CABS(SE13)
     59                   SE32 = CABS(SE14)
```

APPENDIX 11:7 (continued)

```
      SE33 = CABS(SE23)
      SE34 = CABS(SE24)
      ATTENU = 10
      IF(PHASE.EQ.PA)ATTENU = SE31
      IF(PHASE.EQ.PB)ATTENU= SE32
      IF(PHASE.EQ.PC)ATTENU = SE33
      IF(PHASE.EQ.PD)ATTENU = SE34
      PHASE = PHASE * PI/180.0
      S50= ATTENU*CMPLX(COS(PHASE),SIN(PHASE))
      S51= CMPLX(COS(-PHASE),SIN(-PHASE))/ATTENU
      S41=(SI(1)*SI(2)*(S51-SE30))-(SI(2)*SI(3)*(S50-SE30))
     1 -(SI(3)*SI(1)*(S51-S50))
      S42=(SI(1)*(S50-SE30))+(SI(2)*(S51-S50))+(SI(3)*(SE30-S51))
      S11=S41/S42
      SGAM = CMPLX(-1.0,0.0)
      S221 = (S50*(SI(2)-S11)+S11-SI(1))/(SI(2)-SI(1))
      S22 = S221/SGAM
      S12211 = (SI(1)-S11)*(SE30-S22*SGAM)
      S12S21 = S12211/SGAM
      SI6 = (SI(5)-S11)/(S22*SI(5)+S12S21-S11*S22)
      A20 = CABS(SI6)
      A21 = 180.0*ATAN2(AIMAG(SI6),REAL(SI6))/PI
      ZEPERS = ALOG(ATTENU)
      PHASE = PHASE * 180.0/PI
      OUTPUT(108) SA,SB,SC,SD,SE10,SE20,SE11,SE21,SE13,SE14,
     1 SE23,SE24,PA,PB,PC,PD
      OUTPUT(108) SI(1),SI(2),SI(3),SI(4),SI(5),SI6,ATTENU,PHASE
      OUTPUT(108) S50,S51,S11,S221,S12211,SGAM,S22,S12S21
      OUTPUT(108) A1,A2,A3,A4,A5,A6,A7,A8,A9,A10
      OUTPUT(108) SI6
      OUTPUT(108) A20,A21
      OUTPUT(108) ZEPERS
      OUTPUT(108)S41,S42
      GO TO 100
      STOP
      END
```

APPENDIX 11:8

Manual Programme (Double Precision) using Sigma V Computer for reflection coefficient correction using four short circuits.

```
EXTENDED FIV-H, VERSION R01
    1.                IMPLICIT REAL*8(A,B,C,D,L,P)
    2                 IMPLICIT COMPLEX*16(S)
    3                 DIMENSION SI(15)
    4               100 CONTINUE
    5                 READ(105,200) A1,A2,A3,A4,A5,A6,A7,A8,A9,A10
    6               200 FORMAT (10F)
    7                 IF(A1.EQ.0.0000) STOP
    8                 DATA PI/3.1415926535897900/
    9                 A2A=A2*PI/1.800
   10                 A1A=A1*DCOS(A2A)
   11                 A1B=A1*DSIN(A2A)
   12                 SI(1)=DCMPLX(A1A,A1B)
   13                 A4A=A4*PI/1.800
   14                 A3A=A3*DCOS(A4A)
   15                 A3B=A3*DSIN(A4A)
   16                 SI(2)=DCMPLX(A3A,A3B)
   17                 A6A=A6*PI/1.800
   18                 A5A=A5*DCOS(A6A)
   19                 A5B=A5*DSIN(A6A)
   20                 SI(3)=DCMPLX(A5A,A5B)
   21                 A8A=A8*PI/1.800
   22                 A7A=A7*DCOS(A8A)
   23                 A7B=A7*DSIN(A8A)
   24                 SI(4)=DCMPLX(A7A,A7B)
   25                 A10A=A10*PI/1.800
   26                 A9A=A9*DCOS(A10A)
   27                 A9B=A9*DSIN(A10A)
   28                 SI(5)=DCMPLX(A9A,A9B)
   29                 SE30=DCMPLX(1.000,0.000)
   30                 SA=2.0*(SI(1)*SI(3)-SI(1)*SI(4)-SI(2)*SI(3)+SI(2)*SI(4))
   31                 SB = -SI(1)*SI(2)+SI(2)*SI(3)-SI(3)*SI(4)+SI(1)*SI(4)
   32                 SC=SI(1)*SI(2)-2.0*SI(1)*SI(3)+SI(1)*SI(4)*SI(2)*SI(3)
   33                1 -2.0*SI(2)*SI(4)+SI(3)*SI(4)
   34                 SD= SB**2-4.0*SA*SC
   35                 SE10 =(-SB + CDSQRT(SD))/(2.0*SA)
   36                 SE20 = (-SB - CDSQRT(SD))/(2.0*SA)
   37                 SE11 = -2.0*SE10
   38                 SE21 = -2.0*SE20
   39                 SE30 = DCMPLX(1.00000,0.00000)
   40                 SF12 = SE11**2 -4.0*SE30*SE30
   41                 SE22 = SE21**2-4.0*SE30*SE30
   42                 SE13 = (-SE11 + CDSQRT(SE12))/(2.0*SE30)
   43                 SE14 = (-SE11 - CDSQRT(SE12))/(2.0*SE30)
   44                 SE23 = (-SE21 + CDSQRT(SE22))/(2.0*SE30)
   45                 SE24 = (-SE21 - CDSQRT(SE22))/(2.0*SE30)
   46                 PA = 1.800/PI*DATAN2(DIMAG(SE13),DREAL(SE13))
   47                 PB = 1.800/PI*DATAN2(DIMAG(SE14),DREAL(SE14))
   48                 PC=1.800/PI*DATAN2(DIMAG(SE23),DREAL(SE23))
   49                 PD= 1.800/PI*DATAN2(DIMAG(SE24),DREAL(SE24))
   50                 PHASE = 0.00000
   51                 IF(PA.GT.1.00.AND.PA.GE.PB.AND.PA.GE.PC.AND.
   52                1 PA.GE.PD) PHASE = PA
   53                 IF(PB.GT.1.00.AND.PB.GE.PA.AND.PB.GE.PC.AND.
   54                1 PB.GE.PD) PHASE = PB
   55                 IF(PC.GT.1.00.AND.PC.GE.PA.AND.PC.GE.PB.AND.
   56                1 PC.GE.PD) PHASE = PC
   57                 IF(PD.GT.1.00.AND.PD.GE.PA.AND.PD.GE.PB.AND.
   58                1 PD.GE.PC) PHASE = PD
   59                 L1 = CDABS(SE13)
   60                 L2 = CDABS(SE14)
   61                 L3 = CDABS(SE23)
   62                 L4 = CDABS(SE24)
```

APPENDIX 11:8 (continued)

```
      ATTENU = 10.0D0
      IF(PHASE.EQ.PA)ATTENU = L1
      IF(PHASE.EQ.PB)ATTENU = L2
      IF(PHASE.EQ.PC)ATTENU = L3
      IF(PHASE.EQ.PD)ATTENU = L4
      PHASE=PHASE*PI/180.0
      S50 = ATTENU*DCMPLX(DCOS(PHASE),DSIN(PHASE))
      S51=DCMPLX(DCOS(-PHASE),DSIN(-PHASE))/(ATTENU)
      S11 = (SI(1)*SI(2)*(S51-SE30) + SI(2) * SI(3) * (S50-SE30)
     1  -SI(3)*SI(1)*(S51-S50))/(SI(1)*(S50-SE30)+SI(2)*
     2  (S51-S50)+SI(3)*(SE30-S51))
      SGAM = DCMPLX(-1.0D0,0.0D0)
      S221 = (S50*(SI(2)-S11)+S11-SI(1))/(SI(2)-SI(1))
      S22 = S221/SGAM
      S12S11 = (SI(1)-S11)*(SE30-S22*SGAM)
      S12S21 = S12S11/SGAM
      S16 = (SI(5)-S11)/(S22*SI(5)+S12S21-S11*S22)
      A20 = CDABS(S16)
      A21=1.8D2*DATAN2(DIMAG(S16),DREAL(S16))/PI
      ZEPERS = DLOG(ATTENU)
      OUTPUT(108) A1,A2,A3,A4,A5,A6,A7,A8,A9,A10,A20,A21
      OUTPUT(108) S16
      OUTPUT(108) SA,SB,SC,SD,SE10,SE20,SE11,SE21,SE13,SE14,
     1 SE23,SE24,PA,PB,PC,PD
      OUTPUT(108) SI(1),SI(2),SI(3),SI(4),SI(5),S16,ATTENU,PHASE
      OUTPUT(108) S50,S51,S11,S221,S12S11,SGAM,S22,S12S21
      OUTPUT(108) ZEPERS
      GO TO 100
      STOP
      END
```

APPENDIX 11:9

Manual Programme using Sigma V Computer for reflection coefficient correction using four unknown terminations and a reference short circuit.

```
EXTENDED FIV-F, VERSION DC1
    1           C     PROGRAMME FOR 4 UNKNOWN TERMINATIONS AND A REFERENCE SHORT
    2           C SALLY IS THE ACTUAL OUTPUT LOAD ADMITTANCE.
    3           C  PUFFO IS THE IMAGINARY PART OF SALLY DIVIDED BY 2*PI*10**9
    4           C     TO GET STRAY CAPACITANCE IN PF, DIVIDE PUFFO BY F IN GHZ
    5                 IMPLICIT COMPLEX(S)
    6                 DIMENSION SI(6)
    7               100 CONTINUE
    8                 READ(105,200)A1,A2,A3,A4,A5,A6,A7,A8,A9,A10,A11,A12
    9               200 FORMAT(12F)
   10                  IF(A1.EQ.0.0) STOP
   11                  DATA PI/3.1415926536/
   12                  A2A = A2*PI/180.0
   13                  A1A = A1*COS(A2A)
   14                  A1B = A1*SIN(A2A)
   15                  SI(1) = CMPLX (A1A,A1B)
   16                  A4A = A4*PI/180.0
   17                  A3A = A3*COS(A4A)
   18                  A3B = A3*SIN(A4A)
   19                  SI(2) = CMPLX(A3A,A3B)
   20                  A6A = A6*PI/180.0
   21                  A5A = A5*COS(A6A)
   22                  A5B = A5*SIN(A6A)
   23                  SI(3) = CMPLX(A5A,A5B)
   24                  A8A = A8*PI/180.0
   25                  A7A = A7*COS(A8A)
   26                  A7B = A7*SIN(A8A)
   27                  SI(4) = CMPLX(A7A,A7B)
   28                  A10A = A10*PI/180.0
   29                  A9A = A9*COS(A10A)
   30                  A9B = A9 * SIN(A10A)
   31                  SI(5) = CMPLX(A9A,A9B)
   32                  A12A=A12*PI/180.0
   33                  A11A=A11*COS(A12A)
   34                  A11B=A11*SIN(A12A)
   35                  SI(6)=CMPLX(A11A,A11B)
   36                  SA=2.0*(SI(1)*SI(3)-SI(1)*SI(4)-SI(2)*SI(3)+SI(2)*SI(4))
   37                  SB = -SI(1)*SI(2)+SI(2)*SI(3)-SI(3)*SI(4)+SI(1)*SI(4)
   38                  SC=SI(1)*SI(2)-2.0*SI(1)*SI(3)+SI(1)*SI(4)+SI(2)*SI(3)
   39                 1 -2.0*SI(2)*SI(4)+SI(3)*SI(4)
   40                  SD= SB**2-4.0*SA*SC
   41                  SE10 = (-SB + CSQRT(SD))/(2.0*SA)
   42                  SE20 = (-SB -CSQRT(SD))/(2.0*SA)
   43                  SE11 = -2.0*SE10
   44                  SE21 = -2.0*SE20
   45                  SE30 = CMPLX(1.0,0.0)
   46                  SE12 = SE11**2 -4.0*SE30*SE30
   47                  SE22 = SE21**2-4.0*SE30*SE30
   48                  SE13 = (-SE11+CSQRT(SE12))/(2.0*SE30)
   49                  SE14=(-SE11-CSQRT(SE12))/(2.0*SE30)
   50                  SE23=(-SE21+CSQRT(SE22))/(2.0*SE30)
   51                  SE24=(-SE21-CSQRT(SE22))/(2.0*SE30)
   52                  PA = 180.0*ATAN2(AIMAG(SE13),REAL(SE13))/PI
   53                  PB = 180.0*ATAN2(AIMAG(SE14),REAL(SE14))/PI
   54                  PC=180.0*ATAN2(AIMAG(SE23),REAL(SE23))/PI
   55                  PD= 180.0*ATAN2(AIMAG(SE24),REAL(SE24))/PI
   56                  PHASE = 0.0
   57                  IF(PA.GT.1.0E-4.AND.PA.GE.PB.AND.PA.GE.PC.AND.PA.GE.PD)
   58                 1 PHASE = PA
   59                  IF(PB.GT.1.0E-4.AND.PB.GE.PA.AND.PB.GE.PC.AND.PB.GE.PD)
   60                 1 PHASE = PB
   61                  IF(PC.GT.1.0E-4.AND.PC.GE.PA.AND.PC.GE.PB.AND.PC.GE.PD)
   62                 1 PHASE = PC
```

APPENDIX 11:9 (continued)

```
      IF(PC.GT.1.0E-4.AND.PD.GE.PA.AND.PD.GE.PB.AND.PD.GE.PC)
     1 PHASE = PD
      SE31 = CABS(SE13)
      SE32 = CABS(SE14)
      SE33 = CABS(SE23)
      SE34 = CABS(SE24)
      ATTENU = 10
      IF(PHASE.EQ.PA)ATTENU = SE31
      IF(PHASE.EQ.PB)ATTENU= SE32
      IF(PHASE.EQ.PC)ATTENU = SE33
      IF(PHASE.EQ.PD)ATTENU = SE34
      PHASE = PHASE * PI/180.0
      S50= ATTENU*CMPLX(COS(PHASE),SIN(PHASE))
      S51= CMPLX(COS(-PHASE),SIN(-PHASE))/ATTENU
      S41=(SI(1)*SI(2)*(S51-SE30))-(SI(2)*SI(3)*(S50-SE30))
     1 -(SI(3)*SI(1)*(S51-S50))
      S42=(SI(1)*(S50-SE30))+(SI(2)*(S51-S50))+(SI(3)*(SE30-S51))
      S11=S41/S42
      S221 = (S50*(SI(2)-S11)+S11-SI(1))/(SI(2)-SI(1))
      S12211=(SI(1)-S11)*(SE30-S221)
      SGAM=S12211/(S11-SI(5))-S221
      S22 = S221/SGAM
      S12S21 = S12211/SGAM
      SI7=(SI(6)-S11)/(S22*SI(6)+S12S21-S11*S22)
      A20=CABS(SI7)
      A21=180.0*ATAN2(AIMAG(SI7),REAL(SI7))/PI
      ZEPERS = ALOG(ATTENU)
      ZEPERS=ABS(ZEPERS)
      PHASE = PHASE * 180.0/PI
      SALLY = 0.02*(1-SGAM)/(1+SGAM)
      PUFFB = AIMAG(SALLY)/(.002*PI)
      OUTPUT(1C8)A1,A2,A3,A4,A5,A6,A7,A8,A9,A10,A11,A12
      OUTPUT(1C8) SI(1),SI(2),SI(3),SI(4),SI(5),SI(6),ATTENU,PHASE
      OUTPUT(1C8)SI7,A20,A21,ZEPERS
      OUTPUT(1C8) SA,SB,SC,SD,SE10,SE20,SE11,SE21,SE13,SE14,
     1 SE23,SE24,PA,PB,PC,PD
      OUTPUT(1C8) S50,S51,S11,S221,S12211,SGAM,S22,S12S21
      OUTPUT(1C8)S41,S42
      OUTPUT(1C8) SALLY, PUFFB
      GO TO 10C
      STOP
      END
```

APPENDIX 11:10

SOME STATISTICAL DEFINITIONS

The purpose of this appendix is to define and clarify the procedure used in deriving the results of chapters 8 and 9. Most of the information comes from the three main references given at the end of this appendix. Derivation of the equations used here will not be given as they have already been derived in their references.

The definitions and equalities are listed below:-

1: x_i is a measurement value assigned to the "i"th measurement.

2: n is the total number of measurements

3: The mean (X_n) is defined as the average of 'n' measurements of x_i

$$X_n = \frac{1}{n} \sum_{i=1}^{i=n} x_i \qquad \ldots\ldots \quad (11.10.1)$$

4: The weighted mean ($\bar{x}$) is defined as

$$\bar{x} = \frac{\sum_{i=1}^{i=n} \omega_i x_i}{\sum_{i=1}^{i=n} \omega_i} \qquad \ldots\ldots \quad (11.10.2)$$

where ω_i = number of measurements for that particular x_i.

5: The deviation (δ_i) of a measurement x_i in a set of 'n' measurements is defined

$$\delta_i = x_i - X_n \qquad \ldots\ldots \quad (11.10.3)$$

6: The precision or standard deviation (σ) of a set of 'n' measurements is given by

$$\sigma = \sqrt{\frac{1}{n}\sum_{i=1}^{i=n}\delta_i^2} = \sqrt{\frac{1}{n}\sum_{i=1}^{i=n}(x_i - x_m)^2} \quad \ldots\ldots \quad (11.10.4)$$

Note: This is not the definition given by many hand calculators e.g. Commodore type (SR4148R) etc. They use the definition given in 7.

7: The best estimate of the standard deviation (s_m) is defined as

$$s_m = \sigma\sqrt{\frac{(n)}{(n-1)}} = \sqrt{\frac{1}{(n-1)}\sum_{i=1}^{i=n}\delta_i^2} \quad \ldots\ldots \quad (11.10.5)$$

This is the definition given by some hand calculators e.g. Commodore Type (SR4148R) etc.

8: The variance (σ^2) is defined as the square of the standard deviation

$$(\sigma^2) = \frac{1}{n}\sum_{i=1}^{i=n}\delta_i^2 \ldots \quad \ldots\ldots \quad (11.10.6)$$

It follows from 11.10.4 and 11.10.5 that

$$(s_m^2) = \frac{1}{(n-1)}\sum_{i=1}^{i=n}\delta_i^2 \quad \ldots\ldots \quad (11.10.7)$$

9: The standard deviation of the mean $[\sigma(x_n)]$ is given as

$$\sigma(x_n) = \frac{\sigma}{\sqrt{n}} \qquad \ldots\ldots \text{(11.10.8)}$$

10: The best estimate of the standard deviation of the mean $[S_n(x_n)]$ is defined as

$$S_n(x_n) = \frac{s_n}{\sqrt{n}} \qquad \ldots\ldots \text{(11.10.9)}$$

The above is also called the standard error.

11: If the overall result of 'n' measurements (X) is written as

$$X = X_n \pm S_n \qquad \ldots\ldots \text{(11.10.10)}$$

If a Gaussian distribution is assumed, and if

$S_n = s_n$, X is determined with a confidence level of 68.27%
$S_n = 1.65 s_n$, " " " " " " 90.10%
$S_n = 2 s_n$, " " " " " " 95.45%
$S_n = 3 s_n$, " " " " " " 99.73%

12: If $Z = \alpha + ax + by$, where α, a, b, are constants then with 'n' measurements of x and 'm' measurements of y, the best estimate of the true value Z is Z_{nm} and

$$Z_{nm} = \alpha + aX_n + bY_m \qquad \ldots\ldots \text{(11.10.11)}$$

the combined best estimate of precision, $\Delta_{nm}(z)$ is given by

$$\Delta_{nm}(z) = \left[a^2 \Delta_n^2(x) + b^2 \Delta_m(y)\right]^{\frac{1}{2}}$$

..... (11.10.12)

and

the combined best estimate of the standard error $S_{nm}(z)$ is

$$S_{nm}(z) = \left[a^2 S_n^2(x) + b^2 S_m^2(y)\right]^{\frac{1}{2}}$$

..... (11.10.13)

and the measured value Z is given by

$$Z = Z_{nm} \pm S_{nm}(z)$$

..... (11.10.14)

13: If $z = \alpha x^a y^b$, where $\alpha, a, b,$ are constants then with 'n' measurements of x, and 'm' measurements of y the best estimate of the true value of z is z_{nm} and is given by

$$z_{nm} = \alpha (x_n)^a (y_m)^b$$

..... (11.10.15)

and the combined best estimate of precision $\frac{\Delta_{nm}(z)}{z_{nm}}$ is given by

$$\frac{\Delta_{nm}(z)}{z_{nm}} = \left[a^2 \frac{S_n^2(x)}{x_n^2} + b^2 \frac{S_m^2(y)}{y_m^2}\right]^{\frac{1}{2}}$$

..... (11.10.16)

and

$$\frac{S_{mm}(z)}{Z_{mm}} = \left[a^2 \frac{S_m^2(x)}{X_m^2} + b^2 \frac{S_m^2(y)}{y_m^2} \right]^{\frac{1}{2}}$$

..... (11.10.17)

which gives the measured value Z as

$$Z = Z_{mm} \pm S_{mm}(z)$$

$$\therefore Z = Z_{mm}\left[1 \pm \left(a^2 \frac{S_m^2(x)}{X_m^2} + b^2 \frac{S_m^2(y)}{y_m^2}\right)\right] \quad \ldots\ldots \quad (11.10.18)$$

14: If $Z = f(x)$, then

$$Z_m = f(X_m)$$

..... (11.10.19)

$$\delta_m(z) = f'(X_m)\,\delta_m(x)$$

..... (11.10.20)

$$S_m(z) = f'(X_m)\,S_m(x)$$

..... (11.10.21)

References

1 Barford, N.C. 'Experimental Measurements; Precision, Error and Truth' Addison-Wesley Publishing Company Incorporated (1967).

2 Young, Hugh D 'Statistical Treatment of Experimental Data' McGraw Hill Book Co (1962)

3 Braithwaite G & Titmus C, 'Lanchester Short Statistical Tables' English University Press 1967 reprinted 1972, 1973 & 1975.

* * * * * * * * * * *

PAGE/PAGES EXCLUDED UNDER INSTRUCTION FROM THE UNIVERSITY